Synthesis and Characterisation of Photoresponsive Azobenzene-Biomolecule Conjugates

A thesis submitted by

Jack Hayden

to the

National University of Ireland, Maynooth

For the degree of Doctor of Philosophy

Volume 1 of 1

Based on research carried out in the

Department of Chemistry, Faculty of Science and Engineering,

National University of Ireland, Maynooth

under the supervision and direction of

Dr Frances Heaney

Head of Department - Dr Jennifer McManus

2017

Contents

1. Introduction 11

1.1 Molecular switches 11

1.1.1 Introduction 11

1.1.2 Biomolecular switches 12

1.1.3 Photoswitches 13

1.2 Azobenzene 18

1.2.1 Azobenzene isomerisation mechanism. 19

1.2.3 Application of azobenzene photoswitching in biological materials and in biomolecular settings 24

1.2.4 Introduction of azobenzenes to biomolecules 34

1.3 Click chemistry 42

1.3.1 1,3-Dipolar cycloaddition chemistry 43

1.3.2 Copper catalysed azide-alkyne cycloaddition (CuAAC) 43

1.3.2 Nitrile oxide alkyne cycloaddition reactions (NOAC) 47

2. Azobenzenes with dipole and dipolarophile functionalities: synthesis and cycloaddition behaviour 52

2.1 Introduction 52

2.1.1 Major synthetic routes to azobenzenes. 54

2.2 Synthesis of azobenzenes bearing alkyne dipolarophiles at the *ortho*, *meta* and *para* positions 58

2.3 Preliminarily cycloadditions to azobenzenes bearing one or two dipolarophiles: test case reactions 64

2.4 Synthesis of azobenzenes bearing a 1,3-dipole functionality 70

2.5 Preliminary cycloadditions of azobenzenes bearing a 1,3-dipole functionality . 75

2.6 Attempted synthesis of *o*-azobenzene oximes and resulting indazole formation 81

2.7 Summary 95

3. Carbohydrate-Azobenzene Conjugates 96

Introduction 96
3.1 Carbohydrates functionalised with azobenzenes 96
3.1.1 Synthesis of and cycloaddition to carbohydrate dipolarophiles 96
3.1.2 Synthesis and cycloaddition of carbohydrates with dipolarophile functionality 119
3.2 Synthesis and cycloaddition of nucleosides bearing dipolarophile functionality 130
3.3 Summary 134
4. Peptide-Azobenzene conjugates 135
4.1 Background 135
4.2 Solid phase peptide synthesis 136
4.3 Resins and capping 140
4.4 Peptide sequence 141
4.5 Amino acid residues bearing 1,3-dipoles and dipolarophiles 142
4.6 Synthesis of an azobenzene-peptide conjugate through peptide coupling 144
4.7 Cycloaddition to N-terminal azidopeptides: 149
4.9 Cycloaddition to propargylated peptides (CuAAC) 150
4.10 Cycloaddition to azidopeptides (CuAAC) 155
4.11 Cycloaddition to propargylated peptides (NOAC) 157
4.12 Ligation of a peptide with a saccharide 159
4.13 Summary 161
5. Photophysical properties of the conjugates 162
5.1 Photostationary states 163
5.2 Determination of kinetic parameters for the thermal *cis* to *trans* isomerisation 177
5.3 Summary 187
6. Conclusions 188
7. Experimental 190

7.1 Materials and instrumentation 190
7.2 Structural numbering and nomenclature. 192
7.3 Protocols for SPPS 194
7.4 Protocols for determination of photostationary states (PSS) and thermal relaxation measurements 197
7.5 General experimental 199
8. Appendix 310
Full NMR characterisation and assignment of 242 310

Acknowledgements

I would like to thank my supervisor Dr Heaney for her support and guidance during this project.

SFI for making this project possible with their funding.

The project collaborators Prof. Devocelle, Dr Twamly, Dr O'Brien, Dr Valasco-Torrijos and Dr Elmes.

The staff and students in the Chemistry Department Maynooth University. Particularly the technical staff for always being of great assistance. The girls in the office for making my deadline drama successful. Noel for fixing anything and everything.

Andrew, Barry and Chig for the sanity restoring sessions. Ross for the lunchtime escapism to all those chicken delights. Everyone in the synthesis lab, my lab buddy Jusinta and of course the lab fairy for all the gloves.

MoJoe and Emma for their support.

Finally, Michelle for helping me through the struggles of the last 4 years, especially for being able to restore a smile to my face even if it was sometimes involuntary.

Declaration

I hereby certify that this thesis has not been submitted before, in whole or in part, to this or any other university for any degree and is, except where otherwise stated, the original work of the author

Signed:_____ date: / / .

Abstract

This thesis begins by overviewing the literature around the design, synthesis and application of molecular switches with a focus on the field of azobenzene switches, their isomerisation mechanisms and their value as *control* units on biological molecules.

The introductory chapter is followed three synthesis chapters reporting on the application of copper promoted azide alkyne and uncatalysed nitrile oxide alkyne cycloadditions for conjugation of azobenzenes initially with small molecule test case substrates, followed by the synthesis of carbohydrate, peptide and nucleic acid conjugates. The preparation of range of monosaccaride, disaccharide and nucleoside azobenzene conjugates are detailed.

The synthesis of a number of new azobenzenes bearing either 1,3-dipoles or their precursors, or dipolarophiles is described. Biomolecules bearing the complementary functionality are reported. The formation of isoxazole, triazole and ether linked biomolecule conjugates is demonstrated. Peptide conjugates have been prepared by cycloaddition in solution and on the solid phase. Formation of both mono- and divalent conjugates is demonstrated and a range of regioisomeric structures formed. All new compounds have been characterised by a variety of techniques including NMR spectroscopy, IR and UV/Vis spectroscopy, as well as HRMS. The structures of some compounds have been determined by x-ray crystal analysis.

The photophysical properties of a selected range of bioconjugates has been explored: the photostationary states were determined using NMR spectroscopy and the kinetic parameters of the *cis* to *trans* relaxation process determined by a UV spectroscopy study.

The experimental details are reported in chapter 7 and a full bibliography follows. -

Abbreviations

Å	Armstrong
˚C	Degrees Celsius
λ	Wavelength
A	Absorbance
A	Pre-exponential factor
AB	Azobenzene
Arg, R	Arginine
Asp, D	Aspartic acid
Boc	*tert*-butyloxycarbonyl
BOP	(Benzotriazol-1-yloxy)tris(dimethylamino)phosphonium hexafluorophosphate
BOP-Cl	Bis(2-oxo-3-oxazolidinyl)phosphinic chloride
Ch-T	Chloramine T
con^{c}	Concentration
CuAAC	Copper catalysed azide alkyne cycloaddition
d	doublet
D	Debye
DBU	1,8-Diazabicyclo[5.4.0]undec-7-ene
DCC	*N*,*N*′-Dicyclohexylcarbodiimide
DCM	Dichloromethane
DIEA	*N*,*N*-Diisopropylethylamine
DMAP	4-Dimethylaminopyridine
DMTyCl	4,4′-Dimethoxytrityl chloride
DMF	Dimethylformamide
DMP	Dess–Martin periodinane
DMSO	Dimethyl sulfoxide
DNA	Deoxyribonucleic acid
E_A	Activation energy
EDG	Electron donating group
Fmoc	Fluorenylmethyloxycarbonyl chloride
Gly, G	Glycine
h	Planck’s constant
H	Enthalpy
HATU	1-[Bis(dimethylamino)methylene]-1H-1,2,3-triazolo[4,5-b]pyridinium 3-oxide hexafluorophosphate

HBTU	2-(1H-benzotriazol-1-yl)-1,1,3,3-tetramethyluronium hexafluorophosphate
HCTU	2-(6-Chloro-1-H-benzotriazole-1-yl)-1,1,3,3-tetramethylaminium hexafluorophosphate
hr	hour
HMDS	Bis(trimethylsilyl)amine
HOBt	Hydroxybenzotriazole
HPLC	High performance liquid chromatography
HRMS	High resolution mass spectrometry
Hz	Hertz
IDCP	Iodine dicollidine perchlorate
J	Coupling constant
k	Rate constant
K_B	Boltzmann constant
L	Litre
LDA	Lithium diisopropylamide
Lys, K	Lysine
m	Multiplet
min	Minute
MW	Microwave
NBS	*N*-Bromosuccinimide
NCS	*N*-Chlorosuccinimide
NIS	*N*-Iodosuccinimide
NMM	*N*-Methylmorpholine
NMR	Nuclear magnetic resonance (spectroscopy)
NOAC	Nitrile oxide alkyne cycloaddition
OBt	Oxybenzotriazole
PAM	4-(Hydroxymethyl)phenylacetamidomethyl-polystyrene
PCC	Pyridinium chlorochromate
PEG	Polyethylene glycol
Pet. ether	Petroleum ether, (40-60 ˚C)
pH	Logarithmic scale of concentration of hydronium ions
Phe, F	Phenylalanine
pMBHA	4-Methylbenzhydrylamine hydrochloride
ppm	Parts per million
ps	Polystyrene
PSS	Photostationary state
Py	Pyridine
PyAOP	(7-Azabenzotriazol-1-yloxy)tripyrrolidinophosphonium hexafluorophosphate

PyBOP	Benzotriazol-1-yl-oxytripyrrolidinophosphonium hexafluorophosphate
PyBrOP	Bromotripyrrolidinophosphonium hexafluorophosphate
R	Gas constant
RNA	Ribonucleic acid
s	singlet
S	Entropy
Ser, S	Serine
SPPS	Solid phase peptide synthesis
t	Time
t	triplet
T	Temperature
r.t.	Room temperature
TATU	2-(7-Azabenzotriazole-1-yl)-1,1,3,3-tetramethyluronium tetrafluoroborate
TBAHS	Tetrabutylammonium hydrogen sulfate
TBDPS	*tert*-Butyldiphenylsilyl
TBTU	O-(Benzotriazol-1-yl)-N,N,N′,N′-tetramethyluronium tetrafluoroborate
TFA	Trifluoroacetic acid
Thr, T	Threonine
THF	Tetrahydrofuran
TIS	Triisopropylsilane
TLC	Thin-layer chromatography
$TMSN_3$	Trimethylsilyl azide
TPAP	Tetrapropylammonium perruthenate
UV/Vis	Ultraviolet/visible
W	Watts

1. Introduction

1.1 Molecular switches

1.1.1 Introduction

The 2016 Nobel award in chemistry to Jean-Pierre Sauvage, Sir J. Fraser Stoddart and Bernard L. Feringa for the design and synthesis of molecular machines demonstrates the importance of molecules that can exhibit a mechanical response to external stimuli. Molecular switches can be considered as simple machines in that they are compounds that can reversibly respond to external stimuli.[1] The stimuli can be virtually anything *e.g*. changes in pH, temperature, the concentration of recognised guest molecules or ions, or light of a specific wavelength.[2,3] Common responses include changes in colour, fluorescence behaviour, ion or molecule capture or release, and changes in molecular geometry or dipole moment.[4] The scope for utility is massive and molecular switches have commonly been employed in molecular recognition,[4] studies of drug delivery systems,[5] data storage and nanotechnology.[6]

In one example, Harai *et al*. created a pH probe where fluorescent output was controlled by the alteration of molecular shape in response to pH.[7] Above pH 9, there was no interaction between the pendant anthracene units of the sensor **1**, in figure 1, and monomer emission was observed. Upon lowering of the pH, the structure bent allowing interaction between the anthracene centres, causing an excimer emission to be observed.

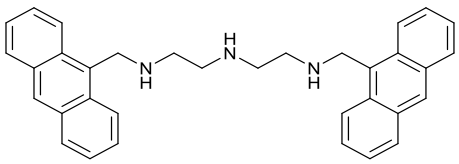

1

Figure 1: Fluorescence responsive pH sensitive molecular switch.[7]

This introduction will review the incorporation of molecular switches to biomolecules including carbohydrates, nucleic acids and peptides, and the utility of such derivatisation in controlling their function.

1.1.2 Biomolecular switches

The structure of biomolecules is intrinsic to their function. The change of a single amino acid can drastically affect the folding of an entire protein, rendering it inactive. Similarly, the change of a single nucleobase can prevent DNA helix formation, making it defunct. The interaction between biomolecules and their substrates is highly specific.[8] Often the lock and key analogy is used to demonstrate the way that biomolecules respond to the specific characteristics of a given substrate. The three dimensional shape, layout and available functionality control interactions between the guest molecule and the host biomolecule, as depicted in figure 2.

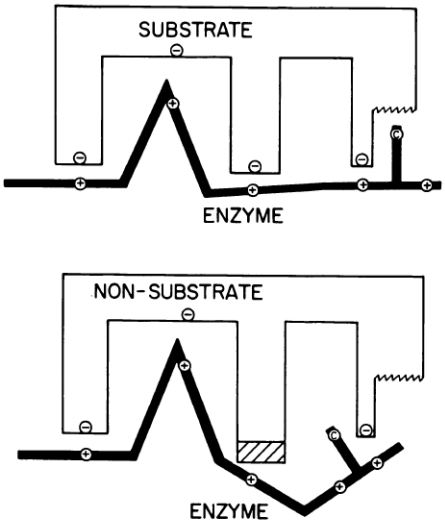

Figure 2: An illustration of the specificity of biomolecular interactions, so-called 'lock and key'.[8]

The design of biomolecular switches tend to be based around units which show, upon external stimulation, significant changes in shape and dipole moment. The choice of stimulus is also an important factor. It is preferable that external stimuli affect switching

on demand but otherwise do not interfere with the biomolecule or its environment. The class of switches that best demonstrates these criteria is photoswitches.

1.1.3 Photoswitches

Photoswitching is particularly attractive for biomolecular applications due to the possibility for non-invasive, controlled triggering and inertness to biological conditions. That is to say, that apart from those specialised to do so, cells are generally unaffected by light irradiation and have moderate permeability to lower energy wavelengths, i.e. between 650 nm and 950 nm.[9] Light also gives excellent switching control in terms of its near instantaneous turning on and off.

The vitamin A derivative retinal is a naturally occurring photoswitch. It is a key molecule in translating light into vision in the human eye. The mechanism of this translation is based upon geometric isomerisation of an extended unsaturated hydrocarbon chain. As shown in figure 3, upon irradiation the single *cis* bond (**2**) isomerises to give the all *trans* form (**3**). Only when in the all *trans* form can the retinal take part in the metabolic pathway which results in the interpretation of light as vision.[10] The wavelength of retinal absorption is dependent on the binding sites of the different opsin proteins, and the on pH of the environment.

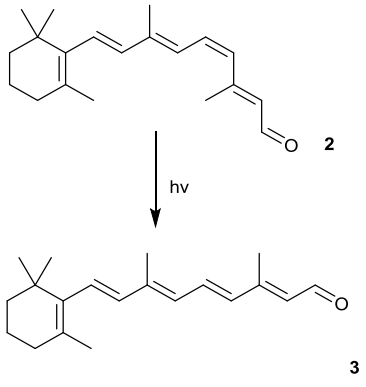

Figure 3: Photoswitching of Retinal.

Spiropyrans, diarylethenes, and azobenzenes are three leading classes of photoswitch. Each has a different response to light stimuli, which in turn has led to different potential applications.

In the early 1950s Fischer and Hirshberg observed that following irradiation with light the C-O bond of spiropyrans could be reversibly broken and reformed.[11] Irradiation in the UV region, typically between 270-380 nm, triggers ring opening, with the reverse process occurring thermally or with irradiation in the visible region, typically between 500-600 nm.[10] For example, the propanol functionalised spiropyran, **4**, shown in figure 4, was opened to its merocyanine form, **5,** with irradiation at 312 nm; it reverted to the ring closed form following irradiation at 590 nm.[12] It was already known that spiropyran-merocyanine isomerisation could occur in both directions thermally, but the observation that it could be photochemically induced caused a rapid growth in the photochromic application of spiropyran containing molecules.

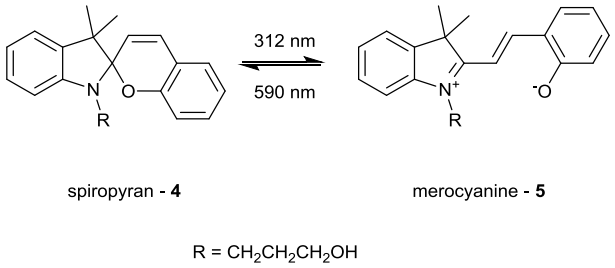

Figure 4: Photoisomerisation between a spiropyran (left) and a merocyanine (right).[12]

The ring closed (spiropyran) and ring open (merocyanine) forms exhibit very different chemical and physical properties. Isomerisation usually coincides with a striking colour change, from the colourless spiroform to the deep blue of the open form. Merocyanines exhibit emission between 600-700 nm whilst spiropyrans display no emission.[13] Geometrically, the merocyanine form is elongated compared to the spiroform.[13] A notable shift in dipole moment also occurs upon photoisomerisation, typically going from 4-6 D in the spiropyran to 14-16 D in the merocyanine form. The merocyanine has a single conjugated system, in contrast the spiroform has two conjugated systems separated at the central, spiro carbon atom.

These dramatic, yet controllable property changes have facilitated a wide range of applications. The incorporation of spiropyran units within photochromic materials is

extremely common. They offer smart materials a range of interesting property changes upon isomersiation, including changes in structure,[14] solubility,[15] colour and spectroscopic behaviour *e.g.* fluorescence.[16] Applications include controlled release of guest molecules/ions[17], visualisation of stress[14,18] and photoresponsive surfaces.[19] Spiropyrans are especially popular switches for fluorescent imaging.[20,21] They have also been used for ion detection as the merocyanine form strongly coordinates to metals ions, particularly through the phenolate oxygen atom, whereas the spiropyran form demonstrates little coordination potential.[22-24]

There are many applications of spiropyran photoswitching in biological settings, for example, as fluorescent imaging probes,[25,26] with the greatest interest being in peptide and protein chemistry.[27,28] The functionalisation of peptides with spiropyrans has been particularly successful in facilitating control of tertiary structure. In one example Lenci *et al*. show that spiropyran-merocyanine, **5↔6**, switching of the modified polyglutamic acid, shown in figure 5, allows turning on and off peptide helical formation.[29,30] Inouye *et al.* also demonstrated photocontrol of peptide helix formation through incorporation of spiropyran units into the peptide chain.[30] Marriott *et al*. have demonstrated that modified spiropyrans can be used to control activity in regulatory proteins. In the ring closed spiropryan form the peptide retains its native activity but the dipolar character of the merocyanine form actively inhibits the function of the protein.[31]

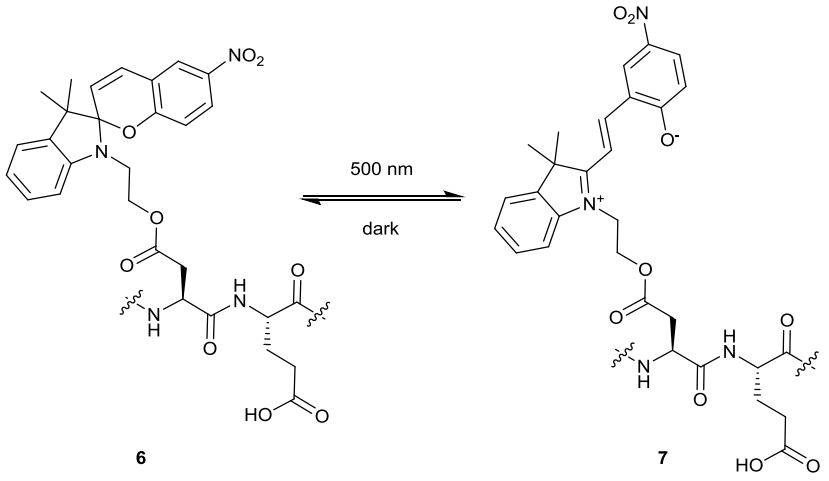

Figure 5: A spiropyran modified polyglutamic acid used to study photo-controlled folding.[29]

Diarylethenes are more recent additions than spiropryans or azobenzenes to the photoswitching family.[32] They share many characteristics with spiropryans. Photoisomerisation, centring upon the opening and closing of a 6-membered ring, as shown for **8↔9** in figure 6, coincides with changes in absorption and other physical

properties of the molecules. The nature of the substituent on the diarylethene is especially important to ensure stability of the ring closed form. Generally, heterocyclic groups are incorporated, particularly thiophenes, and most examples incorporate methyl groups at the 2-positon to avoid oxidation of the central ring.[33,34] Geometrically, the changes induced by photoisomerisation are modest, but significant changes are noted between the absorption spectra of the two forms. The ring open form usually absorbs between 200-350 nm, with the ring-closed form absorbing at around 600 nm. It should be noted that these values may vary significantly depending upon the identity of the aromatic rings and the nature and pattern of their substituents. One drawback of these molecules is a low quantum yield of isomerisation.[35]

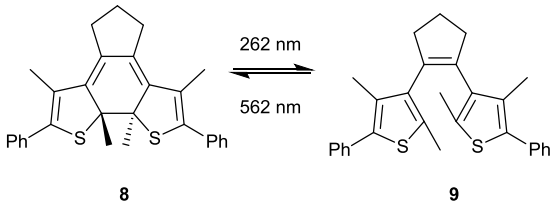

8 **9**

Figure 6: Photoisomerisation between the two forms of a diarylethene.[35]

Diarylethenes differ from many other photoswitches in two major ways: firstly, both forms can exhibit long-term stability, meaning both directions of isomerisation can only be induced by light. Secondly, photoisomerisation does not cause major geometrical/structural changes.[36] These features have led to applications as optical memory devices as photoswitching at a particular wavelength allows for non-destructive reading of optical data.[37] For example, targeted photoswitching was used to write a message on a surface functionalised with a diarylethene based film. Irie *et al*. could observe the image visually and through the change in IR absorbance for the two different forms, as shown in figure 7.[38] Diarylethenes are also attractive for incorporation into materials where photoisomerisation triggered changes in magnetism,[39] or in electronic conductivity,[40] or in liquid crystal properties[41] is desirable.

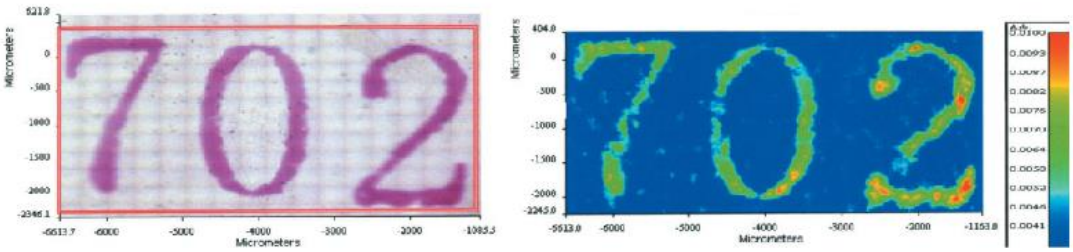

Figure 7:Visual (left) and IR (right) images of a message written into a diarylethene containing photochromic film.[38]

Due to the modest changes in shape and dipole moment between the two isomers relatively few biomolecular applications have been reported for diarylethene switches. In one example, a two-part inhibitor of human carbonic anhydrase I designed around a diarylethene core, figure 8,[42] was shown in the open form, **10**, to be ineffective: in this form it is understood that it was not possible for the two required inhibiting moieties to fit into the active site of the target enzyme. However, upon photoswitching the topology of the molecule changed sufficiently and the ring closed form, **11**, fitted the active site, causing enzyme activity to be switched off.

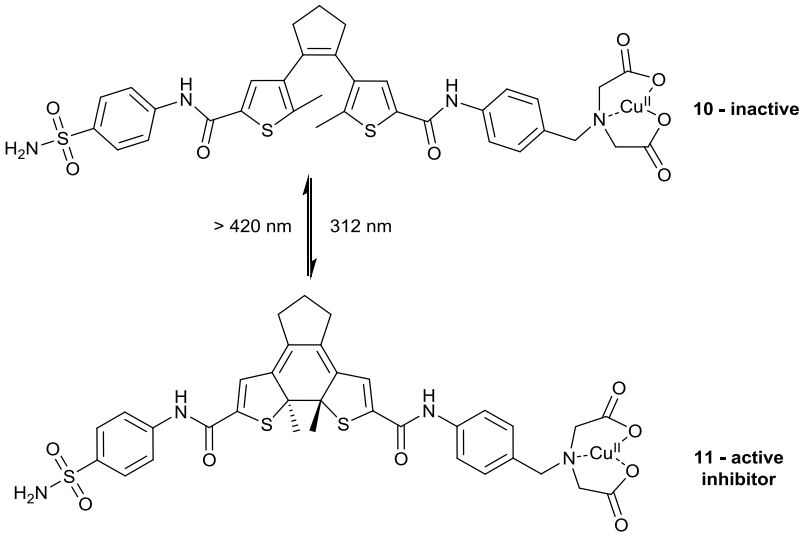

Figure 8: Two part human carbonic anhydrase I inhibitor based around a diarylethene.[42]

Diarylethene switching has also been used to execute light controlled paralysis in simple organisms. It is believed that the electron accepting ability of the closed system

facilitates a disruption of the metabolic pathways. The open ring form does not affect the organism.[43]

The only examples of the incorporation of diarylethene units directly into biomolecules are Singer and Jäschke's examples of nucleoside derivatives **12↔13**, where the nucleobase was substituted by a diarylethene unit, as shown in figure 9.[44] It was proposed that this approach offered a potential opportunity to introduce a photoswitch into the highly structured DNA and RNA systems with minimal disruption to their global structure.

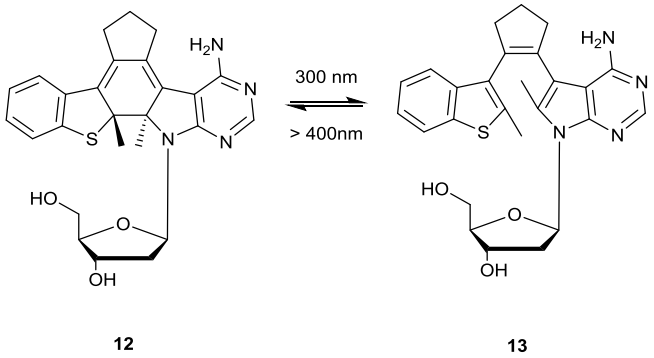

Figure 9: Nucleoside derivative incorporating a photoswitchable diarylethene.[44]

1.2 Azobenzene

Azobenzenes may be photoisomerised around the azo double bond linkage, going from the thermodynamically more stable *trans* form, **14**, to the *cis* form, **15**, as shown in figure 10. Unlike spiropyrans and diarylethenes, there is no colour change upon isomerisation and azobenzenes retain their characteristic orange colour in both forms. Subtle differences are observed in the absorption and emission profile of the two forms; a decrease in the intensity of the peak at ~300 nm and an increase in intensity of the peak at ~450 nm is observed in going from the *trans* form to *cis* form. However, photoisomeriation causes significant changes in shape and dipole moment of azobenzene. The *trans* form is planar and non-polar whilst the *cis* form exhibits a significant dipole moment (~3 D). The *trans* form of the parent molecule is ≈ 42-50 kJ mol^{-1} more stable than the *cis* form and in the dark the *trans* form dominates approaching 100%.[45] The energy barrier for *trans* to *cis* conversion in the parent molecule is around

100 kJ mol^{-1}. Thermal relaxation generally has a half-life in the order of days, but is dependent on factors such as solvent, temperature and substitution.

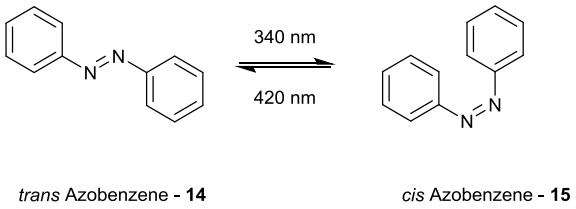

Figure 10: Photoisomerisation of azobenzene

1.2.1 Azobenzene isomerisation mechanism.

The mechanism of azobenzene photoisomerisation has long been a topic of debate with several routes proposed and many reviews published on the subject.[46-50] The main proposals are: inversion, rotation, concerted inversion, and inversion assisted rotation, as summarised in figure 11. Rotational theories suggest that the N=N double bond partially breaks, allowing free rotation around the N-N bond. In contrast, the inversion mechanism maintains the N=N bond and has one of the C-N=N bond angles increasing to 180˚ in the transition state; the concerted inversion route has both C-N=N bonds angles going to 180˚. The inversion assisted rotation mechanism has both twisting of the N-N and an increase in the size of the C-N-N bond angles.

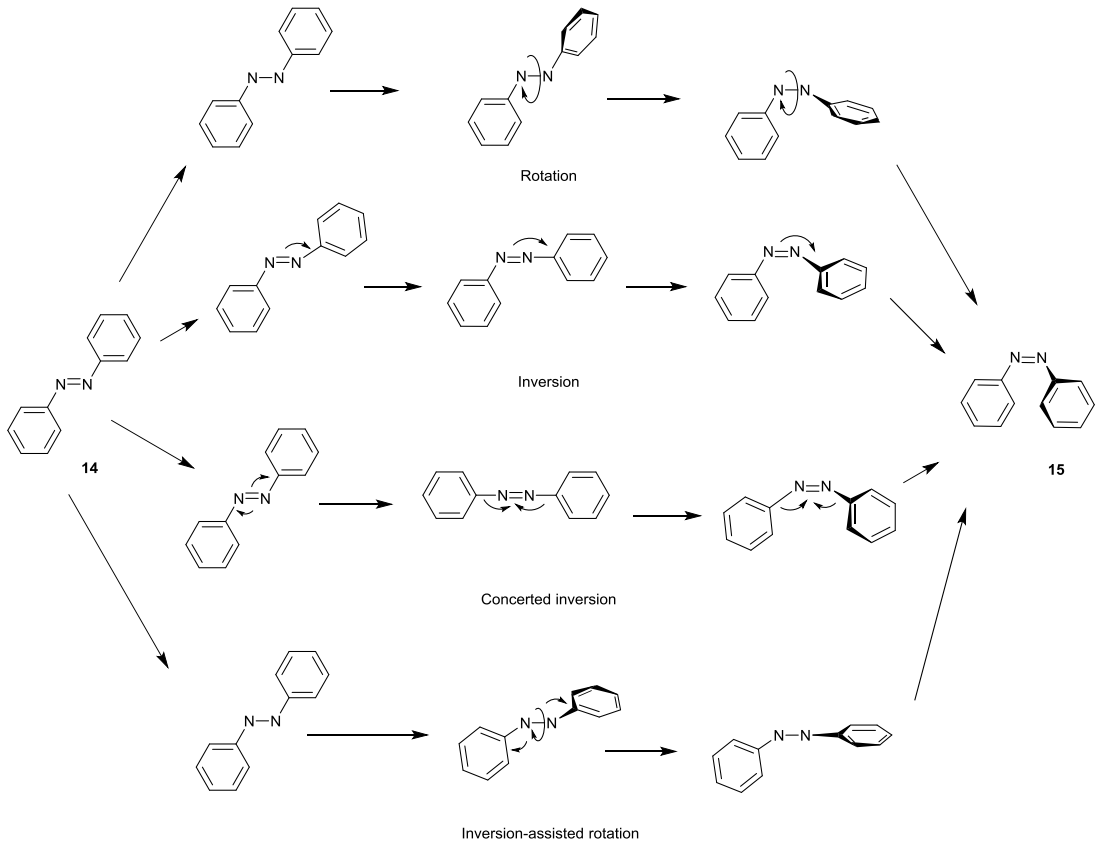

Figure 11: Mechanistic routes proposed for azobenzene photoisomerisation[51]

The absorption profile of the ground state *trans* azobenzene has two well defined bands with the first, and most intense, usually appearing around 310-330 nm, the second, a weaker band usually appears around 440-460 nm, as shown for the parent azobenzene in figure 12 (red trace). The first absorbance corresponds to the symmetry allowed $\pi \rightarrow \pi^*$ transition, and the later band to a symmetry forbidden $n \rightarrow \pi^*$ transition.[52] As a forbidden transition the intensity of the $n \rightarrow \pi^*$ transition will always be lower than that of the $\pi \rightarrow \pi^*$ transition. As the percentage of *cis* form increases the absorption of the $\pi \rightarrow \pi^*$ transition becomes weaker and that of the $n \rightarrow \pi^*$ transition becomes stronger. Data for the parent azobenzene going from the *trans* dominating red trace (t = 0) to the *cis* dominating yellow trace (t = 60 min), can be seen in the figure 12. The $\pi \rightarrow \pi^*$ absorption represents the transition to the S2 ($\pi\pi^*$) energy state and the $n \rightarrow \pi^*$ to the S1 ($n\pi^*$) state.[53] Excitation to either state affords isomerisation in both directions.[54] Ultimately this means that whilst irradiation at 320 nm will favour conversion of the *trans* to *cis* it also facilitate the reverse process meaning complete conversion to one geometrical form is not possible, thus conversion to the *cis* form usually peaks at around

90%. Conversely irradiation at the $n \rightarrow \pi^*$ band, typically around 440 nm, will facilitate *cis* to *trans* conversion, commonly maximising around 80% conversion to the *trans* form.

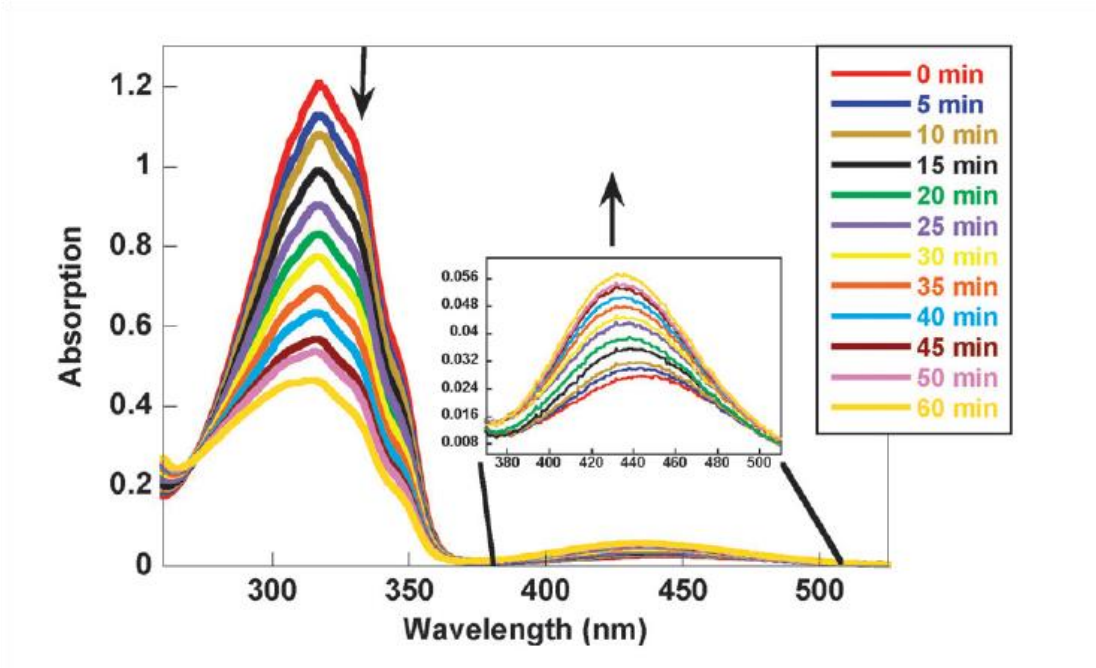

Figure 12: Absorption spectra of azobenzene following irradiation at 316 nm over a 60 min period.[51]

The quantum yield of the $n \rightarrow \pi^*$ is more efficient than the $\pi \rightarrow \pi^*$ transition for both the *trans* to *cis*, and the *cis* to *trans* conversions.[51] The $\pi \rightarrow \pi^*$ transition involves the cleavage of the azo bond to a single N-N bond, making it compatible with a rotational mechanism, whereas the $n \rightarrow \pi^*$ transition is compatible with an inversion pathway.[55] Recent mechanistic studies favour the rotational or inversion assisted rotational pathways as the primary mechanisms,[56-59] with inversion being a possible, but energetically unfavourable route.[60] It is significant that the quantum yield does not equal 1 for either conversion as it infers that more than one isomerisation pathway is in operation

Generally speaking with more polar solvents the quantum yield for the *trans* to *cis* conversion is higher. In contrast, the quantum efficiency of the reverse process is optimal in non-polar solvents.[51]

The *trans* to *cis* conversion is thermally independent and occurs solely upon irradiation. The *cis* to *trans* transformation can be affected thermally or upon photo-activation.

Quantum efficiency is reduced at lower temperatures for isomerisation under both passive relaxation and active irradiation.[61,62]

Photoisomerisation of functionalised azobenzene derivatives is affected by several factors, including: irradiation wavelength, solvent, temperature and substituent nature and pattern. Thus by targeting appropriate experimental conditions a given azobenzene derivative can be isomerised to favour one geometric form. Practically, this is usually achieved by irradiating at a wavelength which has maximum absorption by the *trans*-form and minimal absorption by the *cis*-form or the reverse.

Azobenzenes have been traditionally categorised into three classes, azobenzenes, aminoazobenzenes and pseudostilbenes, based upon the nature of their substituents, as shown in figure 13.

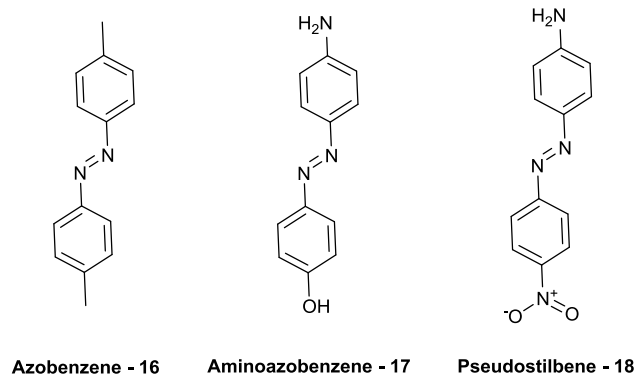

Figure 13: Examples of the three different classes of azobenzenes: azobenzenes, aminoazobenzenes and pseudostilbenes

Azobenzenes, **16**, comprises those structures that retain the absorption characteristics of the parent molecule. Typical substituents for this group are alkyl, aryl, amide, carbonyl and ester. The UV/Vis spectra for this family appear as two well defined bands: a strong $\pi \rightarrow \pi^*$ absorption and a weak $n \rightarrow \pi^*$ band. Similar quantum yields are observed for both directions of isomerisation. On the other hand they exhibit quicker *cis* to *trans* thermal relaxation when compared to that of the parent molecule. This is especially the case for those molecules with multiple substituents and those bearing electron withdrawing groups.[63]

Aminoazobenzenes, **17**, typically have strong electron donating groups, such as amino or hydroxyl, *ortho* or *para* to the azo group. As the number of electron donating groups increases the UV spectra shows a shift of the $\pi \rightarrow \pi^*$ band to a higher wavelength, consequently, the $\pi \rightarrow \pi^*$ and $n \rightarrow \pi^*$ absorption bands become closer.[64] The shift in absorbance coincides with an increase in quantum yield. Electron rich azobenzenes usually demonstrate significantly quicker thermal relaxation than the parent molecule. They have been used by industry as dyes due to their bright colour, for example 'Aniline Yellow', [4-(phenyldiazenyl)aniline], **19**, is a commonly used brightly coloured yellow dye, figure 14.

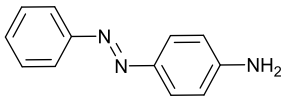

19

Figure 14: Aniline Yellow, a common commercial dye

The **pseudostilbene** class, **18**, are often referred to as push-pull systems as they contain electron donating groups on one ring and electron withdrawing groups on the other. Typically both the substituents are *para* to the azo group. The effect of such substituents is the creation of a significant dipole moment, up to 9.8 D in extreme examples, such as the pseudostilbene **18** in figure 13.[63] Like aminoazobenzenes, pseudostilbenes are often strongly coloured. The electronic imbalance of pseudostilbenes results in a shift of the absorption band of the $\pi \rightarrow \pi^*$ transition to a longer wavelength, to the region typically occupied by the $n \rightarrow \pi^*$ transition.[65] Thermal relaxation rates for the pseudostilbene class are typically extremely fast; this can make the determination of quantum yields difficult. However, where quantum yields have been measured they are often lower than those observed for the parent molecule.

1.2.2 Isomerisation effects

The primary changes observed upon photoisomerisation of the *trans*-form to the *cis*-form are in the geometry and in the dipole moments of the molecules. Whilst for azobenzene the change from zero dipole for the *trans*-form to ~3 D for the *cis*-form is

significant, it is generally the geometric changes that are the 'mechanics' behind the switching operation, figure 15. The *trans*-form is a planar molecule, with recent work identifying it as having C_{2h} symmetry.[66,67] The photoisomerised *cis* form has a bent azo linkage and a twist of one of the aryl rings to around 55˚ out of the plane of the azo bond.[67] These distinct orientations result in considerable differences in distance between, and relative orientation of, substituents on the individual phenyl rings of the *cis* and *trans* isomers of substituted azobenzenes. The extent of such changes for any given molecule can be extrapolated from the observation that the distance between the carbons atoms *para* to the azo linkage (end to end distance) differ by 3.5 Å upon isomersation of the *trans* form to the *cis* form of azobenzene.[68]

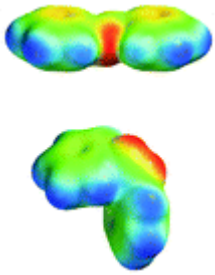

14 - *trans*-azobenzene

15 - *cis*-azobenzene

Figure 15: Electrostatic potential maps of both geometrical forms of azobenzene (positive = red and negative = blue).[69]

1.2.3 Application of azobenzene photoswitching in biological materials and in biomolecular settings

1.2.3.1 Carbohydrate substrates

Azobenzene-carbohydrate conjugates can broadly be separated into those where properties of the carbohydrate are being exploited in modification of the azobenzene unit or those that employ an azobenzene unit to control carbohydrate function. In the case of the former different sugars have been appended to azobenzenes to create desired spectroscopic responses. For example, Shinkai *et al*. created two different amphiphilic azobenzene glycosides, varying only in the choice of glucose or galactose heads.[70] When compressed into films, both molecules experienced shifts in their UV-Vis absorption

behaviour with respect to the uncompressed films, with the glucose form red shifting and the galactose adduct blue shifting.

A second series of amphiphilic conjugates synthesised by Laurent *et al*., e.g. **20**, figure 16, were found to differ in their ability to pack as liquid crystals.[71] It was found that a change in the orientation of a single hydroxyl group of the sugar resulted in significant change to the packing properties of the azobenzene-sugar adducts.

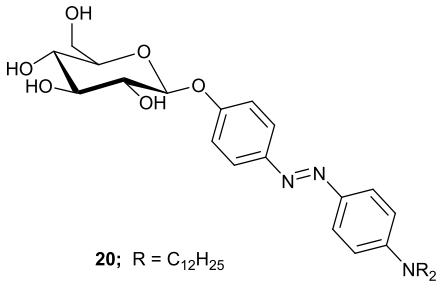

20; R = $C_{12}H_{25}$

Figure 16: Example of an amphiphilic carbohydrate azobenzene conjugate synthesised by Laurent et al.[71]

'Methyl Yellow' is one example of an azobenzene dye about which there are long term concerns about toxicity. This problem was addressed by Valldeperas *et al*.[72] through its functionalisation with a simple monosaccharide. The resulting glucose adduct, **21** in figure 17, had a much reduced toxicity with respect to its parent.[73]

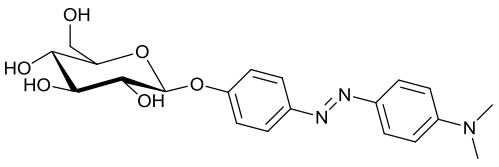

21

Figure 17: 'Methyl Yellow' functionalised with glucose.[73]

Carbohydrate based amphiphilic fluorosurfactants, exemplified by compound **22** in figure 18, have exploited azobenzenes to give control of surface tension and antibacterial properties.[74] Photoisomerisation altered the efficiency of micelle formation, which in

turn affected the solubility of the compound and the growth *Staphylococcus aureus* bacteria.

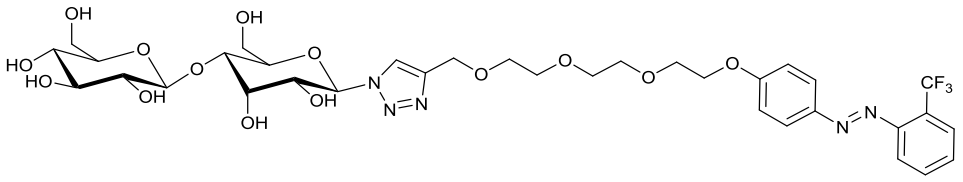

22

Figure 18: Photoswitchable fluorosurfactants with controllable surface tension and antibacterial properties.[74]

The rigid structure of saccharides makes it difficult to directly alter the geometry of individual sugar units. However, azobenzene photoisomerisation offers the potential to change the relative orientation of saccharide units and so to control their interactions with other molecules. Srinivas et al. have demonstrated this by examining the interaction between azobenzene bearing glycoclusters and lectins.[75] They were able to observe that both the *trans* and the *cis* forms of glycocluster **23** had a higher binding affinity for the lectin than the lone saccharide unit, figure 19. Of the two glycocluster forms the *cis* had the highest lectin binding affinity. It was proposed that lectin binding affinity was influenced by the geometry of the azobenzene core, the valence of the glycoclusters, and by the relative orientation of the saccharide units.

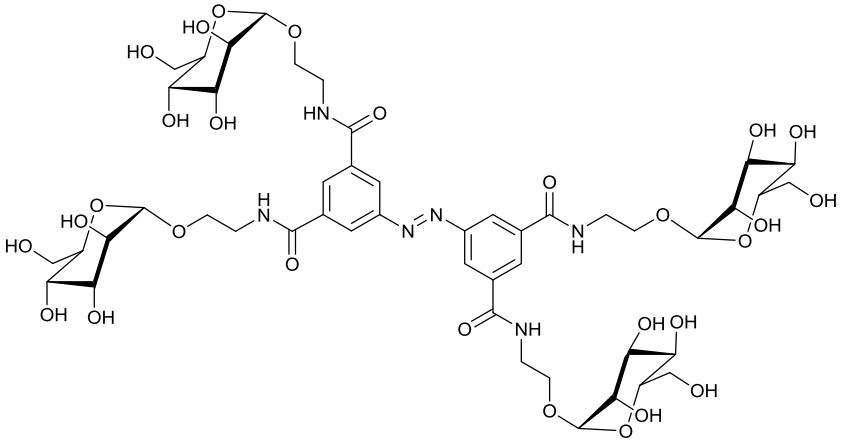

23

Figure 19: Azobenznene scaffolded glycoclusters designed to study saccharide-lectin interactions.[75]

Surface bound carbohydrate-azobenzene adducts have been used to explore potential photocontrol of bacterial adhesion to sugar units.[76] An azobenzene unit has been used to functionalise a surface with mannose. When in the *trans* form the saccharide was capable of interacting with the bacteria. When in the *cis* form no adhesion occurred, as summarised in figure 20. The same group have also demonstrated the photo-control of bacterial adhesion to the surface of a human cell.[77]

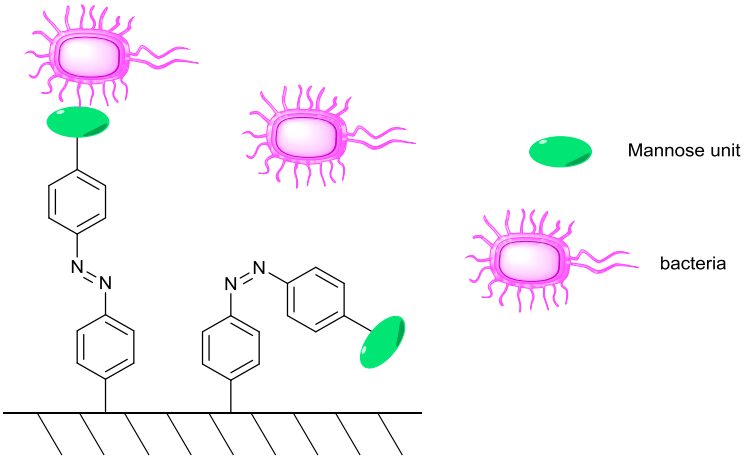

Figure 20: Photocontrol of bacteria surface adhesion.[76]

There have also been applications of azobenzene carbohydrate conjugates in the sensor field. It has been shown that azobenzenes can interact with cyclodextrins, fitting comfortably in the ring cavity.[78] Toda *et al*. exploited this host-guest relationship to create a molecular recognition system.[79] The azobenzene pH indicator Methyl Red was guested into a cyclodextrin ring and so protected from protonation by the bulk medium. Upon addition of a 'suitable' organic molecule, the azobenzene was displaced and the Methyl Red became available for protonation, causing the system to go from yellow to red. Thus, the system acted like a sensor for the 'suitable' organic compound.

With the appropriate linkers, dimeric systems can be created between cyclodextrins covalently modified with azobenzene moieties. The azobenzene unit of each cyclodextrin sits into the cavity of the other, as in figure 21. Described as 'pseudorotaxanes', the dimeric structures disrupt upon photoisomerisation, as the 'guest-host' interaction is unfavourable for the *cis*-azobenzene.[80]

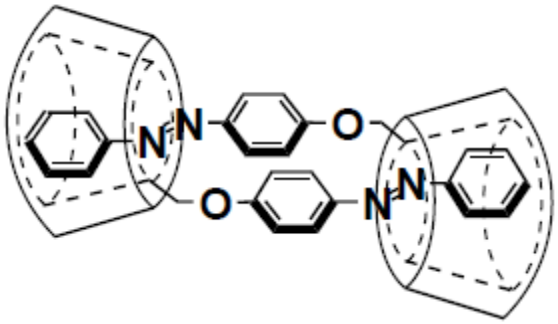

Figure 21: Host-guest type azobenzene-cyclodextrin dimers.[80]

1.2.3.2 Peptides

Functionalisation of peptides with azobenzene units is perhaps the best studied class of biomolecule photoswitch conjugates. This is mostly likely due to the great diversity of peptides and proteins and their important biochemical roles. The wide variety of amino acid sidechain functionalities facilitates targeted, or site specific functionalisation. This is in stark contrast to DNA with its limit of four nucleotide building blocks, or the chemically similar structures of carbohydrates. Secondary, tertiary and quaternary structure is of vital importance to peptide and protein function, and all of these could potentially be photochemically controlled by integration of an azobenzene unit into the biomolecule.

Functionalisation of peptides can be divided into side chain derivatisation and backbone modification. In early work side chain functionalisation was popular as it allowed for the modification of proteins from natural sources. For example, Riklin *et al.* demonstrated the attachment of several azobenzene units to the enzyme papain.[81] The azobenzene units were not regiospecifically introduced at the active site of the enzyme, rather any available lysine residues were functionalised. The derivatised protein, **24** in figure 22, maintained 80% of enzymatic activity when in the *trans* form; upon photoswitching to the *cis* form activity was reduced to 30%. Although somewhat 'simplistic' in approach, this experiment demonstrates that even without targeting a specific site, the structural and dipolar changes accompanying isomerisation of azobenzene units incorporated at the sidechains can have a significant influence on the bioactivity of the resultant protein.

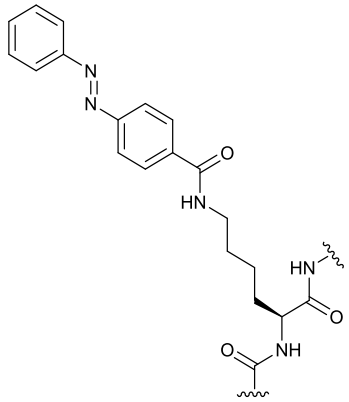

24

Figure 22: Section of papain incorporating an azobenzene functionality.[81]

With the advancement of sophisticated molecular modelling and of synthetic peptide chemistry it became possible to target the introduction of azobenzene units to specific sites within a protein. Amongst the most elegant examples is Kramer *et al.*'s functionalisation of a potassium channel.[82] An azobenzene unit is tethered near the mouth of the ion channel via reaction between the thiol group of a cysteine residue and the maleimide bearing azobenzene **25**. When in the *trans* form, the unit is positioned such that its ammonium functionality covers the opening of the channel. Electrostatic repulsion between the ammonium group and potassium ions effectively blocks the movement of potassium ions across the channel. When the azobenzene core is photoisomerised to the *cis* form the ammonium functionality is pulled away from the opening, allowing the flow of potassium ions, as summarised in figure 23. Further development of this work demonstrated that the azobenzene photoswitches could be used to control neurological activity. This approach has been successful in controlling anion and cation transportation[83,84] ultimately allowing for control of a variety of physiological responses[85,86]

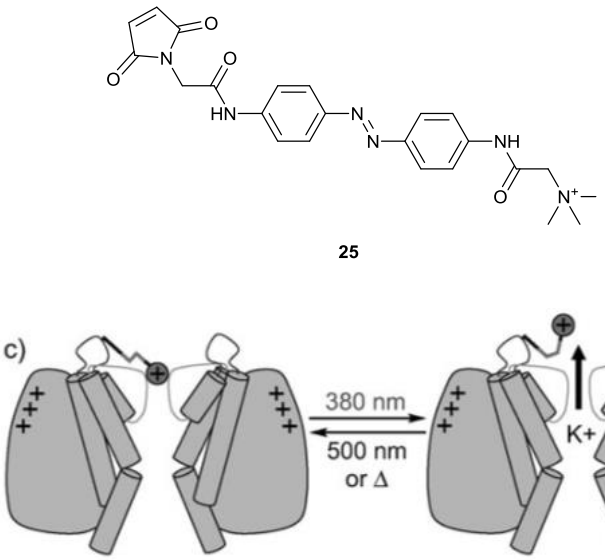

Figure 23: Azobenzene 'arm' developed by Kramer et al. for photo-control of potassium transportation.[82]

Azobenzenes have also been used as cross-linking units in the modification of peptides. The azobenzene unit is attached at two points on the protein through side chain modification and upon photoisomerisation the folding of the protein is disrupted. The distortion in the azobenzene shape is relayed to the peptide, generally the modified conformation is biochemically ineffective. Instructive papers by Woolley *et al*. demonstrate the effects of such cross linking, for example it can be seen that the number of helices in an azobenzene cross-linked protein can be controlled through photoisomerisation.[87,88] In another example Pingoud *et al*. introduced azobenzene cross-linkers to a restriction enzyme and upon photoisomerisation they saw up to 16 fold improvement in DNA cleavage.[89]

In terms of backbone functionalisation, cyclic peptides incorporating azobenzenes have been prepared from azobenzenes bearing both amine and carboxylic acid functionalities. These derivatives are suited to integration through standard peptide coupling. Cyclic peptides constructed with this unit demonstrate different conformational preferences depending on whether the azobenzene unit has *trans* or *cis* geometry.[90,91]

Azobenzenes with amine and carboxylic acid functional groups have also been used to generate synthetic peptides with an azobenzene within the backbone, for example **26**, figure 24, created by Renner *et al.;* [92] β-hairpin folding resulted when **26** was in *cis* form, whilst the *trans* form of same modified protein showed no intricate folding.

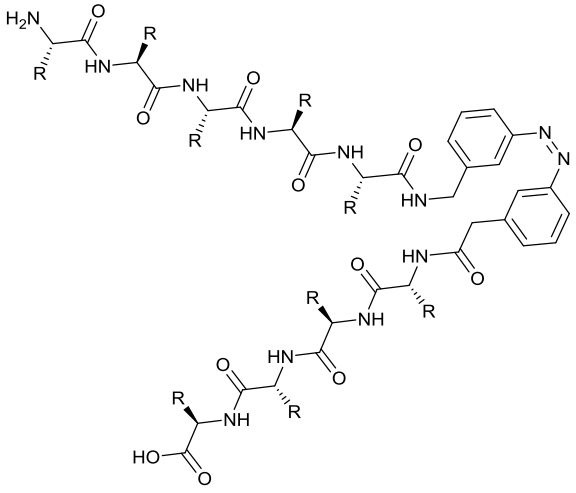

26 R = Typical amino acid sidechains

Figure 24: Peptide incorporating azobenzene: cis geometry mimics β-hairpin folding[92]

1.2.3.3 Nucleic acids

The DNA double helix is arguably the most recognisable of all biological structures; its sequence and shape are critical to its function; the effects of DNA sequence mutation, even the change of a single nucleotide can have dramatic consequences from evolutionary change to cancer causing diseases. Although RNA is more commonly found as a single chain, it still forms complex tertiary structures. These are often helices but folded structures akin to peptides also occur with features such as loops and hairpin folds.[93,94] Azobenzene photoswitches have been exploited in studying the structure and function of DNA and RNA in a manner similar to that demonstrated for peptide studies.

A range of azobenzene photoswitches capable of interacting non-covalently with DNA and RNA have been reported. Applications include control of conformation[95] or interstrand interaction: in one example a bis-1,8-naphthyridine appended azobenzene intercalated DNA as demonstrated in figure 25.[96] The changes to DNA structure resulting from photoisomerisation of the complex **27** can be monitored by changes in absorption at 260 nm and 330 nm.[97]

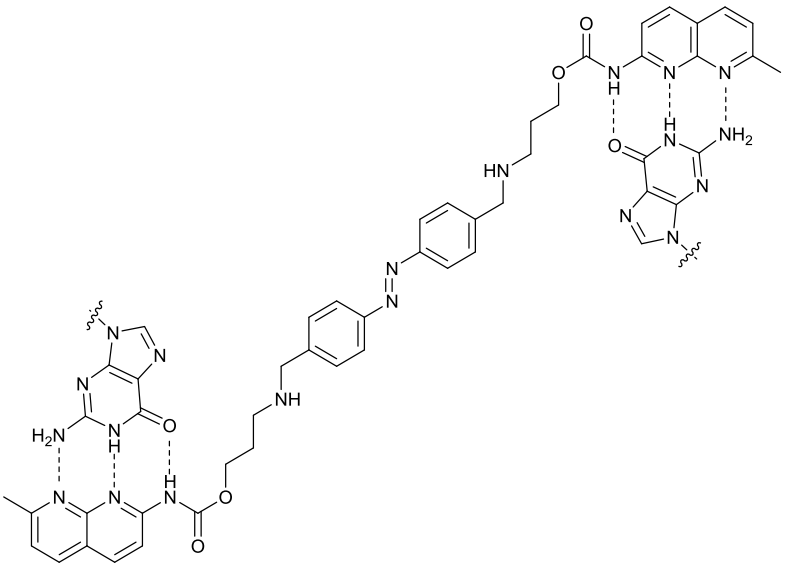

27

Figure 25: DNA intercalating bis-1,8-naphthyridine appended azobenzene developed by Nakatani et al.[96]

By the mid-1990s, DNA sequences incorporating azobenzene motifs capable being photoisomerised were synthesised, this gave greater control of DNA duplex formation/disruption. Introduction of a photoswitchable azobenzene into the DNA phosphate backbone has been demonstrated by Komiyama *et al*.[98] The modified DNA, **28**↔**29** shown in figure 26, retained its ability to form duplexes when the azobenzene was in the *trans* form, **28**, however upon photoisomerisation to the *cis* form, **29**, dissociation into single chains was observed. The switching was observed to be reversible. It was later shown azobenzene modification of the phosphate chain helps to stabilise duplex formation in the *trans* form through π-stacking interactions.[99] In another example, Liu and Sen demonstrated the integration of azobenzene units into a deoxyribozyme, *via* phosphate backbone modification.[100] The RNA cleaving DNA was found to be between 5-6 times more effective when the azobenzene unit was in the *cis* form than in the *trans* form.

The integration of azobenzene units into DNA has facilitated control over its interaction with cleavage enzymes. Komiyama *et al*. reported that Ribonuclease H was more effective at digesting modified DNA sequences when the introduced azobenzene had *cis* configuration compared to *trans* geometry.[101]

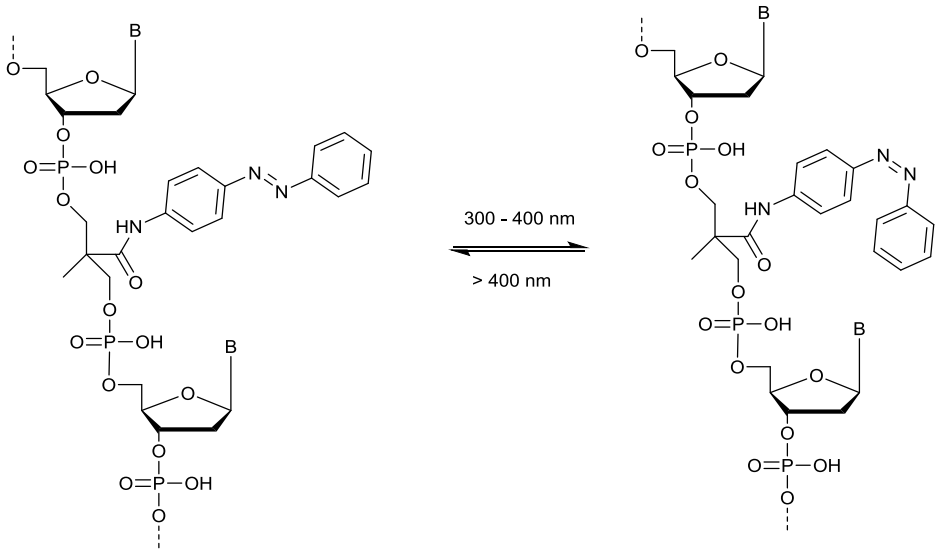

28 29

Figure 26: Photoisomerisation of an azobenzene unit integrated along the phosphodiester backbone of a DNA sequence used to control duplex formation.[98]

An interesting approach to incorporate azobenzene units into nucleic acids developed by Heckel *et al*. involved replacement of the nucleobase from a thymidine residue with an azobenzene unit, i.e. **30** in figure 27.[102] It was found that incorporating this building block into RNA disrupted duplex formation when the azobenzene unit was in the *cis* form. However, whilst in the *trans* form no disruption was observed.

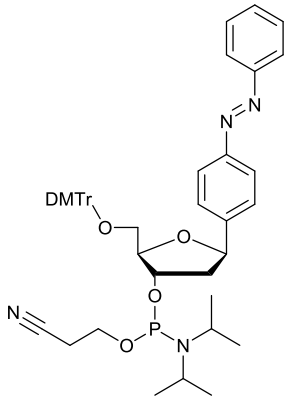

30

Figure 27: Azobenzene modified phosphoramidite building block used to study photocontrol of duplex formation in RNA.[102]

1.2.4 Introduction of azobenzenes to biomolecules

1.2.4.1 Introduction of azobenzenes to carbohydrates

1.2.4.1.1 Glyosidic bond formation with azobenzene acceptors

The majority of carbohydrate derivatives bearing azobenzene units have been synthesised through direct glycosidic bond formation between a suitably functionalised sugar and azobenzene units.[73,76]

Glycosidic bond formation has many attractions as a synthetic approach; the C-1 position can be specifically functionalised without the need for the extensive protecting group manipulation that is often be required for modification at other saccharide positions. For example, pentaacetates, such as **31**, can be reacted with a range of suitable glycosyl acceptors, for example **32-34**, in the presence of carefully selected activating agents to form a variety of glycosides, e.g. **35-37** as shown in scheme 1.

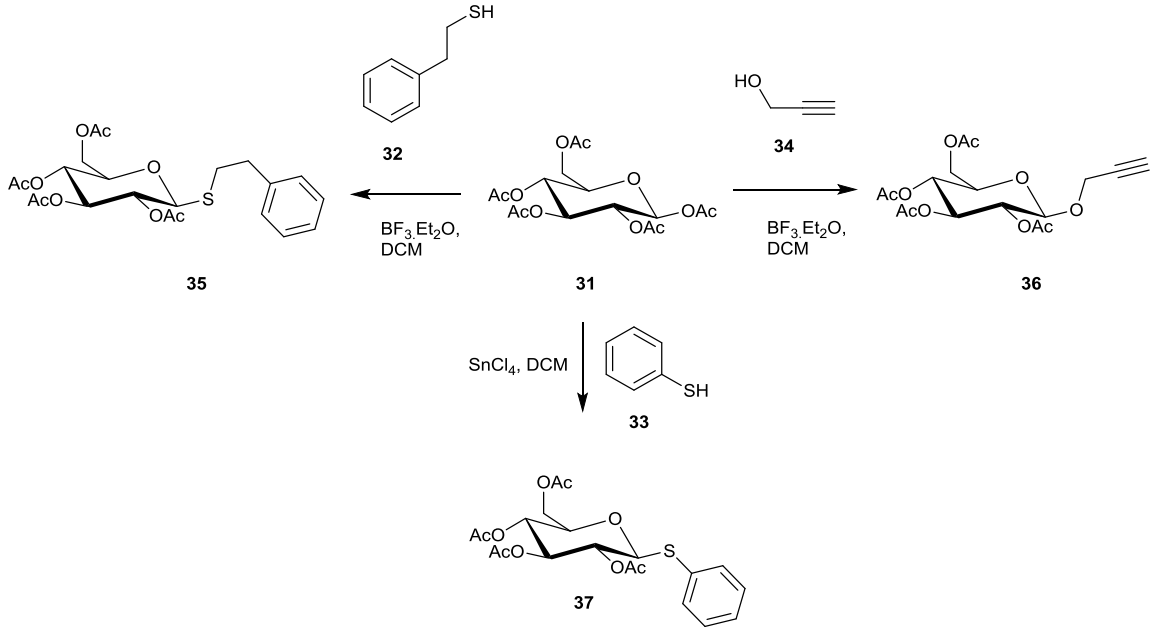

Scheme 1: Representative carbohydrate functionalisation through glyosidic bond formation

Glycosidic bond forming chemistry for the introduction of azobenzene units is well demonstrated by Lindhorst *et al.*, where the simple azobenzene-mannose adduct, **40**, is easily formed in a single step following reaction of 1-*O*-trichloroacetimidoyl-mannose,

38, with 4,4'-dihydroxylazobenzene, **39**, boron trifloride is the activating agent. The adduct was formed in 41 % yield, as shown in scheme 2.[103]

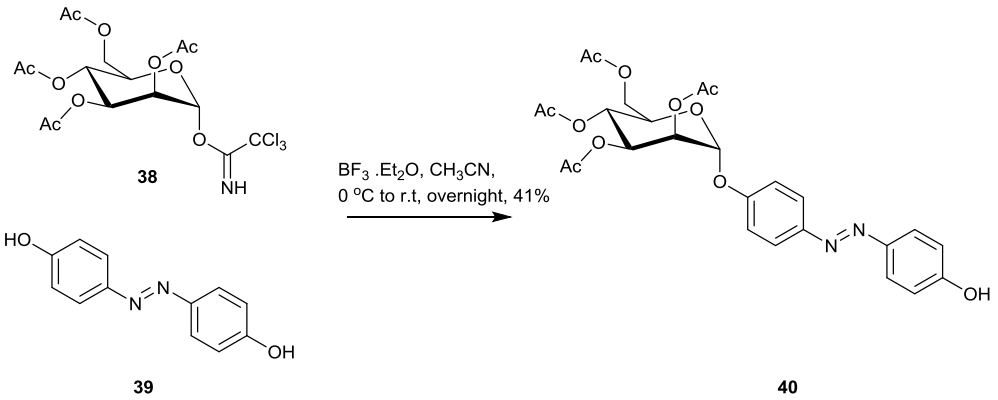

Scheme 2: Azobenzene-mannose conjugate constructed by glycosidic bond formation.[103]

The drawback to glycosidic bond formation is the lack of generality; success is highly dependent upon the choice of saccharide, the protecting groups, glycosidic acceptor and donor and the activation agent. For example, the success of the reaction between protected *N*-pentenyl glucose, **41**, and methanol, depends on the choice of protecting group. Benzyl groups activate the saccharide and the reaction works well. In contrast, protection with benzoyl groups deactivate the saccharide and the reaction fails to proceed.[104] The stereochemical outcome of the reaction is also sensitive to reaction conditions, with the β-isomer, **42**, favoured with iodine dicollidine perchlorate (IDCP) as the activating reagent, whereas activation by a combination of *N*-iodosuccinimide (NIS) and triethylsilyl trifluoromethanesulfonate (Et_3SiOTf) results in a dominance of the α-anomer, **43**, of the product, as shown in scheme 3.

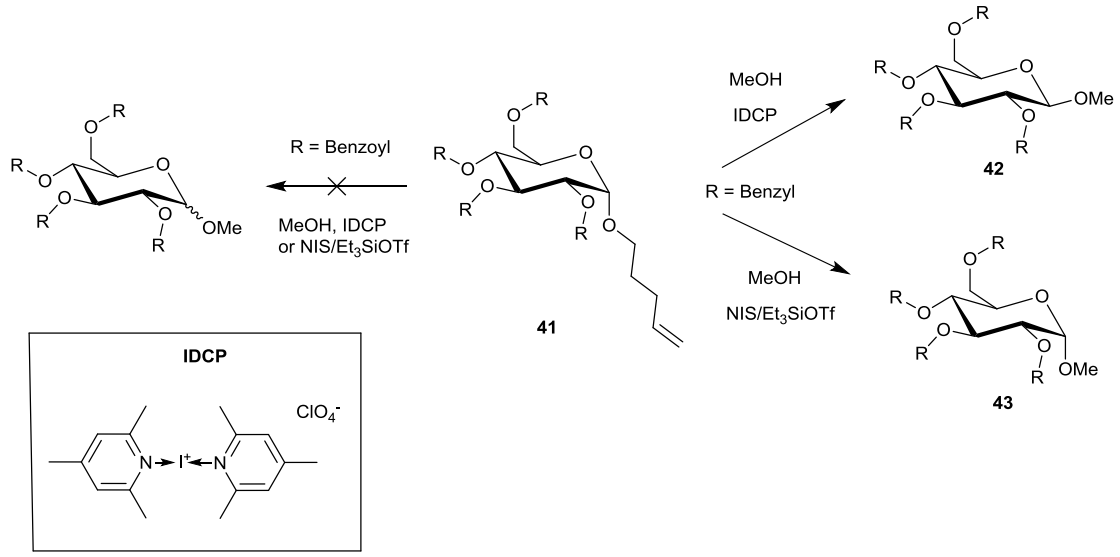

Scheme 3: Sensitivity of glycosylation chemistry to the nature of protecting groups and activating agents.

1.2.4.1.2 Manipulation of C-1 nitrophenyl glycosides

An alternative approach to the synthesis of azobenzene conjugates has involved manipulation of C-1 *p*-nitrophenyl substituted sugars. The nitro functionality of the aryl has served as a precursor to an amino group, which has subsequently been used either to link an azobenzene by condensation chemistry as in the formation of **52**[70,79] or to directly form an azo linkage, via an intermediate diazonium as in the formation of **50**, shown in scheme 4.[71,77] In this example, 4-nitrophenol, **45**, was initally coupled with a glucopyranosyl bromide to give the p-nitrophenyl glycoside **46**.[105] Reduction yielded the anilino glycoside, **47.**[71] Conversion to the diazonium salt, **48**, followed by reaction with phenol afforded the azobenzene-carbohydrate conjugate **50**, scheme 4 path A.[77] Alternatively the aminoglycoside, **47**, could be coupled to an azobenzene bearing carboxylic acid to form the amide linked conjugate. **52**, scheme 4 path B.[70]

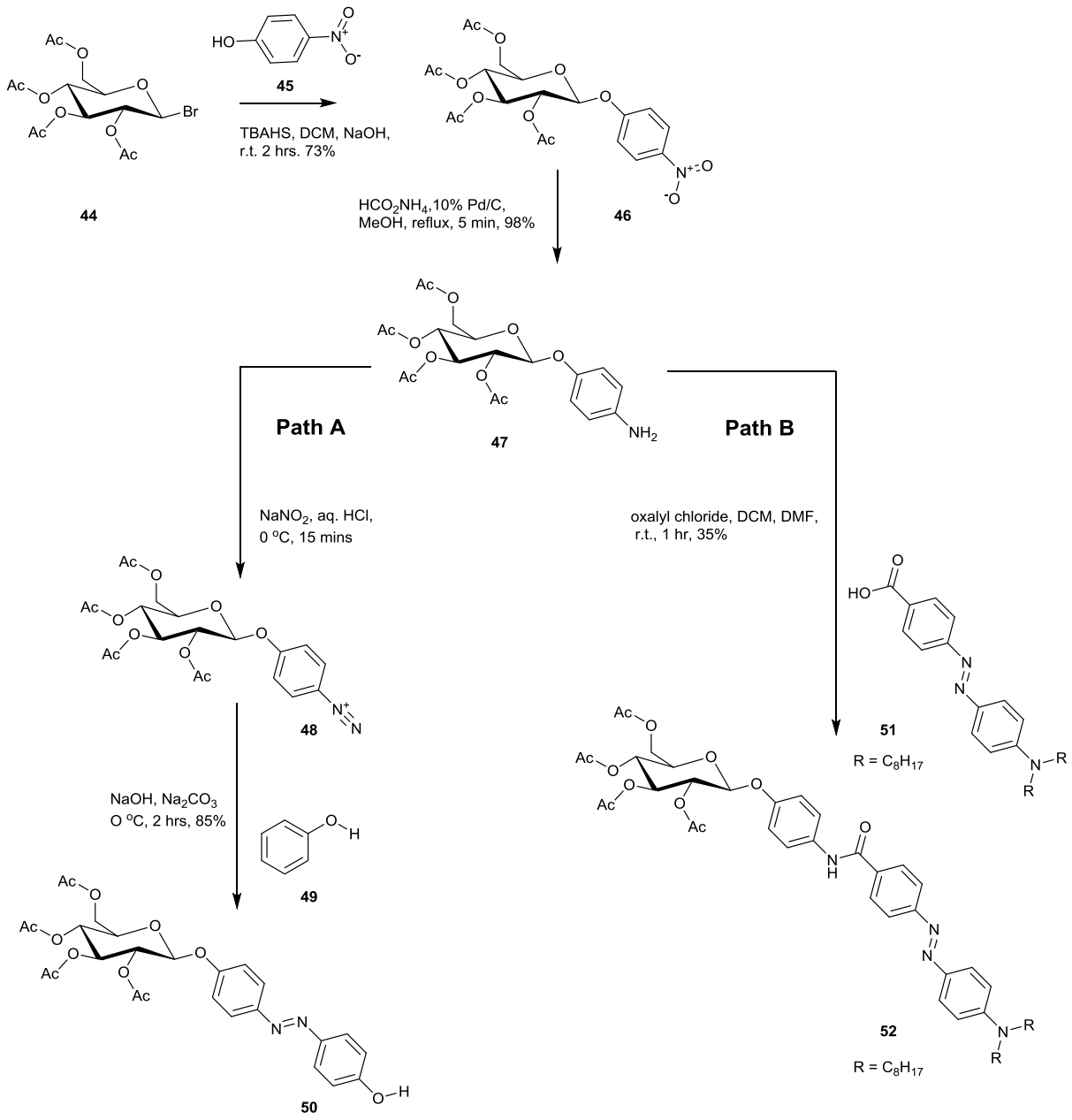

Scheme 4: Formation of azobenzene glycoside derivatives via C-1-p-nitrophenyl glycoside building block.

1.2.4.2 Introduction of azobenzenes to peptides

1.2.4.2.1 Azobenzene units introduced as backbone functionalities

Amide bond formation is the dominant chemistry of peptide functionalisation, particularly for building functionality into the backbone. Therefore, the formation of azobenzenes which bear either, or, both amino or carboxylic acid groups are highly

desirable. One attractive example is 3-[(3-*N*-Fmoc-aminomethyl)phenylazo]phenylacetic acid, **55**, synthesised by Renner *et al*., from Fmoc protected 3-aminobenzylamine, **53** and nitrosophenylacetic acid, **54**, through a Mills reaction, shown in scheme 5.[92] With Fmoc protection, this derivative is an ideal candidate for both manual and automated solid phase peptide synthesis.

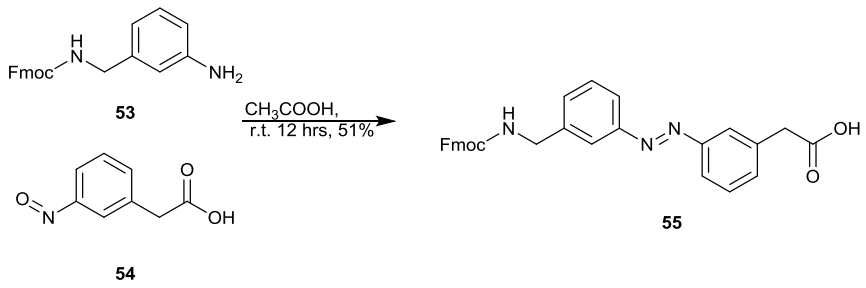

Scheme 5: Synthesis of 3-[(3-N-Fmoc-aminomethyl)phenylazo]phenylacetic acid. [92]

It should be noted that due to their poor nucleophilicity aromatic amines do not easily undergo amide bond formation and linkers between azobenzene and amine functionalities are generally required, however, there are some examples of direct reactions. In one example, 4-aminophenylazobenzoic acid, **58**, synthesed from reaction between nitrobenzoic acid **56** and **57,** scheme 6, was coupled through its carboxylic acid under standard solid phase conditions. The aromatic amine did not require protection and remained unreacted. However, it was subsequently coupled under much more forcing conditions (*N*,*O*-bis(trimethylsilyl)acetamide, DIEA, THF, 40 ˚C) to create an azobenzene linker in the backbone of a peptide.[91]

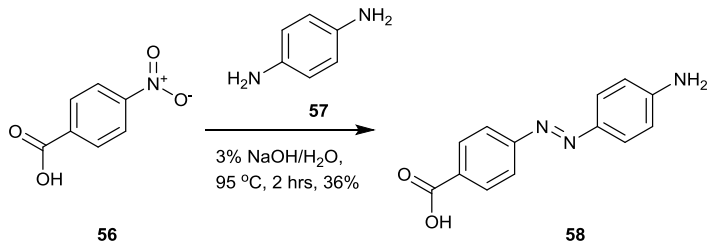

Scheme 6: Synthesis of 4-aminophenylazobenzoic acid.[91]

1.2.4.2.2 Azobenzene units introduced as side-chain functionalities

The chemistry for modification of peptide side chains has largely focused on lysine and cysteine residues. Typically, lysine has been targeted with amide bond formation through reaction with activated esters, but urea and amine bond forming chemistries are also utilised.[106] However, due its unique chemistry and its infrequency in protein sequences cysteine is the most commonly selected residue for side chain modification. The 'thiol-maleimide' reaction has been designated 'click' status due to its efficiency and reliability.[107] Both *mono*- and *bis*- maleimide functionalised azobenzenes have been introduced by this approach.[89,108,109] The simplest mono-substituted azobenzene maleimide, (4-phenylazophenyl)maleimide **61**, has been synthesised in one-step from 4-aminoazobenzene, **59**, and maleic anhydride, **60**, as shown in scheme 7.[110] this derivative has, site specifically, been introduced into calcium binding proteins.[109]

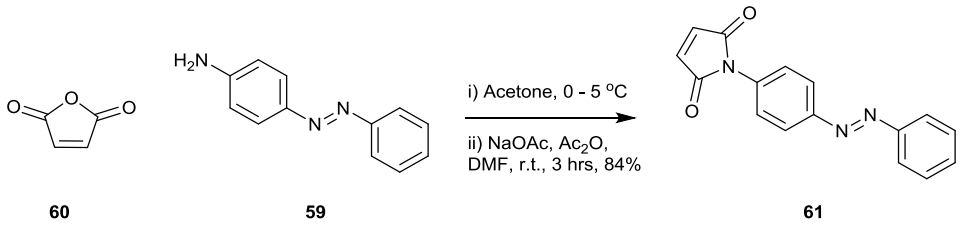

Scheme 7: Synthesis of (4-phenylazophenyl)maleimide.[110]

Functionalisation of tyrosine residues offers an alternative approach to azobenzene functionalised peptides. For example, a tyrosine residue in peptide **62** has been reacted directly with a nitrobenzene diazonium salt, **63**, resulting in the formation of **64** with the azo linkage *ortho* to the tyrosine hydroxyl as shown in scheme 8.[111,112]

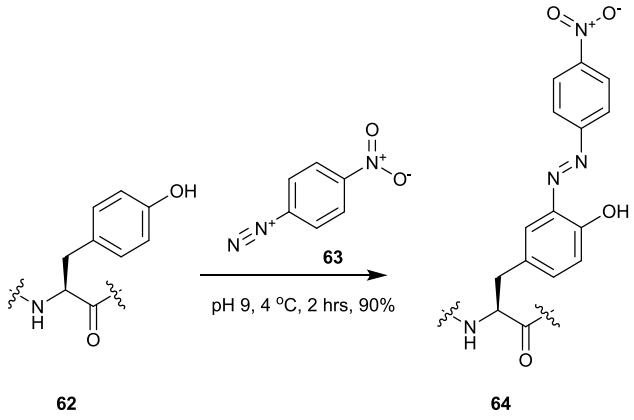

Scheme 8: Introduction of azobenzene into a peptide side chain by reaction of nitrobenzene diazonium with a tyrosine residue.[111]

1.2.4.3 Introduction of azobenzenes to nucleic acids

The introduction of azobenzene units into DNA and RNA strands via automated synthesis is an attractive approach. Therefore, azobenzenes with both a phosphoramidite functionality and a protected alcohol have been important synthetic targets. Although it dates from the late 1990s, the derivatisation of 2,2-bis(hydroxymethyl)propanoic acid, **66**, with 4-aminoazobenzene, **65**, by amide bond formation, remains popular. [113] This reaction forming **67** is shown in scheme 9. One of the equivalent alcohol functional groups of **67** is protected by reaction with 4,4′-dimethoxytrityl chloride. Conversion of the remaining alcohol to a phosphoramidite is typically achieved by reaction with 2-cyanoethyl *N,N*-diisopropylchlorophosphoramidite. The resulting compound **69** has been be used in standard automated oligonucleotide synthesis.

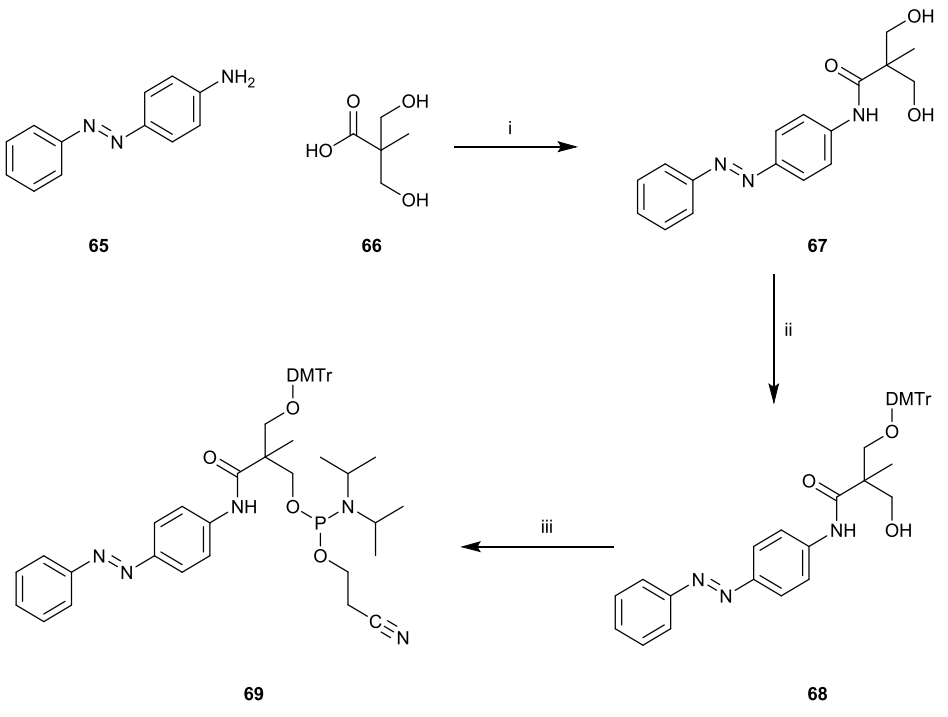

Scheme 9: Synthesis of an azobenzene phosphoramidite from 2,2-bis(hydroxymethyl)propanoic acid.[113]

A significant drawback of this approach is that two diastereoisomers of the phosphoramidite result. As the two diastereoisomers have different stabilising effects on the resultant DNA duplexes, they must be separated before incorporation into oligonucleotides. Komiyama *et al*. by-passed this problem by following a set of reactions similar to those shown in scheme 9, but starting from the optically active D-threoninol, **71**, as shown in scheme 10. Reaction with 4-(phenylazo)benzoic acid, **70**, gave the diol functionalised azobenzene as a signal enantiomer. A series of transformations the phosphoramidite **73**, was obtained as a single diasterioisomer.[114]

Starting from L-threoninol the corresponding azobenzene bearing phosphoramidite could be constructed diastereoselectivity. The DNA constructed from the L-phosphoramidite was destabilised with respect to the native form irrespective of the geometry of the azobenzene unit. Whereas DNA constructed using compound **73** created from D-threoninol showed preferential destabilisation when in the *cis* geometry.

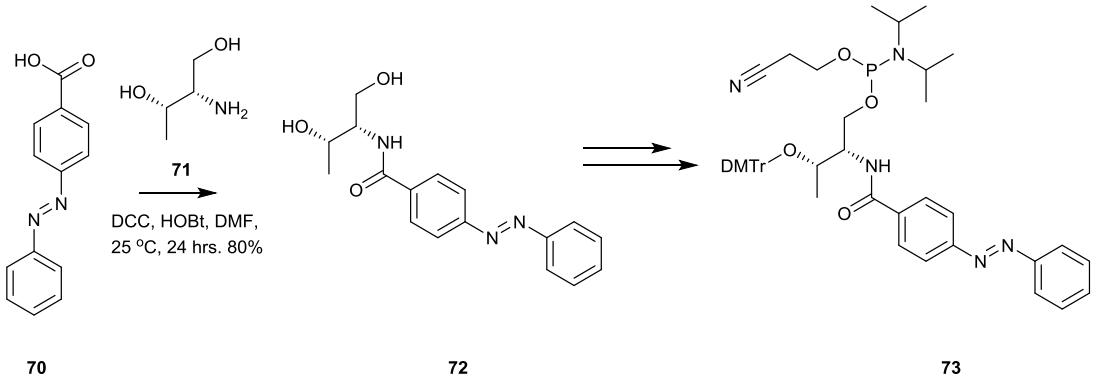

*Scheme 10: Diastereoselectivite synthesis of the azobenzene phosphoramidite **73** starting from D-threoninol.*[114]

As was previously described by Heckel *et al*. substitution of the nucleobase with an azobenzene unit has been achieved. Cleavage of the nucleobase from thymidine by reaction with hexamethlydisilazane and ammonium sulphate resulted in formation of a ribose glycal, **75**,[115] Subsequent Heck reaction with iodo-azobenzene, **74**, resulted in formation of **76** as summarised in scheme 11.[102]

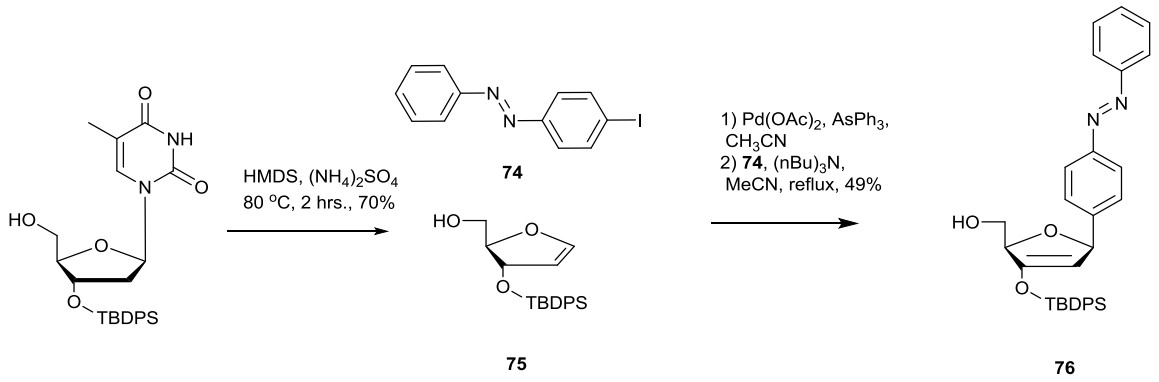

Scheme 11: Synthesis of a nucleoside analogue, where an azobenzene unit replaces the nucleobase.[102]

1.2.4.4 Azobenzene-biomolecule conjugation: closing remarks.

As presented in the previous three sections, the introduction of an azobenzene functionality into biomolecules is most commonly achieved through the traditional chemistry of that particular class of molecule, whether it is glycosidic bond formation for carbohydrates, amide bond formation for peptides/proteins or phosphoramidite chemistry for nucleic acids. This means that methodologies may not be easily transferable from one class to another, and knowledge of the individual chemistry of each biomolecule class is required if azobenzene biomolecule conjugation is to be easily accessed.

Whilst introduction of azobenzene functionalities is well demonstrated for all three classes of biomolecules, there are limitations to the current approaches for example, amide bonds suffer from relatively easy hydrolysis, making them sensitive to water, acids, bases and heat. Drawbacks to other approaches include the necessity to utilise protecting groups. Functionalisation of biomolecules by 1,3 dipolar cycloaddition chemistry could avoid many of these issues, accordingly the following sections will disscuss this class of ring forming reaction.

1.3 Click chemistry

The term click chemistry was coined by Barry Sharpless in the late 1990s, reactions which merit this classification offer high yields, wide substrate scope, inoffensive

byproducts, stereospecificity, simple conditions, and easy separation and purification.[116] Those reaction classifications commonly cited as fulfilling the conditions include: cycloadditions including Diels-Alder cycloadditions and alkyne-azide cycloadditions, nucleophilic substitution of strained rings, and carbonyl chemistry of a non-aldol type, epoxide opening reactions. These reactions are often described as being 'spring loaded' as they have strong thermodynamic driving forces and their use in syntheses has been prolific, for example, entering 'click chemistry' in the literature search engine SciFinder in 2017 generates nearly 15,000 unique citations.

1.3.1 1,3-Dipolar cycloaddition chemistry

Within the broader scope of click chemistry, this work will focus on the use of 1,3-dipolar cycloaddition reactions as a method for conjugating biomolecules with azobenzene photoswitches. As well as the copper cataylsed azide-alkyne cycloaddition (CuAAC), nitrile oxide-alkyne cycloadditions (NOAC) will be explored[117]

1.3.2 Copper catalysed azide-alkyne cycloaddition (CuAAC)

The azide-alkyne cycloaddition, shown in scheme 12, is the best known example of click chemistry. It is renowned for its reliability and effectiveness in connecting two units together. The resulting triazole, **79**, is extremely stable and substitution patterns are highly predictable. However, perhaps the greatest asset of the reaction is the inertness of the starting azide, **78**, and alkyne, **77**, to other modes of reaction. This lack of reactivity allows the groups to be easily introduced into complex substrates where they will lie dormant until the conditions promoting the cycloaddition are provided. Whilst the reaction can occur upon heating, it may be extremely slow and lead to undesirable by-products. However, in the presence of a copper I catalyst, the so called CuAAC (copper catalysted azide alkyne cycloaddition) proceeds rapidly.[118] The active catalyst is often generated *in situ* by reduction of a copper II salt. Typically copper sulphate is used with sodium ascorbate or ascorbic acid. However, it is not uncommon for a copper I salt to be used, such as cuprous bromide. Other catalysts such as ruthenium[119] and silver salts[120] have also been used to promote this reaction.

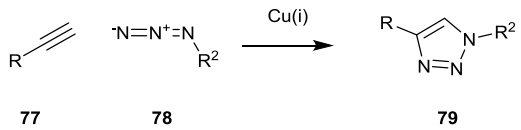

Scheme 12: Copper catalysed azide alkyne cycloaddition (CuAAC).

The reaction mechanism has been studied in detail both experimentally and computationally.[121-123] Recent studies have favoured a dinuclear copper mechanism, as shown in scheme 13.[122,123] Two copper centres coordinate to the alkyne, one adjacent to the π-bond, the other replacing the terminal hydrogen generating species **A**. The azide coordinates to the copper centre engaged with the alkyne, **B**, and a six-membered ring system, **C**, is created. Subsequent ring collapse generates a five-membered ring, **D**, with ejection of one of the copper centres. In the final step, the remaining copper centre is replaced by a proton, furnishing the final cycloaddition product.

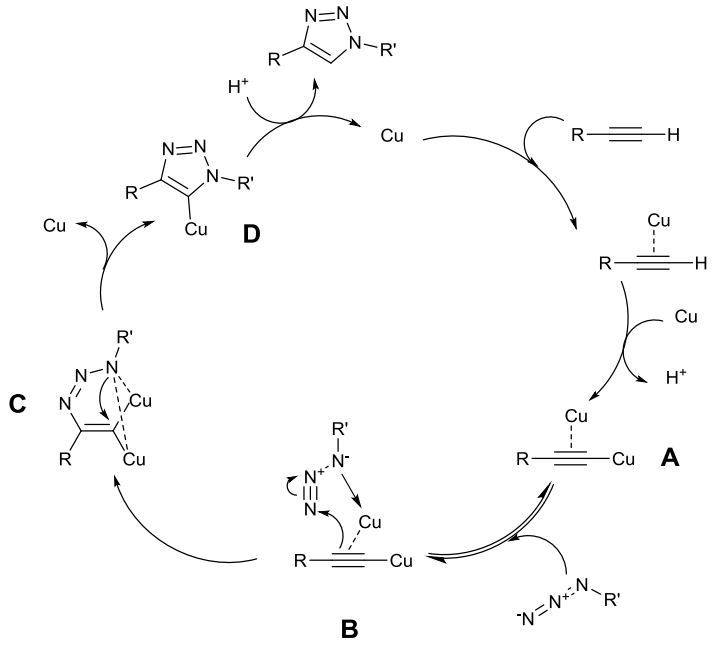

Scheme 13: Mechanism proposed by Worrell and Fokin for CuAAC reaction.[123]

The scope of the CuAAC reaction for derivatisation of carbohydrate substrates is demonstrated in a recent *Chemical Reviews* article.[124] It relates a huge range of 'clicked' glycosides, with applications spanning conjugation to proteins, peptides and lipids, as well as formation of glycoclusters, macromolecules and polymers. A wide range of

carbohydrate substrates bearing the alkyne or azide groups, in a variety of positions have been reported. However, the application the CuAAC to the synthesis of photoswitchable bio-adducts is still underexploited. In particular, there are limited reports of the generation of azobenzene bioconjugates by CuAAC chemistry.

A review by Toth et al. demonstrates the diversity of the CuAAC reaction with peptide substrates.[125] Alkyne and azide functionalities have been introduced to the side chain of a range of different amino acids and amongst other reactions CuAAC chemistry has been used for cross-linking proteins, labelling and tagging proteins and cyclising peptides. Ghadiri et al. have found that a triazole unit can be tolerated in place of a dipeptide e.g. the triazole containing **80** can replace the lysine-leucine unit **81** without effecting α-helix formation of the resulting peptide, figure 28.[126]

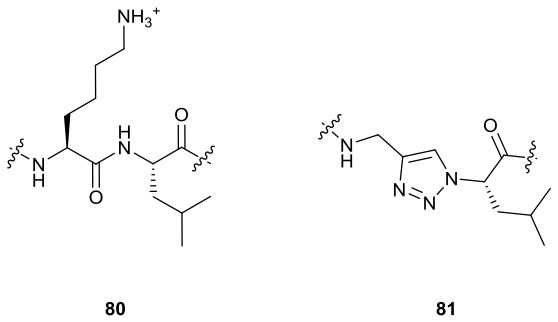

80 **81**

Figure 28: Triazole mimic,81, of peptide, 80.[126]

The CuAAC reaction has also been applied extensively to the functionalisation of DNA and RNA. There are examples where either the azide or the alkyne have been introduced into the ribose, the nucleobase or the phosphate chain.[127,128] Typically triazole formation is used for labelling DNA or connecting DNA strands.[128]

To date azide-alkyne click chemistry has rarely been applied for the conjugation of azobenzenes to biomolecules. Lindhorst and Chandrasekaran have linked C1-linked azido-monosaccharides, **82**, to azobenzene alkynes, **83**, to create *mono* and oligovalent glycosides, **84**, as shown in scheme 14.[129] Azide functionalised cyclodextrins have also been used as substrates in the CuAAC reaction with azobenzene alkynes. The resulting conjugates were used to investigate the effects of isomerisation on the conformational properties of the cyclodextrins.[130,131]

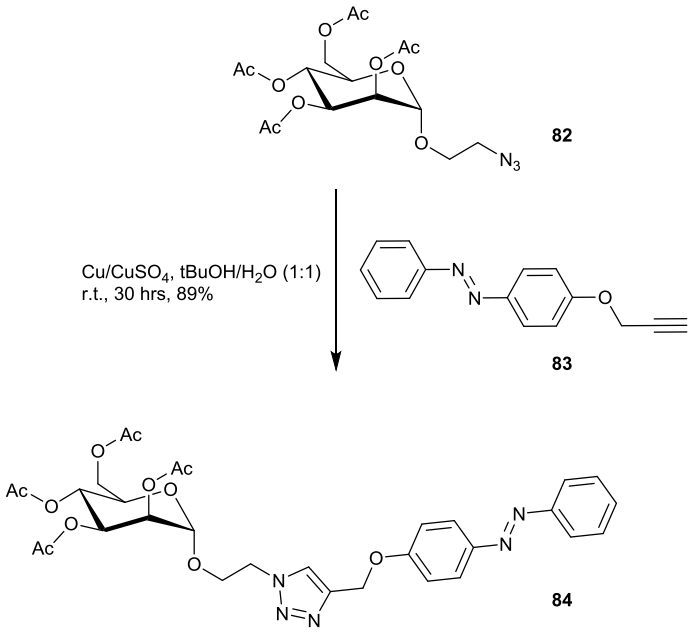

Scheme 14: Azobenzene-glycoside conjugate formed by CuAAC chemistry.[129]

CuAAC chemistry remains unexploited for the formation of azobenzene peptide or nucleic acid conjugates. However, there is some interest in the field. In a recent publication Muller and Lindhorst developed several azobenzene glycosides with azide, alkyne and alkene functionalities with the intention of creating protein cross-linkers through triazole formation, one such building block **85**, is shown in figure 29.[132]

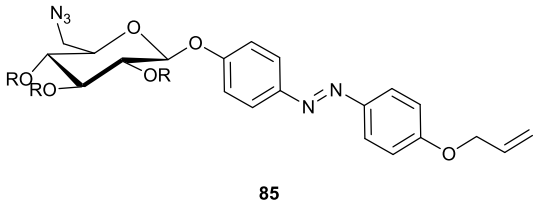

Figure 29: Azide/alkene functionalised azobenzene glycoside designed for future protein cross-linking studies.[132]

Whilst the CuAAC reaction is often considered the best 'click' reaction, it is not without its drawbacks. These are often associated with the potential toxicity and the potential explosive nature of azides. The requirement for a copper catalyst can be a major obstacle in biological and pharmacological settings, where residual ions can be detrimental. One approach to avoiding the need for the copper catalyst is to use more reactive strained alkynes, typically cyclooctynes. However, these substrates generally lack functionality

and introduce large rings to the final conjugate which maybe undesirable in future applications. Therefore, reactive dipoles such as nitrile oxides that can readily react with alkenes and alkynes without the need for catalysts are an attractive alternative to azide cycloadditions.

1.3.2 Nitrile oxide alkyne cycloaddition reactions (NOAC)

In comparison to the azide-alkyne cycloaddition reaction, the isoxazole forming nitrile oxide-alkyne cycloaddition (NOAC) can be considered a more classic 1,3-dipolar cycloaddition. The mechanism was initially debated between a pericyclic concerted reaction and diradical route, however, work by Huisgen helped established the pericyclic route as the preferred mechanism.[133] Nitrile oxides tend to be extremely reactive, short lived species. Thus, conditions for cycloaddition need to be carefully considered to avoid dimerisation[134] or reaction with nucleophilic elements present in the reaction mixture.[135] Nitrile oxides are generally formed in situ from oximes, **86**, hydroximinoyl halides, **88**, or nitro groups, **90**, as summarised in scheme 15.[136] Conversion directly from an oxime to a nitrile oxide through reaction with chloramine-T, (Ch-T), is the most commonly reported route.[137] Another major other route involves inital conversion of an oxime to a hydroximoyl chloride through treatment with *N*-chlorosuccinimide, which subsequently forms the nitrile oxide upon addition of a suitable base[138,139] Alternative reagents for conversion of an oxime to a nitrile oxide include reaction with chlorine gas,[140] sodium hypochlorite[141] or tert-butyl hypochlorite.[142] Examples involving nitrile oxime formation from hydroximinoyl bromides are also reported; oxime bromination can be a achieved by reaction with *N*-bromosuccinimide.[143]

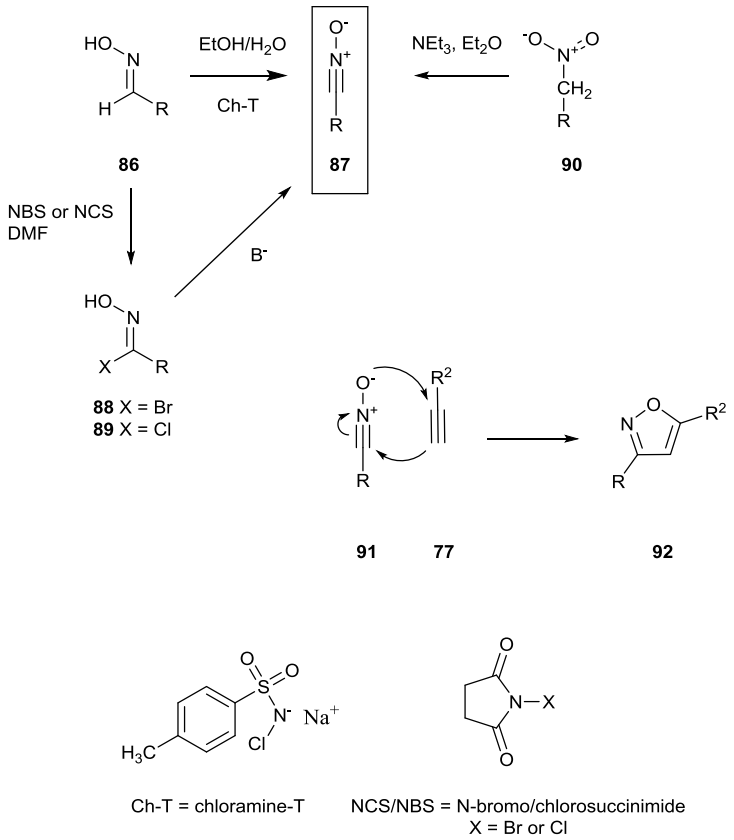

Scheme 15: Nitrile oxide formation and isoxazole formation by cycloaddition of a nitrile oxide with a terminal alkyne

NOAC is popular for its rapid reaction, ease of access to the required oxime precursor and the high degree of regioselectivity. It also avoids the potential safety risks associated with azide dipoles and the need for a metal catalyst associated with the CuAAC chemistry. The isoxazole rings (**92**) formed in the reactions can also be of interest either for incorporation into the final molecules[144,145] or for its potential to ring open and provide further useful functionality, for examples the α–ketonitriles **94** and the highly substituted **95**, which are illustrated in scheme 16.[146-148]

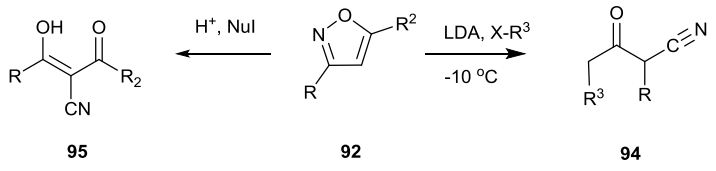

Scheme 16: Ring opening reactions of isoxazoles

Although NOAC reactions are less common than their CuAAC counterpart, they have been used successfully in a range of biomolecular applications. Functionalisation of oligonucleotides, and to a lesser extent peptides and carbohydrates has been reported.[149-151]

The application of nitrile oxide cycloaddition chemistry with carbohydrate substrates includes isoxazoline forming reactions. For example, methylene exo-glucals, **96**, have been reacted with nitrile oxides to generate spiro structures like **98** with potential enzyme inhibition activity, scheme 17.[149]

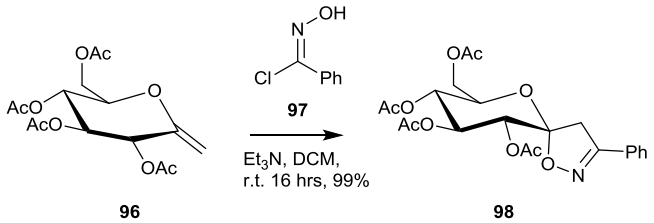

Scheme 17: Nitrile oxide cycloaddition chemistry generating spiro-isoxazoline carbohydrate derivatives.[149]

Methylene exo-glucals have also been used in intramolecular cycloaddition reactions forming bicyclic systems. In these examples it has been demonstrated that the reaction is tolerant to both protected.[152,153] and unprotected saccharides[154]

Bhoseker *et al*. used a nitrile oxide-alkene cycloaddition to form disaccharide and trisaccharide macrocyclic molecules, including **99**. The isoxazoline ring was then opened to give a less rigid macrocyclic structure, **100**, which has additional aminoalcohol functionality, scheme 18.[153]

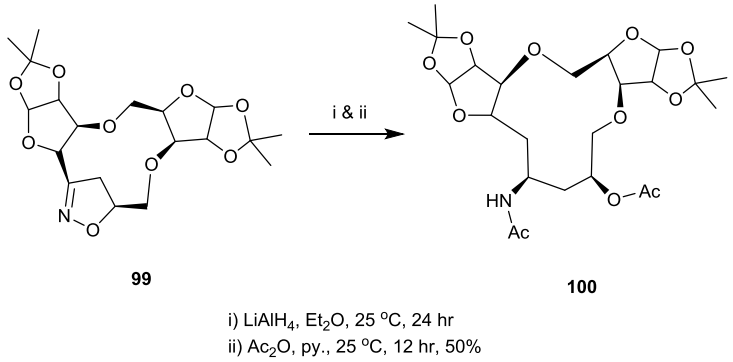

Scheme 18: Disaccharide macrocycles with isoxazoline and aminoalchol functionality.

The highly reactive nature of nitrile oxides and therefore the potential for undesirable side reactions, has somewhat limited the attractiveness of their application in the derivatisation of peptide and protein substrates. In one example, Delft *et al*. report nitrile oxide cycloaddition to the *N*-terminal modified peptide, **101**. Their approach involved adding of the dipole precursor, **103**, in six equal portions over the 12 hours reaction duration. Their reaction resulted in the formation of the isoxazole terminated peptide **104**, shown in scheme 19.[150] The reactive benzonitrile oxide was generated in situ from the parent oxime by reaction with the hypervalent iodine reagent **102**.

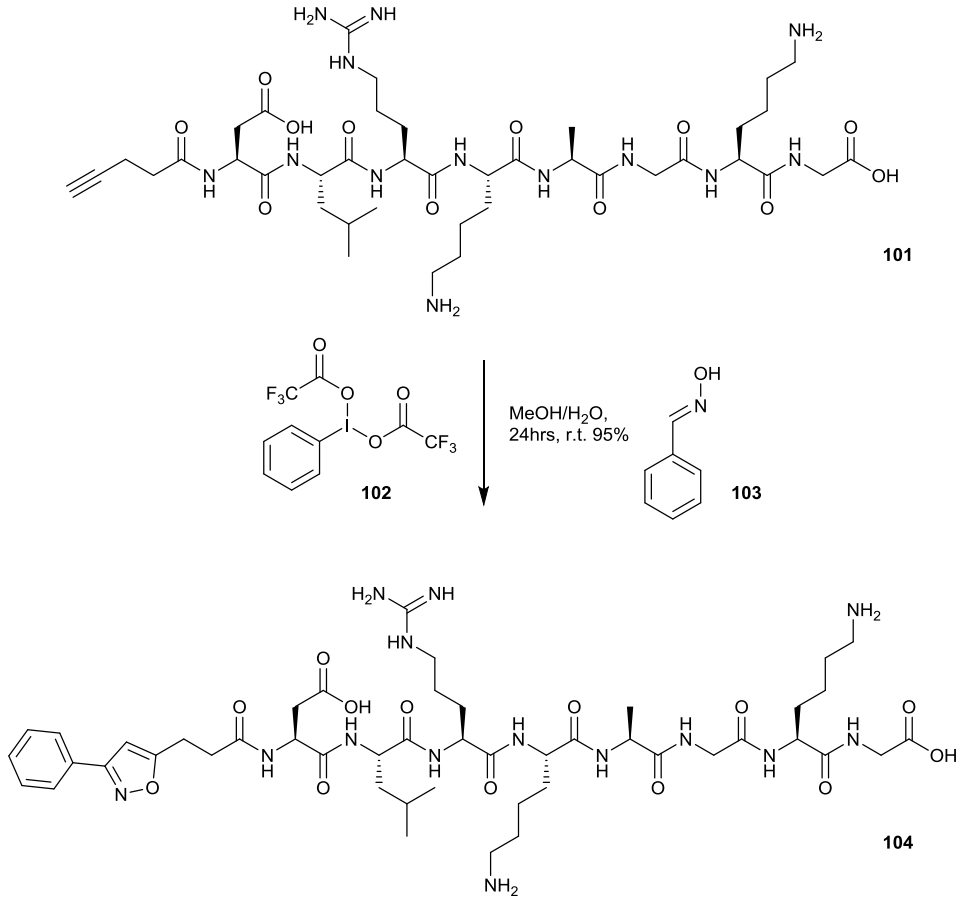

Scheme 19: NOAC between an alkyne functionalised peptide and nitrile oxide generated from benzaldehyde oxime.[150]

In another report, Neumair *et al*. reacted a ^{18}F labelled 4-fluorobenzonitrile oxide with peptides bearing a range of strained and activated alkynes and alkenes, including cyclooctynes, norbornenes and succinimides to great effect.[155]

Delft *et al*. were able to mitigate against the potential difficulties of nitrile oxide self reaction by using reactive strained alkynes and a less reactive nitrone dipole in place of a nitrile oxide.[156] The nitrone was introduced onto the *N*-terminus of a deprotected peptide and successful cycloaddition reactions were achieved under ambient conditions.

In contrast to peptides, nucleic acid substrates have frequently been derivatised by NOAC chemistry. Again, strained alkynes and alkenes are popular dipolarophiles, but terminal alkynes are also utilised. In one example, Carell *et al*. functionalised a nucleoside with a norborene, once built into an oligonucleotide the strained alkene was trapped with a range of functionalised nitrile oxides, including one bearing an azobenzene.[157] Heaney and Singh introduced a cyclooctyne at the terminus of a DNA sequence, **105**, which they used to trap a serval different tags by NOAC chemistry, scheme 20.[158] Further work from the group also demonstrated introduction of an oxime functionality to a phosphoramidite, subsequent conversion to nitrile oxide proceeded cycloaddition to a terminal alkyne.[159] The resulting isoxazole-phosphoramidite was then introduced into a growing oligonucleotide by standard solid phase synthesis. There are a many more examples of the application nitrile oxide-alkyne cycloaddition chemistry in nucleic acid modification included in the microreview by Heaney.[151]

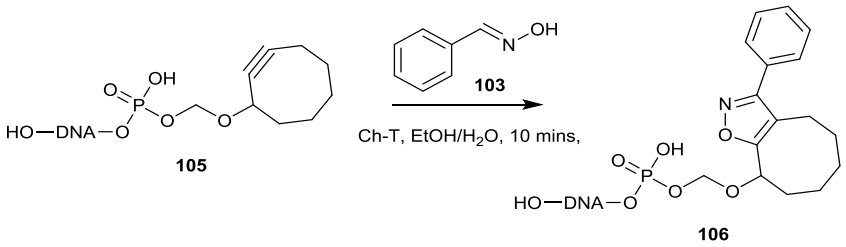

Scheme 20: Reaction between a oligonucleotide with alkyne functionality and benzaldehyde oxime.[158]

2. Azobenzenes with dipole and dipolarophile functionalities: synthesis and cycloaddition behaviour

2.1 Introduction

The objective of this project was to develop a robust and generally applicable methodology for the conjugation of photoresponsive azobenzene units to biomolecular substrates. To this end, a range of azobenzenes bearing either an azide or a nitrile oxide precursor, or an alkyne dipolarophile were desired. Creation of azobenzenes bearing either a dipole or dipolarophile functionality, offered flexibility for the conjugation process in that the azobenzene or the biomolecule could have either of the reciprocal functionalities. Perhaps more importantly, it also offered the possibility of a range of physical and geometric properties to the resulting cycloadducts. As the 3D properties of the cycloadducts were of interest, the potential to prepare regioisomeric azobenzene conjugates was recognised as one important way to create structural diversity. Varying the valency of the azobenzene core further offered access to cycloadducts where one or more individual biomolecule units could be appended.

After designing the range of azobenzenes bearing dipole or dipolarophile functionalities the optimal conditions for cycloaddition were to be investigated. The objective was development of a high yielding reaction, which could be reliably delivered regardless of the nature of the particular biomolecule being ligated. To this end, a number of test case reactions between suitably functionalised azobenzenes with simple aryl dipoles and dipolarophiles were investigated prior to experimentation with biomolecule partners.

The geometric changes affected by photoisomerisation of a functionalised azobenzene derivative are expected to vary depending upon the nature and position of its substituents. Photochemical properties, such as the wavelength of the absorption bands, the quantum yield and rate of the *cis* to *trans* thermal relaxation are also affected by the substituents pattern. As such, it was desired to create a range of functionalised azobenzenes carrying 1,3-dipolar or dipolarophile functionalities in positions *ortho*, *meta* and *para* to the azo functionality, examples shown in figure 30. In search of polyvalent derivatives *bis* substituted compounds, specifically including those with two reactive functionalities on both aryl rings were targeted.

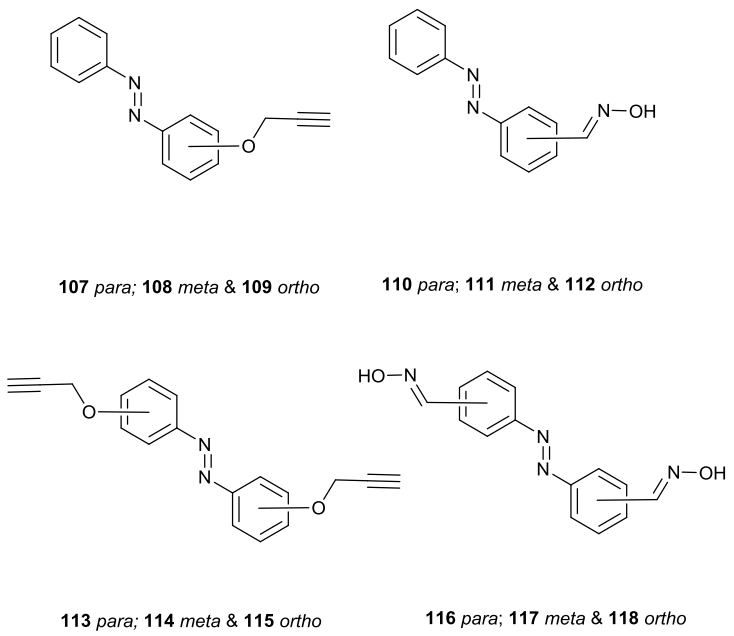

Figure 30: Selection of functionalised azobenzene structures targeted in this research.

Initial target compounds bore an alkyne (**107**-**109**), an oxime (**110**-**112**) or a hydroximinoyl chloride functionality *ortho*, *meta* or *para* to the azo linkage (figure 30). Azobenzenes with either a hydroxyl, **119**, or an aldehyde functionality, **123**, were identified as key synthetic precursors to these targets. The synthetic routes to be adopted are shown retrosynthetically in scheme 21. It was anticipated that the phenolic functionality of **119** would react with propargyl bromide to give easy access to the azobenzene-dipolarophile family (**107**-**109**) and that the aldehyde **123** would react with hydroxylamine (**124**) to give the azobenzene-oxime family (**110**-**112**) which would act as precursors to the corresponding nitrile oxides (**121**).

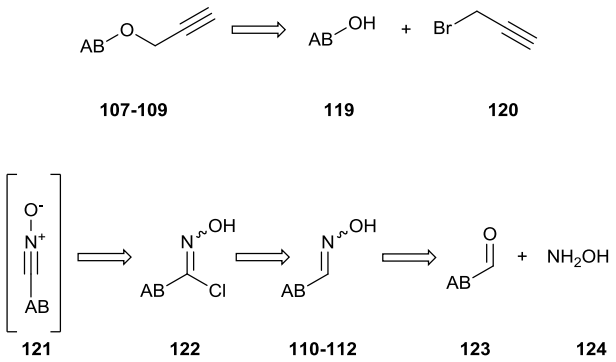

Scheme 21: Retrosynthetic analysis of functionalised azobenzenes.

It was envisaged that some of the targeted molecules could be accessed by modification of commercially available azobenzenes. However, for most formation of the azo linkage would an important first step in the synthesis.

2.1.1 Major synthetic routes to azobenzenes.

Several routes are available for the formation of an azo bond. Those commonly utilised include the Mills reaction, reductive coupling, oxidative coupling and azo coupling; these approaches are summarised in scheme 22.[160]

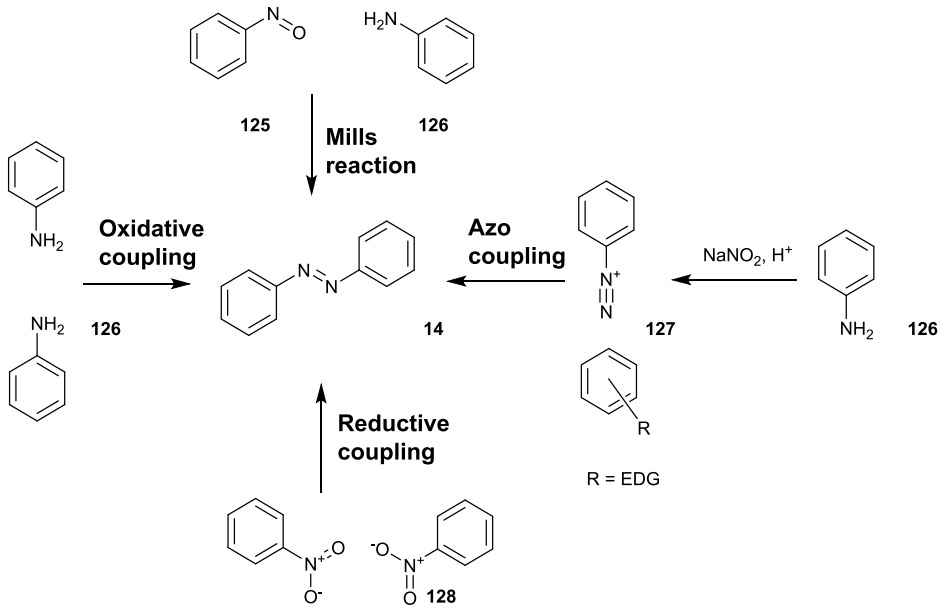

Scheme 22: Major synthetic routes to access azobenzenes.

The '**azo coupling**' reaction is the most popular for synthesising azobenzenes. It is compatible with a range of functionalities and is generally high yielding and fast. It involves formation of an intermediate diazonium salt, formed by nucleophilic attack from an aniline derivative onto nitrosonium ion, generated in situ from the reaction of sodium nitrite with an acid, typically HCl. The partnering aryl generally requires at least one electron donating group (EDG) to facilitate the electrophilic attack on the diazonium salt. Substitution *para* to the EDG is the favoured regiochemical outcome. However, if this site is blocked reaction will occur at the *ortho* position. Apart from the electronic

requirements, the reaction is also sensitive to temperature and pH. The pH of the reaction must initially be acidic enough to facilitate the formation of nitrous acid; later it must not impede the electrophilic substitution by protonation of the EDG on the aryl partner. For example, often a diazonium salt will be reacted with a phenolate, so in the course of the reaction the pH has to be adjusted from acidic to basic. Particular care must also be taken to control the temperature as diazonium salts are known to be unstable above 5 °C. However, these low reaction temperatures often result in poor solubility of the reactants in the aqueous media commonly used. The mechanism for the reaction is demonstrated in scheme 23. Nitrite, **129**, protonation gives rise to nitrous acid, which is further protonated before dehydration to generate NO^+. Attack by aniline, **126**, and a series of proton transfers steps affords diazonium **127**. Attack by phenol and proton elimination gives the final hydroxyazobenzene **131**.

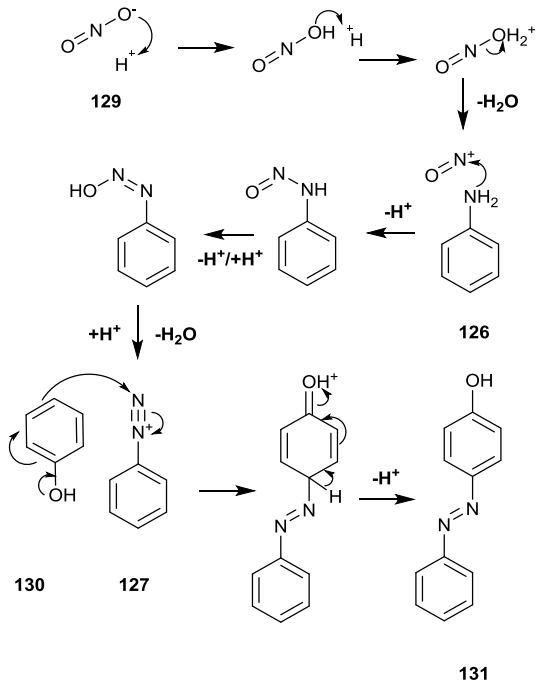

Scheme 23: Mechanism of azo bond formation by the azo coupling reaction.

The **Mills reaction** is also popular for formation of azobenzene derivatives. The mechanism of this reaction involves nucleophilic attack by an aniline derivative on a nitroso functionality followed by proton transfer and elimination of a water molecule, as shown in scheme 24.

While the reaction is usually quick and high yielding, its attractiveness as a synthetic route is can be limited by the range of suitable nitroso species. Whilst nitrosobenzene is commercially available, more highly substituted nitrosoaryls can be challenging to access. Preparation of nitrosoaryls is typically achieved by hydroxylamine oxidation, a reaction that needs to be carefully controlled to prevent over oxidation and which is often poor yielding. The Mills reaction can also be limited by difficulties in product purification with the potential for a variety of by-products to be formed.

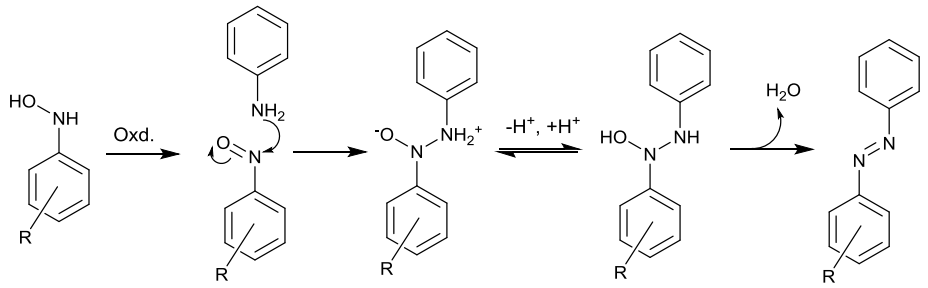

Scheme 24: Mechanism of azo bond formation by the Mills reaction

Reductive couplings offer an efficient route to symmetrically functionalised azobenzenes. In situ generation of nitroso and hydroxylamine species during the reduction of nitro compounds allows for azo bond formation. The key intermediates in the reaction are shown in scheme 25.

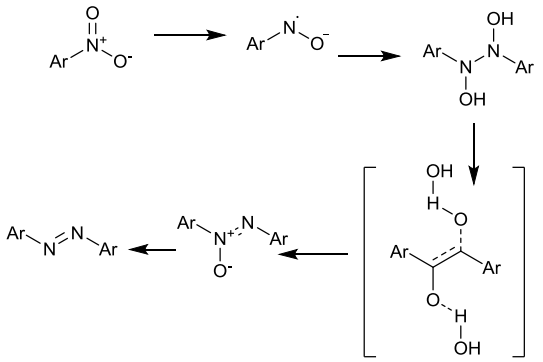

Scheme 25: Key intermediates of azo bond formation by the reductive coupling approaches.

A range of reducing agents including $LiAlH_4$,[161,162] HCO_2^- H^+NEt_3/ Mg,[163] KOH,[164] Zn/NaOH[165] have been reported to be suitable for the transformation. The synthesis of

the parent azobenzene **14** and a selection of substituted derivatives **132-134** by this approach, and the respective reducing conditions, are summarised in scheme 26.

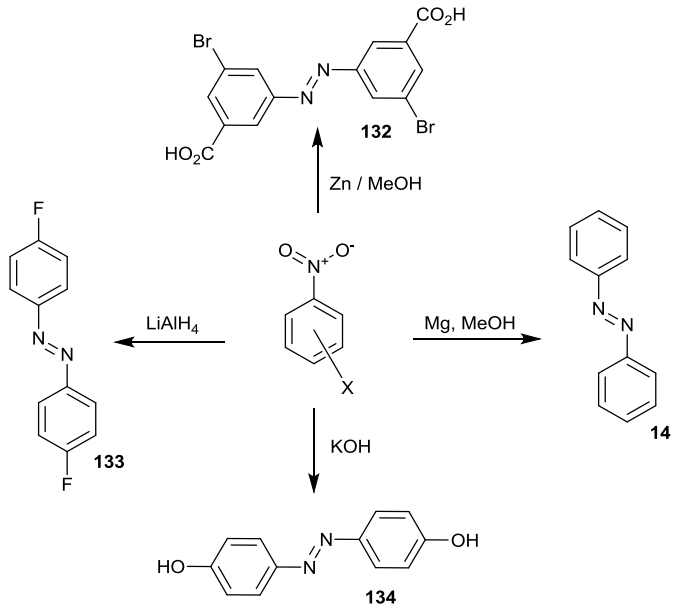

Scheme 26: Reductive routes to symmetric azobenzene derivatives

An alternative route to symmetrically functionalised azobenzenes involves **oxidative coupling** of anilines. A range of oxidising agents have been shown to be effective; these include HgO,[166] MnO_4,[166] $Pb(OAc)_4$[167] and hypervalent iodine species.[168] Oxidative coupling has also been achieved electrochemically[169] and with O_2 in the presence of various metal catalysts. Oxidative azo bond formation is generally a low yielding reaction. It is thought to proceed via a radical mechanism,[170] as shown for the formation of azobenzene **14** in scheme 27. The key step in the mechanism, coupling of the $ArNH^{\cdot}$ radical species **135**, proceeds oxidation of **136**, which furnished the product.

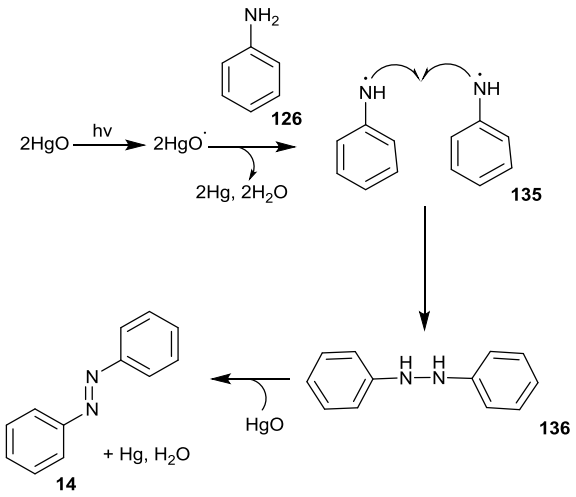

Scheme 27: Mechanism of azo bond formation by oxidative coupling.

2.2 Synthesis of azobenzenes bearing alkyne dipolarophiles at the *ortho*, *meta* and *para* positions

The *mono*- and *bis*-*p*-propargyloxyazobenzenes **107**[171] and **113**,[129] both known in the literature were the initial azobenzene-dipolarophile targets. The corresponding hydroxy parents **131** and **133** were identified as key starting materials. The symmetric 4,4'-hydroxyazobenzene, **133**, was prepared by the reductive route starting from 4-nitrophenol, **137**, according to a literature procedure.[172,173] 4-Nitrophenol was added to potassium hydroxide in a minimum amount of distilled water. The reaction slurry was heated to 300 °C. After several dramatic colour changes, suggestive of a radical mechanism, the product was produced as a yellow solid in 37% yield.[174] Subsequent reaction with propargyl bromide in the presence of potassium carbonate in dry acetonitrile gave the desired *bis*-ether **113** as a golden coloured crystalline solid, in 95% yield. The ^{1}H-NMR spectral data of **133** and **113** agreed with that reported in the literature.[129] For both compounds, a pair of doublets (J = 8.0 Hz) were observed in the aromatic region. For **113** a doublet (2H) and triplet (1H) with reciprocal coupling constants (J = 2.5 Hz) represented the propargyl group. The ^{1}H-NMR spectrum showed **113** presented exclusively in the *trans* form at room temperature in $CDCl_3$.

p-Hydroxyazobenzene, **131**, the precursor to **107**, was formed by an azo reaction. Aniline, **126**, and sodium nitrite were reacted in the presence of hydrochloric acid to form benzenediazonium chloride. A solution of phenol in aqueous sodium hydroxide

was subsequently added.[175] Electrophilic aromatic substitution resulted in the formation of **131** in 57% yield. The ^{1}H-NMR spectroscopic data of **131** was in agreement with that reported in the literature.[176] Alkylation with propargyl bromide in anhydrous acetonitrile in the presence of potassium carbonate, gave **107** as an orange solid in 88% yield. NMR characterisation data match that reported by Yao *et al*.[171] Like its di-substituted version **113**, the ^{1}H-NMR spectrum showed evidence of the *trans* isomer only (r.t., $CDCl_3$).

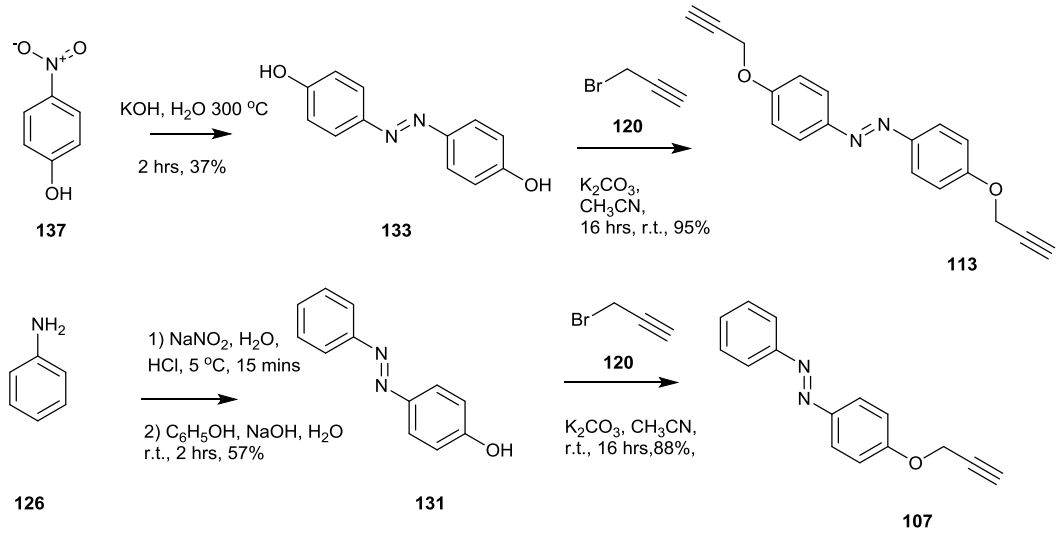

*Scheme 28: Synthetic of **113** and **107**.*

Azo coupling chemistry was not used to target either the *o*- (**138**) or the *m*-hydroxyazobenzene (**141**) regioisomers of **131** were targeted through as the electronics of this reaction are known to favour the *para* regioisomer. However, their syntheses have been reported in the literature through a range of other methods. The difficulty with many of the reported routes is that they proceed from starting materials which are themselves difficult to access, or they involve the use of unconventional reagents. However, Wachtveitl *et al*. have reported synthesis of **138** and **141** in reasonable yield via the Mills coupling of nitrosobenzene, **125**, with either *o*- or *m*-aminophenol, **139**/**140**, in glacial acetic acid (51% and 73% respectively).[177]

Attempts to reproduce either of Wachtveitl's reactions progressed poorly in our hands and the ^{1}H-NMR spectra of the crude products in each case showed a complex mixture. No pure sample of **138** could be isolated from the reaction of *o*-aminophenol, **139**, with

nitrosobenzene, **125**. However, after a difficult separation by flash chromatography the *meta* **141** was isolated in 6% yield from reaction with **140**. Despite the low yield, **141** was reacted with propargyl bromide in the presence of potassium carbonate and the novel **108** was obtained as an orange solid in 87% yield.

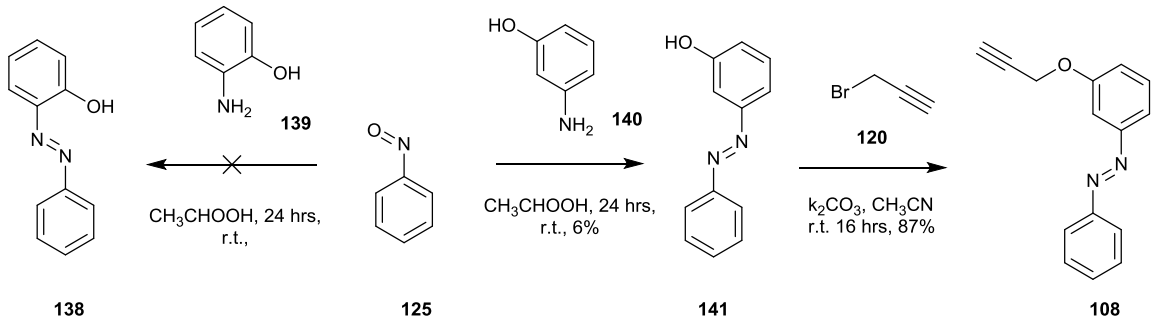

Scheme 29: Attempted synthesis of azobenzenes bearing an ortho or meta dipolarophile..

The ^{1}H-NMR signals arising from the propargyl functionality of **108** mirrored those observed for its *para* regioisomer **107.** The OCH_2 signal occurred at close to 4.8 ppm (d, J = 2.5 Hz) and the terminal alkyne proton was observed at ~2.5 ppm (t, J = 2.5 Hz). Signals representing the aryl protons suggested it presents as 10:1 mixture of *trans* and *cis* geometrical isomers. The signals for the *trans* isomers, which like the resonances of **107,** appear between 7-8 ppm. A second set of low intensity signals represent the aryl protons of the *cis* isomer were present between ~8.3 and 6.4 ppm. The OCH_2 protons of the minor isomer are at ~4.5 ppm and the alkyne resonance appears at ~2.4 ppm, figure 31.

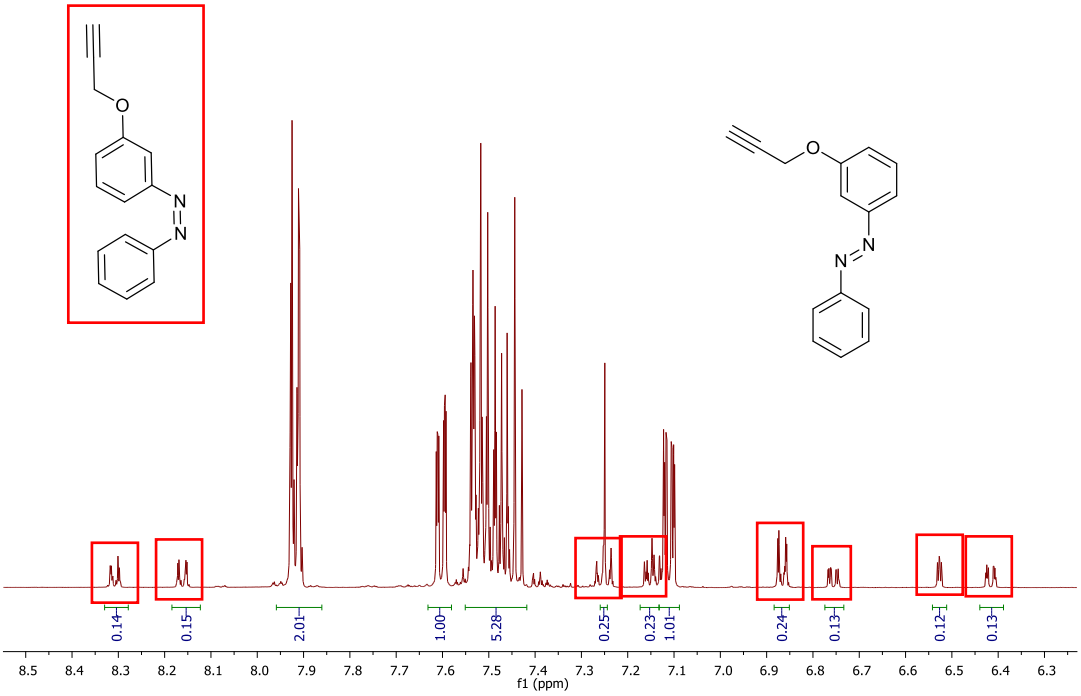

*Figure 31: Aromatic region of the ^{1}H-NMR spectrum of **108**; resonances attributed to the cis isomer are boxed in red ($CDCl_3$, 500 MHz).*

The ^{1}H-NMR spectra of a number of compounds in this series provide evidence of a small amount of the *cis* isomer in equilibrium with the major product having *trans* geometry about the azo double bond. In such cases, a second set of low intensity peaks are observed. The aryl protons nearest the azo bond are those which most frequently appear as separate resonances, distinct from their *trans* counterparts. The signals arising from the *cis* isomer span a wider range of chemical shifts than the corresponding protons of their *trans* counterparts. In particular, a number of resonances of the *cis* isomer appear upfield of the corresponding *trans* protons.[178,179] In the case of **108** the downfield resonances of some of the aryl protons of the *cis*- isomer whilst not rare is less common.

Following the failure to prepare the *ortho* substituted **138** and in continued pursuit of an azobenzene bearing a propargylic dipolarophile *ortho* to the azo linkage, it was proposed to prepare **144**. Although the methyl group at the 5-position limits direct comparisons of the chemical and photophysical behaviour of this compound to its 'regioisomers' **107** and **108**, it does offer an azobenzene with a dipolarophile in the *ortho* position

Since *p*-cresol, **142**, has a 'blocked' *para* position it was believed that an azo coupling with aniline may occur at the *ortho* position, providing **143** as a key intermediate en

route to **144**. A review of the literature shows that *p*-cresol reacts with benzenediazonium chloride to give the 2-hydroxy-5-methylazobenzene **143**.[180] We repeated Black's reaction (65% yield) and the NMR spectral data of the orange solid agreed with that reported. It presented predominantly in the *trans* form with extremely low intensity signals consistent with the presence of a small amount of the *cis* form ($CDCl_3$, r.t.).

To access the novel compound **144** propargyl bromide was reacted with the **143** in the presence of K_2CO_3 in dry acetonitrile. After reaction work up the orange/red product was isolated in 79% yield, scheme 30. The ^{1}H-NMR spectrum of **144** ($CDCl_3$), shown in figure 32, indicates the product was present almost exclusively in the *trans* form with very low intensity signals attributed to trace amounts of the *cis* isomer.

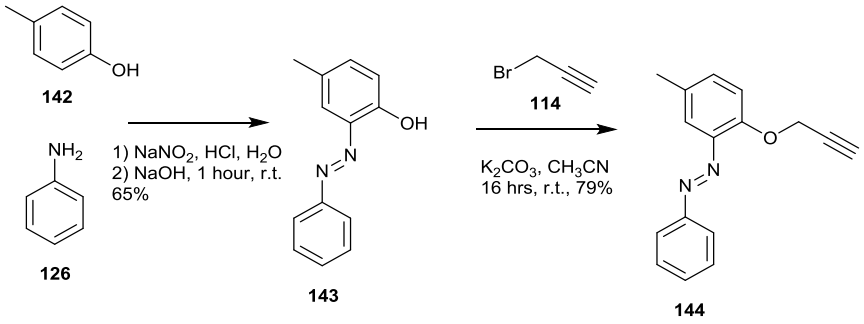

*Scheme 30: Synthesis of 2-propargyloxy-5-methlyazobenzene, **144***

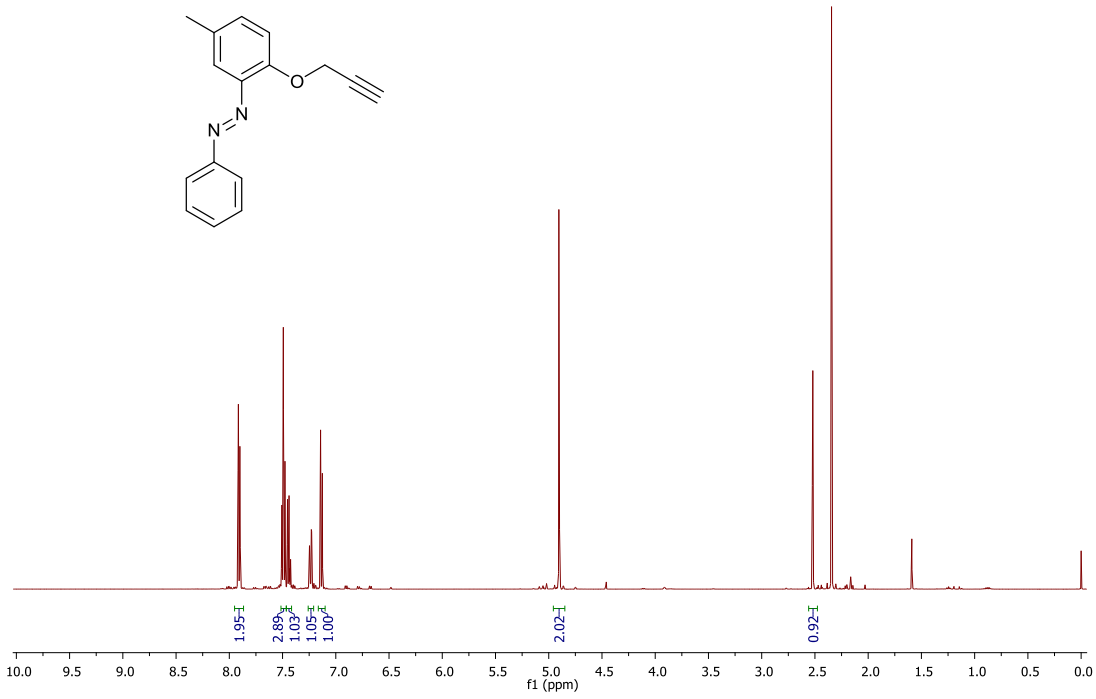

*Figure 32: ^{1}H-NMR spectrum of **144** (500 MHz, $CDCl_3$)*

The symmetrical *o,o*- and *m,m*-dihydroxyazobenzenes **115** and **114** were the next synthetic targets. Reductive coupling of *o*-nitrophenol and *m*-nitrophenol were explored in turn. A solution of the substrate in diethyl ether was added to a stirring suspension of $LiAlH_4$ (5 eq.) in diethyl ether. In both cases a complex mixture resulted. ^{1}H-NMR spectroscopy and TLC analysis suggested formation of a number of species with no dominance of the desired product.

Reaction of either of the nitrophenols with a potassium hydroxide slurry (300 ˚C) also failed to yield the desired compounds.[174] In both cases over reduction was observed and the aminophenols **147** and **148** were found in good yield. An alternative experiment employing sodium hydroxide in ethanol returned, in both cases, the starting materials in quantitative yield.[181] The failure of these reactions, summarised in scheme 31, led to an abandonment of the search for the *o,o*- and *m,m*-dihydroxyazobenzenes **114** and **115**.

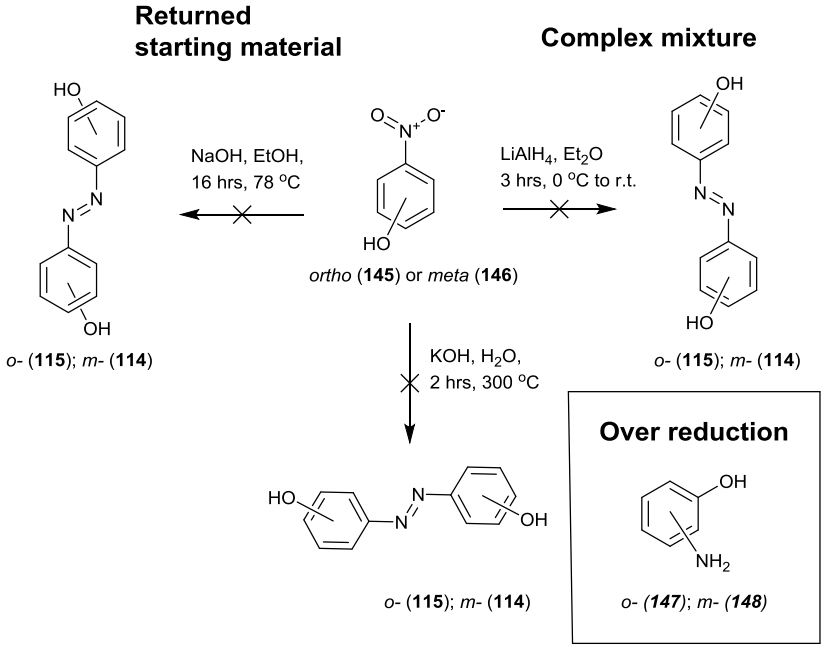

*Scheme 31: Attempted reductive coupling routes to **114** and **115**.*

The final azobenzene alkynes targeted were the known **151** and **152**; **151** has two potential sites for cycloaddition, one alkyne is ether linked and the other ester linked. In contrast, **152** only has the ether linked alkyne. *p*-(*p*-Hydroxyphenylazo)benzoic acid, **150**, was synthesised according to the literature,[182] through azo coupling of *p*-

aminobenzoic acid, **149**, and phenol, **130**, in the presence of sodium nitrite and hydrochloric acid. The alcohol and carboxylic acid groups of **150** were converted to the corresponding ether and ester functionalities respectively through reaction with propargyl bromide in the presence of potassium carbonate in dry acetonitrile. The ester linkage was hydrolysed by treatment with sodium hydroxide to give monovalent **152**, scheme 32. The ^{1}H-NMR data for both the ester **151** and the acid **152** were in agreement with that reported in the literature.[182]

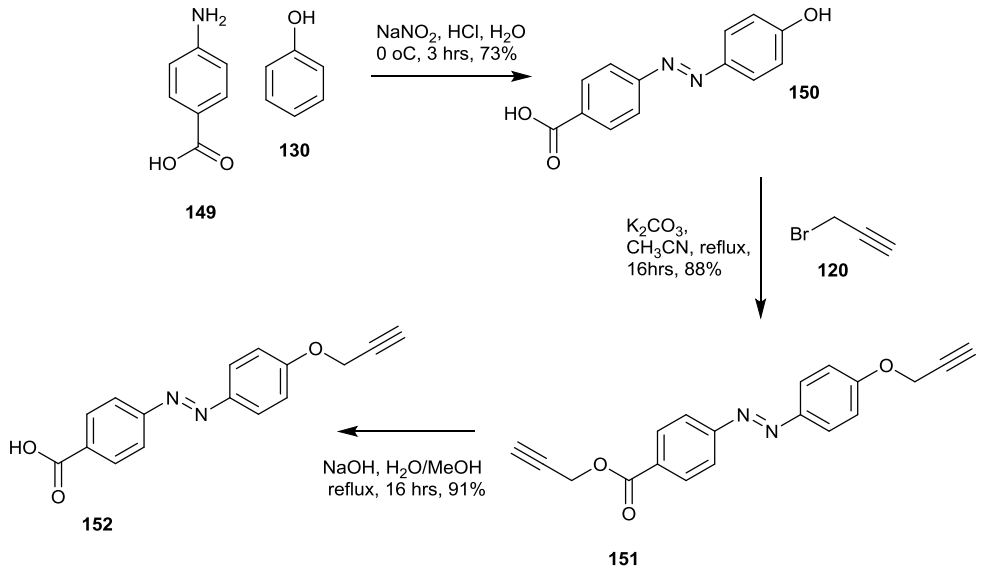

*Scheme 32: Synthesis of 4-(4-propargyloxyphenylazo)benzoic acid **152***

2.3 Preliminarily cycloadditions to azobenzenes bearing one or two dipolarophiles: test case reactions

As previously discussed in section 1.3.2, the generation of nitrile oxides for NOAC reactions can be achieved under a range of conditions. One option involves direct conversion of an oxime to a nitrile oxide by treatment with chloramine-T hydrate (Ch-T). Alternatively the oxime can initially be converted to its chlorinated derivative by treatment with *N*-chlorosuccinimide (NCS) prior to dipole generation following treatment with base. Whilst the direct conversion is often a more straightforward and efficient process, its attractiveness is limited by the poor solubility of Ch-T in organic solvents and reactions generally require aqueous alcohol media. In comparison

conversion of oximes to chlorooximes (or hydroximinoyl chlorides) with NCS is typically undertaken in DMF. The chlorooxime can be isolated and subsequent cycloaddition, if required, can be conducted in solvents other than DMF. The conversion from the hydroximinoyl chloride to the nitrile oxide is extremely rapid upon addition of base whereas dipole formation from reaction of oximes with Ch-T, generally involves premixing of the reactants.

To determine the suitability of either or both the Ch-T or NCS routes for the generation of nitrile oxides and cycloaddition to alkyne bearing azobenzenes, the *p*-propargylated **107** and **116** were reacted in turn with commercially available benzaldehyde oxime, **103**, in the presence of Ch-T, or with the preformed hydroximinoyl chloride **97** .

The isoxazole forming reaction between **107** and the nitrile oxide generated through the treatment of benzaldehyde oxime with Ch-T in ethanol/water was previously known in the group, scheme 33, **route A**.[183,184] The trapping of transient dipole yielded the cycloadduct **153** in 88%.

It was characterised by the appearance of a singlet diagnostic of the isoxazole C-4 proton, at 6.69 ppm in the ^{1}H-NMR spectrum ($CDCl_3$). A shift in resonance of the OCH_2 protons from 4.68 ppm in the starting alkyne to 5.30 ppm also accompanies cycloadduct formation. The aryl proton resonances ($CDCl_3$, 500 MHz) of the azobenzene core of **153** were complex signals. This is due to the magnetic inequivalence of the protons 6 and 6a, and 7 and 7a. Therefore the signals arising from these AA'XX' protons are second order multiplets.

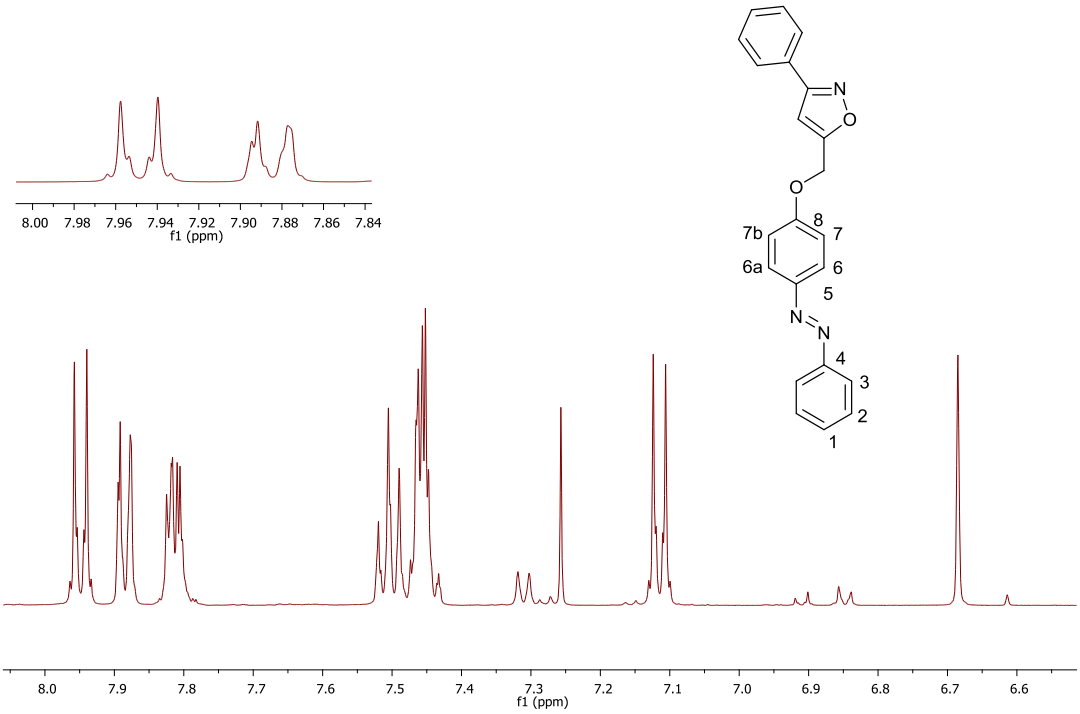

*Figure 33: Aromatic region of ^{1}H-NMR spectrum of **153** CDCl3 500 MHz.*

To evaluate the chlorooxime route to **153,** scheme 33 **route B**, benzaldehyde oxime was initially converted to its hydroximinoyl chloride, **97**, by reaction with NCS in DMF. The success of the reaction was confirmed by the disappearance of the C-H singlet of the imine, at 8.04 ppm, in the ^{1}H-NMR spectrum ($CDCl_3$) of the starting oxime and by a downfield shift in the OH resonance from within the multiplet at 7.49-7.58 ppm to a sharp singlet at 8.13 ppm in the chlorooxime. The hydroximinoyl chloride under the influence of triethylamine in ethyl acetate generated the transient nitrile oxide which reacted in situ with the *p*-propargylated azobenzene **107** to afford the cycloadduct **153** in 76% yield.

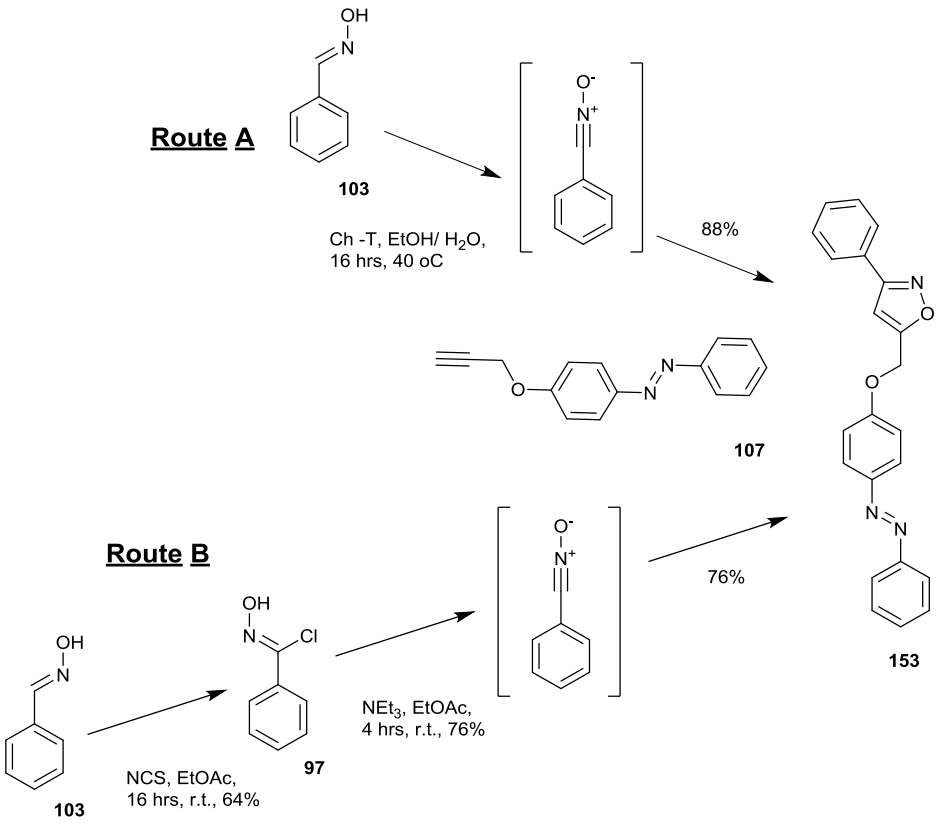

*Scheme 33: NOAC leading to **153**; exploring two routes for dipole formation: Ch-T (route A) and NCS/ NEt_3 (route B).*

In conclusion, both Ch-T and NCS/NEt_3 approaches were effective in generating nitrile oxides which could be trapped in situ by the propargyloxyazobenzene **107**. Starting from benzaldehyde oxime in reaction with Ch-T, the cycloadduct **153** formed in higher yield (88%). The two step oxime to chlorooxime to cycloadduct yields **153** in 48% over the two steps. The lower yield of the cycloaddition step in going from **97** to **157** is possibly due to the faster formation of the nitrile oxide, which facilitates self-reaction of the dipole.

The *p,p*-bis-azobenzene dipolarophile, **116**, had poor solubility in aqueous ethanol and thus cycloadditions utilising Ch-T were not attempted and the hydroximinoyl chloride **97** was used as a precursor to the nitrile oxide.

Dipolarophile **116** was poorly soluble in many common solvents. DMF, DMSO, EtOAc and $CHCl_3$ were found to be the best for solubilising it. DMSO and DMF were unattractive due high boiling points and miscibility with water, therefore, $CHCl_3$ and EtOAc were selected as solvents for cycloadditions leading to **154**. The dipole was

formed in situ by the addition of NEt_3 to a solution containing **116** and 6 equivalents of the chlorooxime **97**.

The success of the reaction was initially estimated by comparing the relative integration of the signals of the isoxazole (6.69 ppm) and OCH_2 protons of the cycloadduct **154** (s, 5.31 ppm) with that of the starting material OCH_2 protons (t, 4.78 ppm). Following purification by flash chromatography the desired cycloadduct **154** was isolated in 81% yield when the reaction was undertaken in chloroform and in 74% yield when ethyl acetate was selected as solvent, scheme 34. The ^{1}H-NMR spectrum of purified **154** ($CDCl_3$, 500 MHz) also suggested restricted rotation about the single bonds, as seen for its monovalent analogue **153**. The aryl protons of the azobenzene unit were second order multiplets due to their magnetic inequivalence.

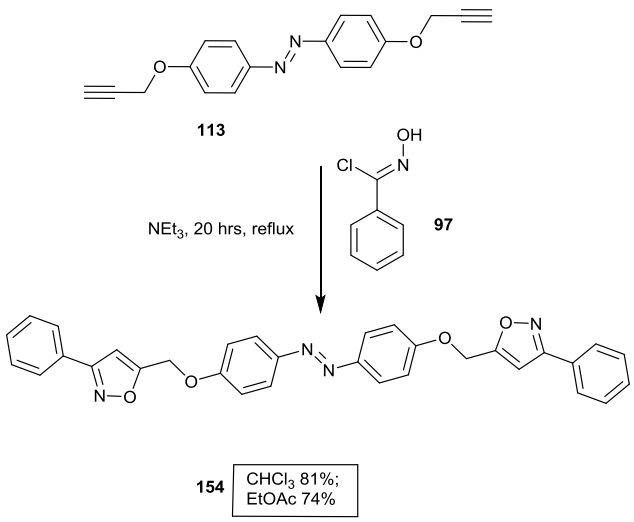

*Scheme 34: NOAC leading to divalent cycloadduct **154***

The potential for the azobenzene dipolarophiles to be trapped with azide dipoles in CuAAC reactions was also of interest. Therefore the cycloadditions of **107** and **116** with benzyl azide were investigated in turn. The dipolarophile and benzyl azide, **155**, were dissolved in a DMSO/H_2O mixture prior to the addition of $CuSO_4.5H_2O$ and sodium ascorbate, followed by stirring for 16 hours at room temperature.

The *mono* alkyne, **107** was reacted with two equivalents of the azide. The catalyst loading was 20 mol % with respect to the alkyne. The cycloadduct **156** was isolated in 89% yield. The *bis* propargyl azobenzene, **116**, was reacted with two equivalents of

azide per alkyne functional group, i.e. four molar equivalents. Catalyst loading was 40 mol % loading per alkyne functional group and the cycloadduct **157** was isolated in 87% yield, scheme 35. The catalyst loading is high, however, it is cheap and readily accessible and the project did not test the loading limits.

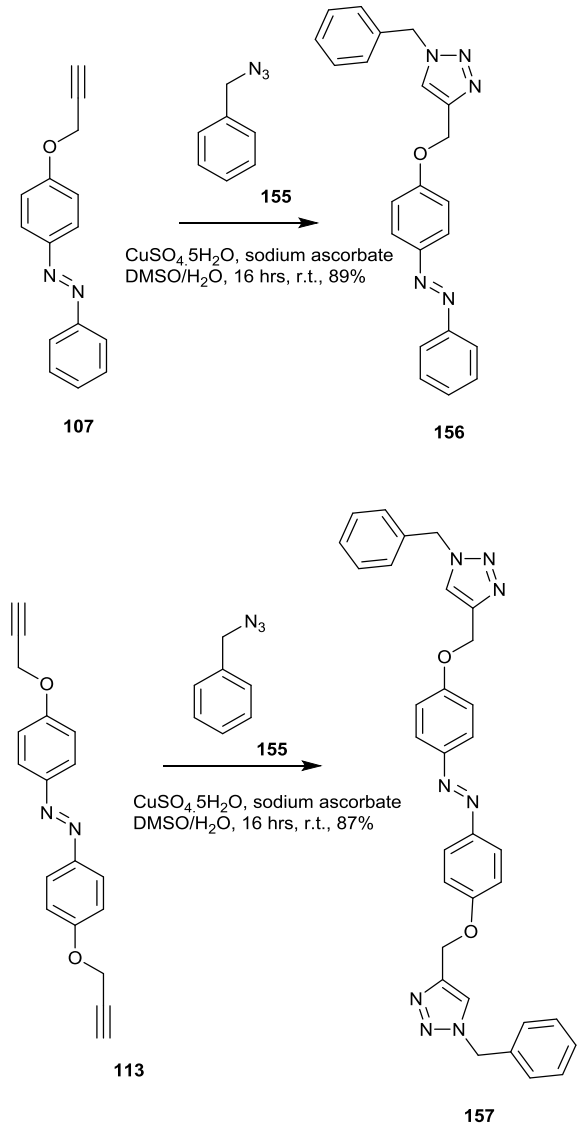

*Scheme 35: CuAAC leading to the mono- and divalent triazoles **156** and **157.***

The ^{1}H-NMR spectra of the cycloadducts **156** and **157** indicate the compounds presents mainly as the *trans* isomers, with low intensity signals for the *cis* isomer in both cases. The ratio of the *cis* to *trans* isomer for **156**, shown in figure 34, was roughly 1:13. The most shielded aryl protons of *cis* form of **156** were observed as far upfield as 6.8 ppm, whilst the most shielded aryl proton of *trans* isomer appears at 7.2 ppm (DMSO-d_6). The triazole CH (8.3 ppm) is much more deshielded than is typically observed for an

isoxazole CH (7.3 ppm) (DMSO-d_6). Both **156** and **157** show the aryl protons of the azobenzene core appeared like first order doublets.

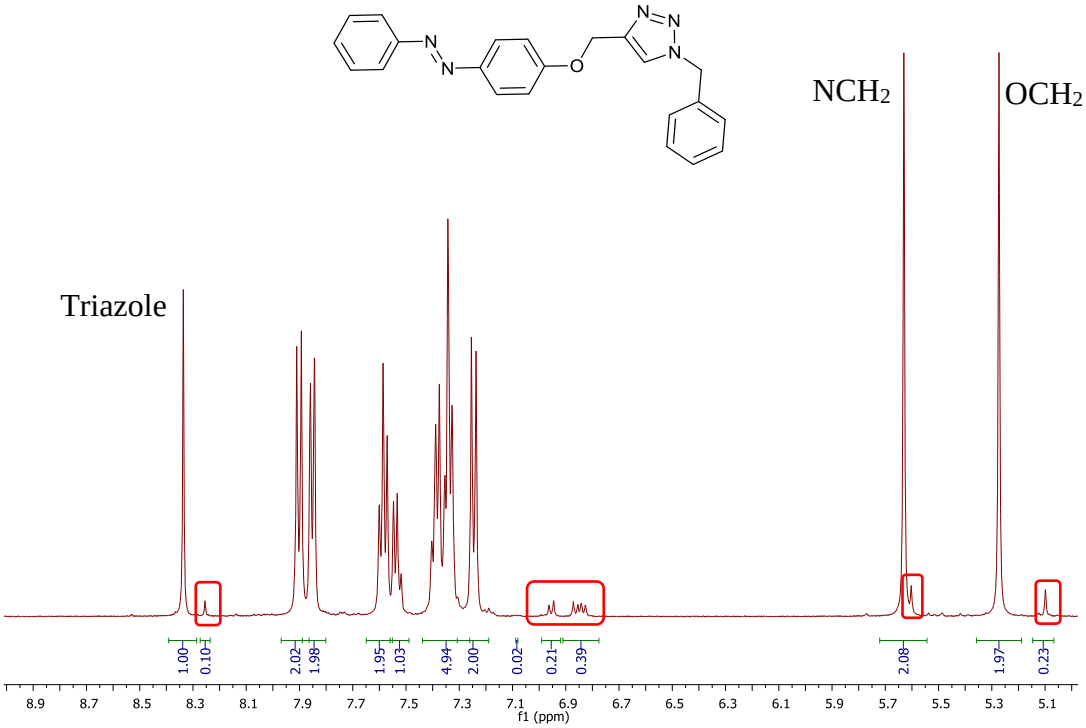

*Figure 34: Region of the ^{1}H-NMR spectrum of cycloadduct **156** showing the dominance of the trans isomer; signals attributed to the cis isomer are identified in red boxes (500 MHz DMSO-d_6)*

2.4 Synthesis of azobenzenes bearing a 1,3-dipole functionality

Following on from the successful synthesis and preliminary cycloaddition reactions of azobenzenes bearing dipolarophile functionalities, the next objective was to develop a range of substrates bearing one or more 1,3-dipole functionalities. The first targets were azobenzenes bearing oxime or chlorooxime groups as precursors to nitrile oxide dipoles. The development of azobenzenes with an azide functionality was also explored.

The first synthetic target was the oxime, **110**, a compound previously synthesised in the group. As summarised in scheme 36, it was accessed from 4-phenylazobenzoic acid, **158**.[184] The carboxylic acid was reduced to the primary alcohol, **159**, ($LiAlH_4$, diethyl ether) followed by controlled oxidation to the aldehyde, **160**, with PCC in DCM in the presence of molecular sieves. The molecular sieves are an important additive since various by-products of the reaction adhere to them allowing the aldehyde be more easily

purified. For example, when the reaction was conducted in the presence of molecular sieves purification by passing the mixture through a silica plug yielded the compound in 81% yield. In contrast, following reaction in the absence of molecular sieves **160** could be isolated in only 65% yield.

Successful oxidation of **159** was also achieved with catalytic amounts (5 mol %) of tetrapropylammonium perruthenate (TPAP) in the presence of *N*-methylmorpholine (NMM) and **160** was isolated in 78% yield. The catalyst was not recovered.

The oxime, **110,** was generated from the aldehyde **160** by reaction with hydroxylamine hydrochloride in ethanol, pyridine was added to liberate the free hydroxylamine.[185] Reaction was initially carried out on a small scale (1.25 mmol) in a Scientific Microwave ((T= 125 ˚C, P = 300 W, t = 1 hr) furnished **110** in 87% yield. However, the reaction scale was limited due to size of the microwave vessels.

The reaction was also successful of a larger scale (9.4 mmol) with conventional heating. The reaction mixture was heated to reflux for 4 hours, the oxime **110** was furnished in 83% yield. Satisfyingly, regardless of the heating method, the oxime **110** was easily isolated by precipitation following the addition of water to reaction solution. It was readily characterised by ^{1}H-NMR spectroscopy (300 MHz, $CDCl_3$); the imine proton resonated at 8.20 ppm.

The Ar-H resonances of **110** overlapped and signals for the and the individual aromatic hydrogens could not be unambiguously assigned. The sample presented as a single isomer about both the azo and oxime functional groups. Oxime stereochemistry is unconfirmed but on steric grounds is assumed to be anti, as shown in scheme 36, (as is the case for all oxime functional groups used in this study).

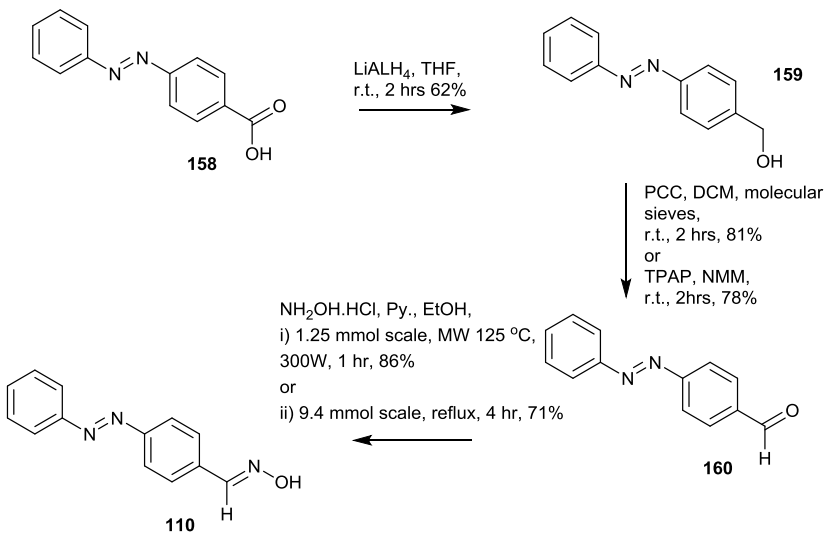

*Scheme 36: Synthesis of the oxime **110.***

The *meta* oxime **111** was also known in the group.[184] It was synthesised, as shown in scheme 37, starting with a Mills coupling between 3-aminobenzyl alcohol, **161**, and nitrosobenzene in the presence of glacial acetic acid to give 3-(phenylazo)benzyl alcohol, **162**. Oxidation to the aldehyde **163** was achieved with PCC in DCM in the presence of molecular sieves. Finally reaction of **163** with hydroxylamine hydrochloride in ethanol in the presence of pyridine yielded the desired oxime **111** as an orange solid, in 82%.[184]

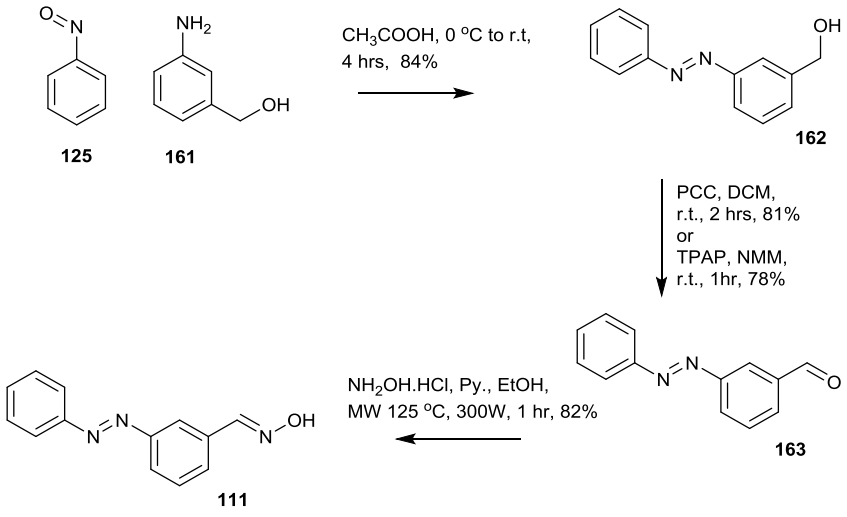

*Scheme 37: Synthesis of the oxime **111.***

To synthesise the symmetrical *bis*-oxime **116**, 4-nitrobenzaldehyde, **164**, was protected with ethylene glycol in the presence catalytic amount of *p*-TsOH.[186] The condensation reaction was conducted in toluene and a Dean-Stark trap was used to remove the water as formed so driving acetal formation to completion. The protected **165,** formed in 84% yield, was subjected to reductive coupling following reaction with $LiAlH_4$ (5eq.) in diethyl ether and **166** was formed in 86 % yield.[187] Deprotection and oxime formation were achieved in one step following treatment of **166** with hydroxylamine hydrochloride in ethanol in the presence of pyridine. Oximation was successful by both microwave (0.74 mmol scale, 53% yield) and conventional heating approaches (4 mmol scale, 44% yield). The compound **116** was found to be insoluble in chloroform, therefore NMR spectra were recorded in DMSO-d_6. The symmetrical compound showed two doublets for the aromatic protons; the imine resonance occurred at 8.26 ppm and the hydroxyl resonance at 11.57 ppm.

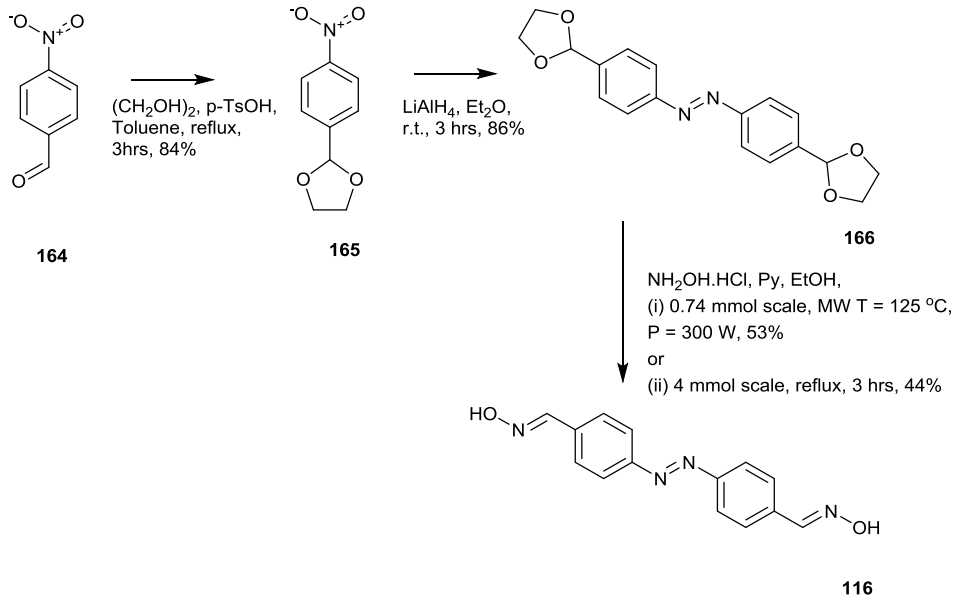

*Scheme 38: Synthesis of bis oxime **116.***

The only preparation of the *m,m*-bis-oxime **117** recorded in the literature involves the reduction of *m*-nitrobenzaldehyde, **167** using Zn power.[188] The paper is ambiguous about the exact reaction conditions, therefore the reported approach was not adopted for this work and a reaction sequence parallel to that used to synthesise *p,p*-dioxime **116** was explored in search of **117** (scheme 39). *m*-Nitrobenzaldehyde was protected with ethylene glycol in the presence of *p*-TsOH,[189] subsequently the nitro groups were reductively coupled ($LiAlH_4$, diethyl ether) to give the protected **169** in 59% yield.[187]

Direct conversation to the oxime **117** was effected by treatment with NH_2OH. However, unlike its *p,p*-derivative **116,** the pure product did not precipitate on addition of water. Instead, purification by flash chromatography was required to separate several minor by-products and **117** was isolated in a modest 48% yield.

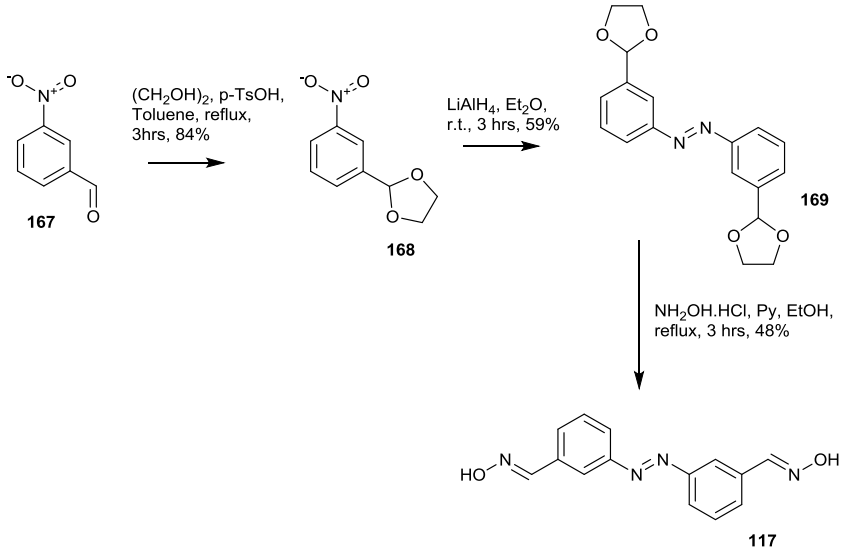

*Scheme 39: Synthesis of m,m-bis-oxime **117.***

4-Azidoazobenzene, **171**, known in the literature,[190] is an attractive target for facilitating direct comparison of the cycloaddition potential of azobenzene azides with azobenzene nitrile oxides. Its structure 'parallels' that of the nitrile oxide accessible from oxime **110**. Potential cycloadducts arising from both the dipoles would have the heterocycle attached directly to the azobenzene unit in the *para* position.

The azide **171** was synthesised from aminoazobenzene, **170**, in a one pot reaction with water as the solvent.[190] The intermediate diazonium salt, generated by reaction with sodium nitrite in the presence of *p*-TsOH, was directly reacted with sodium azide giving the desired product **171** as an orange/red solid in 89% yield, scheme 40.

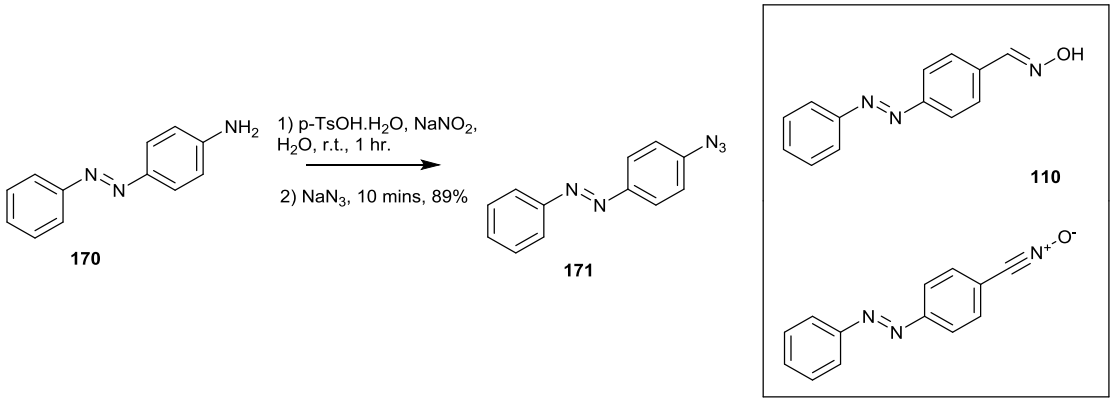

*Scheme 40: Synthesis of the azidoazobenzene **171.***

2.5 Preliminary cycloadditions of azobenzenes bearing a 1,3-dipole functionality

Propargyloxybenzene, **173,** was selected as a simple dipolarophile for investigating reaction conditions suitable for cycloaddition to azobenzene 1,3-dipoles. Its reaction with the *para* and *meta* azobenzene oximes **110** and **111** were previously known in the group;[184] 5 equivalents of either oxime was allowed to mix with chloramine-T in aqueous ethanol for 10 minutes at room temperature before addition of the alkyne and warming to 40 ˚C. A product yield of 89% was reported for the formation of **172** and 46% yield for its *meta* analogue formed via **route B1**, scheme 41.

The reaction of **110** with **173** was revisited to explore the effectiveness of dipole generation by the NCS/NEt_3 approach. Initially a one pot reaction was conducted, **route B2**, scheme 41. Initial conversion of oxime **110** to the hydroximinoyl chloride effected by treatment with NCS in DMF. After 1 hour NEt_3 was added to effect the conversion to the nitrile oxide. The resulting mixture was stirred at room temperature for eight hours. The cycloadduct **172** was ultimately isolated in 73% yield. which is slightly less than the 89% achieved by the Ch-T approach.

In a second experiment (**route A**, scheme 41), the hydroximinoyl chloride **174** was preformed and isolated (81%) prior to dipole formation (NEt_3) and reaction with the alkyne **173**. In this case, the cycloadduct **172** was isolated in 76%. This corresponds to a reduced 62% yield over the two steps starting from oxime **110**.

The ^{1}H and ^{13}C-NMR spectral data for **174** are interesting and show both *cis* and *trans* isomers ($CDCl_3$, 500 MHz). The ^{13}C NMR spectrum of **174** is expected to show nine resonances, five Ar-C and four quaternary carbon signals. Ar-CH signals are seen for the major isomer at 122.9, 123.1, 128.0, 129.2 and 131.6 ppm and for the minor isomer at 120.5, 120.7, 127.8, 128.1 and 128.9 ppm. The quaternary carbons appear at 134.4, 139.4, 152.6 and 153.7 ppm for the major isomer. The quaternary signals for the minor isomer were not observed. The 1H-NMR data suggests two isomers are present in a 5:1 trans to cis ratio .

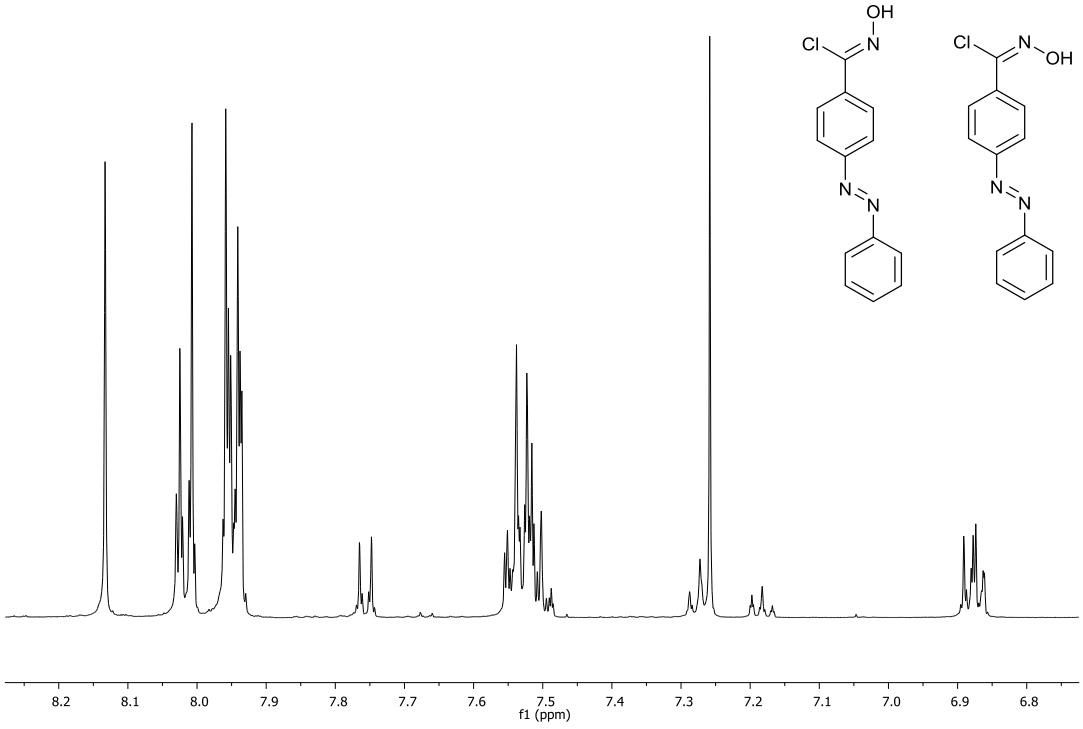

Figure 35: Aromatic region of the ^{1}H-NMR spectra of 174, showing complex multiplicity ($CDCl_3$).

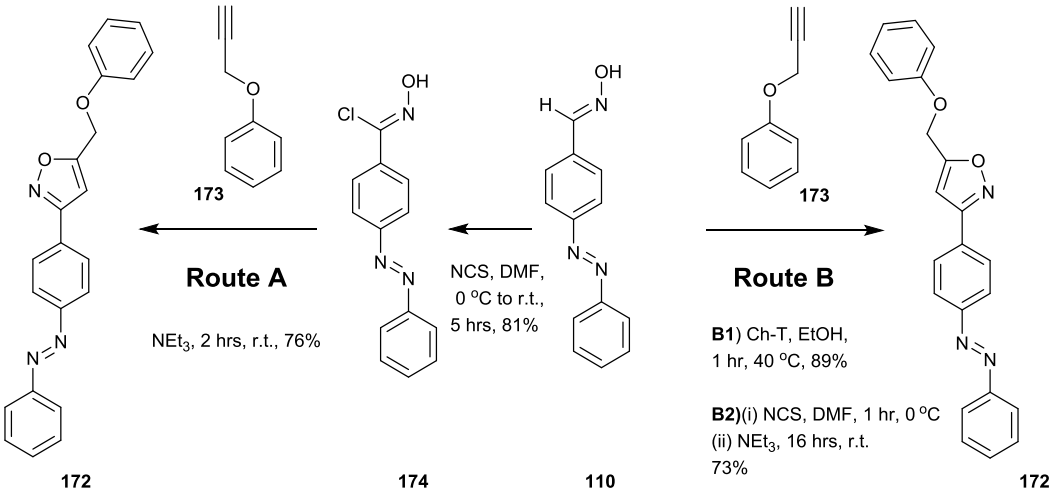

*Scheme 41: Synthesis of the cycloadduct **172.***

The *p,p*-bis oxime **116** was selected as a test case compound to study the potential for formation of divalent conjugates. Substrates with two nitrile oxide functionalities are potentially difficult to work with. To promote good cycloadduct yields from NOAC reactions, in particular to negate any loss of dipole due to dimerization side reactions, the nitrile oxide is generally used in excess. Substrates with two nitrile oxide groups have a much greater propensity for side reactions including dimerization and polymerisation. To minimise self-reaction of the dipole during cycloaddions, an excess of the dipolarophile is generally used.[191,192]

The *bis*-oxime **116** was treated with chloramine-T in an ethanol/water mixture, followed by addition of three equivalents of propargyloxybenzene, **173**, i.e. 50% excess per dipole. The reaction solution was warmed to 40 ˚C for four hours ,table 1, **A1**. Analysis of the crude product by ^{1}H-NMR spectroscopy revealed a complex mixture with no evidence for the formation of the desired *bis* isoxazole **175**, scheme 42.

The reaction was repeated and the dipolarophile excess increased to six molar equivalents (i.e. 3 functional group equivalents) (**A2**). However, the reaction still resulted in formation of a complex mixture. In a third attempt more forcing conditions were applied and the reaction mixture was heated to reflux (**A3**). Again no evidence of the formation of cycloadduct **175** was observed in the ^{1}H-NMR spectrum of the crude product mixture, scheme 42.

The failure to produce **175**, from the reaction between oxime **116** and Ch-T lead us to explore reaction with the *bis*-hydroximinoyl chloride **176,** was synthesised in 72% yield

from **116** by the additions of six molar equivalents (or three functional group equivalents), of NCS in DMF.

The ^{1}H-NMR spectrium of **176**, like its precursor **116**, shows it exists as a single geometric isomer with a pair of AB doublets for the aromatic protons. The hydroxyl proton appears at 12.75 ppm, figure 35.

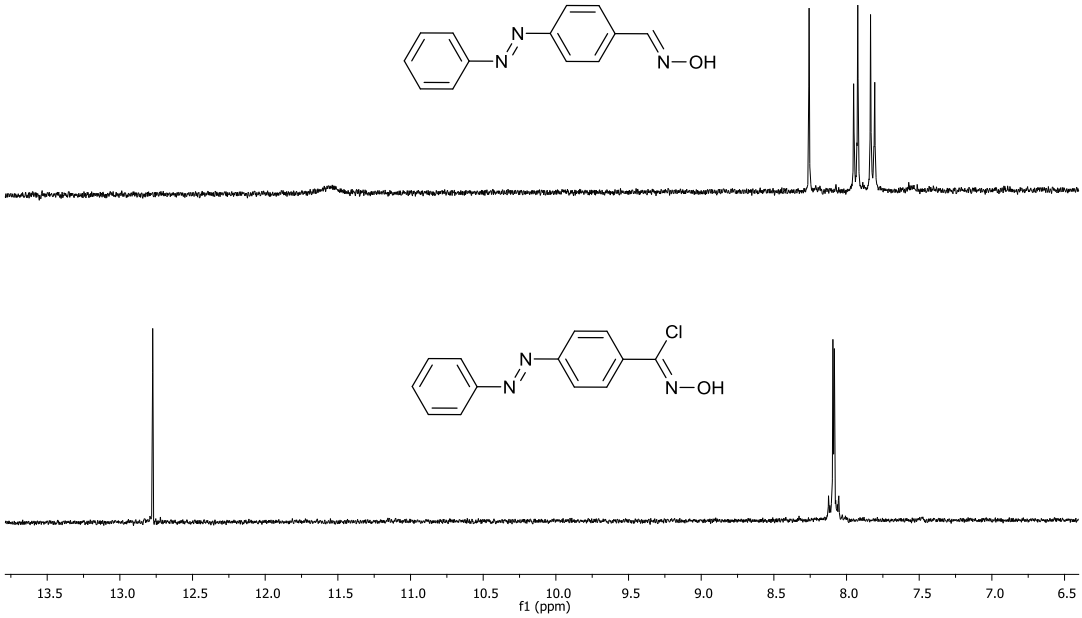

*Figure 36: Overlaid ^{1}H-HMR spectra of the bis-oxime **116** (upper) and its chlorooxime derivative **176** (lower) (DMSO-d_6, 500 MHz).*

The *bis*-chlorooxime **176** was reacted with a six molar equivalents of **173**, i.e. a 3:1 functional group ratio, in the presence of triethylamine, scheme 42 and table 1, route **B1**. Analysis of the ^{1}H-NMR spectrum of the crude material indicated a complex mixture with limited evidence of the desired product **175**, which was finally isolated in just 2% yield after separation by flash chromatography.

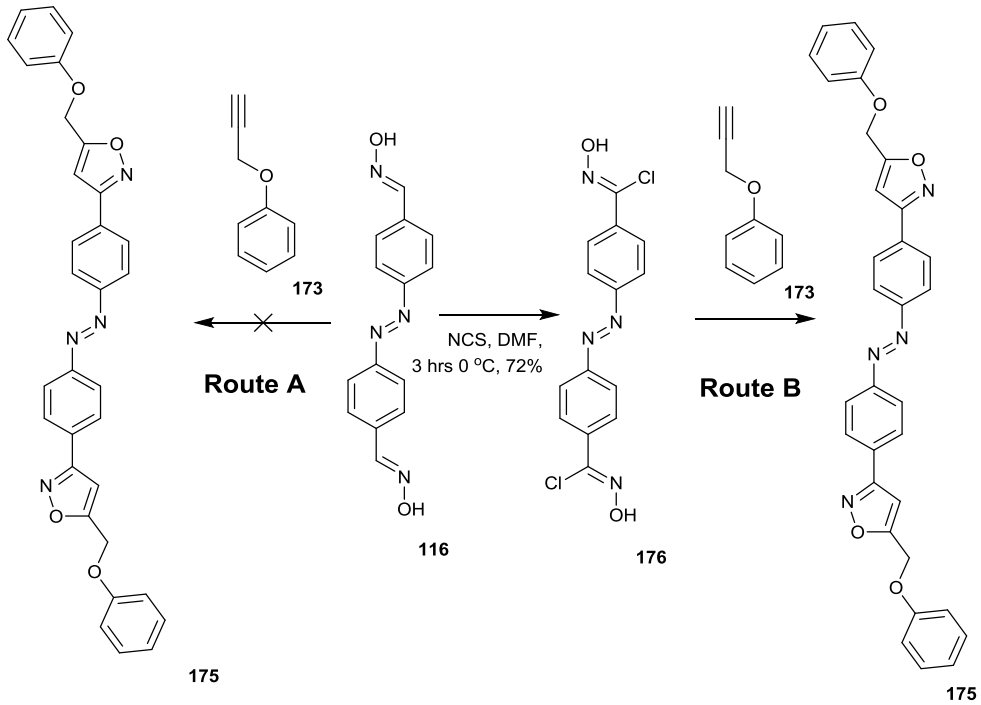

*Scheme 42: Attempted synthesis of **175** with Ch-T and successful synthesis of **175** via **176**, details of explored conditions for route **A** and **B** shown in table 1.*

A search of the literature for NOAC reactions with substrates bearing two or more hydroximinoyl chlorides revealed that slow addition of base reduces the rate at which the nitrile oxide forms and so limits side reactions e.g. dimerization or polymerisation.[191]

In an attempt to optimise the reaction leading to **175,** a solution of NEt_3 in ethanol was slowly added over 40 minutes to the *bis*-hydroximinoyl chloride **176** and the alkyne **173** (**B2**). This revised protocol, resulted in a much improved 21% yield.

Another publication suggested the yields of NOAC reactions may be increased by conducting the reaction under more forcing conditions such as heating to reflux in toluene.[193] All the reagents **176**, **173** (3 mol eq.) and NEt_3 were combined at once and heated to reflux in toluene, after 24 hours **175** was isolated in an increased 32% yield (**B3**).

In an attempt to further increase the yield of **175** an experiment was designed which combined elements of both these approaches. A solution of NEt_3 in ethanol was slowly added to **176** and **173** (3 mol eq.), followed by heating to reflux for 20 hours (**B4**). In this case, **175** was obtained 46% yield.

The appearance of a isoxazole proton resonance, assigned as the singlet at 6.73 ppm, together with the shift in the resonance of the OCH_2 protons, from 4.70 ppm in the starting alkyne to 5.25 ppm in the cycloadduct are consistent with regiospecific formation of the 5-substituted isoxazole at each end of the molecule.

*Table 1: Experimental conditions explored for the synthesis of **175.***

Experiment number	Starting material	Solvent	Con[c] 116/175 (mol/L)	Dipole precursor: alkyne ratio[ǂ]	Reaction duration (hrs)	Temp (˚C)	Out come (isolated product)
A.1	Oxime **116**	EtOH	0.11	1:3	4	40	No **175**
A.2	Oxime **116**	EtOH	0.11	1:6	4	40	No **175**
A.3	Oxime **116**	EtOH	0.11	1:3	4	78	No **175**
B.1	Chloro-oxime **176**	EtOH	0.046	1:6	20	r.t.	**175** - 2% yield
B.2	Chloro-oxime **176**	EtOH	0.046	1:6	20*	r.t.	**175** - 21% yield
B.3	Chloro-oxime **176**	Toluene	0.015	1:6	24	110	**175** - 32% yield
B.4	Chloro-oxime **176**	EtOH	0.046	1:6	20*	83	**175** - 46% yield

[ǂ] Dipole precursor: alkyne ratio is the number of mole equivalents of alkyne to each dipole precursor. Since the oxime **116** or chlorooxime **176** potentially furnish 2 equivalents of nitrile oxide, a 1:3 molar ratio of ratio implies a ratio of 2:3 alkyne to dipole precursor in terms of functional groups,

*In these experiments NEt_3 was added slowly over a 40 minute period, using a syringe pump.

2.6 Attempted synthesis of *o*-azobenzene oximes and resulting indazole formation

With the *p*- and *m*-azobenzene oximes **110** and **111** successfully synthesised, the *o*-isomer **112** was targeted to complete the regiosomeric series. At the outset of this investigation, it was known that the route developed for the *p*- and *m*-derivatives was not suited to the generation of **112.**

It had been noted in the group, the aldehyde **179** could not be obtained by oxidation of the hydroxymethyl precursor and reaction with DMP resulted in formation of a colourless compound, scheme 43. The loss of colour indicated a reaction in which the azo group had been consumed. Subsequently analysis by X-ray crystallography showed the product of the reaction between **178** and DMP to be the 2-phenyl-*2H*-indazole, **180**.[194]

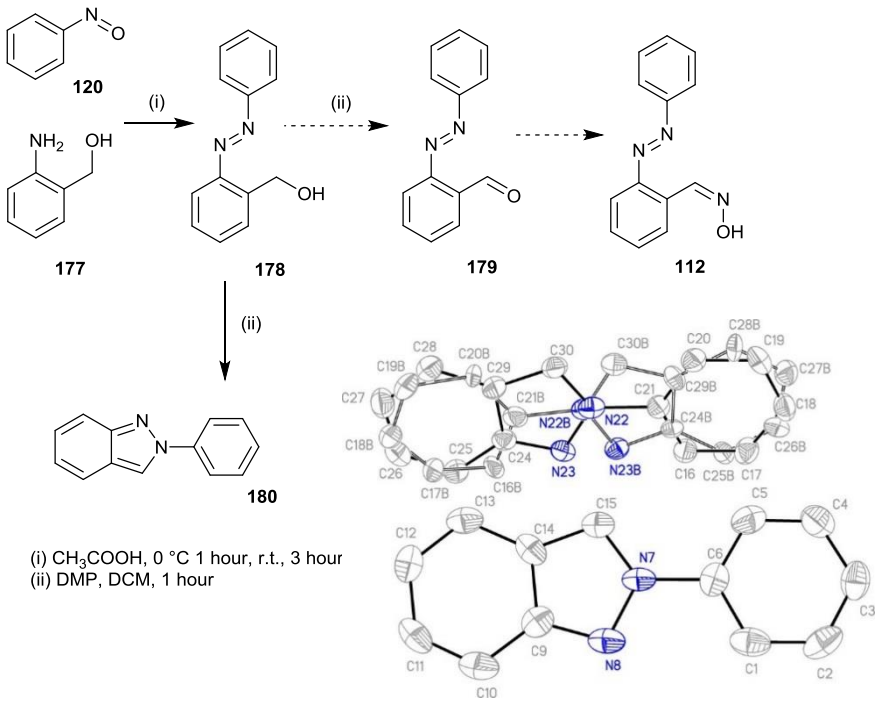

*Scheme 43: Synthetic route planned to access **112;** formation of the indazole **180.**[184]*

Whilst the mechanistic details for the generation of **180** from **178** are unknown, several papers report indazole formation from azo substrates. For example, Xi created the same

indazole **180** in a reaction involving an initial rhodium catalysed insertion of an olefin *ortho* to the azo linkage, prior to cyclisation as shown in scheme 44, **route A**.[195] An second group report I_2 mediated attack of the azo linkage on an *ortho* methyl group **route B**, as shown in scheme 44, Route B.[196]

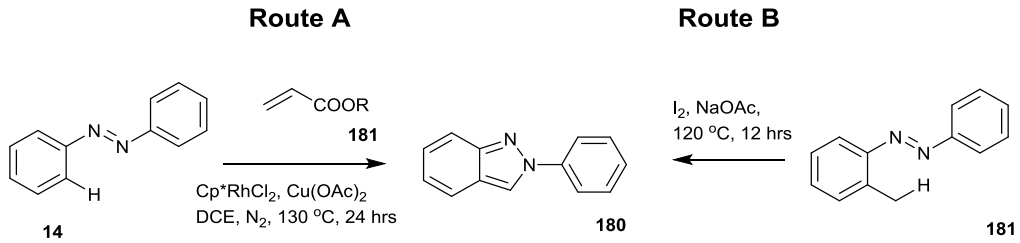

Scheme 44: Indazole formation from azobenzene substrates.[195,196]

It is further reported that nucleophilic azo attack of azobenzenes bearing adjacent electrophilic centres readily furnishes the indazole skeleton.[197,198] In particular, Hecht et al. observed cyclisation of the acetal **182** during an attempted deprotection with 1M HCl in acetone, scheme 45**.** They proposed indazoles **183** and **184** arose by pathways **A** and **B** respectively involving attack of the azo group on an adjacent oxonium species (**route A**) or on a protonated aldehyde **(route B**).[199]

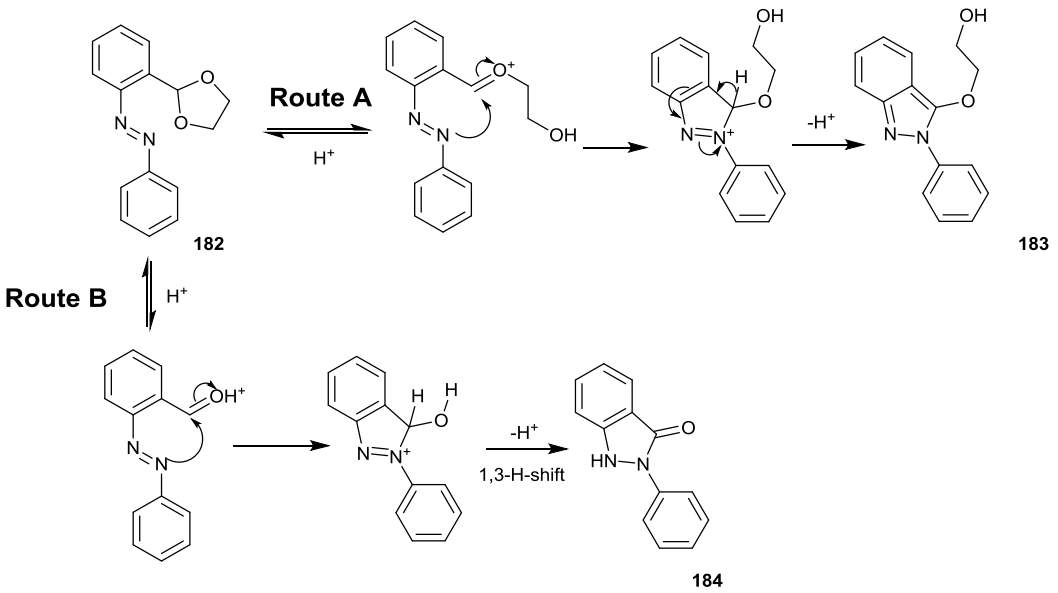

*Scheme 45: Mechanism of formation of indazoles **183** and **184** from acid induced reactions of **182.***

With Hecht's work in mind, we sought a new synthetic route to oxime **112** which would avoid the potential incompatibility between the proximate aldehyde and the azo functional group of **179**. A Mills coupling between nitrosobenzene **125** and 2-amino benzaldehyde oxime **186** was planned, as shown in scheme 46.

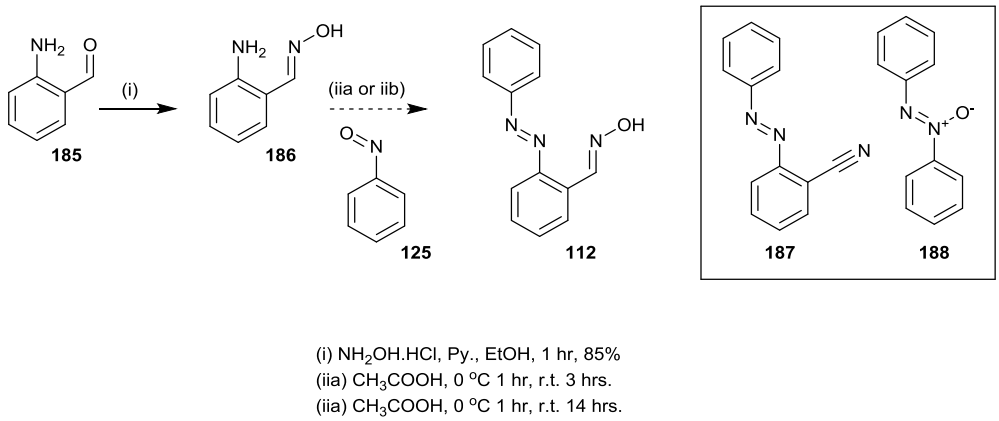

(i) $NH_2OH.HCl$, Py., EtOH, 1 hr, 85%
(iia) CH_3COOH, 0 °C 1 hr, r.t. 3 hrs.
(iia) CH_3COOH, 0 °C 1 hr, r.t. 14 hrs.

*Scheme 46: Attempted synthesis of oxime **112** and isolated by-products.*

2-Aminobenzaldehyde **185** was converted in good yield to the required oxime **186**.[200] It was subsequently treated with nitrosobenzene **125** under typical Mills coupling reaction conditions.[201,202]

Initially oxime **186** was added to nitrosobenzene, **125,** in glacial acetic acid. After an hour at 0 °C, followed by 3 hours at room temperature, the crude mixture was analysed by ^{1}H-NMR spectroscopy.[201] The data failed to support the formation of the desired product, there was no peak observed for the expected aryl aldoxime C<u>H</u>=NOH which would typically be a singlet between 7.5-8.5 ppm. The following compounds were isolated following separation by flash chromatography: *o*-cyanoazobenzene **187** (9%), azoxybenzene **188** (6%) and unreacted oxime **186** (28%). The cyanoazobenzene **187**[203] and azoxybenzenes **188**[198] are known compounds and the ^{1}H NMR spectra of the isolated materials match those reported in the literature.

The mechanistic origins considered for formation of **187** are summarised in scheme 47; it may have arisen either from the dehydration of the starting oxime leading initially to the aminonitrile **189** followed by Mills coupling (**path A**) or by dehydration from the targeted product **112**, **path B** scheme 47.[204-206] There is literature precedence for the dehydration of an aryl aldoxime following heating first to reflux in acetic acid, and then in acetic acid in the presence of hydrochloric acid.[207] Aldoxime dehydration has also

been observed under basic conditions[208] and has been promoted by a variety of catalysts.[209,210] In one example dehydration of a dimethlyamino analogue of **112,** has been observed upon treatment with $CuSO_4$, NEt_3 and DCC in chloroform.[211]

To explore the possibility that **187** involved initial oxime dehydration, a solution of oxime **186** was stirred at room temperature in glacial acetic acid for 3 hours (73 mmolar, 0.73 mmol scale). After this time, the oxime was returned in quantitative yield, ruling out the possibility that **189** was an intermediate en route to the cyanoazobenzene **187**, **path A**, scheme 47.

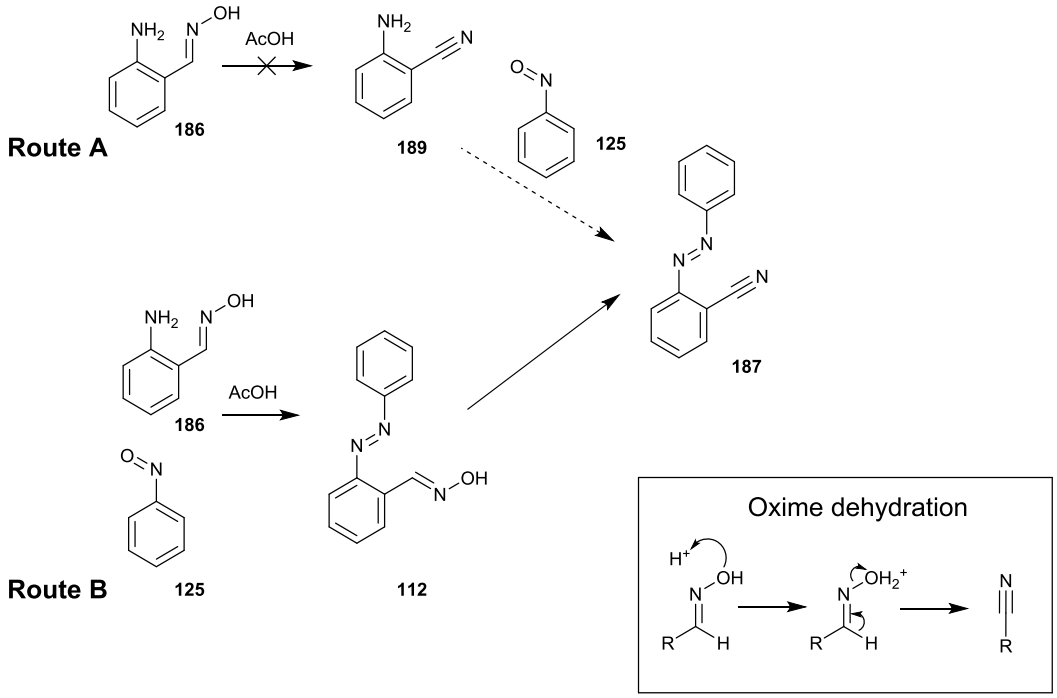

*Scheme 47: Possible routes to o-cyanazobenzene **187** from the reaction between aminobenzadehyde oxime and nitrosobenzene.*

The failure of **186** to dehydrate on exposure to acetic acid may be explained by the examining the relative pKas of its amine and the oxime functional groups.[212,213] It is likely that the more basic amine is the preferred site of protonation, making acid induced oxime dehydration of **186** unlikely. It remains possible that the reaction between **125** and **186** did lead to **112** and that it its dehydration accounts for the failure to isolate **112**.

In considering the origin of azoxybenzene **189**, we have found that there is precedence for formation azoxy products from the coupling of anilines and nitrosobenzenes under typical Mills coupling conditions, for example, the highly substituted **192** resulted from

the reaction between diaminodurol and 4-(dimethylamino)nitrosobenzene, as shown in scheme 48.[214] However, the origin of the azoxy derivative **189,** from the reaction between **186** and nitrosobenzene is not easily accounted for since in addition to coupling, the mechanism must account for loss of the oxime functional group for **193** or one of its derivatives as shown in scheme 49, **route A**. However, whilst the elimination of oxime functional groups under flash vacuum pyrolysis has been observed[215] such as reaction is not likely under the conditions employed in this experiment.

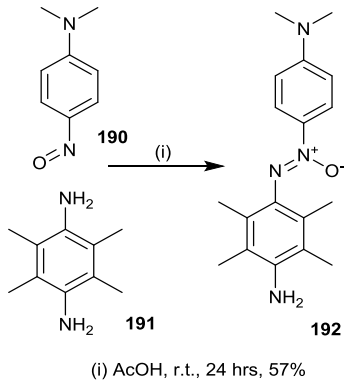

*Scheme 48: Reaction between diaminodurol and 4-(dimethylamino)nitrosobenzene under Mills conditions leading to the azoxy dervitive **192**.*

It could also be considered that azoxybenzene **189** may have resulted from self-reaction of nitrosobenzene, scheme 49 **route B.**[216,217] However, such couplings normally require drastic conditions, for example, treatment with elemental carbon in an arc reactor.[218] These conditions are very forcing compared to those employed in our experiments and nitrosobenzene dimerization is not the likely origin of the unsubstituted azoxybenzene **189**.

Finally, **189** may be considered to arise from reaction between one molecule of nitrosobenzene with a molecule of phenyl hydroxylamine **194**, generated in situ by reduction of nitrosobenzene, scheme 49, **route C**.[217]

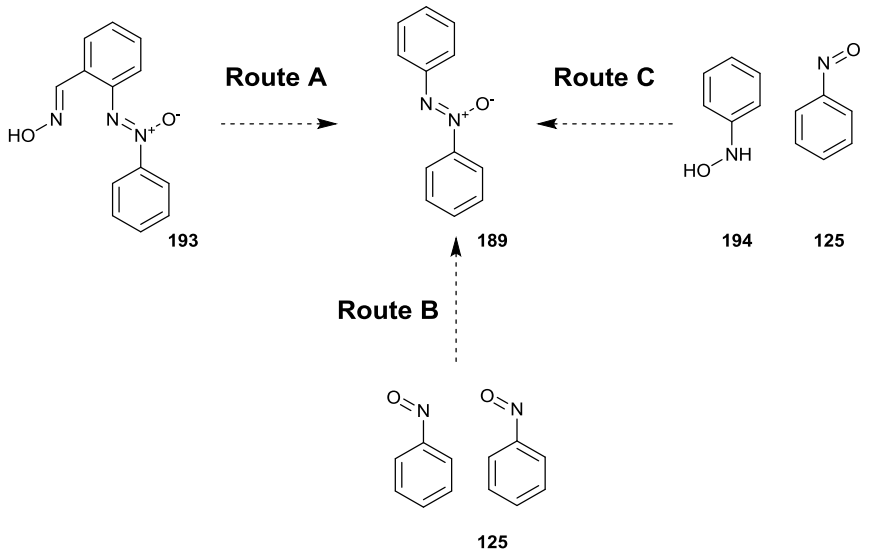

*Scheme 49: Proposed mechanistic origins of azoxyazobenzene **189.***

In a second experiment targeting the *ortho* substituted azobenzene aldoxime **112,** the Mills coupling reaction between the amino oxime **186** and nitroso benzene was repeated and its duration was extended to 14 hours. Following flash chromatography the reaction products were the starting oxime **186** (15%), azoxybenzene **187** (28%), and *o*-cyanoazobenzene **188** (24%). The desired product was not found in the mixture.

The failure of the Mills approach to furnish **112** prompted a change in direction and the symmetrical dioxime **118** was the new target. The approach to **118** was centred around a reductive coupling of the acetal protected nitrobenzaldehyde **196**, shown retrosynthetically in scheme 50. Aldehyde protection was used to avoid potential cyclization between azo and aldehyde functionalities. It was hoped that direct conversion from the acetal **197** to the bis-oxime **118** would be possible. If the oxime was insufficiently electrophilic indazole formation could be prevented and **118** could be isolated from the reaction.

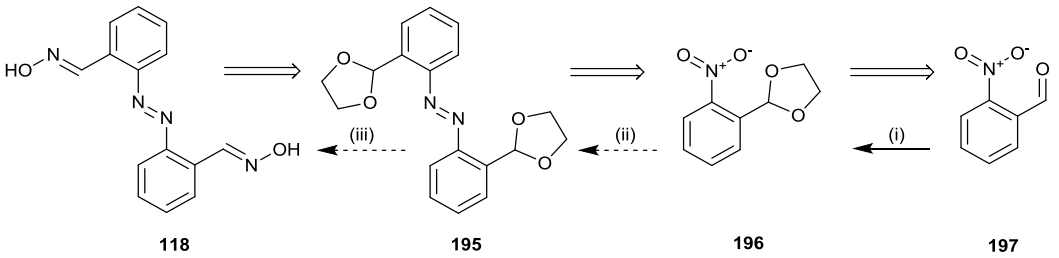

(i) Ethylene glycol, p-TsOH, toluene, reflux, 3 hrs.
(ii) $LiAlH_4$, Et_2O, -82 °C to r.t., 3 hrs.
(iii) $NH_2OH.HCl$, EtOH, Py., reflux, 14 hrs.

*Scheme 50: Retrosynthetic route and proposed forward reaction for formation of the bis-oxime **118**.*

Treatment of *o*-nitrobenzaldehyde **197** with ethylene glycol in the presence of an acid catalyst gave the acetal protected **196** in 64% yield.[186] $LiAlH_4$ in diethyl ether was used in the attempted reductive coupling of **196**[187] and reaction work up involved the addition of dilute sulphuric acid. ^{1}H-NMR spectroscopic analysis of the orange coloured crude products showed a complex mixture. However, a singlet at 5.55 ppm ($CDCl_3$) was interpreted as potentially representing the acetal CH proton of **195**. The upfield shift of this signal compaired to the corresponding proton in the starting **196** (6.32 ppm in $CDCl_3$) was thought to be in keeping with transformation of the nitro group of **196** to the less electron withdrawing azo group of **195**.[217] Encouraged by the orange colour and the appearance of the new 'acetal CH singlet' in ^{1}H NMR spectrum, the product mixture was treated with hydroxylamine hydrochloride without purification in an attempted one step deprotection/oximation sequence.[185] The crude mixture from this reaction was analysed by ^{1}H NMR spectroscopy and was found to comprise of one major, asymmetric product, which was isolated as a colourless solid following trituration with diethyl ether and pet. ether.

The ^{1}H-NMR spectral data of this colourless product included singlets at 7.79 and 11.52 ppm, characteristic of the CH and OH resonances of an oxime. A further ^{1}H singlet resonance at 8.73 ppm and ^{13}C resonances at 122.4, 128.8, 139.4 and 149.4 ppm, together with the lack of colour a suggested the product may have been the oxime indazole **198** (figure 36).

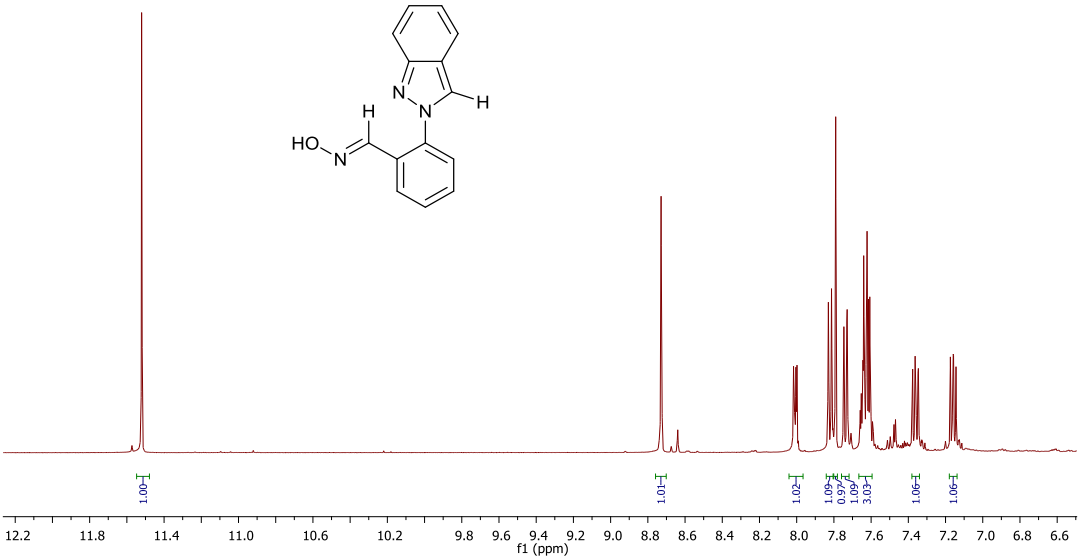

*Figure 37: ^{1}H-NMR spectrum of indazole **198** (DMSO-d_6, 500MHz).*

The structure was unambiguously identified as **198** following analysis by x-ray crystallography, figure 37. Crystals were grown by the vapour diffusion technique. The compound was dissolved in methanol and slow diffusion of chloroform allowed quality crystals to be obtained. The crystallographic data showed that the phenyl ring is rotated roughly 35˚ out of the plane of the bicycle. The packing diagram shows intermolecular hydrogen bonding between the hydroxyl of one oxime and the N-2 nitrogen atom of the indazole of another molecule (N···H-O distance 2.785 Å).

To avoid the possibility that **198** resulted from cyclisation of **195** induced by the acid used in work up of the $LiAlH_4$ reduction reaction, the coupling experiment was repeated and the reaction work up based around the Fieser method of quenching.[219] involving quenching of excess $LiAlH_4$ by slow addition of water and NaOH followed by removal of the salts by filtration. Surprisingly, under the modified experimental conditions the indazole **198** was once again the major product from the reaction (46% yield).

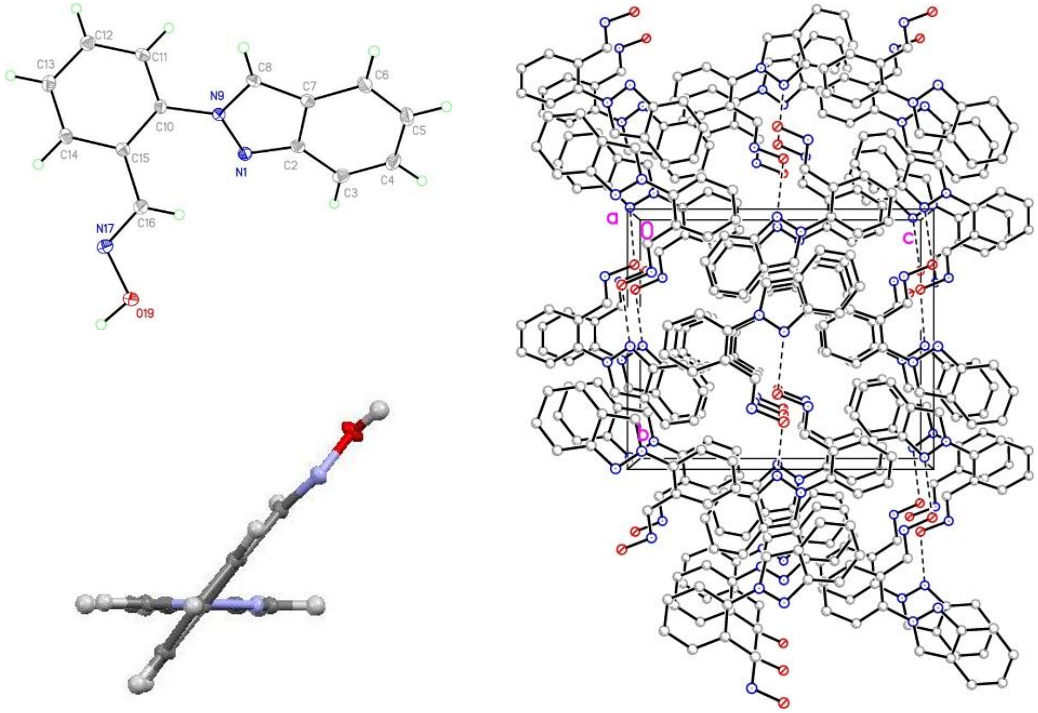

*Figure 38: **Left**: Molecular structure of **198** with atomic displacement parameters shown at 50% probability; **right**: Packing diagram of **198** viewed down the a-axis. Hydrogen atoms omitted for clarity.*

It is difficult to be unambiguous about the mechanistic origin of indazole **198**, however, the lack of a 2-oxo or a 2-hydroxyethoxy substituent suggests it did not form by mechanisms parallel to those suggested by Hecht et al. for the mono-protected analogue **182**, scheme 45.

To reduce the potential for azo-cyclization and to promote formation of **118**, we wanted to avoid intermediates bearing aldehyde functional groups. Direct reductive coupling of *o*-nitrobenzaldehyde oxime **199** was investigated.

o-Nitrobenzaldehyde, **197**, was converted to oxime **199** and its potential as a precursor to **118** was explored under a range of conditions, scheme 51.[185] $LiAlH_4$ promoted reductive coupling of **199** in diethyl ether produced a complex mixture of products, the ^{1}H-NMR spectrum was not consistent with survival of the oxime group, scheme 51 (ii). In a second experiment KOH was used as the coupling promotor and the reaction was conducted using the conditions which had been successful in the reduction producing **113** (300 ˚C).[220] Analysis of the resulting complex mixture by ^{1}H-NMR spectroscopy failed to support the formation of the **118**, scheme 51 (iii).

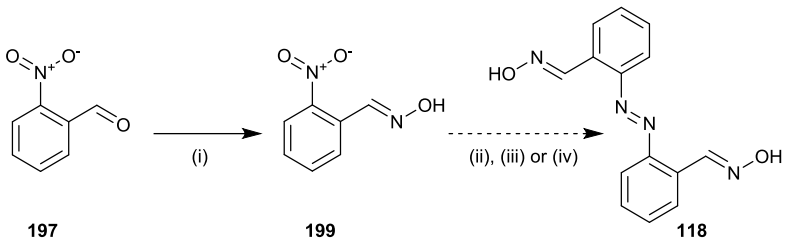

(i) $NH_2OH.HCl$, py. EtOH, 3 hrs., reflux, 86%
(ii) $LiAlH_4$, Et_2O, -82 ^oC to r.t, 4 hrs.,
(iii) KOH, H_2O, 300 ^oC, 4 hrs
(iv) $NaBH_4$, DMSO, 80 ^oC, 5 mins - 24 hrs

*Scheme 51: Attempted formation of bis-oxime **118** by reductive coupling of 2-nitrobenzaldehyde oxime.*

The reductive coupling of **199** was further explored with $NaBH_4$, scheme 51 (iv). The reduction was first attempted at low temperature (-82 °C) in diethyl ether. Under these conditions unreacted oxime was returned. There is literature precedence for $NaBH_4$ promoted azobenzene formation in DMSO at 80 °C from a wide range of aromatic nitro compounds.[221] Reaction of **199** with $NaBH_4$ was repeated at 80 ˚C (DMSO). At shorter reaction times (t = 5 mins - 1.5 hrs), the starting oxime was returned, at longer times (t = 6-24 hrs) complex mixtures were produced. ^1H NMR spectral data of a number of isolated products supported the presence of the starting oxime **199**, 2-aminobenzaldehyde oxime, **186**[200] and benzaldehyde oxime, **103**, as the main contributors in the product mixtures.[222]

In a further attempt to access **118,** a final year student doing a research project in the laboratory explored a reductive coupling of **196** employing zinc and hydroxide, scheme 52 (**ii, a**).[223] After flash chromatography of the complex product mixture, small orange crystal were isolated directly from the column fractions (diethyl ether : pet. ether, 1:1). Analysis by x-ray crystallography unambiguously identified the structure as 2,2'-(1,3-dioxolane)azobenzene (**195**). The structure, shown in figure 38, indicates in the solid state, as expected, the azo functional group adopts the *trans* geometry. Disappointingly the isolated yield was small. No other products were identified from the complex mixture.

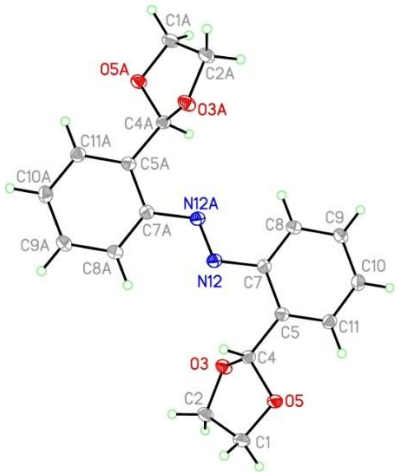

*Figure 39: Molecular structure of **195** with atomic displacement parameters shown at 50% probability.*

The ^{1}H-NMR spectrum of **195** showed the acetal proton resonance ~0.5 ppm downfield of the corresponding signal in the starting material **196.** Thus negating the earlier interpretation that the azoacetal **195** was an intermediate species present amongst the products of $LiAlH_4$ reduction of **196**, (scheme 50) the species identified in that reaction, with the upfield singlet resonance remains unidentified.

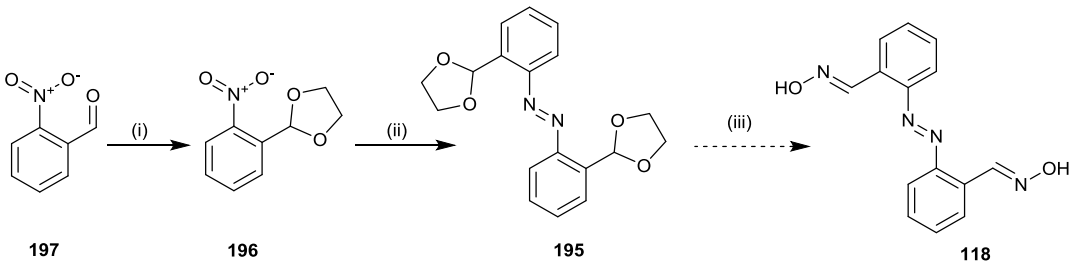

(i) Ethyl glycol, p-toluenesulfonic acid, toluene, reflux, 3 hours.
(ii, **a**) Zn (2 eq.), NaOH, EtOH/ H_2O, 3 hrs, reflux, trace amounts
(ii, **b**) Mg (5 eq), MeOH, 30 mins, reflux, 14%
(ii, **c**) Mg (5 eq), MeOH, 16 hrs, reflux, 11%
(ii, **d**) Mg (10 eq), MeOH, 30 mins, reflux, (over reductionl)
(ii, **e**) Zn (10 eq.), NaOH, EtOH/ H_2O, 3 hrs, reflux, azoxy product
(ii, **f**) Zn (20 eq.), NaOH, EtOH/ H_2O, 3 hrs, reflux, complex mixture
(iii) $NH_2OH.HCl$, Py., EtOH, 3 hrs, reflux

*Scheme 52: Attempted synthesis of the bis-oxime **118.***

The reductive coupling of nitroaryl compounds was also reported with Mg in MeOH.[224] In an attempt to access **195** in higher yields, **196** was heated to reflux with five mole equivalents of magnesium (30 mins) scheme 52 (**ii, b**), the masked aldehyde **195** was isolated in 14%. To try to improve the yield further, the reaction was repeated on the same scale but was heated to reflux and left at this temprature overnight, scheme 52 (**ii, c**), however, the yield did not improve. The reaction was also repeated with double the

quantity of magnesium, scheme 52, (**ii, d**) however in this case over reduction of the nitro group occurred and protected aminobenzaldehyde oxime was observed as the major product. In this case none of the desired **195** could be isolated from the experiment.

Since the yields of **195** isolated from the magnesium induced reductions were so modest, the reduction of **196** was repeated with an increased quantity of zinc (10 eq.).[225,226] Following 3 hours of reaction time, the ^{1}H-NMR spectrum indicated the starting material was completely consumed, however the known azoxy product, **200**,[225] dominated the product mixture. In a subsequent experiment, the reaction was repeated with 20 equivalents of zinc to facilitate the conversion of any of the intermediate azoxy **200**. The ^{1}H-NMR spectrum showed a complex mixture formed with no identifiable products.

The protected azoxy **200** was successfully converted to the novel di-oxime **201** by treatment with hydroxylamine in the presence of pyridine in ethanol when the solution was heated to 125 ˚C in a Scientific Microwave, scheme 53. The *bis* oxime, isolated in 86% yield does not undergo intramolecular cyclisation as azoxy groups have quite different reactivity to their azo analogues.[226,227]

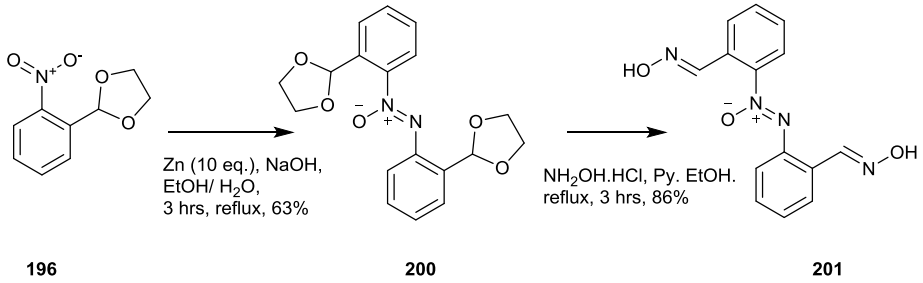

*Scheme 53: Reductive coupling leading to the azoxybenznene **200** and its subsequent conversion to bis-oxime **201**.*

Due to the failure of the various experiments designed to access either the *o*-oxime **112** and the *o,o*-bis-oxime **118** and because of the potential problems of intramolecular cyclisation or possible issues with intermolecular cycloaddition of an azobenzene bearing in *ortho* substituted nitrile oxide (scheme 54), a decision was made to abandon the pursuit of azobenzenes with oxime functional groups in the positions *ortho* to the azo bond.

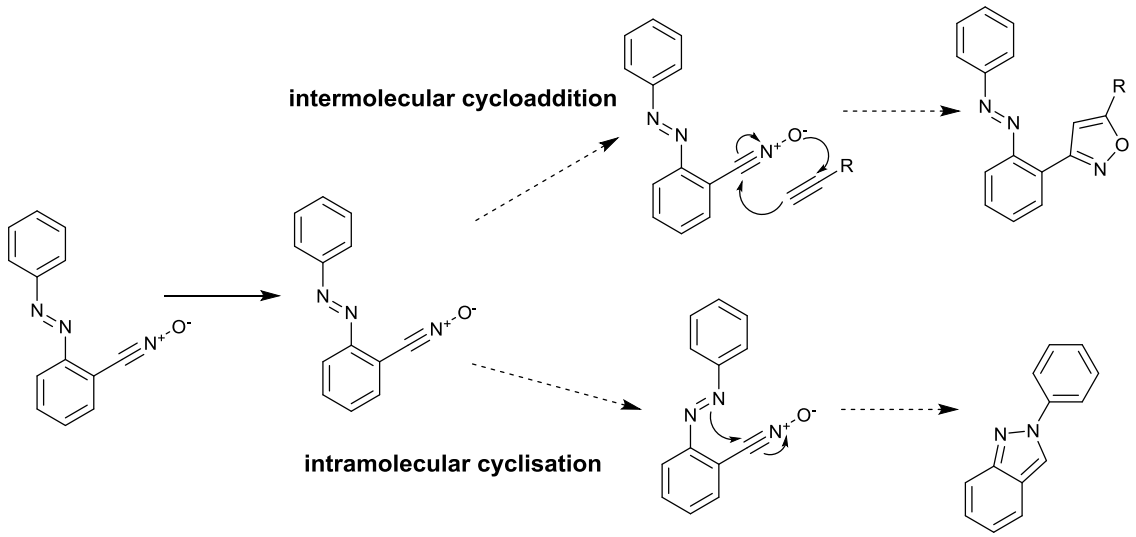

Scheme 54: Potential intramolecular cyclisation and intermolecular cycloaddition reactions of an azobenzene with ortho substituted nitrile oxide.

It was noticed during TLC analysis that the indazole oxime **198** was weakly fluorescent and its fluorescence emission spectrum was recorded in THF (12 µM), figure 39.

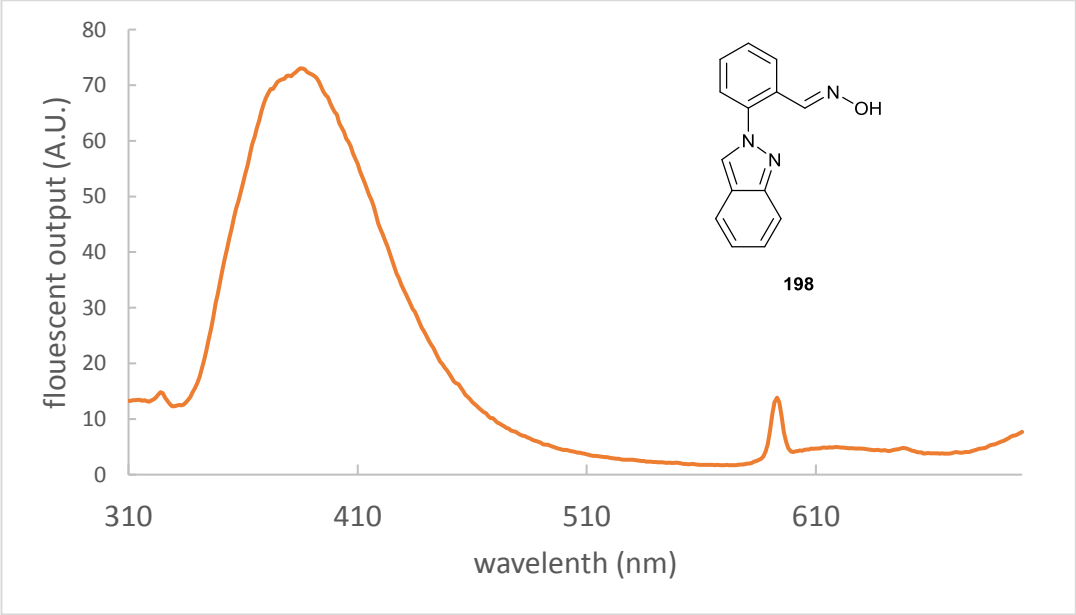

*Figure 40: Fluorescence emission spectrum of Indazole **198** (12 µM, THF, ex. 295 nm).*

It was proposed that the oxime of **198** might provide handle to introduce a fluorescent indazole tag on a substrate of interest. Several attempts were made to promote NOAC reaction between **198** and propargyloxybenzene (**173**), scheme 55. The oxime **198** was

treated with Ch-T in ethanol before addition of the alkyne and stirring for 16hrs. The resulting product was dominated by the starting oxime **198**. In a second experiment, chlorination of **198** with NCS in DMF was attempted, however, a complex mixture resulted. In a final experiment a one pot chlorination/dehydrochlorination cycloaddition sequence was explored. Treatment with NCS in DMF for an hour followed addition of the alkyne **173** and finally the slow addition of triethylamine also resulted in a complex mixture with no evidence of isoxazole formation in the ^{1}H-NMR spectrum of the crude product.

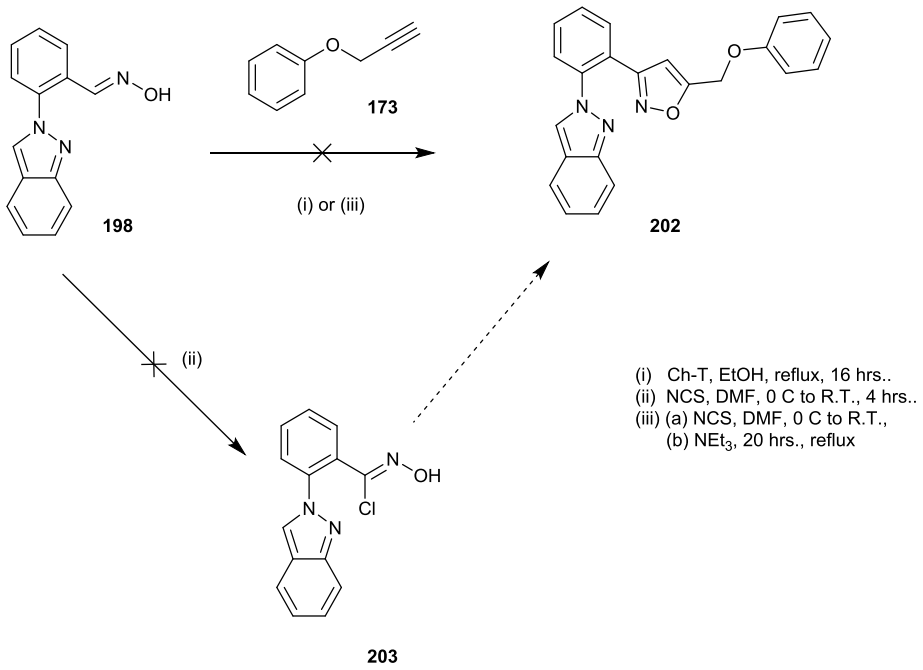

*Scheme 55: Attempted NOAC to the indazole oxime **198.***

2.7 Summary

- A range of azobenzenes bearing 1,3-dipoles, precursors to 1,3-dipoles or dipolarphilic functionalities were synthesised
- An alkyne functionality was introduced *ortho*, *meta* or *para* to the azo-linkage; a symmetrical *p*,*p*-disubstiuted azobenzene bearing two alkyne groups was also successfully synthesised.
- Azobenzene-alkynes were successfully reacted with simple "1,3-dipole partners"; several routes were found effective for formation of putative nitrile oxides from precursor oximes.
- Azobenzenes with an oxime functionality in the *para* or *meta* position were synthesised; symmetrical *m*,*m*- and *p*,*p*-bisoximes were also accessed.
- Test case reactions showed cycloaddition with monofunctional oximes could be effected by multiple routes, but that those azobenzenes with two oximes requiredmore specific reaction conditions.
- Synthesis of an azobenzene bearing an oxime functionality in the *ortho* position was difficult. In particular, cyclisation between the azo functionality and any adjacent electrophilic centre was found to form indazole structures.

3. Carbohydrate-Azobenzene Conjugates

Introduction

Following the successful synthesis of a range of azobenzenes bearing either 1,3-dipole or dipolarophile functionalities and the subsequent exploration of conditions suitable for their cycloaddition to 'simple' partners, the next aim was to apply this knowledge to form azobenzene-biomolecule conjugates.

The biomolecules desired for conjugation included peptides, nucleic acids and carbohydrates. Structures of a diverse range of azobenzene appended biomolecules can be found in the introduction of this thesis. These molecules, with wide rangeing applications have been accessed by a variety of chemistries. In this research we aimed to develop cycloaddition chemistry as a general route to form azobenzene-biomolecule conjugates.

In this work the biomolecule targets were split into two categories: carbohydrates and nucleic acids, and peptides. The peptide substrates offered very different synthetic challenges and will be considered separately from the carbohydrate and nucleic acid class which would be functionalised by the introduction of cycloaddition handles to hexose and deoxyribose units respectively.

3.1 Carbohydrates functionalised with azobenzenes

3.1.1 Synthesis of and cycloaddition to carbohydrate dipolarophiles

Galactose, **204**, mannose, **205,** and lactose, **206**, were selected as the representative saccharide units to be conjugated with an azobenzene unit. Their structures are shown in figure 41.

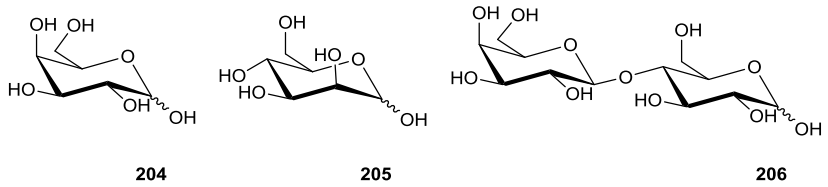

Figure 41: The structures of galactose, mannose and lactose, with undefined stereochemistry at the anomeric position.

Galactose, the C-4 epimer of glucose, is commonly found in the human body in glycolipids, glycoproteins and antigens. It plays an important role in cell recognition processes. Mannose, the C-2 epimer of glucose, is also an important biological molecule. In particular it has been a popular choice for studying carbohydrates-lectin interactions. The disaccharide lactose is a major component of milk, metabolically it is broken down into its constituent galactose and glucose units, which are consumed for energy. It has various applications in the food industry.

The multitude of hydroxyl functional groups on a carbohydrate substrate means protecting group chemistry is often extensively utilised in accessing selectively functionalised derivatives. Several protection and deprotection steps can make syntheses somewhat laborious. In this project we wished to use the C-1 position as the anchor point for sugar conjugation and acetyl protection was an attractive choice. Galactose and mannose pentaacetates, and lactose octaacetate are reliable substrates capable of controlled glycosidic bond formation.

2-Propynyl-tetra-*O*-acetyl-β-D-galactopyranoside, **209**, 2-propynyl-tetra-*O*-acetyl-α-D-mannopyranoside, **211**, and 2-propynyl-octa-*O*-acetyl-β-D-lactose, **213**, were the initial target carbohydrate bearing dipolarophile compounds. They were accessed through a two-step synthesis, which has been applied to a wide range of related carbohydrate substrates.

Galactose, mannose and lactose were fully protected by heating to reflux in acetic anhydride in the presence of sodium acetate. The products were purified by crystallisation. Acetylation of saccharides generally favours formation of the β-isomer.[228] The reaction between the hydroxyls and anhydride in the presence of a weak base, typically sodium acetate, is slow and anomerization occurs more rapidly and reaction by the more nucleophilic β-hydroxyl is favourable so resolving the α/β mixture towards the β-isomer.

Following protection, glycosidic bond formation was achieved by reaction with propargyl alcohol. Boron triflouride ethrate ($BF_3.OEt_2$) was selected as the activating agent as the activating agent and anhydrous DCM as the solvent.[229] The reaction product was isolated exclusively as the β-isomer for the galactose and lactose substrates. The mannose derivative was isolated as the α-isomer. The synthesis of the galactose and mannose substrates are shown in scheme 56. The yields for the propargylated sugars were 73% for the galactose derivative **209**, 83% for the mannose counterpart **211** and 74% for lactose analogue **213.**

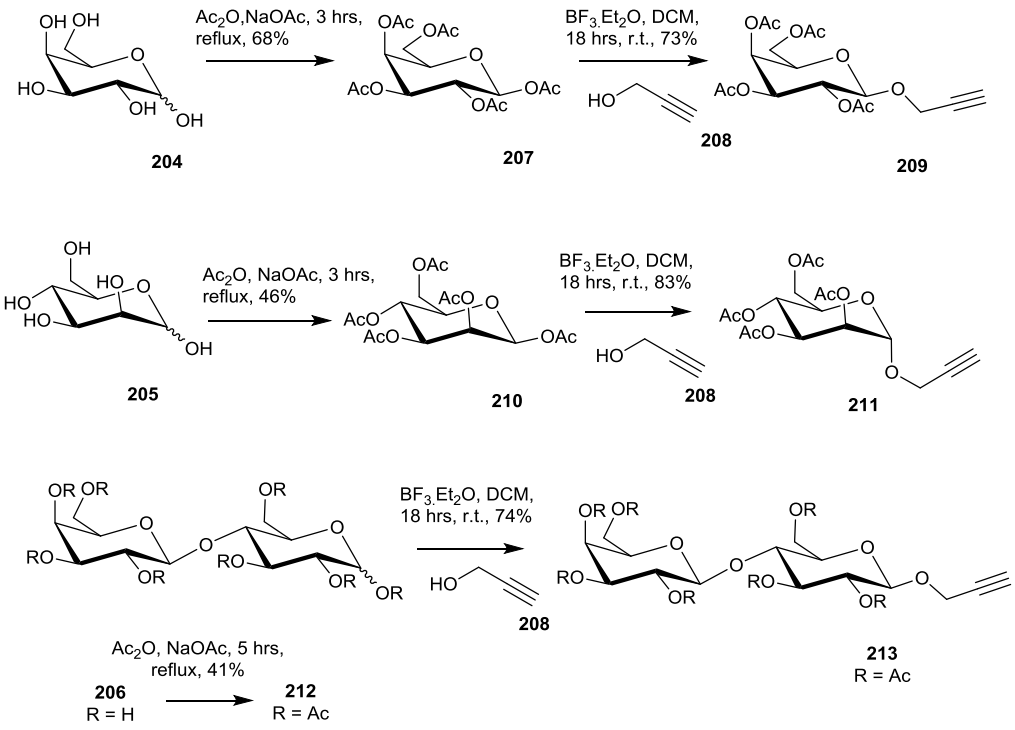

Scheme 56: Synthesis of 2-propynyl-tetra-O-acetyl-β-D-galactopyranoside, 2-propynyl-tetra-O-acetyl-α-D-mannopyranoside and 2-propynyl-octa-O-acetyl-β-D-lactose.

The stereochemistry of the propargylation reaction can be explained by examining the reaction mechanism. The acetyl at the 2-postion of acetylated sugars is important for controlling the stereochemistry of reactions at the anomeric centre. Reactions are typically promoted by a Lewis acid, which facilitates the leaving of the anomeric acetyl. Attack by the 2-postion acetyl on the adjacent electrophilic centre forms a cyclic oxonium. The cyclic oxonium species then undergoes S_N2 nucleophilic attack resulting in inversion of stereochemistry, as shown in scheme 57. Therefore, if the substituent at the 2-position is equatorial, as in glucose or galactose, the β-product is favoured.

Conversely where the 2-postion substituent is axial, as in mannose, the α-product is favoured.

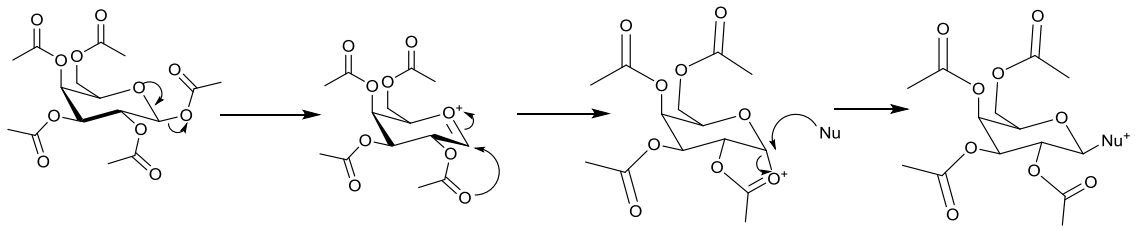

Scheme 57: Mechanism of stereocontrolled glycosylation of a galactose pentaacetate.

Attempted formation of **214** by cycloaddition between the propargylated galactose **209** and the nitrile oxide derived from the oxime **106** was initially conducted by both the chloramine-T route and by the transient hydroximinoyl chloride route. The same reaction conditions which had been successful in the cycloaddition between **106** and the test case dipolarophile propargyloxybenzene were employed, scheme 58. Complex mixtures resulted from both reactions, with only limited evidence of isoxazole formation evident in the ^{1}H-NMR spectrum of the crude reaction products. TLC analysis indicated several different products containing azobenzene and carbohydrates units were present in the mixture – the former can be visualised as orange coloured spots and the latter by the appearance of dark spots upon charring (heat gun) of the plates.

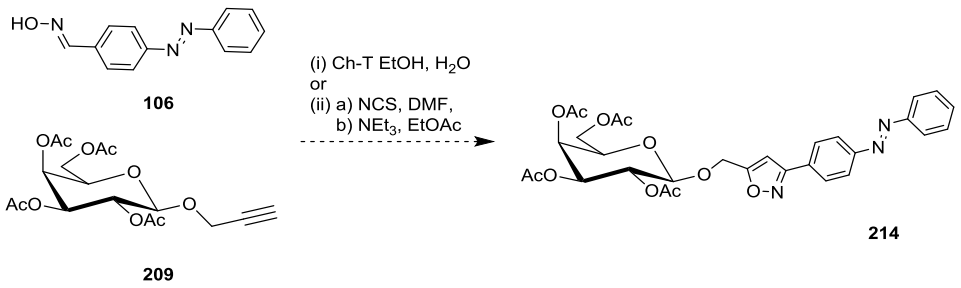

*Scheme 58: Attempted synthesis of carbohydrate-azobenzene adduct **214***

In a subsequent attempt to form the adduct **214** the hydroximinoyl chloride **174** was performed. Triethylamine was added over the course of 4 hours with a syringe pump to a solution of **174** and propargyl galactose **209** in an approximately 3:1 molar ratio. The

resulting solution was heated to reflux for a further 16 hours. Following purification by flash chromatography the desired adduct **214** was isolated in 79% yield, scheme 59. The ^{1}H-NMR spectrum of this protected compound showed the *trans* form dominated and only low intensity signals could be seen for the *cis* form. The OCH_2-isoxazole protons of **214** are diastereotopic and present as a pair of doublets (at 4.84 and 5.02 ppm, J = 14.0 Hz, 500 Hz, $CDCl_3$), which contrasts to the starting galactose dipolarophile, **209,** where the OCH_2 presents as a singlet.

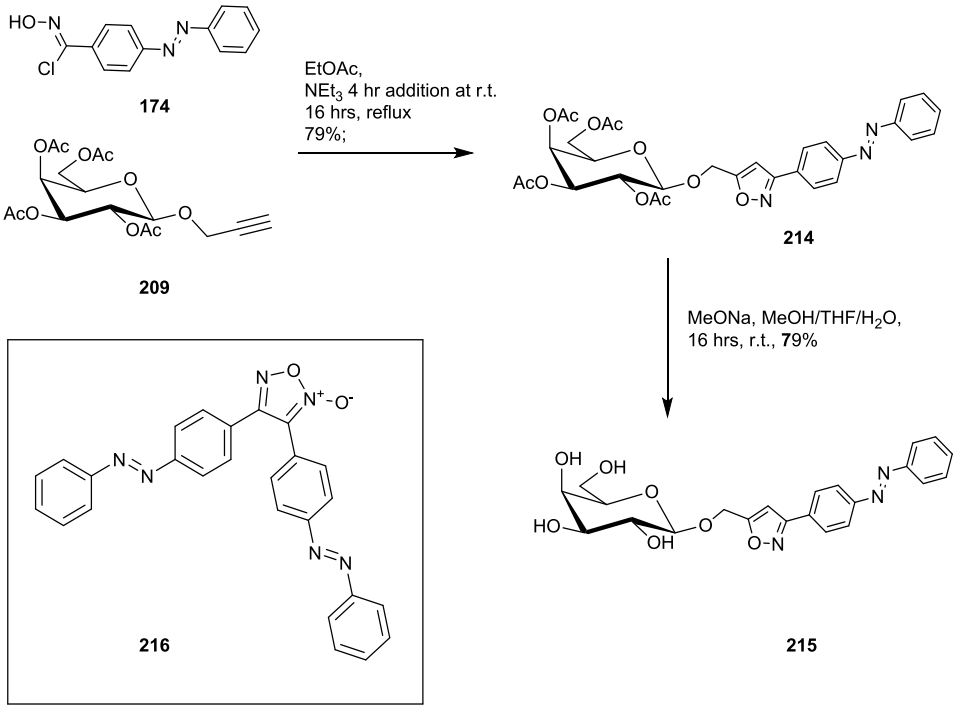

*Scheme 59: Synthesis of the galactose-azobenzene cycloadduct **215.***

During the purification of the cycloadduct **214** by flash chromatography, another orange coloured product was isolated. It crystallised via the vapour diffusion technique. It was dissolved in DCM and pet ether was allowed to diffuse into the solution. Upon standing for three days orange needles formed. They were analysed by X-ray diffraction and the solved structure was found to be the furoxan **216**, as shown in figure 42. The formation of furoxans is the common result of nitrile oxide dimerization and its formation could possibly have been avoided if a smaller excess of chlorooxime **174** was used.[230]

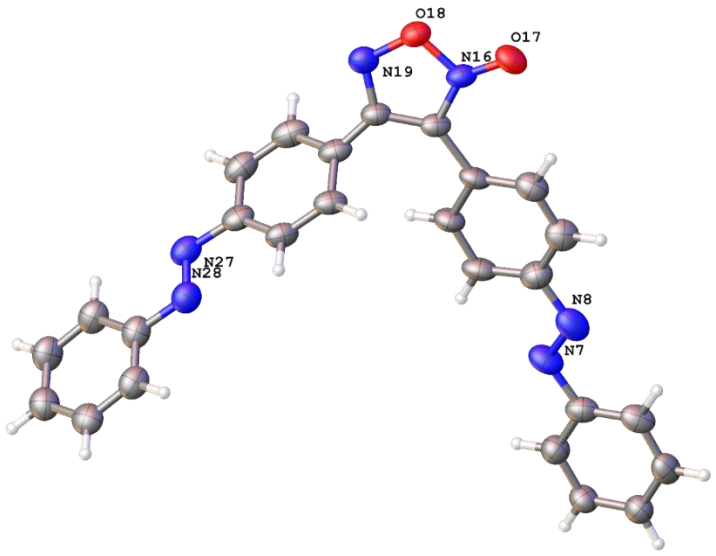

*Figure 42: Structure of the furoxan **216**, solved by X-ray crystallography.*

The mannose adduct **217** was also formed starting from the preformed chlorooxime **174**, again the sugar alkyne was used in approximately 3 fold excess, scheme 60. The slightly reduced yield of 73% for the mannose adduct with respect to its galactose analogue **214**, is attributed to mechanical loss rather than a lower conversion of the reaction, as both the starting material and product were very difficult to handle due to their sticky nature. The ^{1}H-NMR spectrum for the mannose derivative shows very low intensity signals for the *cis* isomer and the major adduct is the trans-azobenzene conjugate **217**.

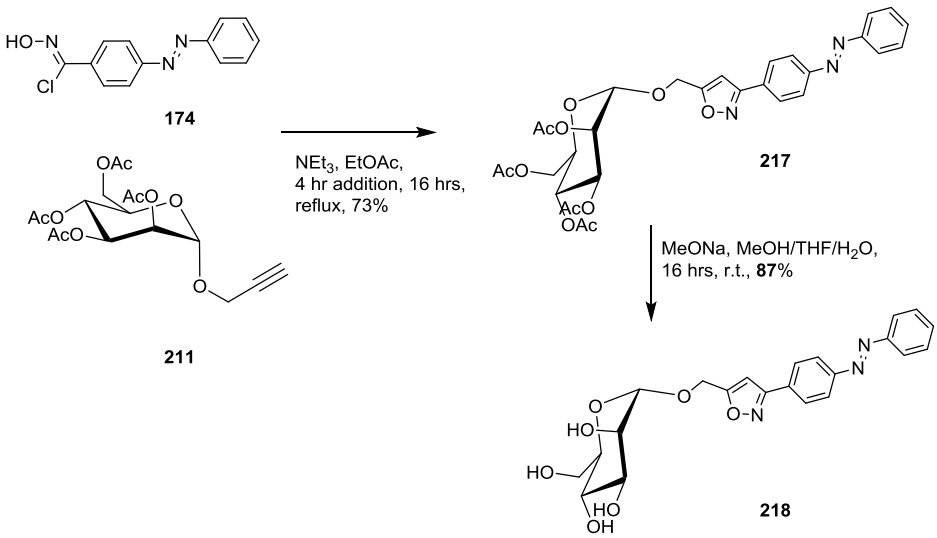

*Scheme 60: Synthesis of the mannose azobenzene conjugate **218.***

Following their successful cycloaddition reactions the conjugates **214** and **217** were deprotected. Deprotection of the galactose cycloadduct **214** was attempted using the Zemplén method. The adduct in aqueous methanol was treated by a catalytic amount of sodium methoxide at room temperature for 16 hrs.[231] After which the product, only partially soluble, was found to be incompletely deprotected. TLC analysis showed a variety of products likely material in various stages of deprotection.

In a second reaction, the protected cycloadduct was initially dissolved in THF before the addition of methanol and finally water. The conjugate remained in solution in the three component mixture and sodium methoxide was added in catalytic amounts. After stirring overnight, the pH of the reaction solution was adjusted with addition of acidic Dowex resin. When the mixture became slightly acidic an orange precipitate formed. The solid product together with the resin beads was collected by filtration and washed with aqueous methanol. The product was separated from the resin by washing with DMF. The resulting solution was concentrated to provide the pure cycloadduct **215** as an orange solid in 79% yield.

The ^{1}H-NMR spectrum of the deprotected product **215** presented as an all *trans* form. Unfortunately, some of the C<u>H</u> signals of the galactose unit are obscured by the residual <u>H</u>$_2$O in the solvent. However, the spectrum was extremely well resolved, and showed each O<u>H</u> resonance as a doublet or triplet. When partially exchanged with deuterium oxide the intensity of the OH signals reduced, as can be seen in figure 43.

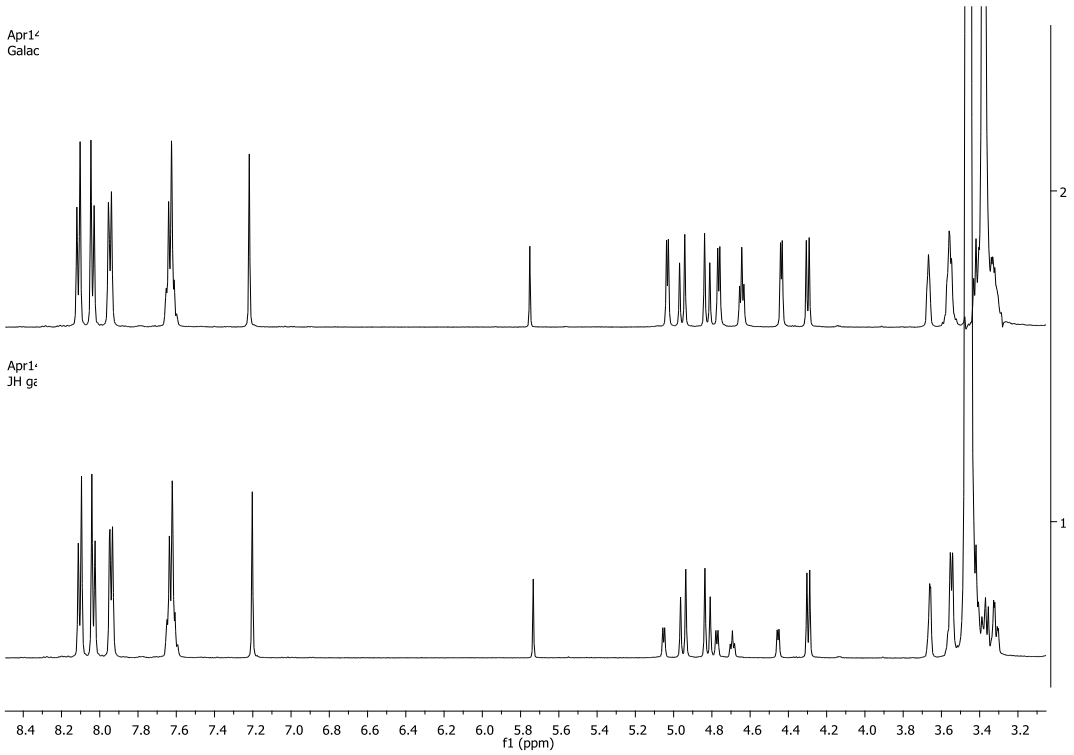

*Figure 43:1H-NMR spectrum of **215** in DMSO-d_6 (top) and DMSO-d_6 with D_2O added (bottom), showing reduced intensity of partially exchanged OH signals; 500 MHz.*

Deprotection of the mannose derivative **217** was approached in the same way, however no precipitate formed upon acidification of the crude products. TLC analysis of the solution indicated the reaction had been a success. Therefore the solution was concentrated under vacuum until a precipitate did form. Work up following the usual way yielded the deprotected product **218** in 87% yield.

With successful formation of the monosaccharide-azobenzene conjugate demonstrated, the next objective was to prepare the disaccharide analogues. Reaction between the chlorooxime **174** and the propargylated lactose **213** (3 eq.) was conducted using the same conditions as had been successful in synthesising the adducts **214** and **217**, scheme 61. Purification proved difficult and the cycloadduct product **219** could not be completely isolated from the propargylated lactose starting material. The partially purified material was deprotected with sodium methoxide in a THF/MeOH/H_2O mixture. The deprotected product **220** precipitated upon acidification and was isolated in 55% yield.

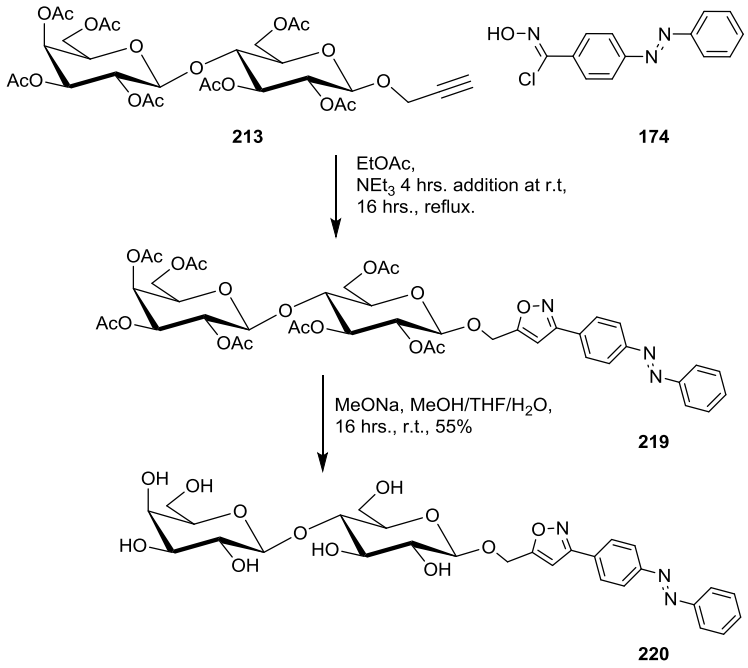

*Scheme 61: Synthesis of the lactose-azobenzene conjugate **220**.*

The ^{1}H-NMR spectra of the mannose and lactose conjugates **218** and **220** are rather typical of unprotected carbohydrates, unlike the galactose analogue **215** (figure 42), no defined hydroxyl resonances can be seen. Instead a broad peak appears between ~3.0-4.0 ppm representative of the residual water and various OH protons. Often obscuring many of the C-H resonances of the carbohydrate, which can be seen the ^{1}H-NMR spectrum of the lactose adduct **220** is shown in figure 44.

Several attempts were made to crystallise the deprotected conjugates. The galactose and mannose cycloadducts **215** and **218** but not the lactose conjugate **220** crystallised under the conditions explored. The compounds were dissolved in methanol and chloroform was allowed to slowly diffuse into the solution, which was left to stand at room temperature. Both **215** and **218** presented as small cubic crystals after a period of weeks. Unfortunately, those of the galactose adduct **215** proved unsuitable for X-ray analysis due to twinning. Despite a small amount of disorder, the crystals of the mannose cycloadduct **218** were solved by Dr Brendan Twamley, TCD. Significant images are present in figures 45-47.

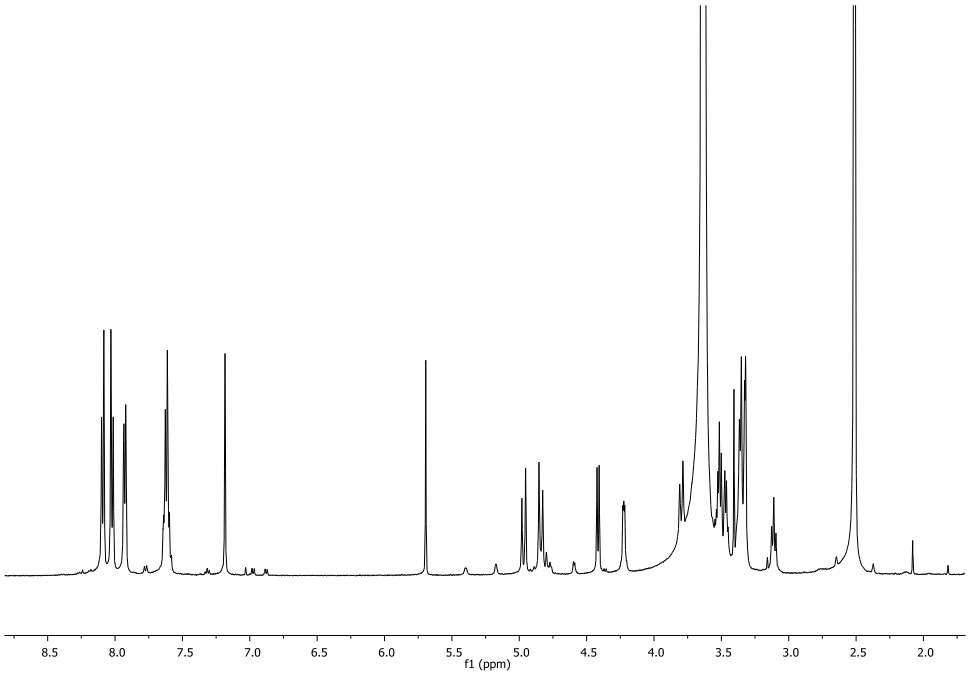

*Figure 44: 1H-NMR spectrum of **220** in DMSO-d_6 (500 Mz), showing broad OH signal at ~3.5 ppm obscuring C-H resonances, 500 MHz.*

A

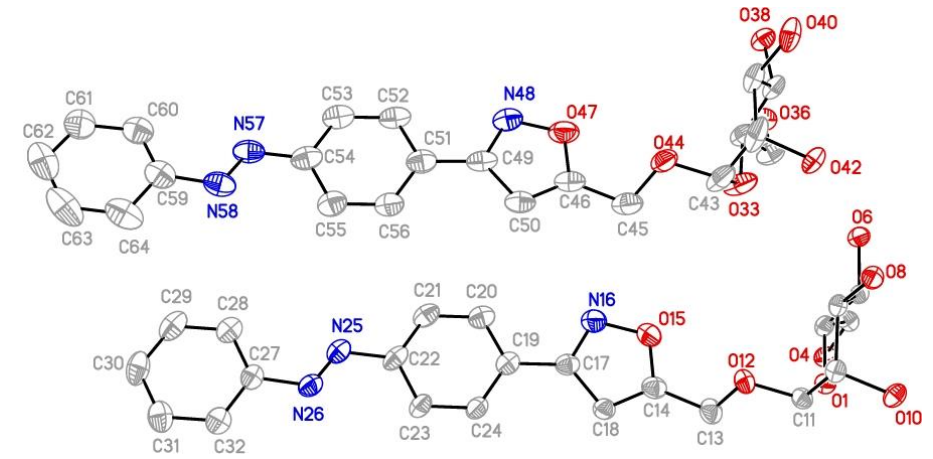

B

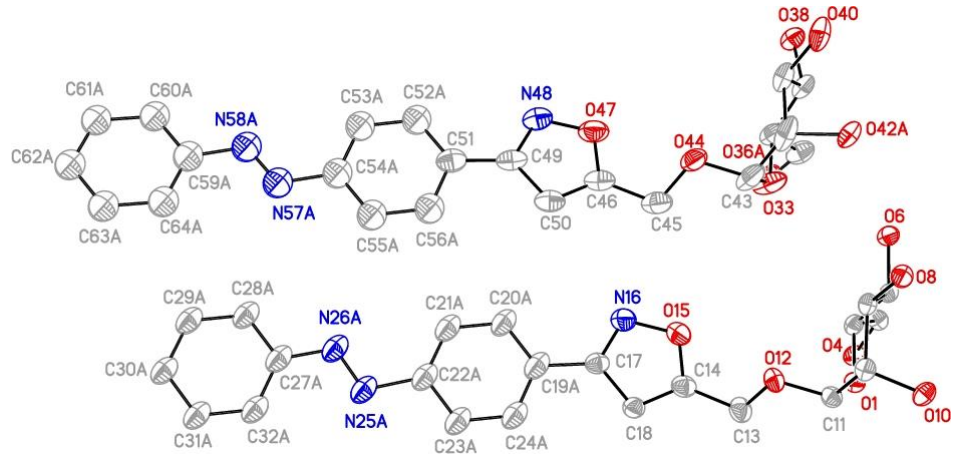

*Figure 45 Disordered moieties of **218** as separate images (A) 78 and 70% and (B) 22 and 30% occupied. Sugar carbon atoms unlabelled and hydrogen atoms omitted for clarity.*

The crystal data shows the molecules present as two district dimer units, labelled A and B in figure 45. The key difference between the two dimers is the relative orientation of the isoxazole and the azo linkage about the aryl ring that connects them. In dimer unit A, the C=N bond of the isoxazole has a trans-relationship to the azo bond across the aryl ring, we label this conformation transoid. In contrast, in dimer unit B unit there is a cis-relationship between the isoxazole C=N and the azo bond and the aryl ring that connects them. We described presentation B as having a cisoid conformation. A report by Sharma and Bharadwaj, discusses potential limitations on rotational freedom (about both sigma and N=N bonds) of divalent imidazole-appended azobenzenes, creating cisoid and transoid conformations. They describe how rotational motions in the structure create disorder, which can be observed in crystal structures.[232]

The isoxazoles in both the A and B dimer units are only slightly out of plane with adjacent azobenzene aryl ring, interplane angles of 3 degrees and 7 degrees suggest partial conjugation between the heterocycle and the azobenzene.

The basic packing unit of the crystals was based around an asymmetric dimer of the two geometric forms. Two hydrogen bonds occurred between the saccharides of the dimer unit as part of an extended network in the full packing structure (O···H-O

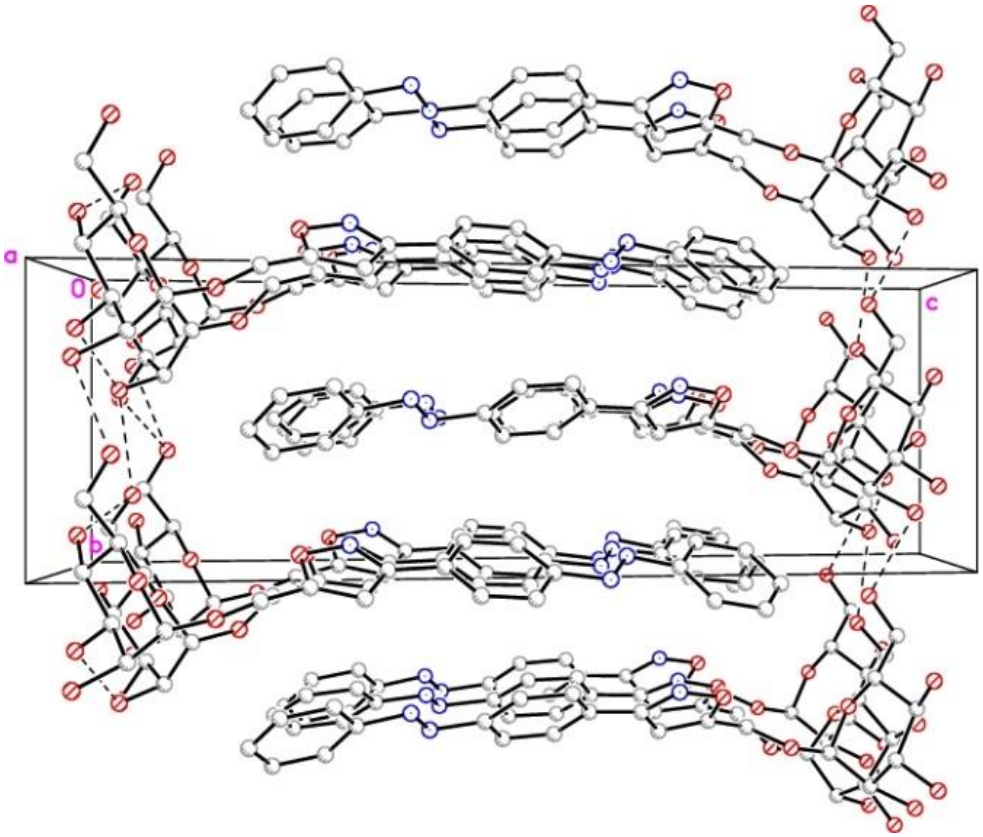

*Figure 46: Packing diagram of **218** viewed down the a-axis. Dashed lines indicate strong hydrogen bonding. Hydrogen atoms omitted for clarity.*

distance 2.947 Å). The azobenzene and isoxazole units do not show any π-stacking, with only weak intermolecular interactions observed. Overall the packing structure is based around interlocking azobenzene units between saccharide walls, as shown in figure 46.

The saccharide unit in the X-ray structure was observed to be in the favourable chair conformation. The crystal structure also confirms the α-glycosidic linkage. An expansion of the sugar region of the structure is shown in figure 47.

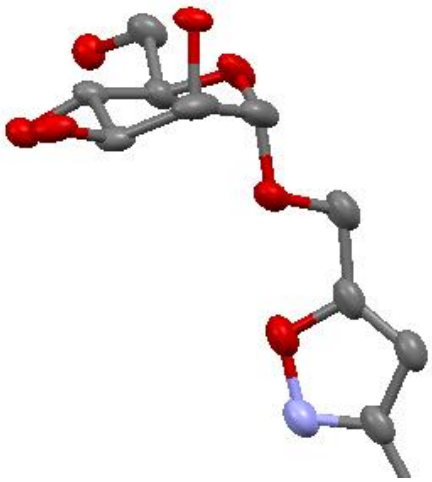

*Figure 47: Expanded saccharide region of the X-ray structure of **218**. Hydrogen atoms omitted for clarity*

An expansion of the aromatic region of the ^{1}H NMR spectrum of **218**, figure 48, shows the signals are the expected second order multiplets due to the magnetic non-equivalence of the chemically equivalent protons

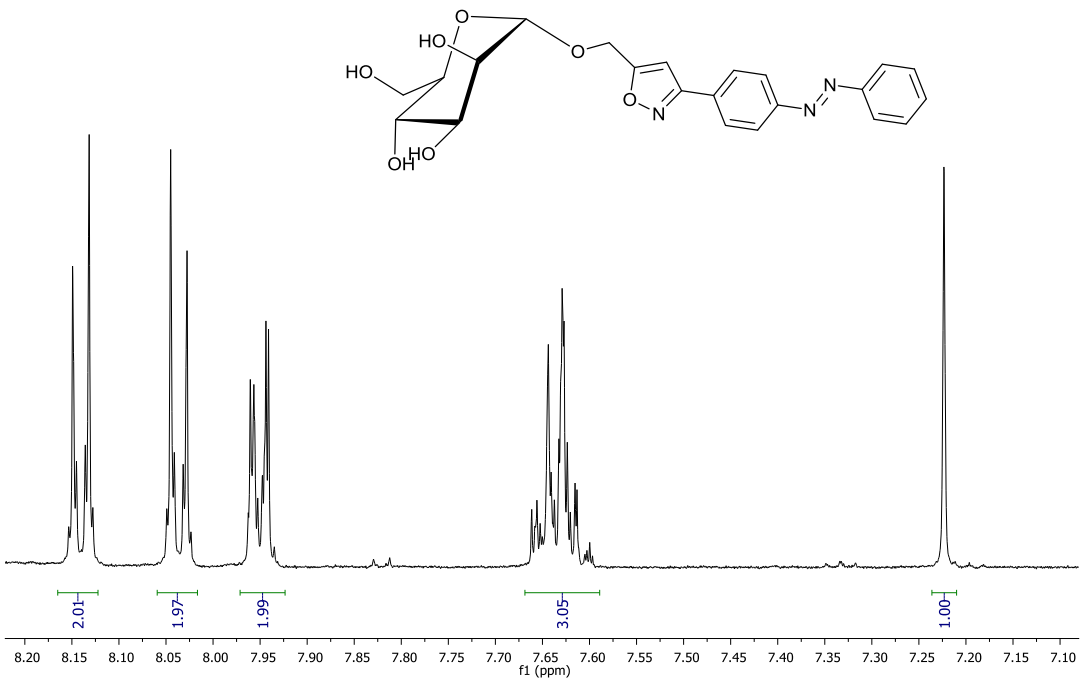

*Figure 48: Expansion of the aromatic region of the ^{1}H-NMR spectrum of **218** (DMSO-D_6, 500 MHz).*

Conjugates with one azobenzene unit separating two carbohydrate moieties were the next synthetic targets. The *p*,*p*-bishydroximinoyl chloride **176** and the propargylated galactose **209**, in a 1:2 molar ratio or 1:1 functional group ratio**,** were dissolved EtOH at room temperature before the slow addition of triethylamine, followed by heating to reflux overnight. Following work-up the cycloadduct **221** was obtained in a modest 34% yield. Poor solubility of the starting chlorooxime in EtOH was viewed as limiting the success of the reaction and it was subsequently repeated in ethyl acetate, scheme 61. This reaction gave the product in a much improved 69% yield. Like its *mono* ligated analogue **214**, ^{1}H-NMR spectrum of **221** shows it presenting mainly as the *trans* isomer in solution ($CDCl_3$).

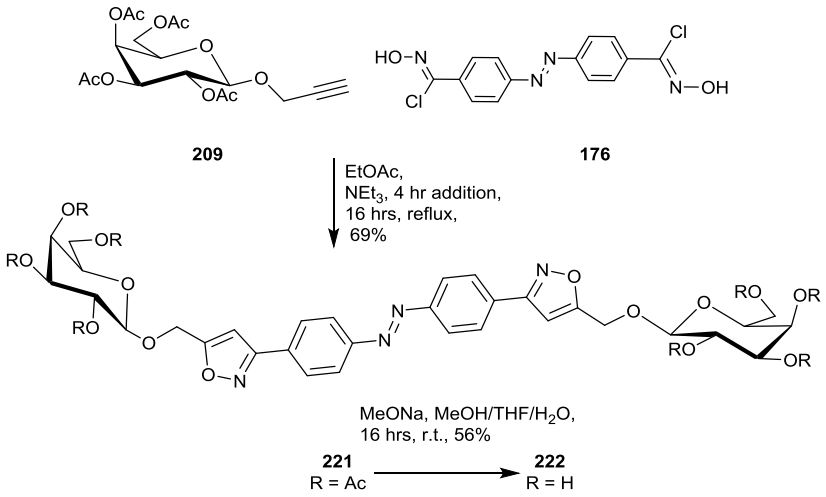

*Scheme 62: Synthesis of galactose-azobenzene conjugate **222.***

Whilst the isolated yield of **221** for the reaction in EtOAc (20 hrs., 77 ˚C) was satisfactory, options to further increase the yield were explored. A review of the literature suggested NOAC reactions might proceed faster under microwave activation.[233,234]

The reaction between the chlorooxime **176** and **209** was repeated with heating in a scientific microwave (80 ˚C, 30 mins). The potential to use a syringe pump to facilitate a slow addition of the base is problematic with microwave vessels and an all in approach was adopted. After work up the product was isolated in 53% yield. In an attempt to control the effective concentration of nitrile oxide, the reaction was repeated and the

NEt_3 was added in 6 portions with 10 minutes of heating between additions. However, these revised conditions failed to lead to an improved yield.

Another paper suggested the yields of NOAC reactions could be greatly increased by activation involving non-thermal microwave effects.[235] The latter work utilised a domestic microwave and a solvent free system where the reactants were coated on alumina. We wished to explore this approach, however it was difficult to strictly follow the conditions of the paper since it was ambiguous about the type of alumina used. As the reported reaction lacked a base, which is generally required for in nitrile oxide formation from a chlorooxime, it was thought that basic alumina might best facilitate the reaction.

To coat the alumina with **176** and **209** the compounds were dissolved in DCM, basic alumina was then added and the solvent removed under vacuum. The synthesis reported in the literature used eight equivalents of the nitrile oxide precursor with respect to the alkyne. However, we considered the risk of dimerization or polymerisation with the *bis* substrate **176** was high and an equimolar ratio of reactants (i.e. 2:1 chlorooxime to alkyne functional group ratio. 50 mg of alumina was employed with a 0.05 mmol loading of alkyne. The reactants were heated in a domestic microwave at 800 W for 3 minutes. Following work up and purification by flash chromatography, the cycloadduct **221** was isolated in 42% yield. This reaction was undertaken on an extremely small scale due to safety concerns around the use of a domestic microwave.

In the interest of reproducibility, the reaction was repeated on doubled scale in a scientific microwave, with heating to 100 ˚C (80 W, 30 mins) with vigorous stirring. Analysis of the crude products by ^{1}H-NMR spectroscopy allowed an estimate of the conversion to the cycloadduct at ~40%.

A clumping of the reaction material due to the sticky nature of the carbohydrate substrate **209** was identified as potentially limiting the success of the reaction. To try to limit aggregation the reaction was repeated with an increased quantity of alumina. Initially it was increased from 100 mg to 200 mg, however, the problems surrounding the aggregation of the material remained. Subsequent increase to 1000 mg of alumina afforded loaded material with a uniform appearance as a fine and free flowing power. The revised conditions led to a crude product with an improved conversion of 50%.

In an attempt to further optimise the reaction the solvent used during the initial adsorption of **209** (0.1 mmol) onto the alumina (1000 mg) was changed from DCM to EtOAc, this resulted in a conversion of 55%.

In a further reaction the ratio of chlorooxime to alkyne was doubled to 2:1 (4:1 molar ratio). Analysis of the crude product by ^{1}H-NMR spectroscopy suggested near complete conversion at 94%. With this much improved conversion the crude product was subject to flash chromatography and cycloadduct was isolated in a 55% yield.

The series of experiments exploring MW activated, alumina supported cycloaddition reactions are summarised in table E3 in the experimental section. Their uncertain outcome lead to the conclusion that they did not provide a viable route for accessing further bioconjugates.

To access the mannose analogue of **221**, *p*,*p*-chlorooxime **176** and dipolarophile **211** were dissolved in ethyl acetate before the addition of triethylamine over four hours, followed by heating to refluxing overnight. The cycloadduct **223** was isolated in 68% yield.

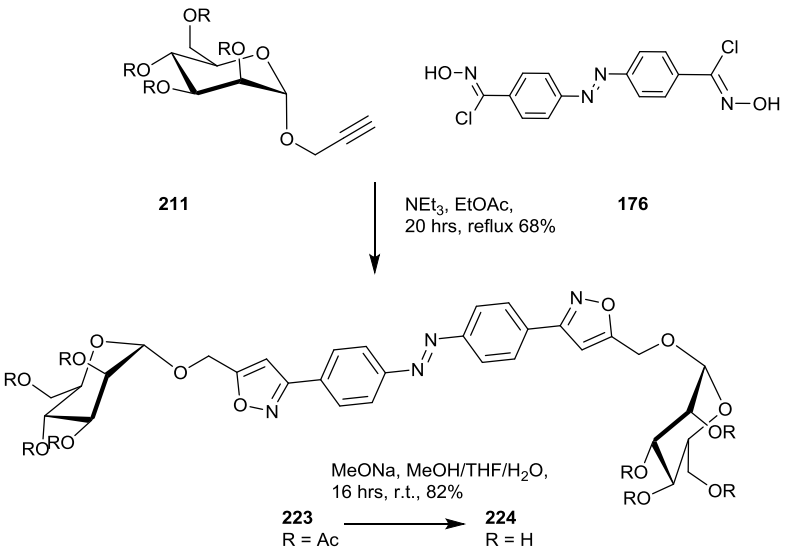

*Scheme 63: Synthesis of the divalent carbohydrate-azobenzene conjugates **223** and **224**.*

Deprotection of the symmetric products **221** and **223** was achieved by treatment with NaOMe in THF/MeOH/H_2O. Each product precipitated upon acidification with Dowex resin. The ^{1}H-NMR spectra of the mannose products **223** and **224** were more complex

than expected. Several unexpected resonances were observed, in particular, for each compound three signals were observed in the isoxazole region: at 6.71, 6.72 and 6.73 for the protected **223** ($CDCl_3$), and at 7.20, 7.23 and 7.25 for the deprotected **224** (DMSO-d_6), spectra Figure 49. There were also four extra sets of doublet signals in the aromatic region for both compounds. The relative integration of the Ar-H and the isoxazole-H signals suggested one major structure where the proton resonances of the isoxazole rings at each end of the molecule were the same (7.23 ppm for **223**) and a second minor structure where there was a higher degree of asymmetry and in which the isoxazole-H at each end of the molecule has a unique signal (7.20 and 7.25 ppm for **223**).

To confirm that the two structures were not geometrical isomers about the N=N a sample of **224** was irradiated with light at 365 nm to induce photoisomerisation. This experiment confirmed that none of the extra peaks arose from the *cis* isomer. In fact, the spectrum of the irradiated sample showed resonances for the *cis* counterparts of both structures present in the dark adapted sample, figure 49.

We hypothesise that the extra signals in the dark adapted sample arise from a second asymmetric conformation, brought about by restricted rotation – likely of the *cisoid*/*transoid* nature observed in the solid state structure of **218** (page 112). To investigate this possibility the ^{1}H-NMR spectrum of **224** was also recorded at 50 ˚C in the hope that rotational freedom might be facilitated at this elevated temperature. However, aside from a very slight shift in the resonance position, no significant change was observed in the downfield region between the spectra recorded at room temperature and at elevated temperature spectrum, figure 50.

It is possible the energy barrier for rotation about the single bonds was not reached when heating to 50 ˚C and further elevation of the temperature may have induce convergence to a single conformation.

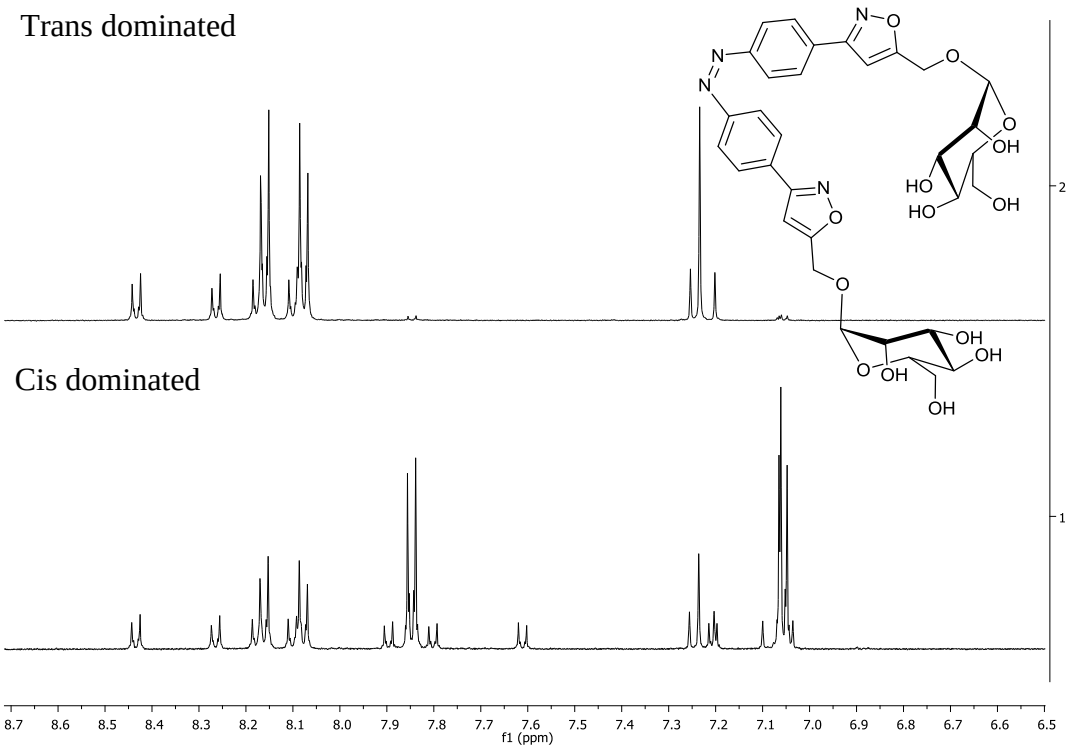

*Figure 49: [1]H-NMR spectra of **224**, top: all trans isomer; bottom: cis isomer dominated mixture (DMSO-D_6, 500 MHz).*

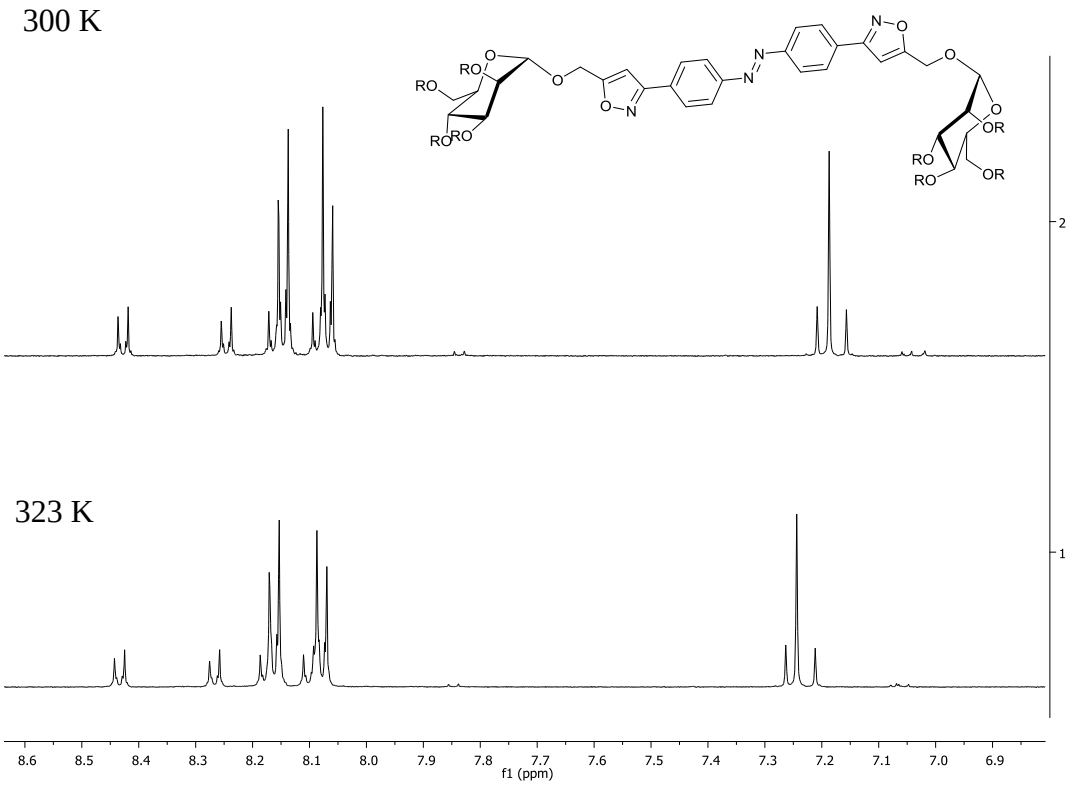

*Figure 50: [1]H-NMR spectra of **224**, top: spectrum recorded at 300 K; bottom: spectrum recorded at 323 K (DMSO-D_6, 500 MHz)..*

To increase the structural diversity *meta* substituted azobenzene sugar conjugates were targeted. In order to access these, the novel *m*-chloroxime **225**, was prepared. It was obtained in 91% yield from the precursor oxime **111** by treatment with NCS in DMF. The ^{1}H-NMR spectrum of **225** presented as *trans* isomer in $CDCl_3$ trace amounts of the *cis* form. Its NOH singlet appeared within the aromatic signals at 8.06 ppm.

The *m*-chlorooxime **225** and the propargylated galactose **209** were dissolved in ethyl acetate followed by addition of triethylamine over four hours, the reaction mixture was then heating to reflux overnight. Following work up and purification, the galactose-azobenzene conjugate **226** was isolated in a slightly disappointing 56% yield, scheme 63 (i). An improvement in yield to 76% was achieved when the reaction repeated with heating to reflux from the beginning, scheme 63 (ii). With this success, the slow addition of the base (4 hrs.) to a refluxing solution of the chlorooxime and dipolarophile was established as the standard approach for all future NEt_3 induced NOAC reactions. Under these conditions the mannose alkyne **211** and m-chlorooxime **225** were reacted to give the mannose-azobenzene conjugate **228** in 68% yield.

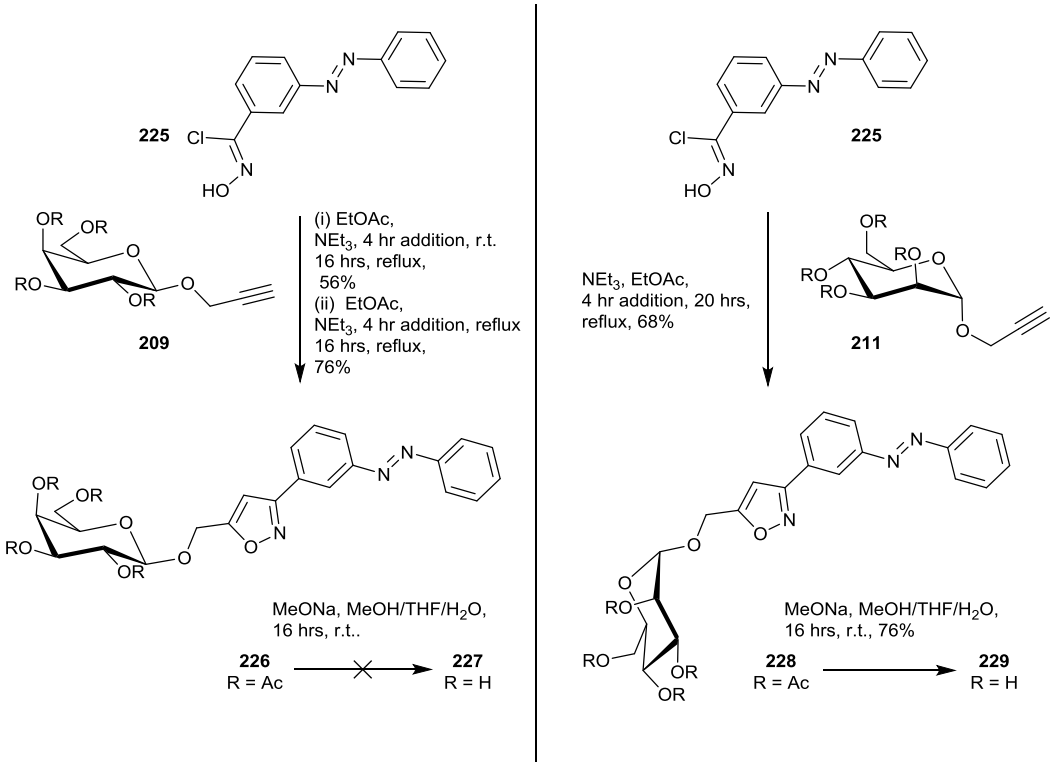

*Scheme 64: Synthesis of the carbohydrate-azobenzene conjugates **227** and **229**.*

Unlike their *para* regioisomers **214** and **217**, the ^{1}H-NMR spectra of **226** and **228** both showed considerable amounts, up to 20%, of the *cis* isomer. However, substitution pattern does not affect the resonance position of the isoxazole CH, which resonated at ~6.7 ppm in all cases.

Deprotection of **226** and **228** was attempted by treatment with NaOMe in a THF/MeOH/H_2O solution. Whilst the mannose conjugate **228** could be deprotected in good yield under these conditions, the carbohydrate unit of **226** suffered from degradation. Two isoxazole peaks were observed in the ^{1}H-NMR spectrum, the less intense one corresponded with the diastereotopic OCH_2 signals, indicating some survival of the desired product (shown in red). However the major isoxazole peak corresponded to a singlet OCH_2 peak likely indicating loss of the carbohydrate functionality (shown in blue). The isoxazole singlets and methylene protons are highlighted in figure 51.

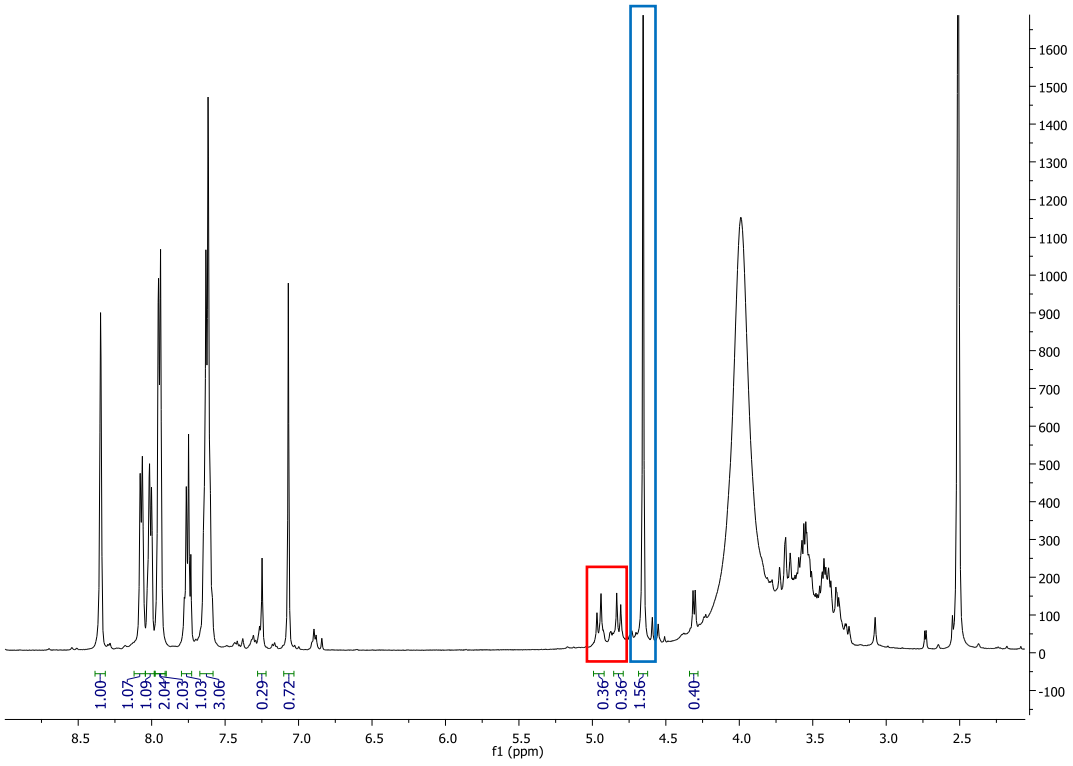

*Figure 51: ^{1}H-NMR spectrum of degraded material in the attempted deprotection of **226** (DMSO-D_6, 500 MHz).*

To gain access to divalent *meta* substituted cycloadducts, the *m,m*-bischlorooxime **230** was an important target. It was synthesised from the parent oxime **112**, by treatment with NCS in DMF for 5 hours. The chlorooxime **230** was insoluble in chloroform and its ^{1}H-

NMR spectrum was recorded in DMSO-d_6, the NOH signal appeared at 12.65 ppm. Like its *mono* substituted analogue **225**, the ^{1}H-NMR spectrum was dominated by signals of the *trans* isomer.

The *m,m*-symmetric galactose and mannose adducts **231** and **233** were formed in a series of experiments, using the conditions discussed above for the synthesis of **226** and **228**. The compounds were isolated after purification by flash chromatography in 72% and 74% yield respectively scheme 65. Once again, these *meta* products showed a greater amount of the *cis* isomer than had been observed for their *para* counterparts. The *cis* isomer represented up to 25% of the material in solution in $CDCl_3$ when analysed by ^{1}H-NMR spectroscopy, as can be seen in figure 52.

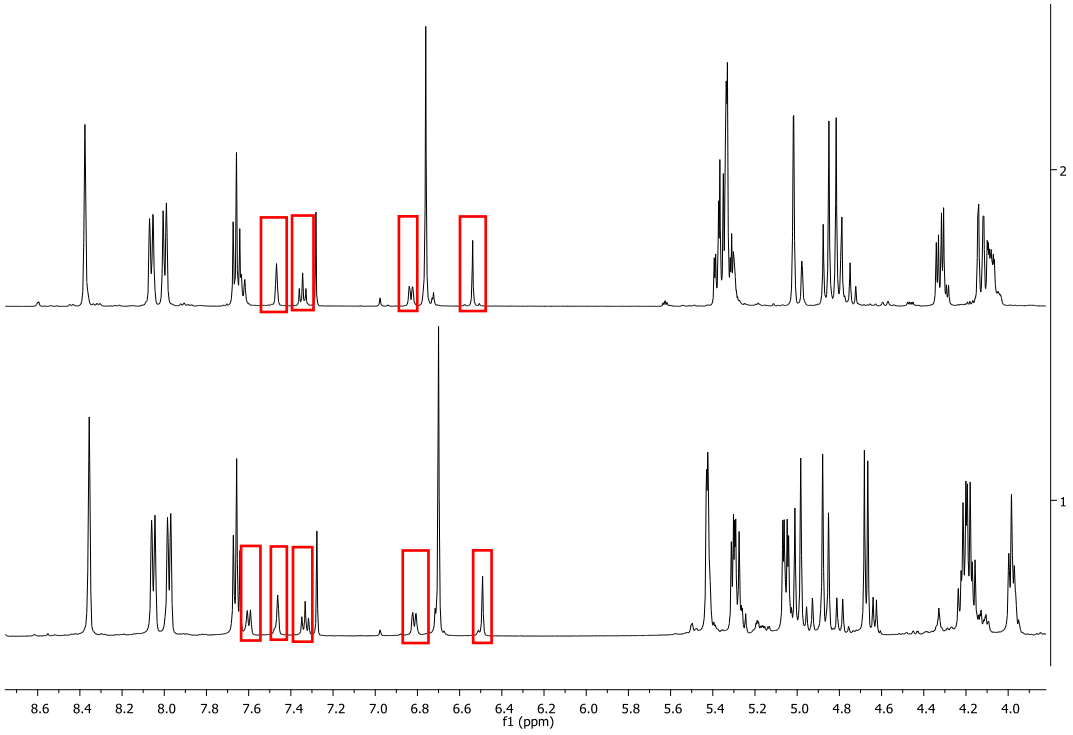

*Figure 52: Portion of the ^{1}H-NMR spectra of **231** (top) and **233** (bottom) showing the signals for the cis isomer boxed in red ($CDCl_3$, 500 MHz)*

Following deprotection in the usual manner (NaOMe, THF/MeOH/H_2O), the products **232** and **234** were isolated in 83% and 81% yield respectively, scheme 65. In contrast to their parents, only low intensity signals were observed for the *cis* isomer and their ^{1}H-NMR spectra were dominated by signals arising from the *trans* isomer (DMSO-d_6, 500 MHz).

The protected propargylated saccharides **209** and **211** were also suitable substrates for reaction with the azidoazobenzene **171.** Copper sulphate pentahydrate and sodium ascorbate were used to generate the copper (I) catalyst in aqueous DMSO and reaction between equimolar amounts of the dipole and dipolarophile was allowed to continue overnight at room temperature. After purification by flash chromatography, the protected galactose adduct **235** was isolated in 80% yield. The ^{1}H-NMR spectrum revealed the compound presented in solution as an approximately 10:1 ratio of *trans* to *cis* isomers ($CDCl_3$).

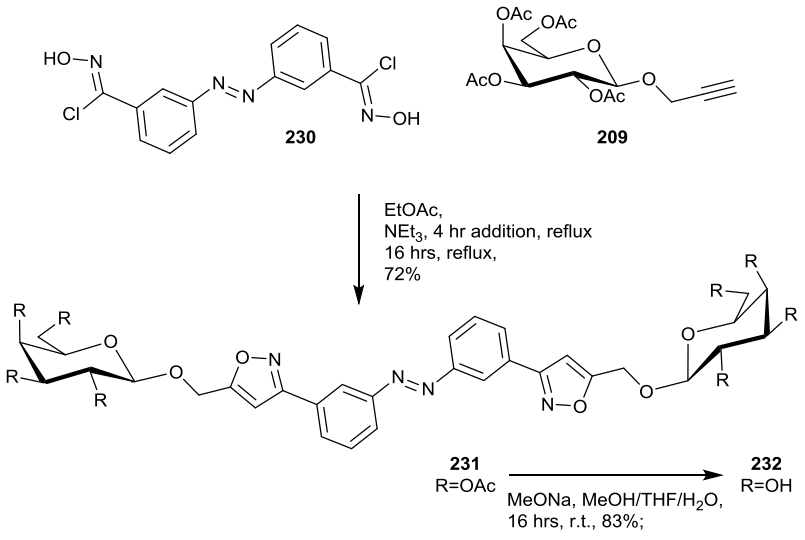

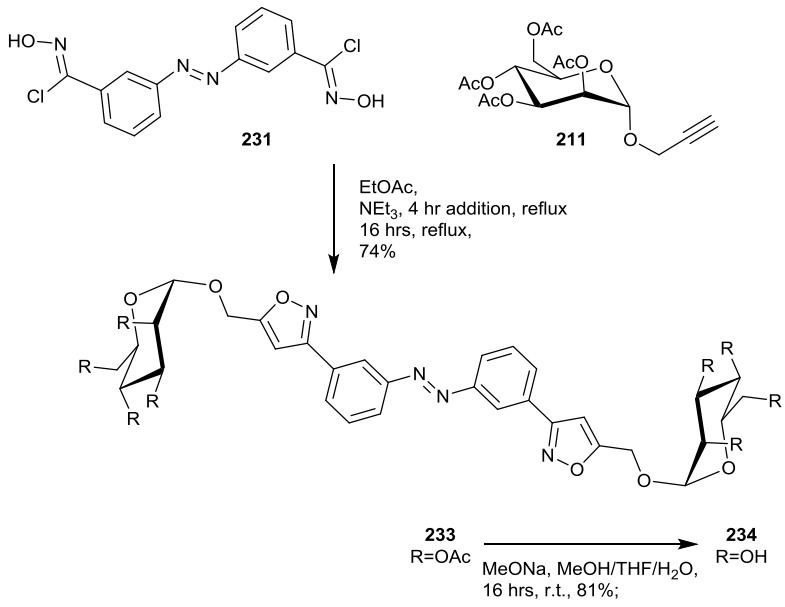

*Scheme 65: Synthesis of divalent isoxazole ligated azobenzene-carbohydrate conjugates **232** and **234.***

Following an analogous reaction, the ^{1}H-NMR spectrum of the crude product from the reaction with the mannose substrate **211** suggested a successful cycloaddition. However, the mannose adduct **237** could not be successfully isolated. After several attempts at purification, the partially purified material was taken on for deprotection.

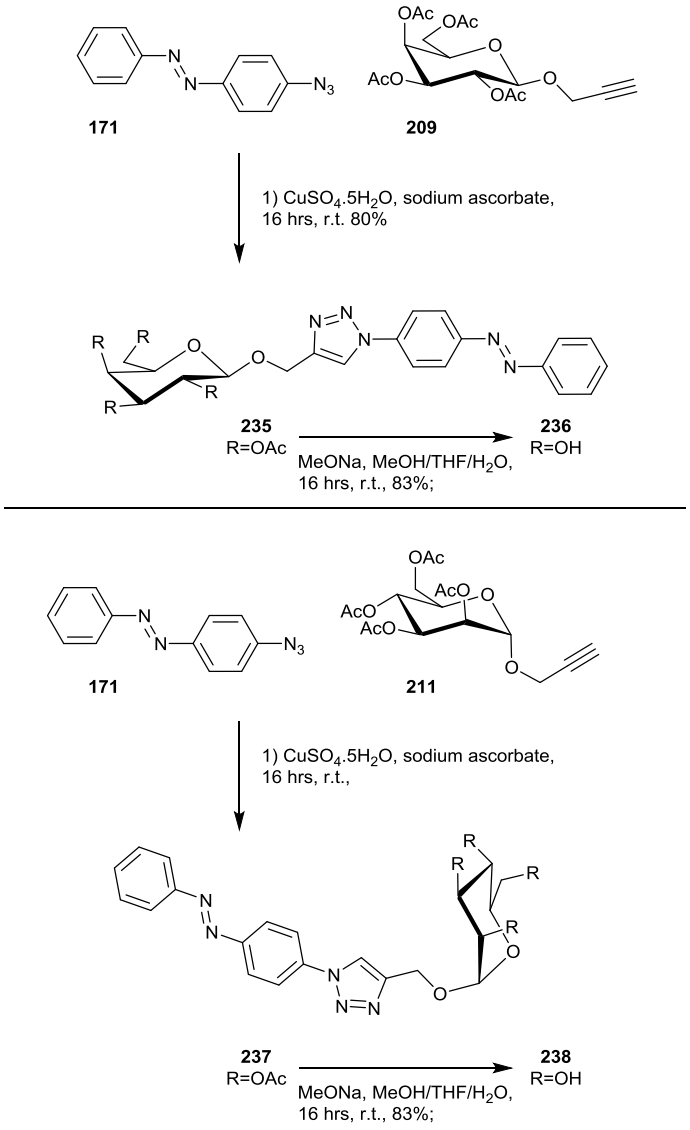

*Scheme 66: Synthesis of triazole ligated azobenzene-carbohydrate conjugates **236** and 2**38.***

Both pure **235** and incompletely purified **237** were fully deprotected using sodium methoxide in THF/MeOH/H_2O and **236** formed from **238** in 83% yield, i.e. in 66% over the 2 step cycloaddition and deprotection sequence. In contrast, **238** was isolated in 80% yield over the deprotection and cycloaddition steps. Both the deprotected conjugates **236**

and **238** presented with very limited amounts of the *cis* isomer. The ^{1}H-NMR spectrum of **238** presented as second order for its aromatic protons, figure 53, due to magnetic non-equivalence. Several peaks are present for the triazole proton, suggesting the possibility of several conformers.

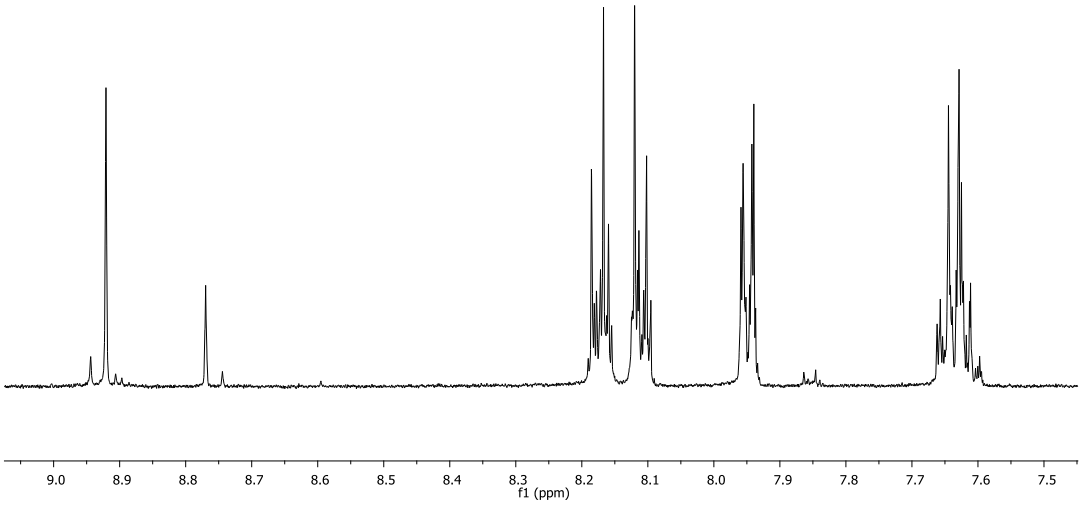

*Figure 53: 1H-NMR spectrum of **238**, showing triazole resonances at 8.77 and 8.92 ppm.*

3.1.2 Synthesis and cycloaddition of carbohydrates with dipolarophile functionality

To illustrate the versatility of the cycloaddition approach to azobenzene carbohydrate conjugation, we turned our attention to developing carbohydrates with dipole functionality. A search of the literature revealed while several azide bearing saccharides are known, including the attractive 1-O-azido-tetraacetate pyranoses, there are relatively few oxime bearing substrates. For our purpose, **241** was attractive as it offered a saccharide bearing an aryl aldoxime, which may have been expected to have a similar reaction profile to the test case benzaldehyde oximes. It is based on the naturally occurring compound helicid **239** which has been converted to its oxime derivative for investigation as potential inhibitors of acetylcholinesterase and mushroom tyrosinase.[236,237] Following the literature procedure **239** was protected with acetic

anhydride prior to oximation with hydroxylamine hydrochloride in the presence of pyridine to obtain **241** in 70% yield.

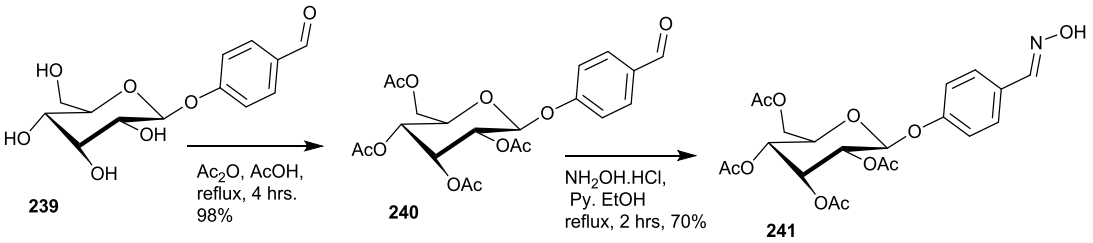

*Scheme 67: Synthesis of the sugar oxime **241**.*

Attempts at the chlorination of oxime **241** with NCS in DMF proved unsuccessful and generation of the desired nitrile oxide was explored by treatment with Ch-T (ethanol/water). A total of eight equivalents of the nitrile oxide precursor were reacted with *bis* alkyne **113**. The oxime and Ch-T (8 eq.) were added portion wise on four occasions at 90 minute intervals to the alkyne in aqueous EtOH. Eight molar equivalents of the nitrile oxide precursor equates to a four-fold functional group excess as **113** bears 2 alkyne groups. The product **242** was obtained in 59%, scheme 68. Only very low intensity signals were present for the *cis* form in the ^{1}H-NMR spectrum.

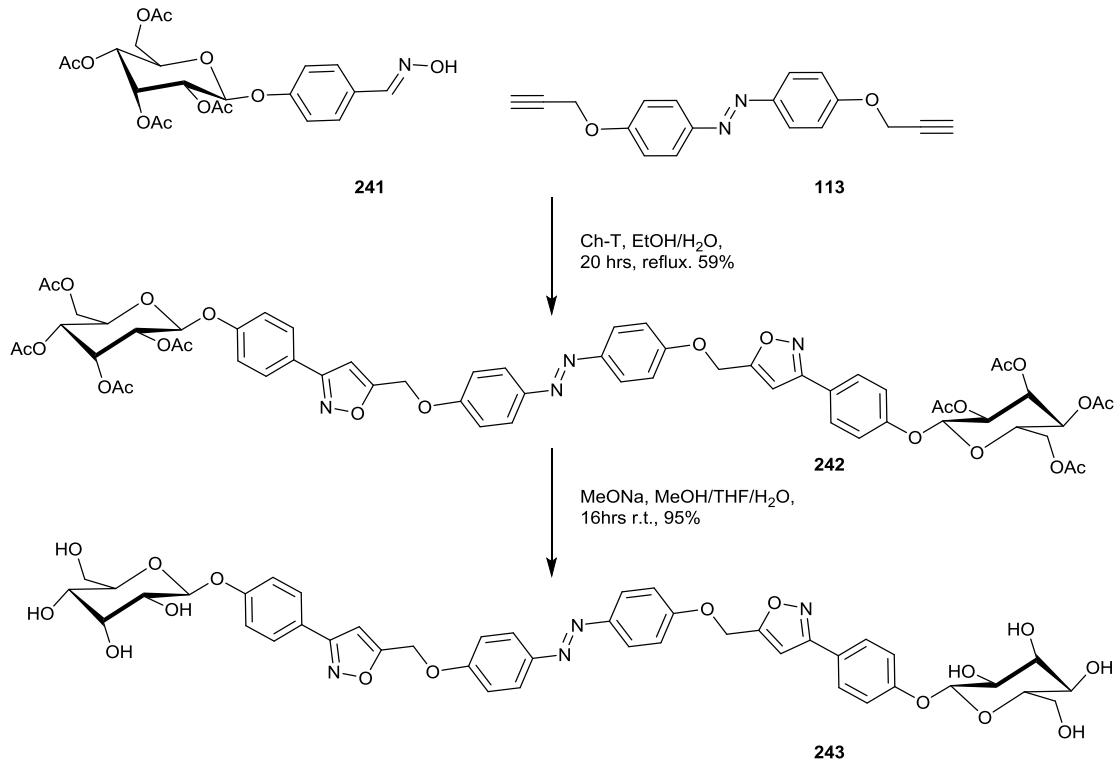

*Scheme 68: Synthesis of the helicid-azobenzene conjugate **243**.*

The cycloadduct was deprotected with sodium methoxide in THF/MeOH/H_2O to give **243** in 95% yield. Like its parent the contribution of the *cis* isomer in the ^{1}H-NMR spectrum was insignificant (DMSO-d_6).

Although the helicid was an attractive substrate for nitrile oxide formation, the allose sugar has limited biological appeal; the C-3 epimer of glucose is rarely observed in nature and applications involving this unit are infrequent compared to other aldohexoses. Therefore, we were keen to develop galactose or mannose derivatives of **241** and targeted the oximes **248** and **249.**

The pentaacetates of both galactose and mannose were prepared and treated with hydrobromic acid in acetic acid, to give the brominated mannose **244** in 76% and the brominated galactose **245** in 85% yield. They were allowed to react with 4-hydroxybenzaldehyde in a biphasic system of chloroform and aqueous sodium hydroxide solution; with tetrabutylammonium bromide was present as a phase transfer catalyst.[236] After a somewhat difficult purification by flash chromatography the desired ethers were isolated, the mannose adduct **247** in 78% yield and the galactose adduct **246** in 73% yield. Unfortunately, treatment of either aldehyde with hydroxylamine failed to yield the desired oxime, instead in each case a complex mixture was obtained with no

evidence for the formation of the desired oxime was observed in the ^{1}H-NMR spectra of the crude products.

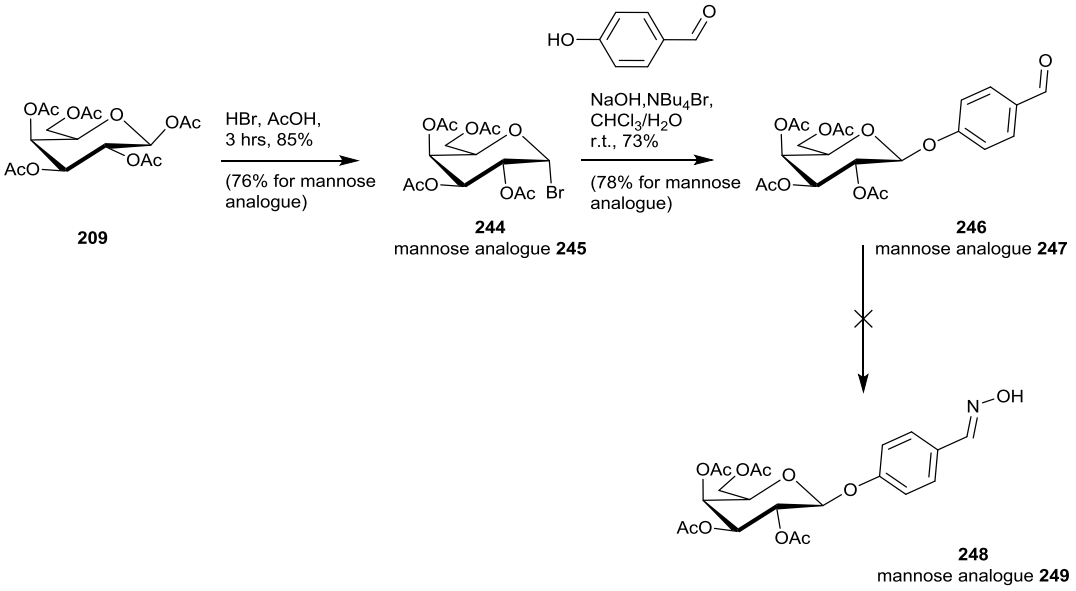

*Scheme 69: Attempted synthesis of the galactose and mannose oximes **248** and **249**.*

Due to the failure to form the helicid derivatives **248** and **249**, structures with an aryl oxime unit linked at the 6-position of the pyranose were targeted. To facilitate this reaction galactose was protected as the 1,2- and 3,4-acetonides by treatment with acetone in the presence of catalytic amounts of iron chloride.[238] The remaining 6-position hydroxyl of **250** was free for the introduction of a mesylate leaving group, achieved by reaction with mesyl chloride in neat pyridine.[239] The reaction of the mesylated **251**, with 4-hydroxylbenzaldehyde, **252**, was attempted under a range of conditions. K_2CO_3 was used as a base and acetonitrile as a solvent; no conversion was observed. It was thought that a stronger base would more readily facilitate hydroxyl deprotonation. Therefore, the reaction was repeated in the presence of DBU again, as shown by ^{1}H-NMR spectroscopy, no indication of formation of the desired ether. Neither did any of the starting aldehyde structure. It is presumed that the deprotected hydroxylbenzaldehyde may have been removed in the aqueous wash during work-up.

It was reported in the literature that montmorillonite K10 can facilitate ether formation between mesylates and phenolic compounds.[240] However attempts to utilise this approach in promotion of the reaction between **251** and hydroxybenzaldehyde failed.

No carbohydrate products were observed in the ^{1}H-NMR spectrum of the crude products.

Another publication suggested KOH in a toluene/DMSO mixture[241] could be effective but we found these conditions did not promote formation of **250**. The reaction was also attempted in the 'reverse' manner with the benzaldehyde bearing the leaving group, **255**, in reaction with galactose derivative **250**; however, it was without success. A complex mixture was observed with at least four aldehyde products were observed in the ^{1}H-NMR spectrum.

Finally an attempt to react hydroxylbenzaldehyde mesylate **255** and protected galactose **250** in the DMF in the presence of either $CsCO_3$ (DMF)[242] or potassium *tert*-butoxide (DMF or CH_3CN)[240] failed. In each case, a complex mixture resulted.

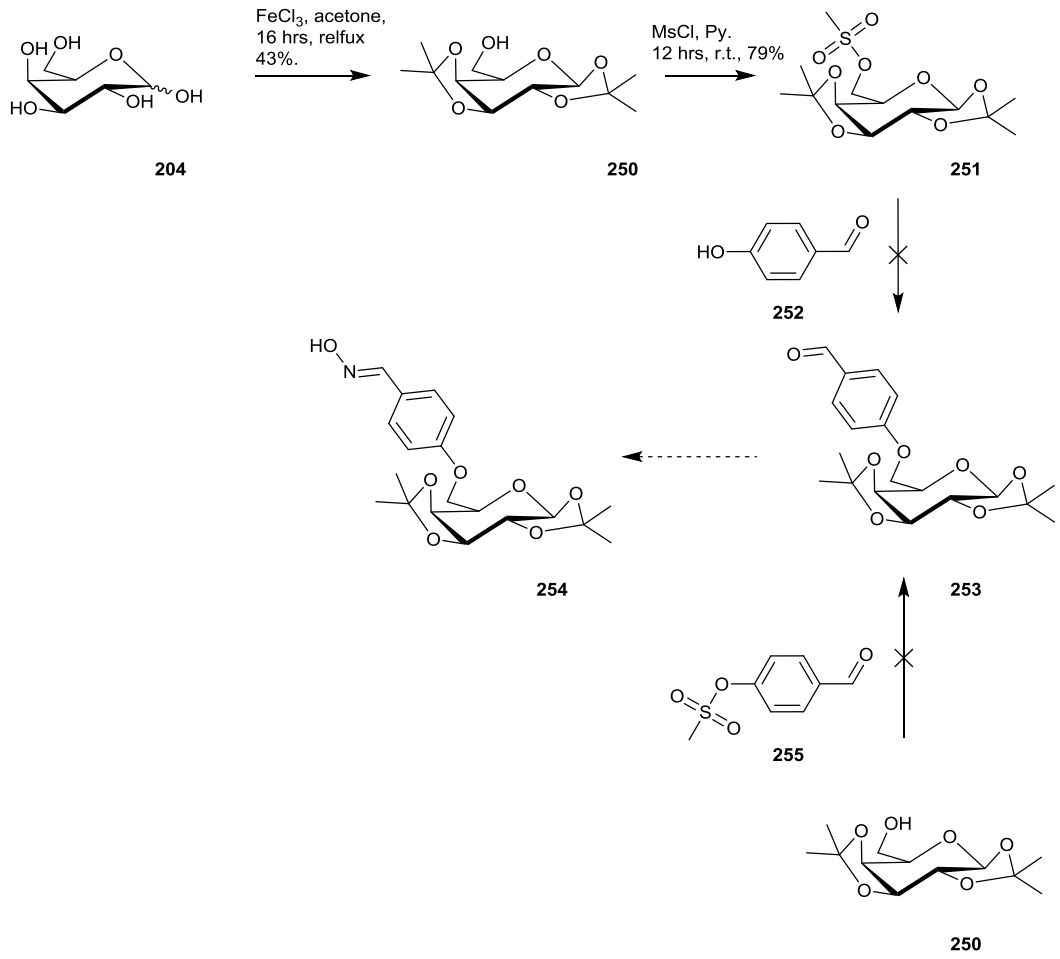

*Scheme 70: Attempted synthesis of the galactose-aldoxime **254**.*

In view of the failure to introduce a 'benzaldehyde' functionality to the 6-postion of galactose we considered the ability to exploit the secondary alcohol of the acetonide protected galactose remained a possibility. In particular the controlled oxidation of the secondary alcohol **250**, followed by conversion through to the chlorooxime **253** is known in the literature, and has been shown to take part in cycloaddition reactions.[243] The conversion of the alcohol **250** to the oxime **254** followed the synthesis reported by Streicher and Wünsch with some adaptations.[244] Firstly, by oxidation with PCC in DCM in presence of molecular sieves. This was followed by with reaction with $NH_2OH.HCl$ in the presence of sodium acetate in ethanol to give the oxime. Finally the oxime was chlorinated with NCS in DMF to form the hydroximoyl chloride **253,** scheme 71.[243]

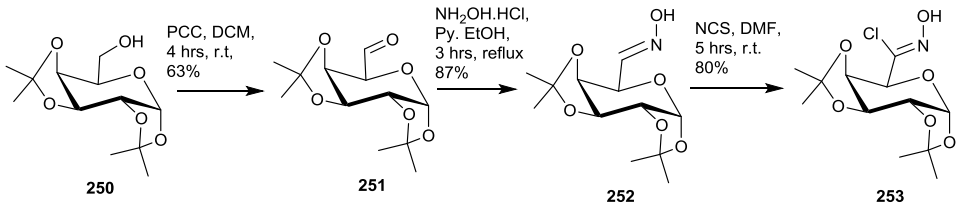

*Scheme 71: preparation of the chlorooxime **254.***

The chlorooxime **253** was reacted with the bis-propargylated azobenzene **113** by mixing the two compounds in ethyl acetate followed by addition of triethylamine over the course of 4 hours and finally heating to refluxing overnight, scheme 72. Initial analysis by ^{1}H-NMR spectroscopy and TLC revealed a complex mixture of products. Within the mixture there was strong support for the formation of the desired cycloadduct. In particular, the appearance of a singlet resonating at ~6.5 ppm in the 1H-NMR spectrum was indicative of isoxazole formation; a singlet at ~5.2 ppm was suggestive of the OCH_2 protons. The presence on the TLC plate of an orange coloured compound which charred when heated after staining with sulphuric acid in ethanol, further supported the formation of the divalent azobenzene carbohydrate cycloadduct **254**.

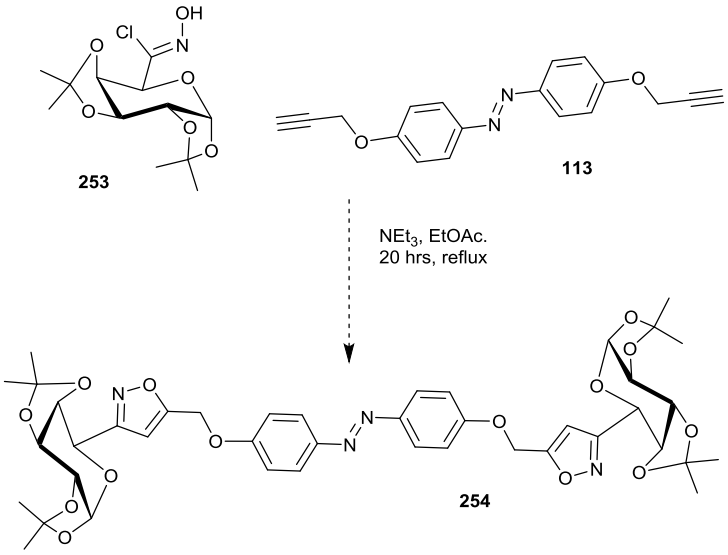

*Scheme 72: Attempted synthesis of the divalent galactose-azobenzene conjugate **254**.*

Several attempts were made at isolating the cycloadduct by flash chromatography utilising different solvent systems (DCM/MeOH; Ether/pet ether; EtOAc/cyclohexane/pet. ether). Unfortunately, the product proved impossible to isolate. Despite the range of solvents a carbohydrate reaction by-product consistently maintained almost exactly the same R_f as the product. Ultimately, only a single fraction from the last chromatography attempt was found to contain only **254.** The small quantity of material was enough for analysis by NMR spectroscopy and further structural characterisation data could not be obtained. Both the ^{1}H-NMR and ^{13}C-NMR spectra strongly supported formation of the desired cycloadduct **254**. The proton data showed five peaks for the saccharide unit, a singlet for the isoxazole at 6.45 ppm, and the OCH_2 protons at 5.15 ppm. A pair of doublets for the aryl protons of the azobenzene units were observed. The ^{13}C-NMR spectrum accounts for all expected signals and does not contain any unexpected resonances, both spectra are shown in figure 54.

Separation of the compound was complicated by the fact that acetal deprotection would have resulted in a mixture of isomers at the anomeric position. The potential for generating both α and β mixture as well as pyranose and furanose isomers made separation of a deprotected mixture an unattractive prospect and we discontinued experiments with **254**.

Focus turned to carbohydrates substrates with azido functionality. Bromination of the pentaacetates followed by reaction with sodium azide[245] or direct azide transfer from trimethylsilyl azide ($TMSN_3$) with activation by tin (IV) chloride are the two most

common routes to access the azides at the anomeric position.[246] Both the mannose (**256**) and galactose (**255**) azides were synthesised using the $TMSN_3$ route, scheme 73.

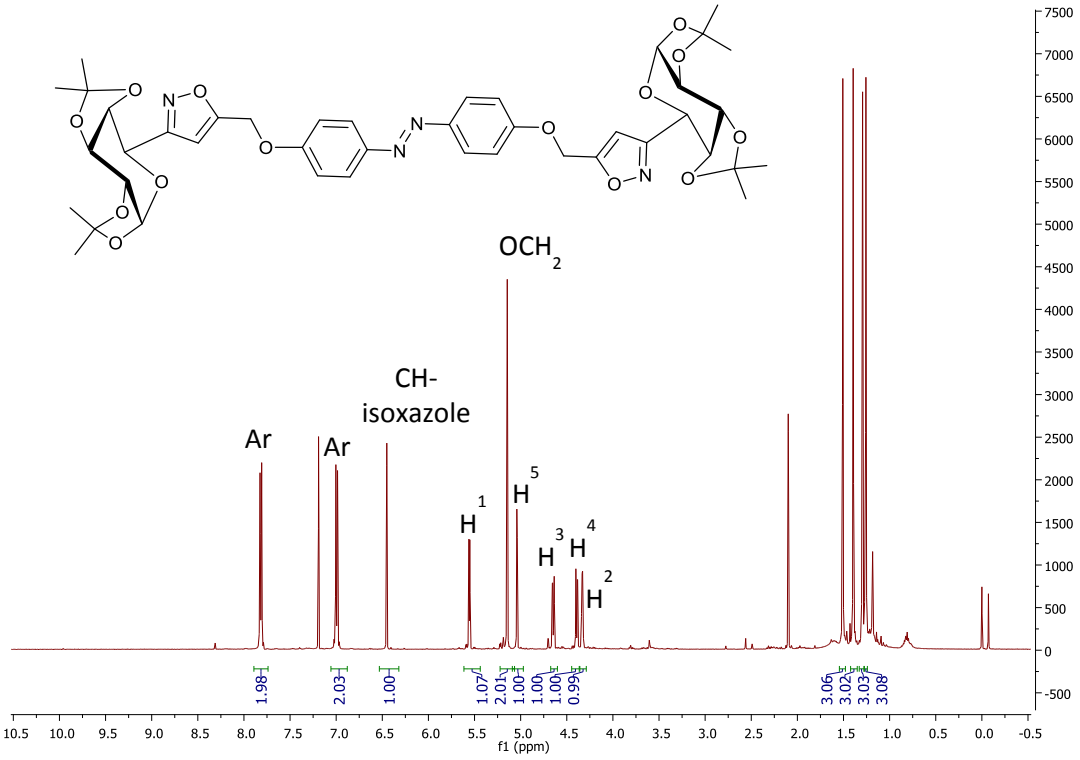

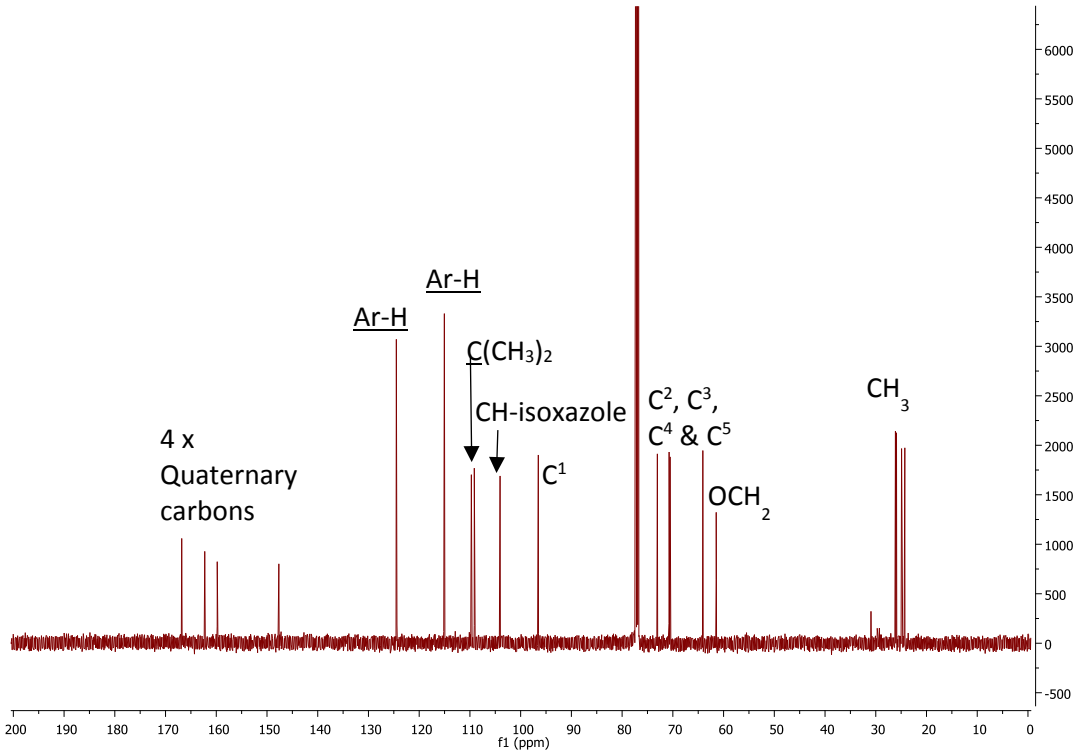

*Figure 54: 1H and 13C-NMR spectra of symmetrical cycloadduct product **254** ($CDCl_3$, 500 MHz)*

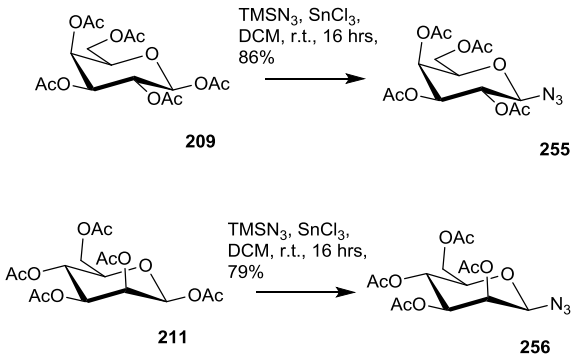

Scheme 73: Azide transfer from $TMSN_3$ to galactose and mannose pentaacetates

The azidosaccharides were dissolved in DMSO alongside the *p*-propargylated azobenzene **107** or the *p,p*-diproparglyated azobenzene **113**. The copper catalyst, generated by adding copper sulphate and sodium ascorbate to distilled water was added the solution. A 10% catalyst loading per alkyne functional group was used scheme 74. The reaction mixture was stirred overnight, followed by work-up and purification by flash chromatography. The monovalent cycloadducts were isolated in 77% yield for the galactose derivative **257** and 84% yield for the mannose derivative **259**. Both samples were found to contain a significant amount of the *cis* isomer when analysed by ^{1}H-NMR

spectroscopy, with a 1:0.25 ratio of *trans* to *cis* observed for both compounds. The proton NMR spectrum no longer distinguishes the diasterotopic OCH_2 protons.

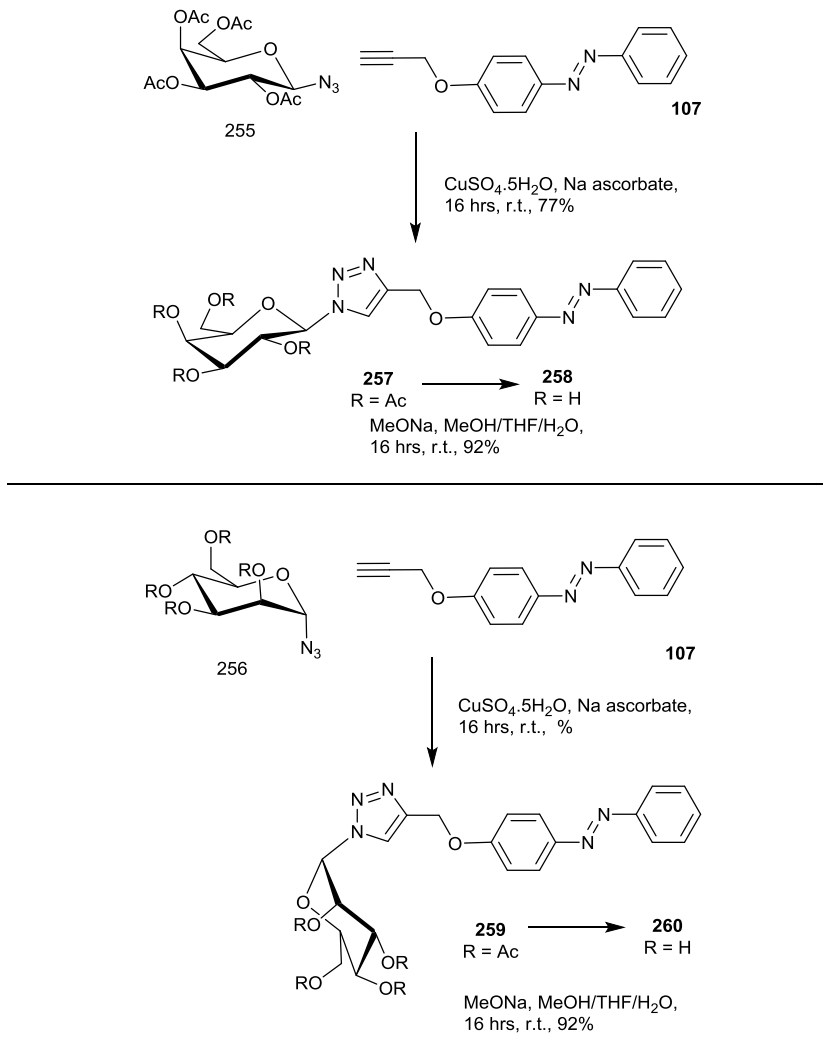

*Scheme 74: Synthesis of triazole ligated azobenzene-carbohydrate conjugates **258** and **259.***

The symmetric galactose adduct **261** formed in a slightly higher yield at 74% compared to the mannose adduct **263** at 71% yield, scheme 72. Both compounds show minor peaks representative of the *cis* form in their respective ^{1}H-NMR spectra.

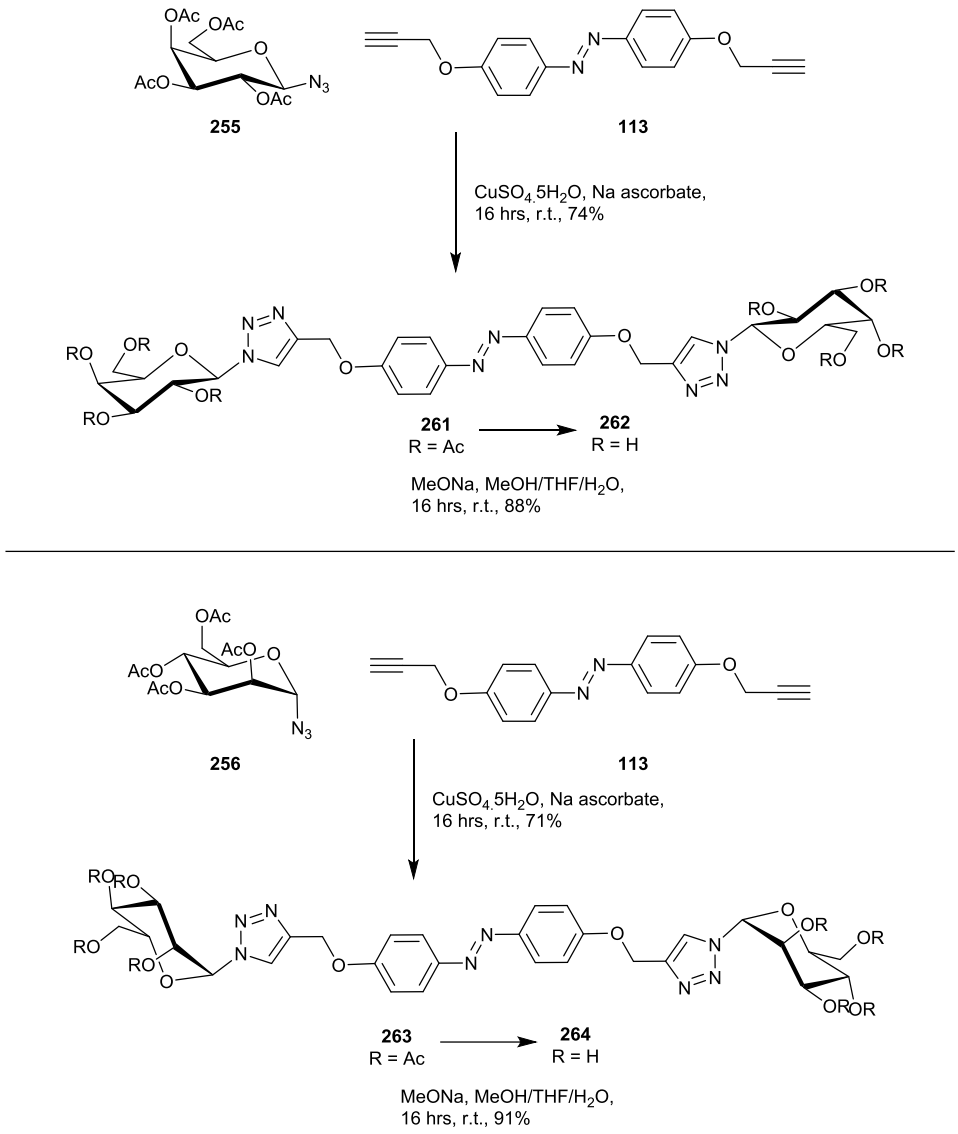

*Scheme 75: Synthesis of divalent, triazole ligated azobenzene-carbohydrate conjugates **262** and **264.***

The same catalyst loading in an aqueous DMSO solution was found to be suitable for the conjugation of the galactose azide **255** with the *ortho* substituted azobenzene **265** with cycloadduct **265** being isolated in 85% followed by deprotection in 86% yield, scheme 76. ^{1}H-NMR spectroscopy revealed the protected product to be present in 1:0.22 *trans* to *cis* ratio ($CDCl_3$) whilst the deprotected product was found to consist of 1:0.4 *trans* to *cis* ratio in DMSO solution at room temperature.

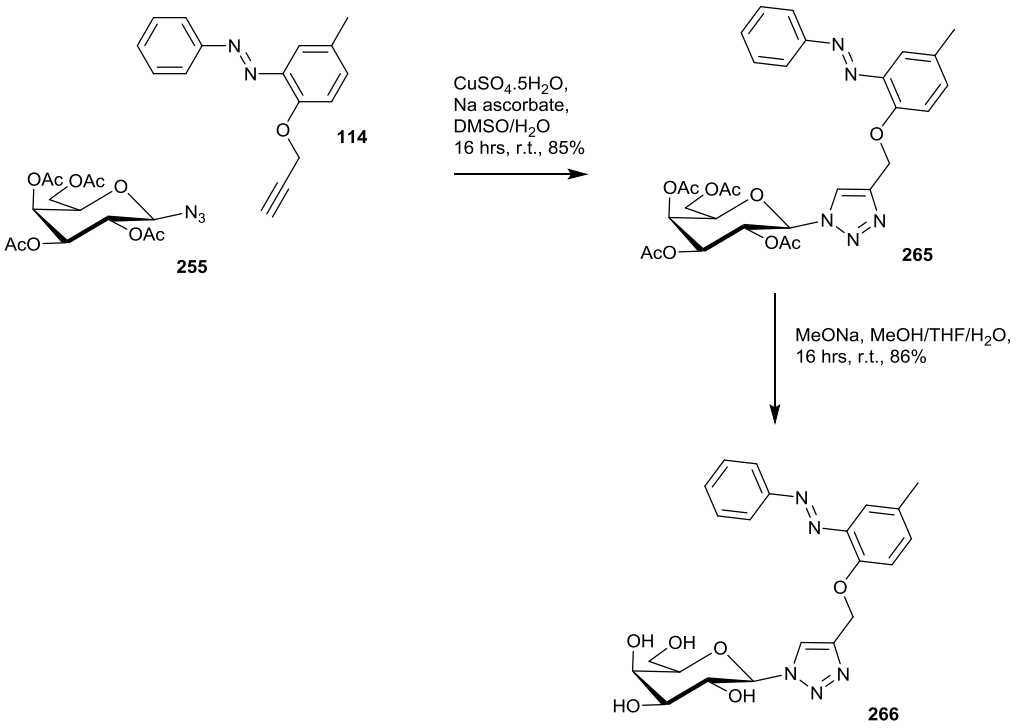

Scheme 76: Synthesis of the carbohydrate-azobenzene cycloadduct.

3.2 Synthesis and cycloaddition of nucleosides bearing dipolarophile functionality

Following the synthesis of a range of azobenzene carbohydrate conjugates, the application of this chemistry to the ribose units of nucleosides was planned. While functionalisation of the ribose can affect the ability of the nucleobase to be built into a DNA sequence it generally has a lesser effect upon the nucleobase pairing. On the other hand, functionalisation of the nucleobase can avoid disruption of the sugar-phosphate backbone, but it often affects the nucleosides ability to bind to its nucleobase counterpart, disrupting DNA duplication.

Functionalisation of either the 3'- or 5'- hydroxyl of nucleic acids blocks any potential for oligonucleotide growth in that direction, as the site becomes unavailable for phosphoramidite coupling. However, the hydroxyl groups at the 3- and 5-postions of the ribose can allow for the introduction of alkyne functionality. Selective protection of the 5'- primary alcohol by using bulky protecting groups offers an important synthetic advantage to introduction of alkyne functionality to C-3 secondary alcohol.

Thymidine was 5'-protected with trityl chloride in the presence of pyridine in DMF. Alkylation of the 3'-hydroxyl followed by treatment with propargyl bromide, after deprotonation by sodium hydride in a one-pot reaction, scheme 77.

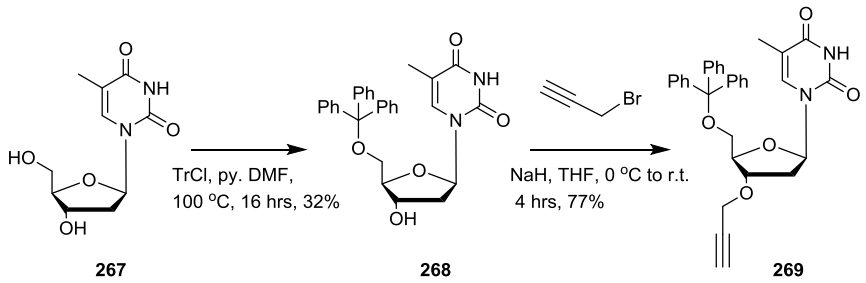

*Scheme 77: Synthesis of thymidine alkyne **269.***

Having synthesised the thymidine alkyne **269**, cycloadditions with the various azobenzene nitrile oxide precursors and azidoazobenzenes were attempted. Initially controlled addition of NEt_3 to a refluxing solution containing a threefold excess of *p*-chlorooxime azobenzene **174** and the propargylated thymidine was attempted, synthesis details are summarised in scheme 78. After separation by flash chromatography the cycloadduct **270** was isolated in 57% yield. The ^{1}H-NMR spectrum showed a roughly 4:1 ratio of the *trans* to *cis* isomers ($CDCl_3$, 500 MHz). Finally, the trityl protecting group was removed by stirring the cycloadduct in a solution of dichloroacetic acid and DCM at room temprature, to give the thymidine azobenzene adduct **271** as an orange solid in a 67% yield. The relative amount of *cis* form in the ^{1}H-NMR was half that of the protected parent molecule at 6:1 *trans* to cis

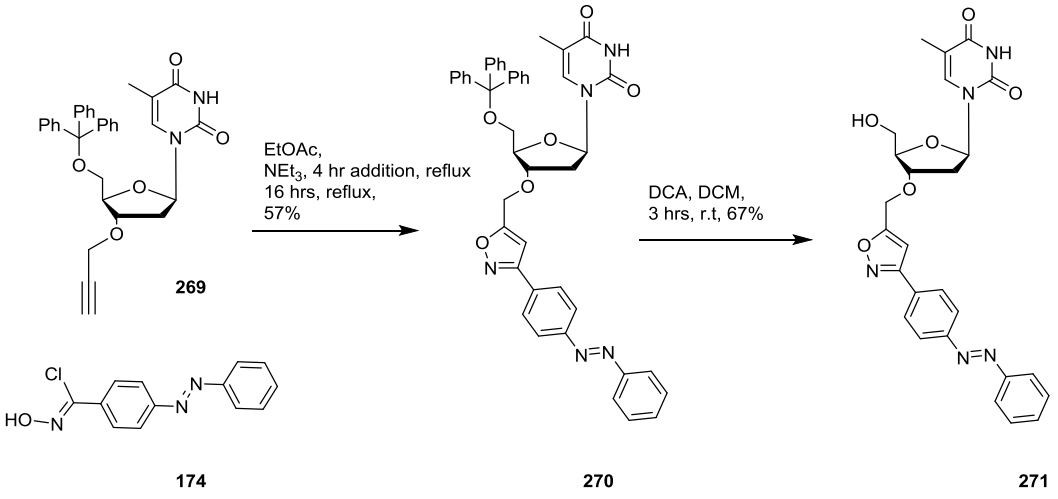

*Scheme 78: Synthesis of azobenzene-thymidine cycloadduct **271.***

Under the same reaction conditions, cycloaddition of *m*-chlorooxime **225** and the thymidine derivative **269** proceeded to give **272** in 73% yield, scheme 79. Treatment with dichloroacetic acid gave the deprotected product in 70% yield. Unlike the protected *para* analogue **270**, the *cis* form of **272** could only be seen as very low intensity signals in the proton NMR spectrum. The deprotected showed a 5:1 ratio of *trans* to *cis* isomers, similar to its *para* analogue.

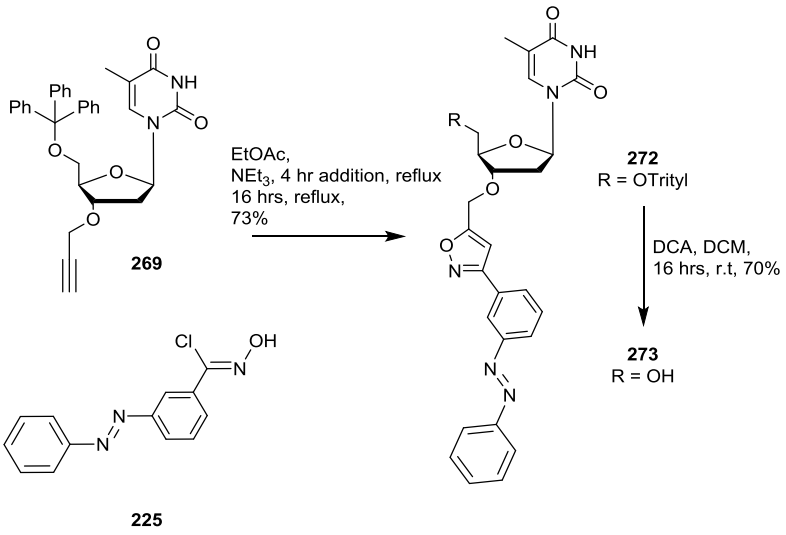

*Scheme 79: Synthesis of azobenzene-thymidine conjugate **273.***

With the success of these two conjugation reactions, the next targets were the divalent adducts **274** and **275**. Again the slow addition of NEt_3 to a refluxing solution of the alkyne and chlorooxime reagents was utilised, scheme 80. In the case of the divalent substrates a 6-fold molar excess of the thymidine alkyne **269** was used, (i.e. three equivalents of alkyne to each nitrile oxide functionality). The reactions gave the protected cycloadducts moderate yields of 65% for **274** and 46% for **275**. However, after characterisation, there was insufficient material left to undertake deprotection. As all the other trityl deprotections proceeded without difficulty, there is little to suggest deprotection would not have been successful. The ^{1}H-NMR of both compounds showed a dominance of the *trans* form with only weak intensity signals present for the *cis* isomer in deuterated chloroform.

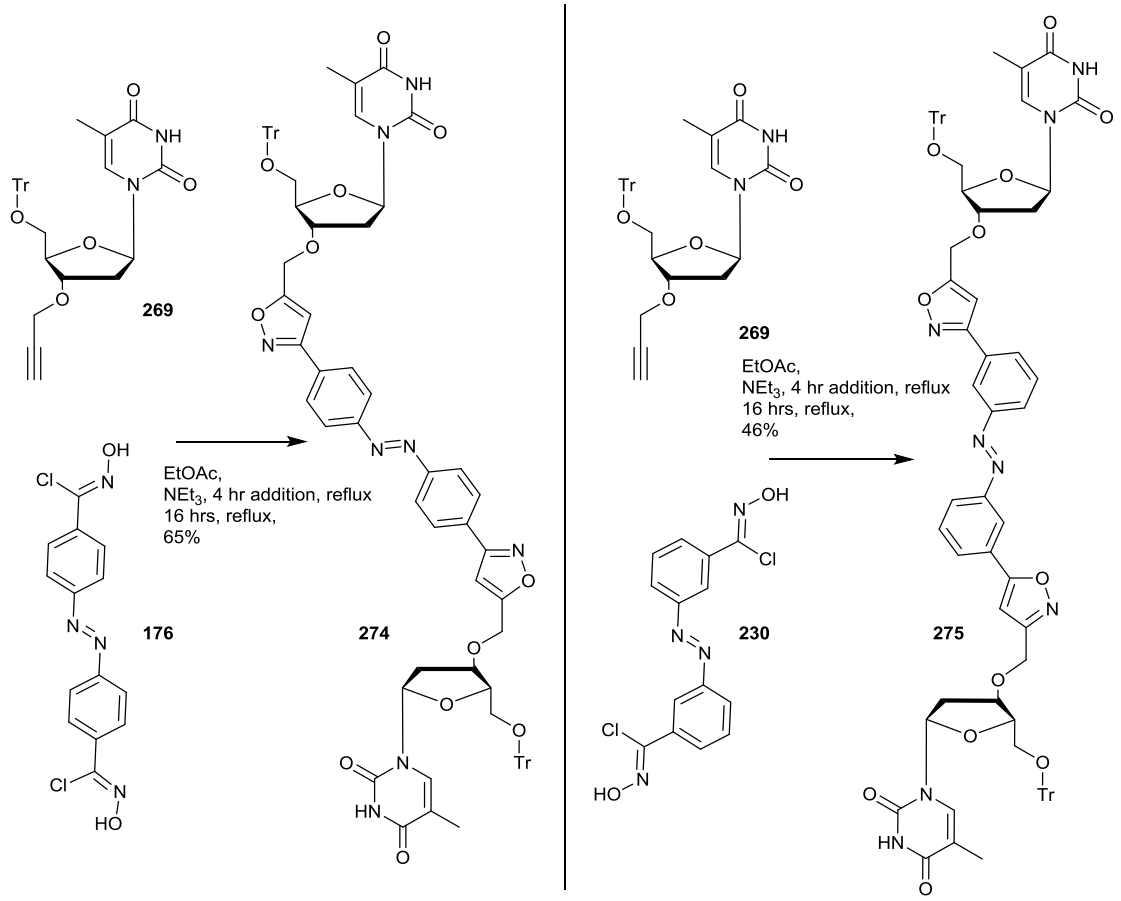

*Scheme 80: Synthesis of the divalent azobenzene-thymidine cycloadducts **274** and **275.***

Conjugation of the propargylated thymidine **269** and the azidoazobenzene **171** was also explored. A 1:1 ratio of the azide and alkyne were dissolved in DMSO and followed by addition of sodium ascorbate and copper sulphate in distilled water. After stirring overnight the cycloadduct **276** was isolated in 84% yield, scheme 81. The trityl group was removed by treatment with dichloroacetic acid in DCM to give the deprotected **277** in 76% yield. NMR spectroscopy showed both samples were heavily dominated by the *trans* form with only minor evidence of the *cis* form ($CDCl_3$ 500MHz).

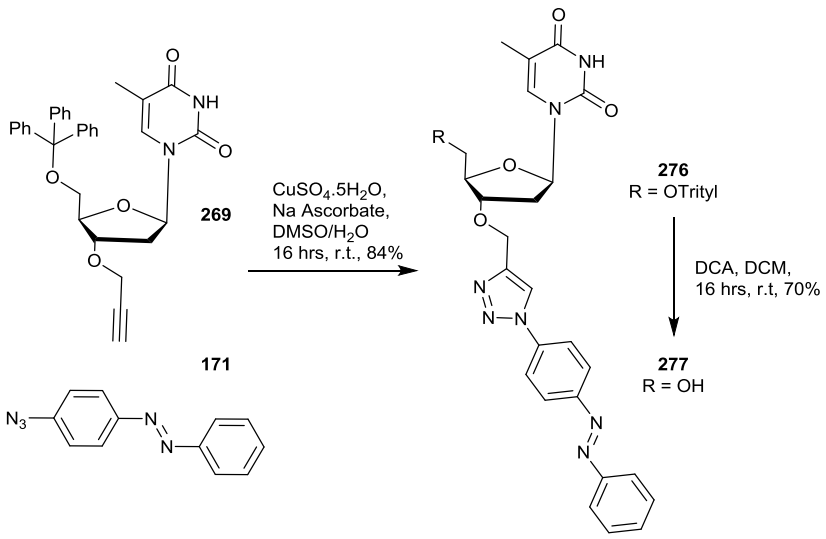

*Scheme 81: Synthesis of azobenzene-thymidine conjugate **277.***

3.3 Summary

- Glycosidic bond formation reactions allowed a family of carbohydrates bearing an alkyne dipolarphile to be synthesised.
- These were successfully reacted in cycloadditions with nitrile oxide and azido bearing azobenzene substrates.
- The introduction of an oxime functionality into a carbohydrate substrate was found to be more challenging..
- Several azido-carbohydrates, accessed through know chemistry, were subsequently reacted with azobenzene-alkynes to produce carbohydrate-azobenzene cycloadducts.
- A nucleoside bearing an alkyne dipolarphile was synthesised and successfully conjugated to a range of azobenzene bearing 1,3-dipoles.

4. Peptide-Azobenzene conjugates

4.1 Background

As discussed in the introduction, the integration of photoswitches, such as azobenzenes, into peptides and proteins has been the focus of much research. Due to their binding site specificity, the structure of proteins is key to their function. The introduction of azobenzene photoswitches to peptides can be very effective for controlling their bioactivity as changes in geometry often result in the turning 'on' and 'off' function in a peptide.

The most common routes to introduce photoswitches into peptides include amide coupling reactions[81,247] and succinamide-cysteine reactions.[109,110] Other routes include CuAAC reactions, and on occasion either azide or alkyne functional groups have been introduced into peptides either along the backbone or within the sidechains positions.[125,126] The application of NOAC chemistry to peptide modification is much more limited and only a few examples of alkyne bearing peptides in reaction with nitrile oxide moieties have been reported.[150,155]

We aimed to create a range of peptides bearing either a dipolarophile or 1,3-dipole (or its precursor) for use in conjugation by cycloaddition to azobenzenes bearing the reciprocal functionality. It was intended to introduce the reactive functionalities at the N-terminal position or in the middle of peptide by building in residues with either azido or alkyne functionalities into the peptide sequence. We considered exploring the conjugating cycloaddition reactions by both solid phase peptide synthesis (SPPS) and solution phase synthesis.

The introduction of reactive functionalities into peptides presents a range of challenges. In particular, the cycloaddition precursors or their partners need to be stable during both the solid phase coupling steps and the final deprotection and cleavage steps.

4.2 Solid phase peptide synthesis

While solution phase peptide synthesis is viable and is attractive under certain conditions, SPPS has become the standard for peptide synthesis.[248] The original Boc protection SPPS methodology has largely been replaced by Fmoc protocols. Currently Boc protocols are attractive for synthesis of peptides prone to aggregation or those containing base sensitive moieties.[249] The Fmoc group is deprotected with a piperidine solution, while the Boc group is removed with a TFA solution.The attractiveness of Fmoc chemistry is that it allows the use of milder reaction conditions. In particular, cleavage in Fmoc protocols involves a TFA based mixture whilst Boc protocols require HF for resin cleavage. The latter requires specialist handling. [248]

Both Fmoc and Boc SPPS follow cycles of coupling and deprotection steps. Rapid, controlled formation of peptides can be achieved. The reactions summarising the processes are shown in figure 55. Initially the resin must be deprotected if necessary. This is followed by coupling of the first C-activated, and ,if necessary, sidechain protected, N-protected amino acid. N-terminal deprotection then follows. The next coupling can proceed with an N-protected C-activated residue. When all the required amino acids in the sequence have been added, the final deprotection can be undertaken, leaving the N-terminus as the free amine. Alternatively a capping reaction, such as acetylation can be applied. When under-taking SPPS the greatest care must be applied to washing the resin bound material between steps, particularly after deprotection. This is important as any residual base present during the coupling steps will cause insertions and the prematurely deprotected material can polymerise. To optimise the final yield of the peptide, it is usually required that each coupling and deprotection step maintains at least 95% yield. Finally, the peptide is cleaved from the resin and all sidechain protecting groups are removed by treatment with a cleavage cocktail.

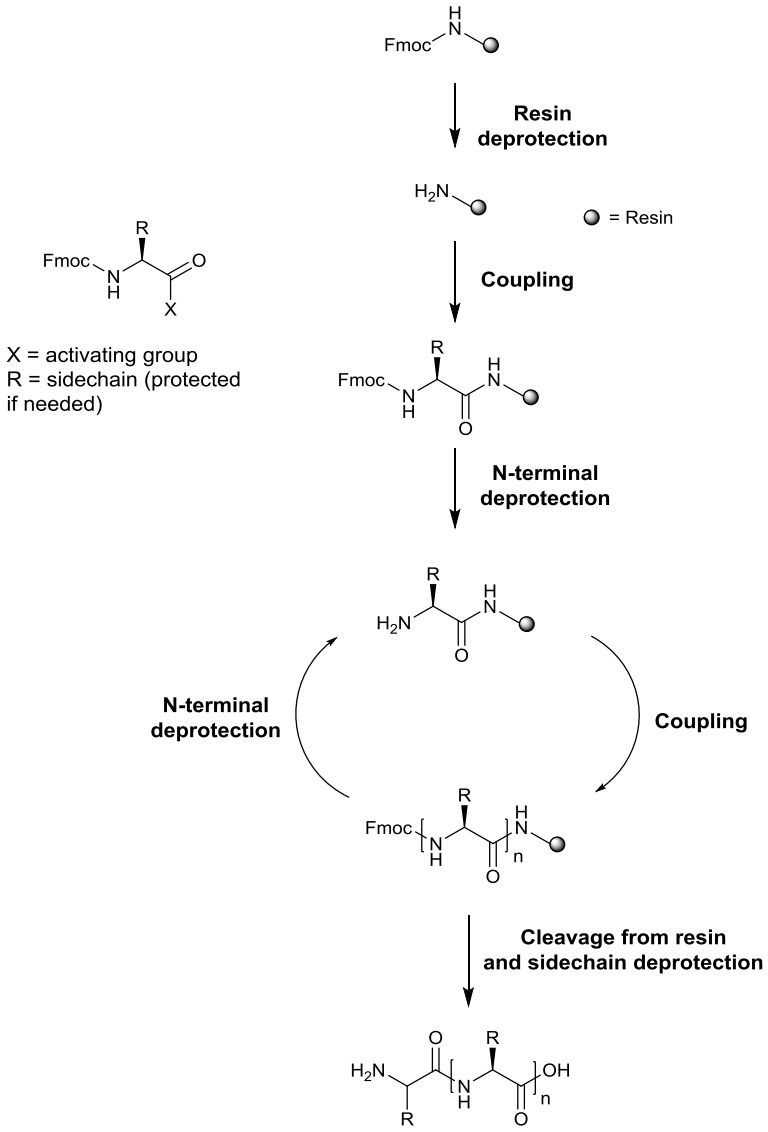

Figure 55: Flow diagram of a typical solid phase peptide synthesis.

The mechanism for the coupling step varies depending upon the choice activating agent. Usually the carboxylic acid of the residue to be coupled is first activated to induce nucleophilic attack by the free amine of the growing peptide. Most modern coupling agents operate by a two-part mechanism. Initially the carboxylic acid is activated in a reaction with a phosphonium or uronium species. This is followed by reaction with an oxybenzotriazole (OBt^-) ion. The resulting OBt ester is then readily attacked by the terminal amine of the resin bound peptide. The desired amide bond is formed without racemisation of the coupled residue. The mechanism of benzotriazol-1-yl-oxytripyrrolidinophosphonium hexafluorophosphate (PyBOP) activated coupling as a typical example is shown in scheme 82.

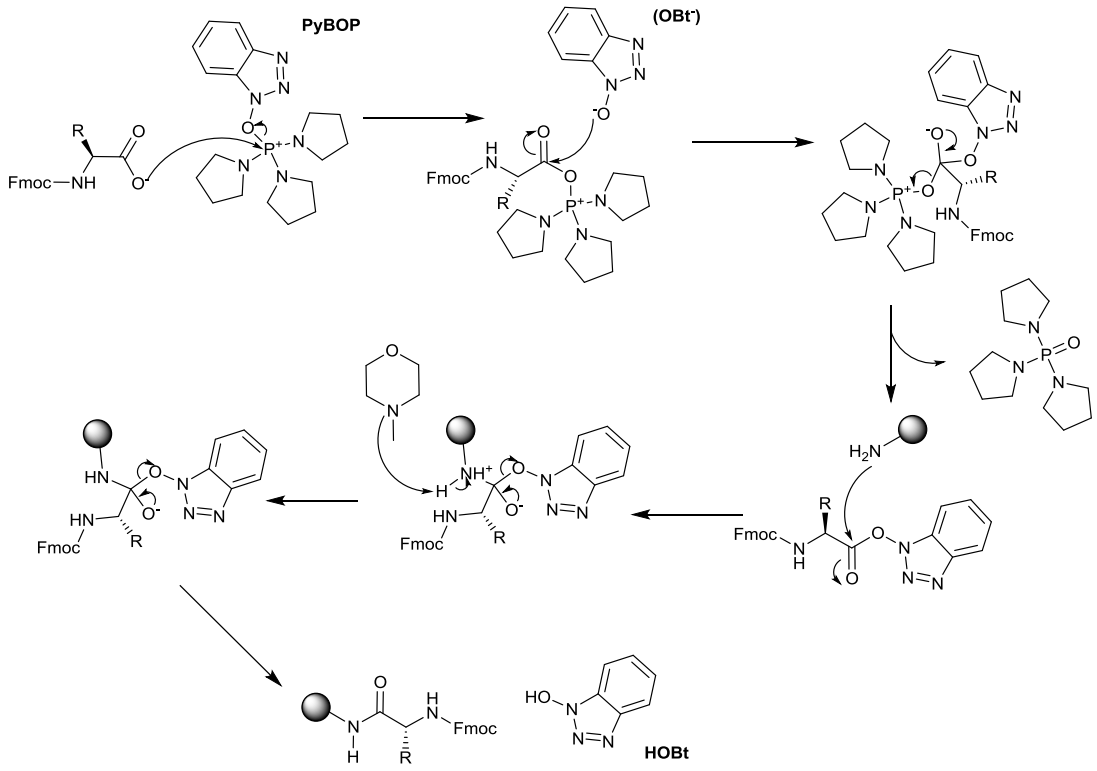

Scheme 82: Mechanism of peptide coupling with PyBOP as activating agent.

A great many coupling agents for SPPS have been developed, however, most modern syntheses are based around HBTU and BOP couplings. Even within each of these groups there are a range agents including BOP, PyBOP, PyAOP, PyBrOP, BOP-Cl, HATU, HBTU, HCTU, TATU, TBTU (all acronyms are listed in the table of abbreviations). Each agent has its own advantages and disadvantages typically offering trades in terms of cost, toxicity and coupling efficiency. For manual peptide coupling experiments PyBOP is often selected as the activating agent as it offers rapid couplings whilst suppressing racemisation and avoiding toxic by-products. HATU is a popular selection for automated synthesises.

The choice of reagents to effect terminal deprotection depends on the protecting group used. Typically a TFA solution is used for Boc chemistry and a piperidine solution for Fmoc chemistry. Weak bases like piperidine mediate Fmoc deprotection following attack of the acidic hydrogen in the 9-postion of the fluorene aromatic system. This results in formation of dibenzofulvene and a carbamate ion which eliminates carbon dioxide and is protonated to give the free amine. Dibenzofulvene adduct has distinctive absorption properties which can be used to determine the efficiency of the deprotection

step and therefore indirectly inform on the success of the previous coupling or resin loading steps. The mechanism of Fmoc deprotection is shown in figure 56.

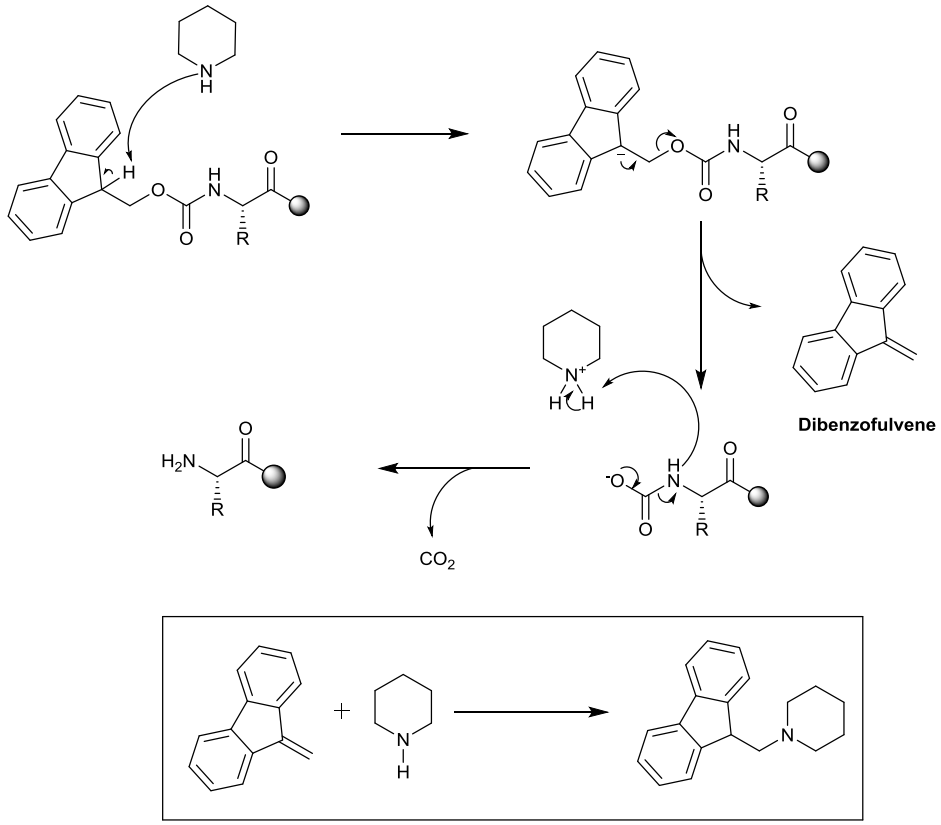

Figure 56: Mechanism of piperidine mediated Fmoc deprotection.

Manual and automated solid phase peptide synthesis (SPPS) are both commonly used and both methods are applicable for the synthesis of the majority of peptides. Automated synthesis drastically reduces the amount of time need to make a given peptide, offering advantages both in terms of overall synthesis time and in active participation time. However, the automated synthesis generally consumes much more materials. Often up to 10 equivalents of each amino acid and of the coupling agents are used for each coupling. Automated SPPS also often utilises *N*-methyl-2-pyrrolidone (NMP) as a solvent which is expensive, whereas manual syntheses typically uses DMF. Another drawback to automated peptide synthesis is that it can only produce peptides on a limited scale.

4.3 Resins and capping

The most popular resin choices for SPPS are polystyrene (PS) or polyethylene glycol (PEG) based. PEGs are favoured for Boc syntheses for their greater TFA stability. Polystyrenes are favoured in Fmoc syntheses because of their higher loading capabilities.[250] The loading of resins generally lie with in the 0.1-1.0 mmol per gram range, with lower loadings being favoured for the synthesis of hydrophobic peptides. There is a wide range of resins within each category and they each offer a different terminal functionality upon cleavage. For example, an oxymethylphenylacetamidomethyl (PAM) resin would be selected for a Boc protocol if a free acid was required. A Wang resin would be selected if the terminal acid was required from an Fmoc synthesis. A Rink amide (Fmoc), or a paramethylbenzhydrylamine (pMBHA) (Boc) resin, would be suitable if an amide was required at the C-terminus.[250] The structures of each of these resins are shown in figure 57. Irrespective of the resin, the N-terminus of the peptide can be left as the free amine or capped, for example by acetylation.

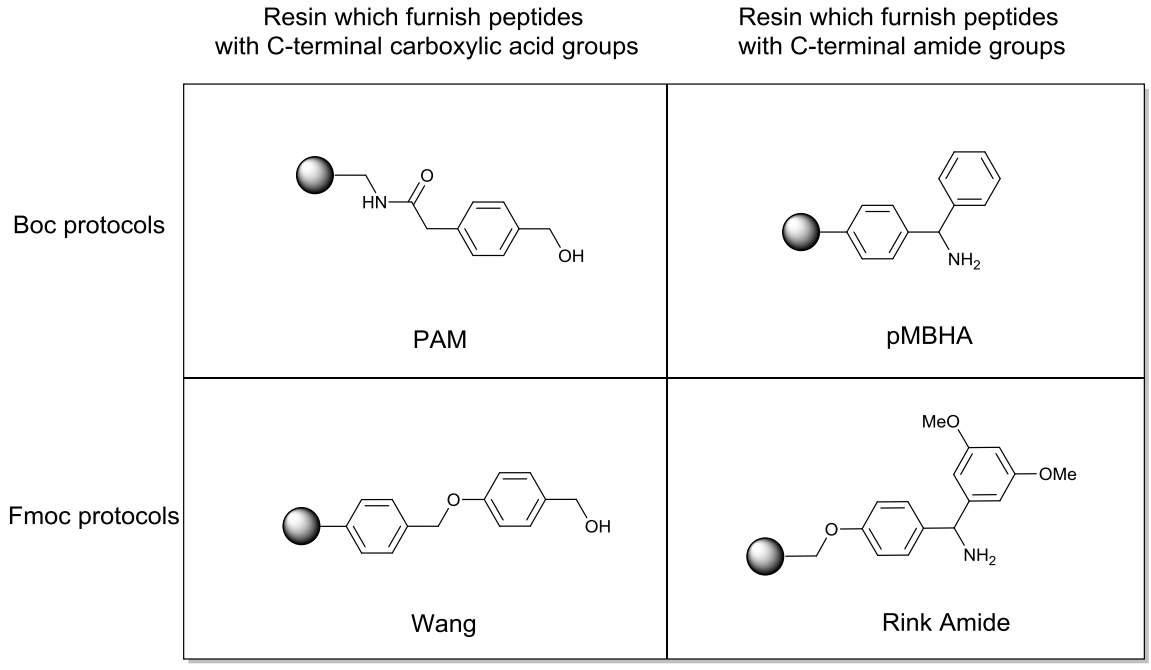

Figure 57: Common resins for SPPS

The ability to control the functionality at the terminal positions is important since derivatisation at these points can have a significant effect on the overall properties of a

peptide, especially in short sequences. For example, peptides with capped termini generally adopt the characteristics of longer peptides. In biological settings, capped peptides are more likely to be recognised as if they were part of a protein and are less likely than their uncapped counterparts to be digested by exopeptidases.[251] However, it should be noted that capping can have a negative effect the solubility of a peptide.[252]

4.4 Peptide sequence

We wished to demonstrate the potential to conjugate an azobenzene unit to a peptide through click chemistry and chose a short, biologically relevant peptide to demonstrate the chemistry. RGD peptides were identified as a simple template from which to work, as well as providing relevance to the work of biomolecule-azobenzene conjugation

RGD peptides contain the tripeptide sequence of arginine (Arg, R), glycine (Gly, G) and aspartic acid (Asp, D). The structure of the tripeptide is represented in figure 58. The RGD motif is a recurring feature in cell recognition processes.[253] RGD peptides are known to interact with integrin receptors of cell membranes to control adhesion of peptides to cells. Although the RGD sequence has since been shown to feature in many proteins, it was initially discovered as the cell recognition motif of fibronectin, a molecule involved in cell growth, cell migration and many other cellular roles.[254] Since their initial discovery RGD peptides have been used in a plethora of applications, ranging from tissue engineering[255] to targeting apoptosis.[256]

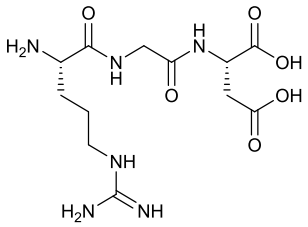

278
H-Arg-Gly-Asp-OH
H-RGD-OH

Figure 58: RGD tripeptide

4.5 Amino acid residues bearing 1,3-dipoles and dipolarophiles

There are two main routes to introducing functionality into a peptide. Side chain modification is possible through incorporation at any point along the peptide sequence of a suitable substituted unnatural amino acid. Alternatively, the functionality can be introduced at one terminus after peptide growth. The introduction of alkynes and azides to the terminal and internal positions of peptides has been reported in papers describing the synthesis of a range of peptide cycloadducts.[125] While some examples of NOAC have been reported for peptide substrates,[150,155] the reactive nature of this dipole may make it less attractive than the azide dipole for peptide modification. NOAC is potentially more problematic since the broad range of functional groups present in peptide side chains could allow side reactions with nitrile oxides to compete with desired cycloadditions.

Several side chains are suitable for the introduction of azide and alkyne functional groups into a growing peptide. Serine, threonine, cysteine and tyrosine are the amino acids most commonly targeted to introduce alkynes following reaction with propargyl bromide.[257-259] Azide transfer has typically been applied to a range of residues including arginine, glutamic acid, serine and threonine.[259] The side chain of Fmoc protected lysine can be converted to an azide in one step.[250,251] The prominence of CuAAC chemistry has rendered many of the azide and alkyne modified amino acid residues commercially available, however, they are often prohibitively expensive.

The azidolysine **281** was the first building block targeted in this research. It was synthesised in 83% yield by the reaction of Fmoc-Lys-OH with the hydrogen sulphate salt of imidazole-1-sulfonyl azide, **280**,[*260] in the presence of pyridine in DMF.[261] This residue was suitable substrate for SPPS synthesis.

The propargylated serine **285** was the second building block targeted. Starting from Boc protected serine, treatment with sodium hydride was followed by reaction with propargyl bromide to give the Boc protected **283**. The Fmoc analogue was required as a SPPS substrate so the Boc group was removed by treatment with TFA in DCM, followed by protection with 9-fluorenylmethyl *N*-succinimidyl carbonate (Fmoc-OSu) in DMF.[262]

[*] imidazole-1-sulfonyl azide should be handled with care. It is known that some salts have explosive properties. It should only be isolated as its hydrogen sulphate salt **280**. The synthesis of **280** is detailed in reference 260, along with a number of precautionary measures.

The overall yield of the three step synthesis (**282** → **285**) was 56%. The synthesis of both of the derivatised Fmoc amino acid cycloaddition partners are shown in scheme 83.

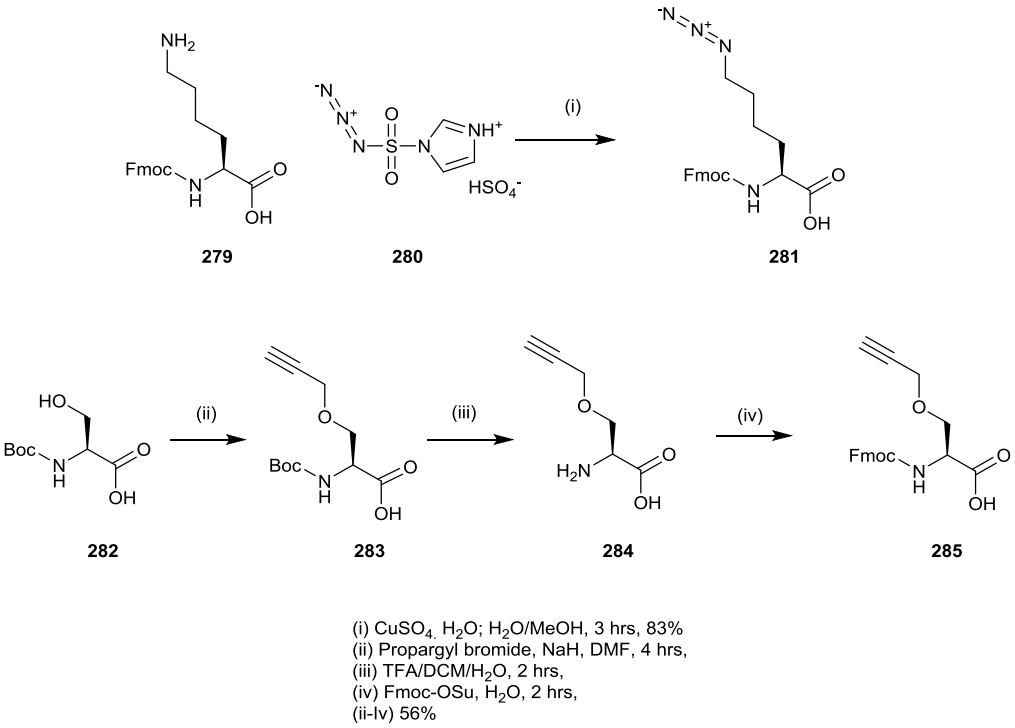

Scheme 83: Syntheses of azidolysine (above) and propargylated serine (below) residues suitable for Fmoc SPPS.

Alkyne and azide functionalities have commonly been introduced at the N-terminus of peptides through alkylation and azide transfer reactions respectivly.[252,253] We considered access to N-terminal azides by direct azide transfer from imidazole-1-sulfonyl azide.H_2SO_4 **280.**[251,254] In an alternative strategy we also explored the reaction of 2-bromoacetic acid, **289**, with sodium azide in search of 2-azido acetic acid, **290**, scheme 84[263,264] which we believed would be a suitable substrate for peptide coupling chemistry, effectively yielding an azido glycine N-terminal residue.

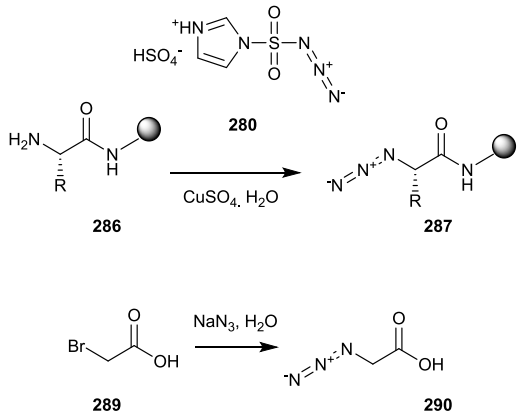

Scheme 84: Routes to be explored for the introduction of azido functionality at the N-terminal position of a peptide.

4.6 Synthesis of an azobenzene-peptide conjugate through peptide coupling

Initially, the short RGD peptide-azobenzene conjugate **295** was targeted by two routes involving reactions with the supported peptide H-GRGDG-resin. The routes considered for constructing the conjugate are summarised in scheme 85. Although all routes are potentially suitable for solution phase chemistry, solid phase conditions were more attractive for the initial syntheses.

Route 1 –Direct coupling chemistry between a growing peptide (**291**) and a preformed azobenzene carboxylic acid (**292**).

Route 2: On resin cycloaddition to an azidopeptide (**293**) and an azobenzene alkyne (**107**).

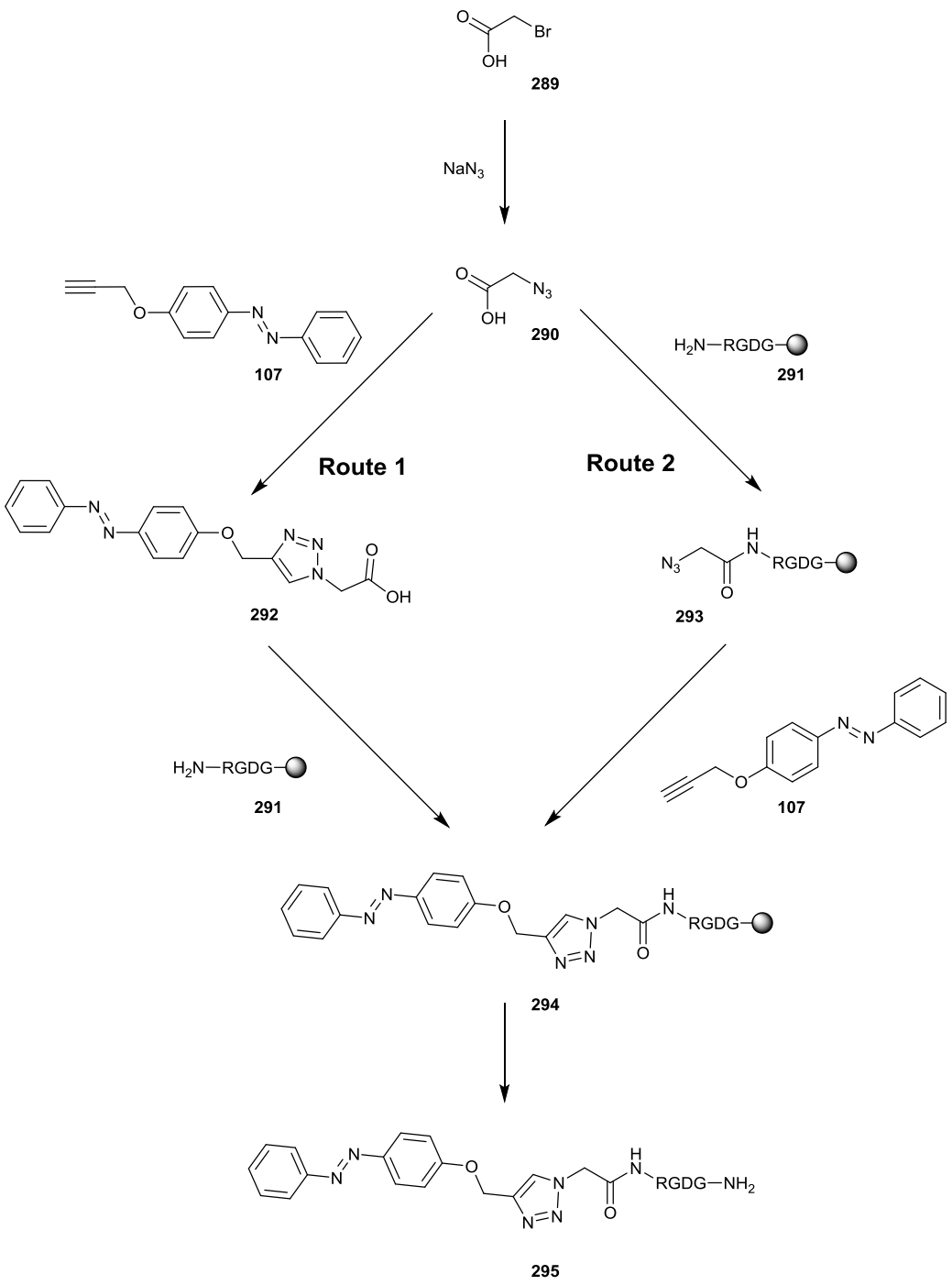

*Scheme 85: Synthetic routes explored for access to the N-terminal peptide-azobenzene conjugate **295.***

Initially **route 1** was explored. The synthesis of peptides is the costly and time-consuming component and this route involves a 'traditional' amide bond forming reaction and so it was deemed to minimise the risk of reaction failure and loss of material.

Azidoacetic acid **290** was reacted with the propargylated azobenzene **107** in the presence of copper sulphate and sodium ascorbate. The cycloadduct **292** was obtained as one major isomer in 61% yield.

The supported tetrapeptide **291** (H-RGDG-Resin) was synthesised manually using Fmoc amino acid building blocks with the standard SPPS protocol on a Rink amide resin at a 0.311 mmol scale and using PyBOP as the activating agent. A small portion of the material was deprotected and cleaved from the resin and analysed by mass spectrometry, which supported formation of the desired sequence. The coupling of the triazole linked carboxylic acid terminated azobenzene **292**, to the resin bound peptide was achieved through treatment of PyBOP under standard SPPS conditions. The success of the reaction was inferred by the strong orange colour imparted to the washed resin which is attributable to the incorporation of an azobenzene unit.

The supported peptide-azobenzene conjugate **294** was cleaved from the resin and the side chain protecting groups simultaneously removed by treatment with a TFA/H_2O/TIS mixture (30 minutes, r.t,). The product was isolated following precipitation by the addition of diethyl ether. The solid was collected by centrifugation and the supernatant discarded. After several washing steps (diethyl ether) the solids were dissolved in water and the minimum amount of acetonitrile before lyophilisation. The crude product **295** was obtained as an orange solid. The synthesis of **295** is shown in scheme 86.

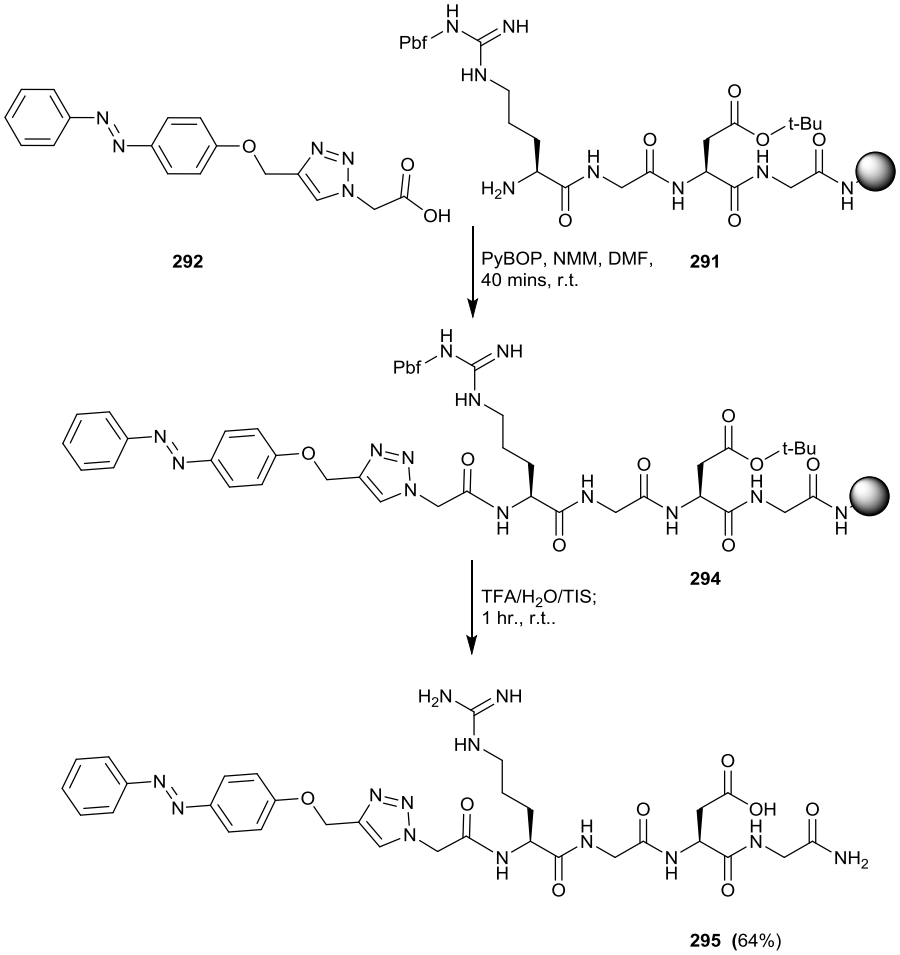

*Scheme 86: Sold phase synthesis of azobenzene-peptide conjugate **295.***

The crude product was analysed by HRMS and HPLC, and was purified by semi-preparative HPLC (H_2O/CH_3CN). Following lyophilisation of the isolated fractions, the product **295** was obtained as an orange solid in 64% yield[†]. HRMS and analytical HPLC were used to support formation of the desired structure and its purity, figure 59.

[†] The yields of the peptides are based on the initial loading of the resin, and so are representative of all amino acid couplings as well as the cycloaddition and cleavage steps.

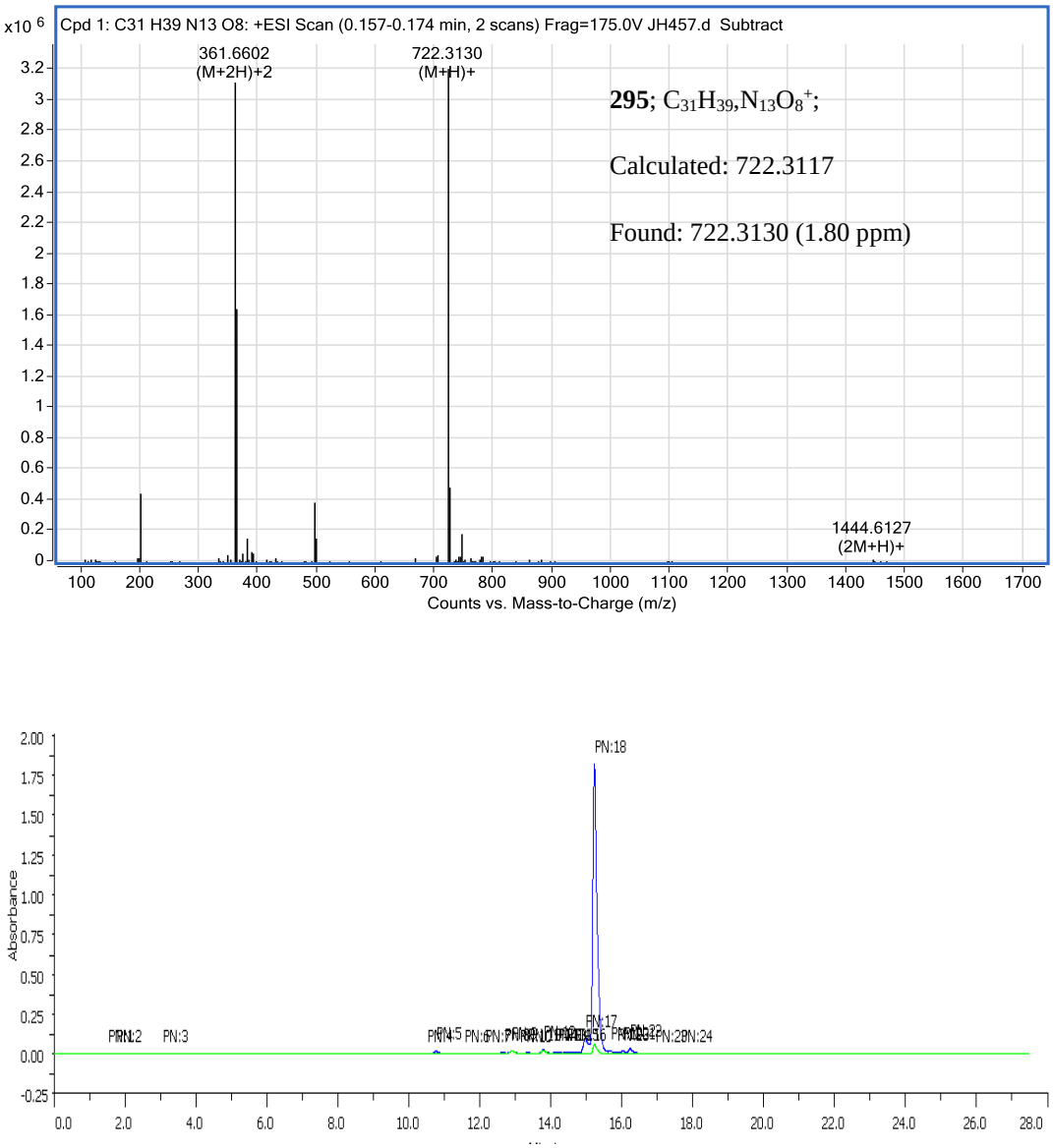

*Figure 59:HRMS and HPLC (UV/Vis 256 nm, CH_3CN/H_2O) data in support of formation of peptide-azobenzene conjugate **295**.*

4.7 Cycloaddition to N-terminal azidopeptides:

To better explore the potential of cycloaddition chemistry as a general approach to peptide and protein conjugation, solution phase cycloaddition to azidopeptides was studied. This time the supported pentapeptide, H-GRGDG-resin **291**, was synthesised by automated SPPS on a 0.1 mmol scale. While still on the resin the terminal amino group was converted to an azide by treatment with the azide transfer reagent **280** in DMF in the presence of DIEA. The resulting azidopeptide was cleaved from the resin by treatment with TFA/H_2O/TIS, in a reaction that also caused deprotection of the sidechains. The peptide **296** was precipitated by addition of diethyl ether. HRMS analysis of the crude material, supported survival of the azido functionality after the cleavage process ($M+H^+$ calculated: 486.2168; found: 486.2183; difference: 3.16 ppm).

Cycloaddition to **296** was attempted using the crude material which was dissolved in DMF. The propargylated azobenzene **107** was added followed by copper sulphate and sodium ascorbate in H_2O, scheme 87. After stirring overnight at room temperature, the solvent was removed under vacuum without heating. The resulting oily material was purified by HPLC (CH_3CN/H_2O). The collected fractions were dried by lyophilisation and the cycloadduct **295** was isolated as an orange solid in 51% yield. The synthesis of **295** is shown in scheme 87. HPLC and HRMS data was in agreement with that obtained with the material obtained from the synthesis by the on-resin peptide coupling approach.

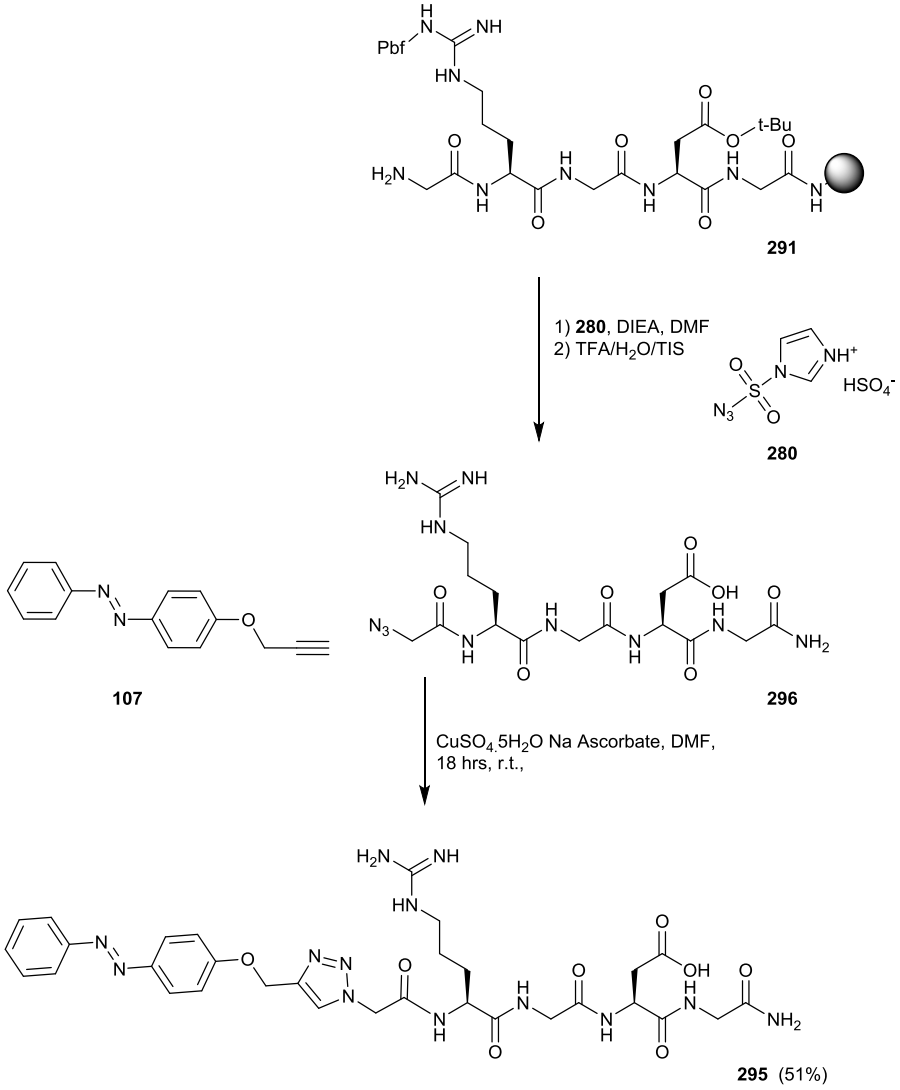

*Scheme 87: Solution phase synthesis of azobenzene-peptide conjugate **295**.*

4.9 Cycloaddition to propargylated peptides (CuAAC)

The sequence H-RGDSTF-OH was selected for the introduction of a dipolarophile into the side chain of a peptide; this sequence was taken directly from the α-chain of fibrinogen.[265] The peptide was manually synthesised using the Fmoc SPPS protocol on a 0.3 mmol scale. The propargylated serine derivative **285** was used as direct replacement for natural serine. The N-terminus was capped by treatment with acetic anhydride in the presence of pyridine and the final supported peptide has the structure Ac-RGDS*TF-resin‡, **297**, scheme 88.

‡ A residue marked with an asterisk indicates one modified with a cycloaddition partner

While still on the resin, the peptide (**297**) was reacted with 4-azidoazobenzene, **171**, in the presence of copper sulphate and sodium ascorbate. The success of the cycloaddition was strongly inferred by the vivid orange colour afforded to the washed resin. When the resin bound peptide was treated with the cleavage cocktail (TFA/H_2O/TIS 95:2.5:2.5), **conditions 1**, scheme 88, it unexpectedly turned black. Following the addition of diethyl ether to the TFA solution a light brown precipitate was observed. It was washed several times with diethyl ether and lyophilised from water/acetonitrile to give an off white powdery solid (89%).

The off-white sample was analysed by HRMS and by HPLC which supported the presence of two products. The mass spectrum showed a pair of peaks at 895.4171 (H+) and 448.2152 (2H+), and a second pair at 984.4501 and 492.7292, figure 60. The HPLC trace showed 2 peaks; one at ~10 minutes and the other at ~15 minutes. Following irradiation of the sample with light at 365 nm, the peak at ~10 minutes did not change, whilst the peak at ~15 minutes decrease in size and was largely 'replaced' by a new peak with a retention time of ~14 minutes. Since the product which eluted at ~15 minutes photoisomerised it is likely that it gives rise to the mass 984.4445 and 492.7292, since these masses are in keeping with that expected for the azobenzene conjugate **300**. The HPLC data shown in figure 61.

The failure of the peak eluting at ~10 minutes to photoisomerise, suggests the molecule giving rise to it has lost its azo functionality. A search of the literature revealed that under certain conditions, TIS can reductively cleave the azo linkages.[90,266] If this had occurred in our experiment, the anilino product **299** would be the likely product. The HRMS peaks at 448.2154 and 895.4234 are consistent with the formation of **299**. It was decided in future experiments that TIS would not be used in the cleavage protocols of azobenzene containing peptides.

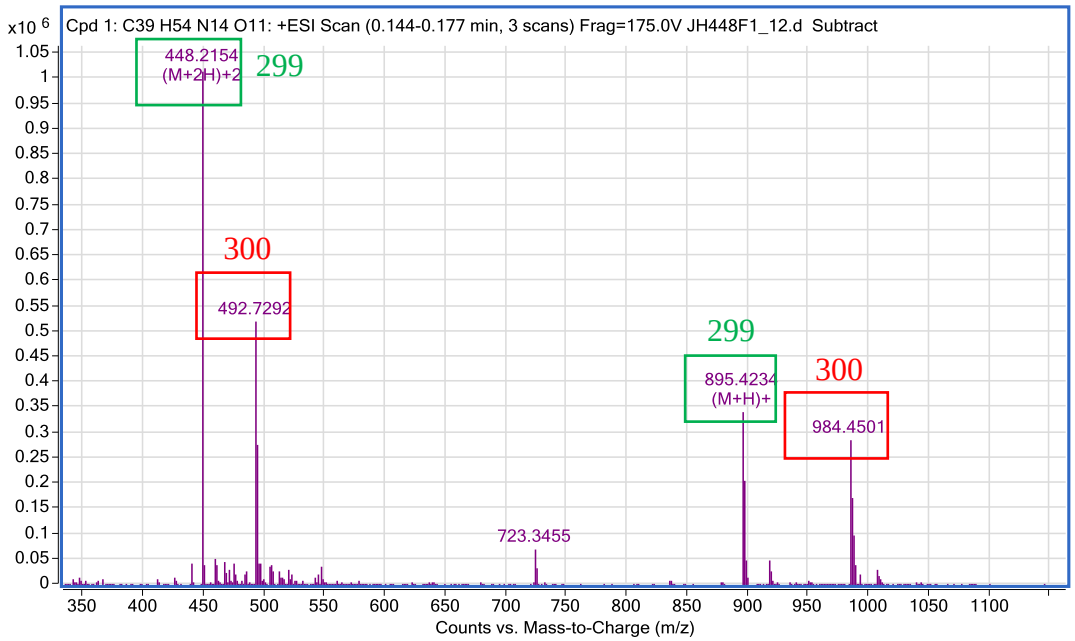

*Figure 60: HRMS data for the crude products of cycloaddition between **297** and **171** involving cleavage conditions 1: supporting formation compounds **299** and **300**.*

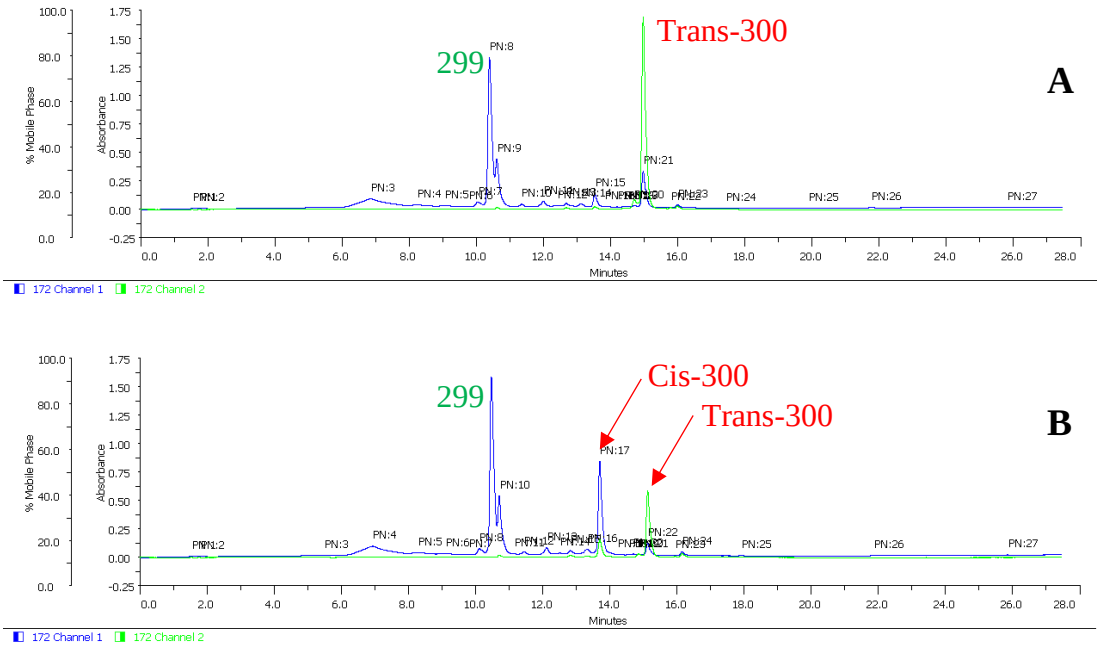

*Figure 61: HPLC traces in support of **299** as an aminopeptide conjugate and **300** as an azobenzenepeptide conjugate; the reaction products of cleavage and deprotection of **298**. **A**: sample kept in the dark; **B**: sample irradiated with light at 365 nm. (Blue trace 330 nm, green trace 430 nm. H_2O/CH_3CN).*

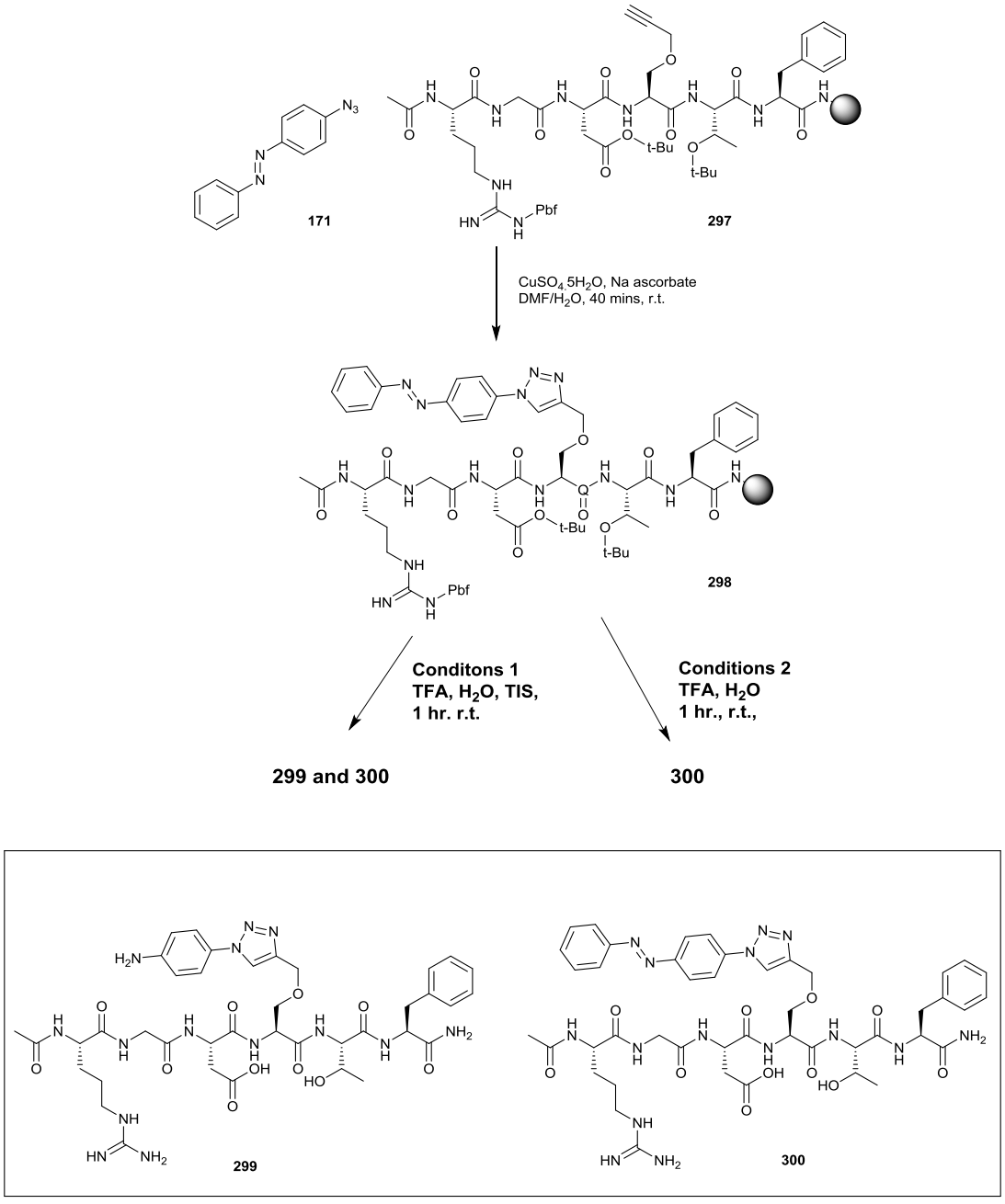

*Scheme 88: Synthesis of peptide conjugates **299** and **300.***

The supported peptide **297** (Ac-RGDS*TF-resin) was synthesized through automated SPPS (0.1 mmol) and deprotected and cleaved from the resin with a TFA/H_2O/TIS mixture. HRMS confirmed the desired peptide **301** had formed. Together with 4-azidoazobenzene **171**, it was dissolved in DMF and an aqueous solution of copper sulphate and sodium ascorbate was added and the mixture left to stir overnight at room temperature. The synthesis is shown in scheme 89. Attempts to precipitate the product by addition of diethyl ether failed. Therefore, the reaction mixture was concentrated under vacuum. The resulting material was subjected to purification by semi-preparative

HPLC. Several sets of fractions were collected. However, the HRMS data of no fraction group was consistent with that expected for the desired product **300**.

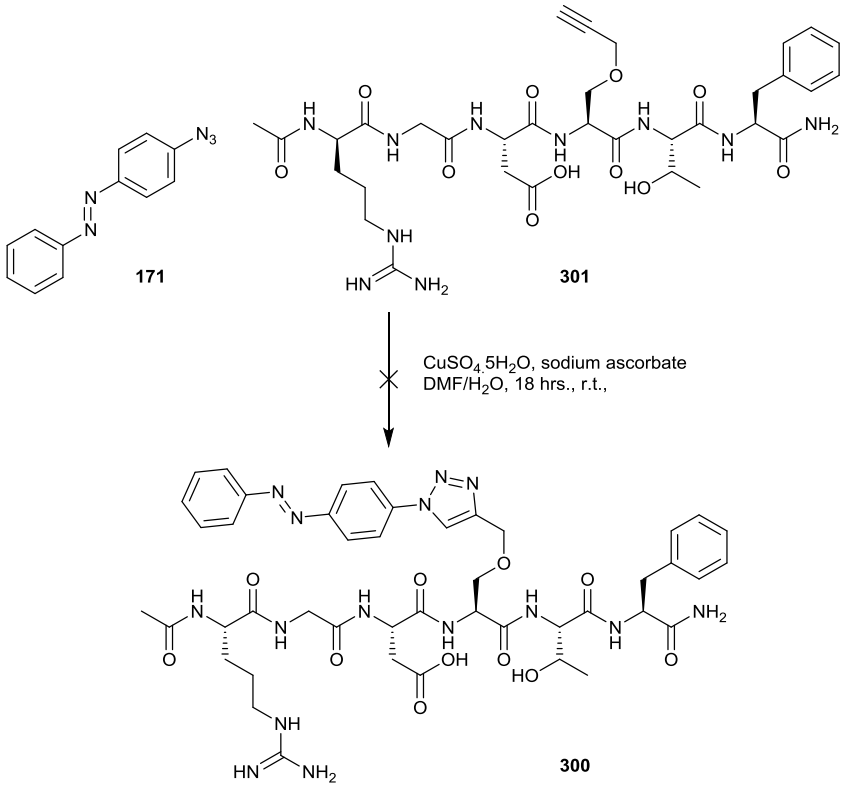

*Scheme 89: Attempted solution phase formation of peptide-azobenzene conjugate **300.***

The difficulties encountered with TIS in the deprotection protocol for on-resin (scheme 88) and the complexity of the product mixture for the off resin approach to **300** (scheme 89) resulted in a return to an on-resin approach. The supported peptide **297** was once again synthesised (manual, 0.305 mmol scale) and was reacted with the azidoazobenzene **171** under the same conditions as before ($CuSO_4$, sodium ascorbate, DMF, r.t.), scheme 88. Once again the resin was a vivid orange colour. In this case, crucially, the final deprotection and cleavage was conducted with TFA and H_2O (95:5) in the absence of TIS, scheme 88 **conditions 2**. With this modification the solution remained orange and following addition of diethyl ether an orange precipitate was returned. Following purification by HPLC and lyophilisation, the desired product **300** was returned as an orange solid in 69% yield, ($[M+H]^+$ calculated: 984.4435, found: 984.4420; difference: 1.52 ppm).

4.10 Cycloaddition to azidopeptides (CuAAC)

The sequence SRK*RGDS was selected for integration of an azidolysine residue. It was manually synthesised on rink amide resin and **302** was prepared on a 0.16 mmol scale. Propargylated azobenzene **107**, copper sulphate and sodium ascorbate in DMF/H_2O were added to the resin bound azidopeptide **302**. Following reaction at room temperature for one hour the liquid phase was removed and the resin washed, The resin was now a yellow/orange colour. Cleavage of the peptide from the resin and sidechain deprotection was carried out using a TFA/H_2O mixture. The resulting orange solution was diluted with ether until precipitate formation. The precipitate was washed three times with diethyl ether and lyophilised to give the crude product as a yellow/orange solid. The synthesis of **303** is shown in scheme 90.

The material was subjected to purification by HPLC and the desired product **303** was isolated as a yellow/orange solid in 56% yield. HRMS data of the compound is shown in figure 62.

In a parallel experiment preparation of **303** was attempted by solution phase conjugation chemistry. The supported azidopeptide Ac-SRK*RGDS-resin **302** was again manually synthesised on a 0.16 mmol scale. It was then deprotected and cleaved from the resin upon treatment with a TFA/H_2O solution and precipitated by addition of ether. After isolating the peptide by centrifugation it was dissolved in DMF. The propargylated azobenzene **107** and an aqueous solution of copper sulphate and sodium ascorbate were added. After stirring overnight, the solution was concentrated under vacuum without heating to give the crude material as a brown oil. This was subjected to purification by HPLC whereupon the desired cycloadduct **303** was isolated as an orange solid in a much reduced 14% yield. The HRMS data agreed with that of the conjugate formed by the on resin reaction, figure 62.

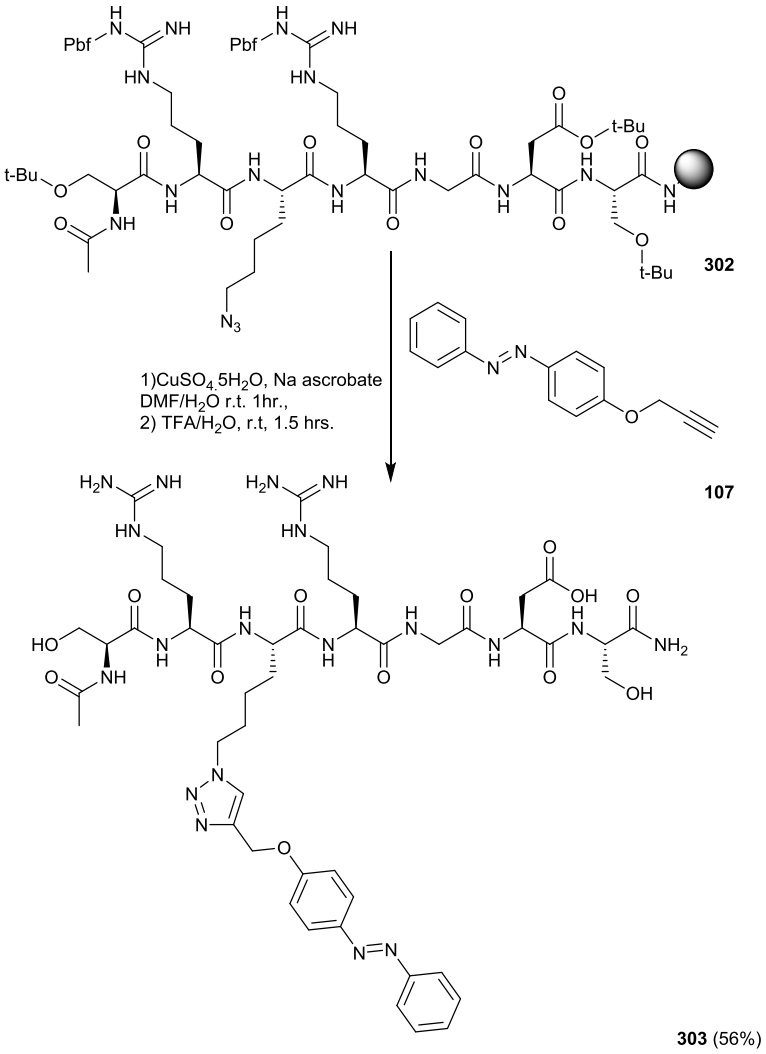

*Scheme 90: Synthesis of internally modified peptide-azobenzene conjugate **303**.*

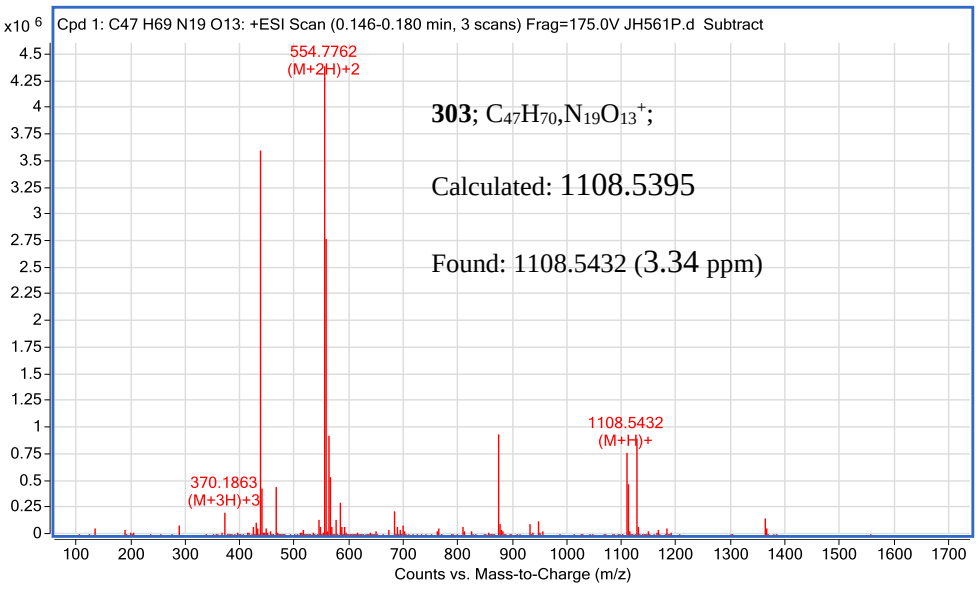

*Figure 62: HRMS data of the peptide-azobenzene conjugate **305.***

4.11 Cycloaddition to propargylated peptides (NOAC)

Following from the successful synthesis of a range triazole linked azobenzene-peptide conjugates, NOAC reactions were explored in search of isoxazole analogues. The base sensitive nature of chlorooximes makes them incompatible with Fmoc SPPS conditions. Oxime functional groups could potentially be integrated into a peptide sequence but the resin swelling is poor in aqueous alcohol solutions and would most likely hinder the cycloaddition efficiency. These limitations restricted us to the use of an azobenzene oxime or chlorooxime in partnership with a dipolarophilic peptide. As it would lead to **304** the 'isoxazole analogue' of the triazole ligated **300**, reaction between the chlorooxime **174** and the supported propargylated peptide **297** was selected for study. The resin bound peptide was selected as SPPS had proven more successful than the solution phase chemistry for the generation of **300**.

The nature of the SPPS vessels makes the slow addition of base difficult, as they are not easy adapted to allow deliveries to be made with a syringe pump. To compensate for the established advantages of slow dipole generation, a large excess of chlororoxime was utilised. We were not concerned about work-up difficulties, since in common with all solid phase reactions, any solution phase by-products and unreacted material could be easily washed away from the supported product at the end of the reaction. The resin bound Ac-RGDS*TF peptide **297** was treated with a threefold excess of both chlorooxime and base. The reaction mixture was agitated for 30 minutes, the solution was drained from the resin followed by washing and exposure to a further three equivalents of both the dipole precursor and base, followed by agitation for an additional 30 minutes. After the post reaction washes, the resin only retained a faint orange colour. The reaction sequence is summarised in scheme 91.

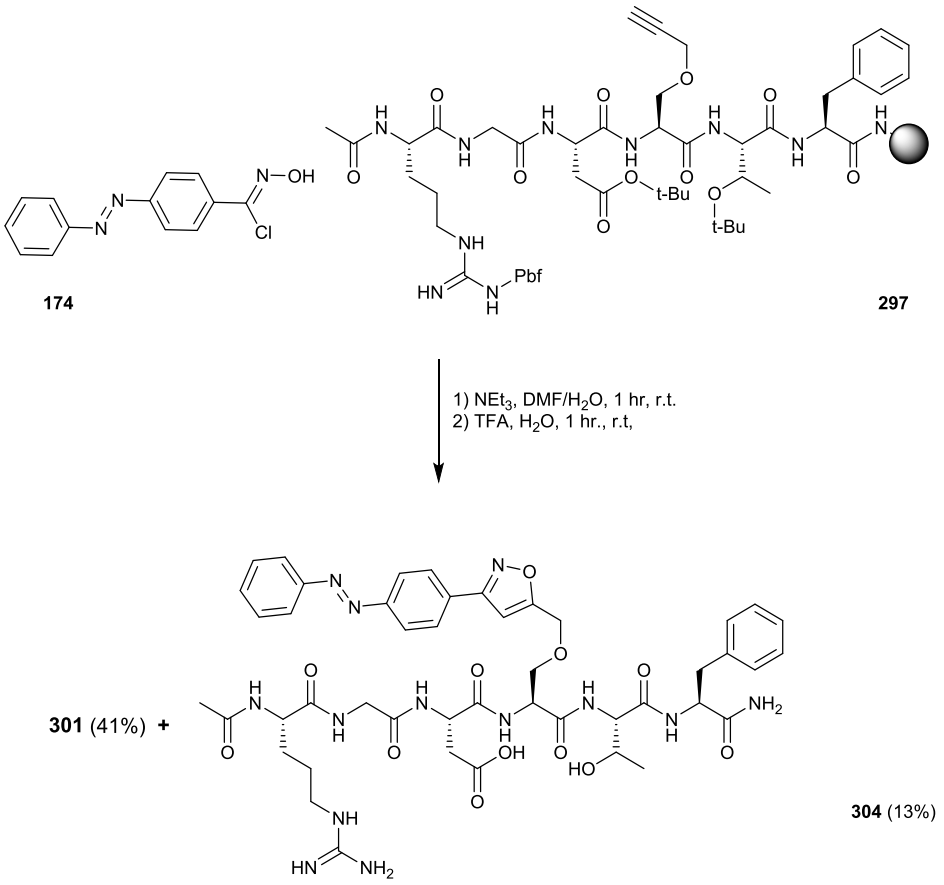

*Scheme 91: Synthesis of the isoxazole ligated azobenzene peptide conjugate **304** by on resin NOAC.*

Deprotection and cleavage from the resin by treatment with TFA and water gave the crude reaction products. Following precipitation induced by diethyl ether, the crude material was isolated as a faint orange solid. After separation by HPLC, the propargylated peptide **301** was isolated in 41% and the azobenzene-peptide conjugate **304** in 13%. The HRMS data of **304** is shown in figure 63. The poor yield of **304** (13%) with respect to the 56% obtained for analogous triazole adduct **300** may be a consequence of side-reactions of the more reactive transient nitrile oxide dipole. Future experiments aiming to optimise the yields of isoxazole ligated peptide conjugates may examine protocols which allow greater control of dipole formation.

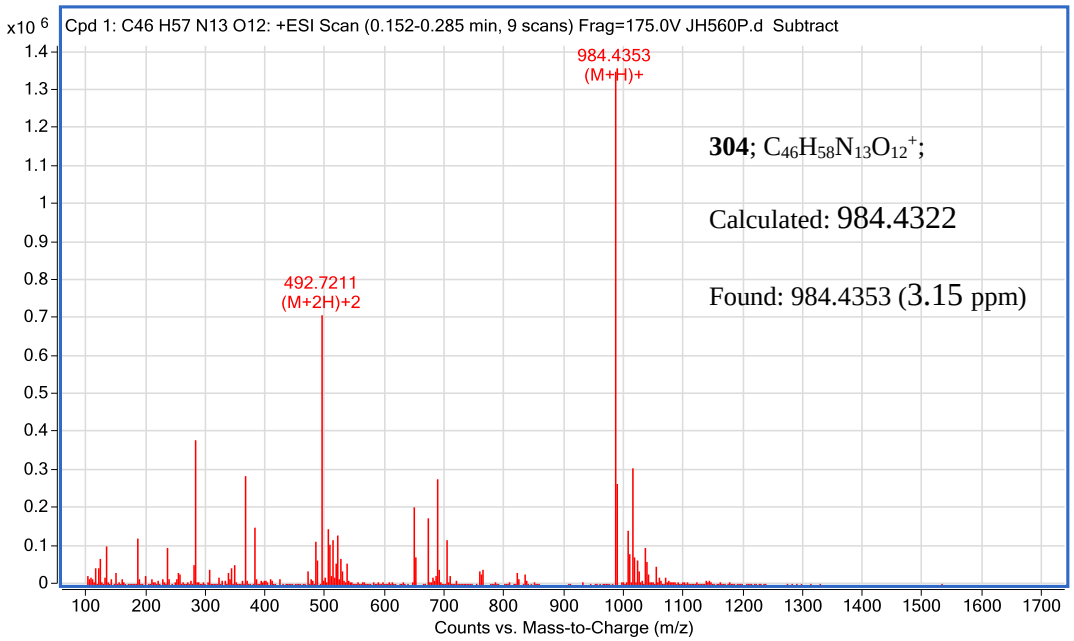

*Figure 63: HRMS data of isoxazole ligated peptide-azobenzene conjugate **304***

4.12 Ligation of a peptide with a saccharide

Finally, we wished to demonstrate the use of this chemistry to make highly functionalised molecules and chose to conjugate a saccharide to a peptide, with a photoresponsive azobenzene spacer between the biomolecule units. For the purposes of demonstrating this possibility we aimed to ligate a galactose unit with a pentapeptide, as shown in scheme 92. The azobenzene **152**, with both alkyne and carboxylic acid functionalities, was coupled to a resin bound GRGDG peptide **291** using the standard SPPS protocol. The success of the coupling was verified following cleavage and deprotection of a small sample by HRMS (calculated: 722.3117, found: 722.3130, difference 1.79 ppm). The resulting orange coloured supported peptide **305** was reacted with the azidogalactose **255** in the presence of a copper I catalyst generated in situ from copper sulphate and sodium ascorbate. The peptide was deprotected and cleaved from the resin using a TFA/H_2O mixture. The adduct was precipitated by addition of diethyl ether, giving the crude product as an orange solid. The reactions are summarised in scheme 92.

Following purification by HPLC and lyophilisation **306** was isolated as an orange solid in 24% yield. Unreacted N-terminal azobenzene-alkyne **307** was recovered in 39% yield.

Deprotection of the sugar unit in **306** was not attempted as it is likely that the aqueous basic solution required would degrade the peptide. Future work in the area might include a 'repeat' of this experiment with protecting groups which could be removed without the need for strong acid, base, or heating.

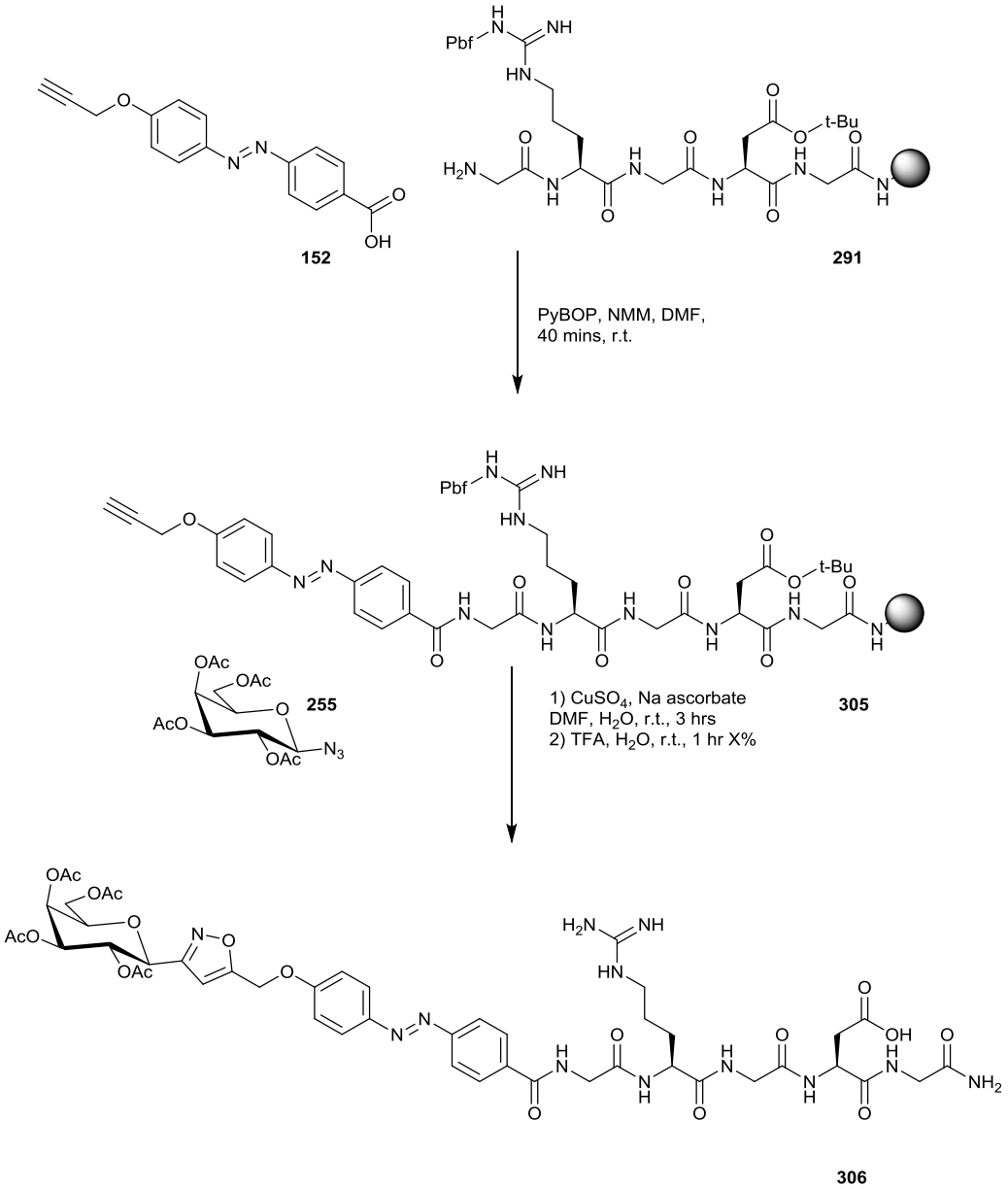

*Scheme 92: Synthesis of azobenzene spaced glycopeptide conjugate **306.***

4.13 Summary

- Simple peptides integrating 1,3-dipoles, their precursors, or an alkyne functionality were synthesised by both manual and automated solid phase peptide synthesis.
- Azide-alkyne cycloadditions between peptides and partnering azobenzene units were successful where the azide was located at the terminal or at a sidechain position of the peptide.
- Conjugation by CuAAC was demonstrated for a peptide with a sidechain alkyne functionality.
- Conjugation by NOAC was demonstrated for a peptide with a sidechain alkyne functionality .
- A carbohydrate-peptide conjugate with an azobenzene spacer was formed via cycloaddition reaction.

5. Photophysical properties of the conjugates

We wished to investigate the photophysical properties of a selection from amongst the wide range of azobenzene biomolecule conjugates synthesised in this project. We wished to establish, firstly, the photostationary states of the selected compounds and secondly, their thermal relaxation rates from the *cis* isomer to the *trans* isomers.

We considered that the compounds selected for investigation should include those which would allow direct comparisons of the influence of the following: (1) the biomolecule structure: mannose vs galactose, *mono* vs disaccharide and sugar vs nucleoside (2) the nature of the linkage: isoxazole vs triazole, heterocycle vs ether (3) the relative orientation of the biomolecule about the azobenzene skeleton: *para* substitution vs *meta* or *ortho* substitution and (4) valency: *mono* substituted vs divalent conjugates.

The influence of the biomolecule on the properties of the conjugates is of interest as the size of the 'substituents' is known to affect the rates of isomerisation,[267] for example slowing the *trans* to *cis* and facilitating the *cis* to *trans* conversion for bulky substrates.[268]

The nature of the linkage between the azobenzene and biomolecule motifs is also potentially an important influencer of the photophysical properties of the conjugates. Electron donating or withdrawing properties of substituents are known to have a significant effect upon the properties of an azobenzene. As well as influencing the efficiency of the isomerisation, it has been proposed that the mechanism of isomerisation may change with the electronic nature of the substituents, with electron donating groups favouring rotation mechanism and electron withdrawing groups favouring inversion pathways.[269,270]

Typically, as might be expected from their weak to moderate electron donating or withdrawing properties groups like aryl, alkyl, halide, carbonyl and amide are viewed as having very little effect upon the photophysical properties of an azobenzene. In contrast, amino or hydroxyl functionalities show significant effect upon the position of absorption bands of azobenzene so substituted.[51] This parameter is important since when irradiating substituted azobenzene at a fixed wavelength, the rate of isomerisation is impacted by the absorption intensity at that particular wavelength.

The effect of electron donating groups on an azobenzene photophysical properties is also dependent upon the position at which the substitution is present with respect to the azo

group. Ortho and *para* electron donating substituents have a greater influence than *meta* positioned groups.

However in general comparisons of the physical properties of families of azobenzenes is somewhat understudied; from what is known, *meta*- and *ortho*- substitution can have effects beyond their electronic donating/withdrawing properties.[271,272] In particular, substitution *ortho* to the azo linker can cause destruction of planarity and a reduction in the efficiency of isomerisation processes.[273]

In light of the structural diversity within the biomolecule conjugates prepared in this research and their potential value as probes in biological settings we wished to characterise the photostationary states and thermal relaxation parameters for a range of conjugates.

5.1 Photostationary states

The photostationary state for any given azobenzene is the point at which the rates of formation of *trans* to *cis* isomerisation and *cis* to *trans* isomerisation become equal. The point at which is this equilibrium is reached is dependent upon a number of factors[54]:

- The nature and pattern of substituents on the azobenzene core.
- The wavelength of irradiation.
- Environmental factors including solvent and temperature.
- The wavelength of irradiation

Whilst the exact processes of isomerisation are somewhat complicated by the various modes by which it can take place. The absorption associated with the π→π* transition, typically between 300-400 nm, is more intense than that associated with the n→π* transition, 400-500 nm, for the *trans* isomer. The inverse is the case for the *cis* isomer.[271] This means that to optimise the *trans* to *cis* isomerisation that the wavelength of the light selected should be as close to the λmax of the π→π* band as possible whilst being as far from the n→π* (nm) absorption as possible. Conversely light of a wavelength as near the λmax of n→π* band and as far away from the π→π* band would be favourable to promote *cis* to *trans* isomerisation.

In order to support the choice of wavelength of light to be used for determining the photophysical states of the compounds in this series the UV/Vis spectra of a number of compounds were recorded. The UV/Vis spectra of **215** recorded in DMSO (25 μM), is shown in figure 64. The blue trace is the spectrum of a sample left in the dark for a period of several days, the sample, dominated by the *trans* isomer is referred to as the 'dark adapted' spectra. The intense π→π* band appears with a λmax at ~ 335 nm, with the weak n→π* band having a λmax at ~ 435 nm. The *cis* dominated PSS_{365} is shown as an orange trace. The n→π* band has an approximately similar λmax but is more intense than that of the dark adapted sample.

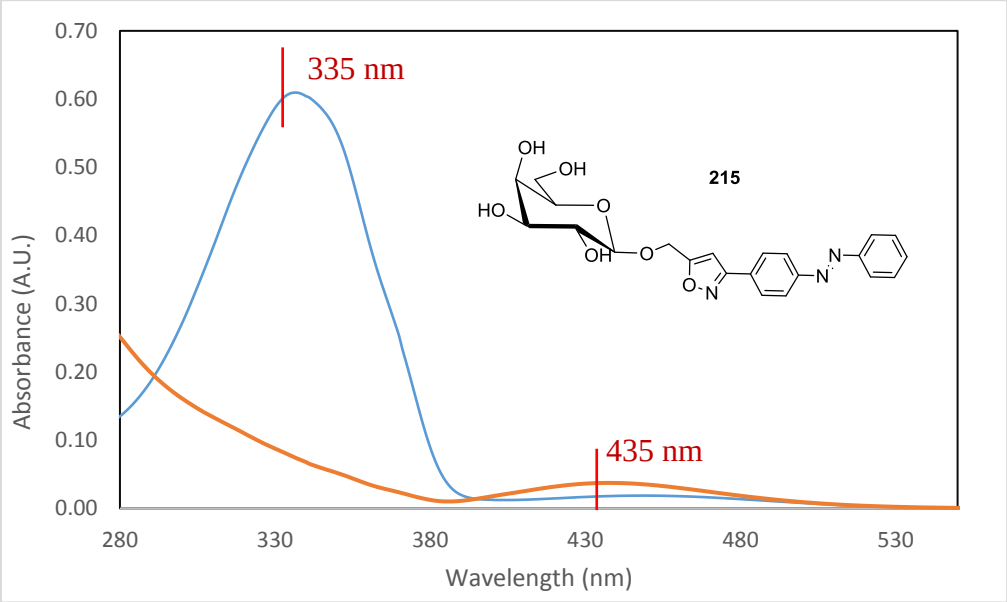

Figure 64: UV/Vis spectra of 215 (25 μM, DMSO); Dark-adapted sample in blue and cis photostationary state in orange

Electron donating substituents are known to cause a shift to longer wavelengths for the π→π* band,[274,275] as is observable for the ether ligated **258,** with respect to isoxazole linked adduct **218**, figure 65. The λmax (π →π*) ~ 350 nm, while the n→π* band is essentially uninfluenced and for both **218** and **258** appears at 440 nm.

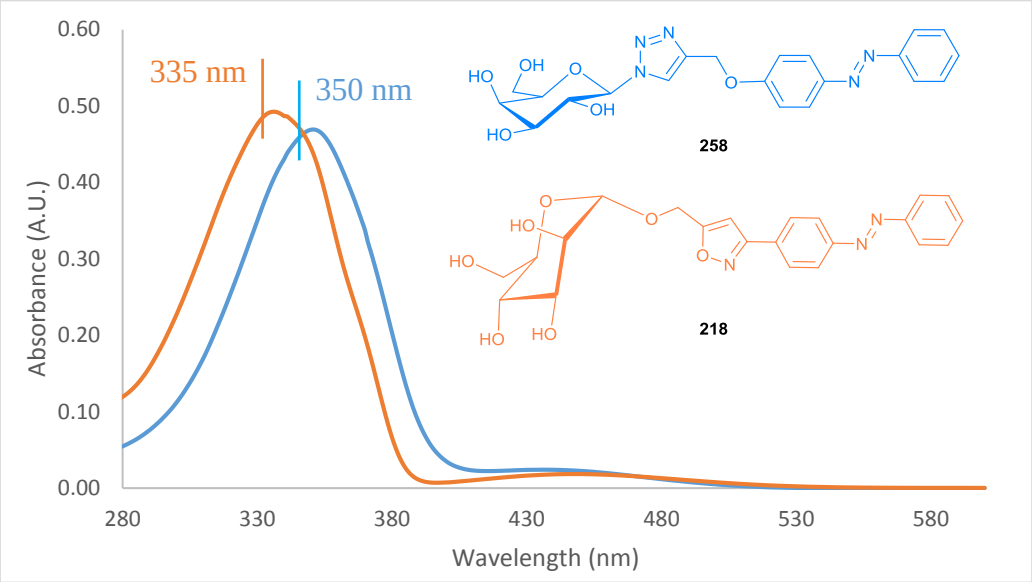

*Figure 65: UV/Vis spectra of **258** and **218** (25 µM, DMSO); **258** in blue, **218** in orange*

In idealised situations photostationary state studies utilise a range of light sources to irradiate each molecule at a wavelength as close as possible to the λmax of each band.[276] However, in other cases, like ours commercial diode lamps are used. We purchased two diodes which irradiate at 365 nm and 420 nm as these wavelengths are a very good compromise for the λmax of the compounds selected for study. Therefore the photostationary state study will identify characteristics of the isomerisation processes at these particular wavelengths rather than at the wavelengths at which maximum efficiency may be obtained.

The photostationary states of azobenzenes have been determined using a number of ^{1}H-NMR spectroscopy techniques.[276-280] Typically the integral values of signals respresentive of a single geometric isomer are determined and these values used to calculate the ratio of the *cis* and *trans* isomers under the experiment conditions.

The choice of solvent has a significant effect upon the quantum yields of the isomerisation processes. Polar solvents facilitate higher quantum yields for *trans* to *cis* isomerisation. Non-polar solvents are more conducive to the *cis* to *trans* process.[51] It is therefore important to ensure that all experiments to characterise a series of compounds are conducted in the same solvent. DMSO and DMF were found to be the solvents in which the compounds had good solubility, and, DMSO was selected.

Whilst temperature does not effect the *trans* to *cis* process, the quantum efficiency of the *cis* to *trans* isomerisation increases with increased temperatures.[55] Therefore, all experiments to determine photostationary states were conducted at 25 ˚C.

Each adduct was made up to a known concentration in deuterated solvent (5 mM). These samples were left in the dark for a period of no less than 3 days. The ^{1}H-NMR spectra of the so called dark adapted samples were recorded and all the resonances of the *trans* form identified and assigned.

The samples were irradiated at 365 nm to effect the *trans* to *cis* photoisomerisation as described in the general experimental (7.4 protocols for determination of photostationary states (PSS) and thermal relaxation measurements). Spectra were recorded periodically until the photostationary state, PSS_{365}, was reached and the relative integrations of the resonances of the *trans* and *cis* isomers remained constant. At the PSS_{365} the relative amounts of the two isomers was determined by examining and relating the relative integrations of signals attributed to each isomer in the aromatic region of the spectrum. The process was then repeated with irradiation at 420 nm to follow the *cis* to *trans* isomerisation and establish the PSS_{420}.

The process for determining the percentage of the *cis* isomer in each sample from the proton NMR spectra at the photostationary state is detailed using the conjugate **218** as an example.

1. The spectrum was recorded for the dark adapted sample, spectrum 1, figure 66.
2. Spectra were recorded, following irradiation at 365 nm, at one minute intervals until no further change was observed, Spectrum 2, figure 66.
3. The spectrum of the PPS_{365} was recorded, spectrum 3, figure 66.
4. Spectra were recorded, following irradiation at 420 nm, at 1 minute intervals until no further change was observed, spectra 4, figure 66.
5. The spectrum of the PPS_{420} was recorded, spectrum 5, figure 66.

- From the dark adapted sample the peaks A (2H), B (2H), C (2H), D (3H) and E (1H) were assigned as the *trans* isomer resonances (9 Ar-H and the isoxazole-C-H), spectrum 1.
- As the photoisomerisation was induced, the resonances F (2H), G (2H), H (1H), I (1H), J (2H) and K (2H) continued to grow in intensity as the resonances for A-E fell in intensity, in the spectrum 3

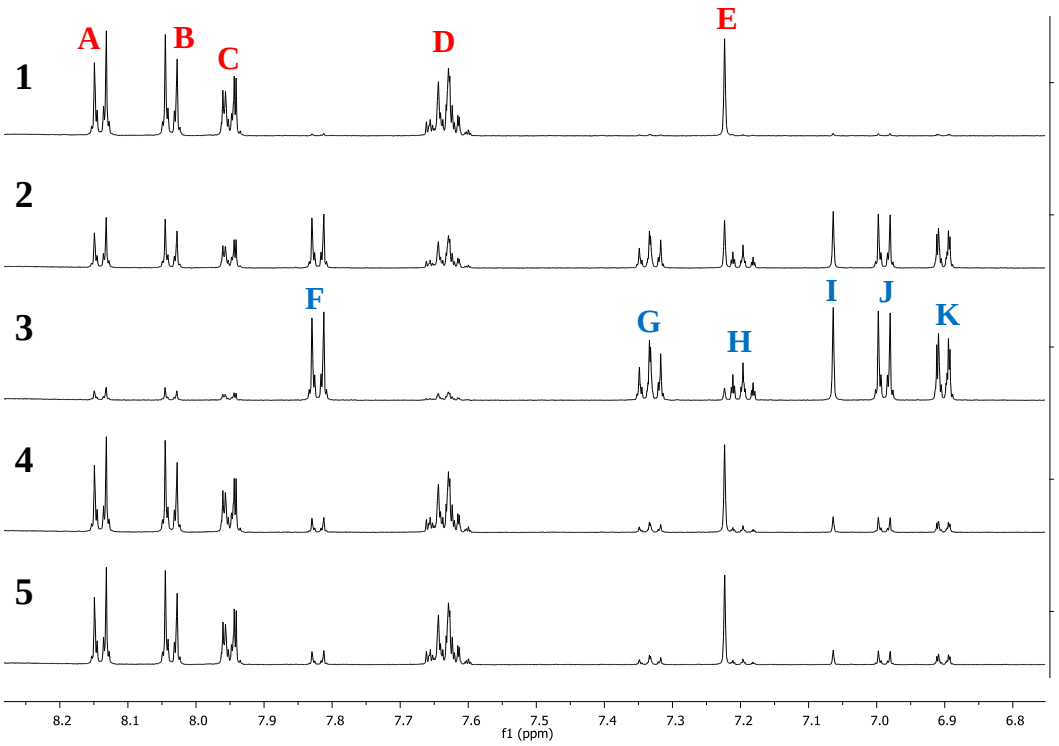

*Figure 66: Selected spectra (aromatic region, 500 MHz, DMSO-d_6) from the photoisomerisation of **218**: From top to bottom: (1) dark adapted sample, (2) irradiation at 365 nm for 1 minute, (3) irradiation at 365 nm for 4 minutes, (4) irradiation at 420 nm for 1 minute and (5) irradiation at 420 nm for 3 minutes.*

- Upon reaching the photostationary state, PPS_{365}, (spectrum 3) i.e. when no change was observed in the spectrum upon further irradiation, the relative amounts each isomer were calculated. All the resonances were integrated, except where signals of the *cis* and *trans* isomers overlapped. In the case of **218** the signals E and H were not included in the analysis because the isoxazole C-H *trans* resonance (E) overlapped with an Ar-H *cis* resonance (H). The integration of the resonances associated with the *trans* and *cis* isomers of **218** at the PSS_{365} is shown in the spectrum in figure 67 and summarised in table 2.

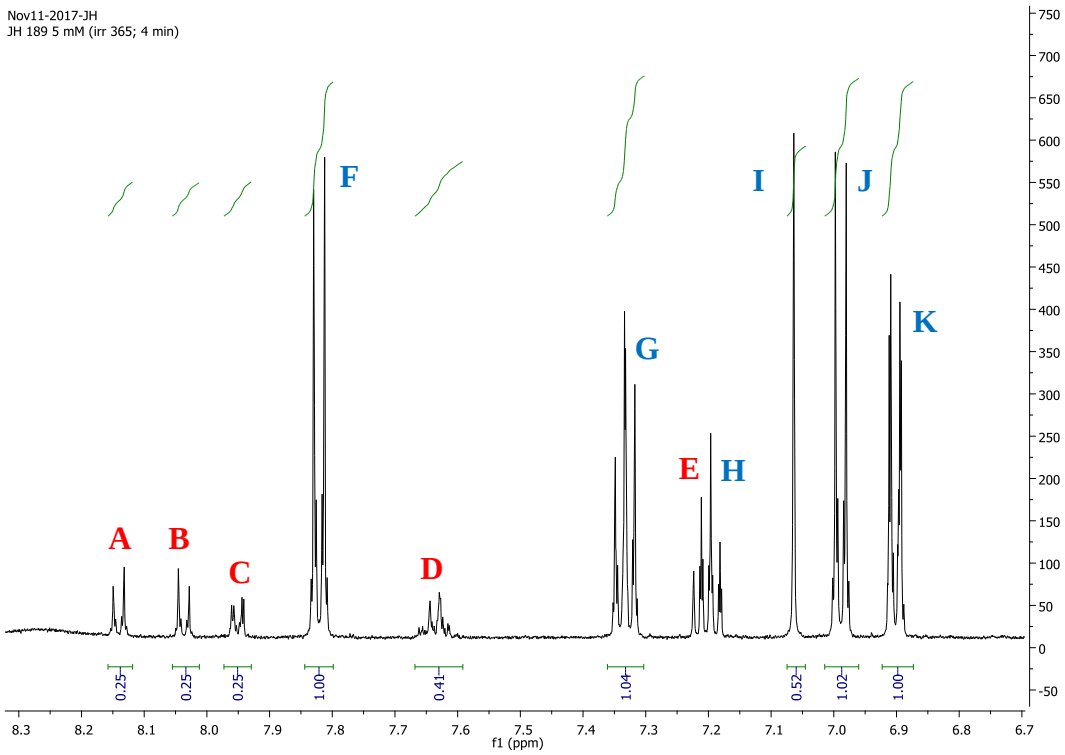

*Figure 67: Expansion in the PSS365 of the ^{1}H-NMR spectrum (DMSO-d_6, 500MHz) of **218** showing the integration of both the trans and cis isomers*

- The integration values were divided by the number of hydrogens that each signal represented. For example, resonance **A** with a relative integration of 0.25 was divided by the 2 as it represents 2H, to give a value of 0.125 per proton. These values were determined for all the signals associated with *trans* and with *cis* isomers. The average intensity of a ^{1}H signal for each isomer in the PSS_{365} samples was determined in this way, This allowed all the available integration values to be used for the average without concern for having an equal amount of proton signals from the *trans* and *cis* isomers. From the two averages the ratio between the geometric forms or the percentage of either *cis* or *trans* isomer can easy be calculated.
- Manipulation of the data, shown in table 2 reveals a 20:80 ratio of *cis* to *trans* isomers for 218 at the PSS_{365} in DMSO-d_6 (r.t.).

*Table 2: Data manipulation of the integrations of the resonances of the trans and cis isomers of **218**.*

Trans- isomer			**Cis-isomer**		
Signal	Integration (H per signal)	Integration per H	Signal	Integration (H per signal)	Integration per hydrogen
A	0.25 (2H)	0.125	**F**	1.00 (2H)	0.50
B	0.25 (2H)	0.125	**G**	1.04 (2H)	0.52
C	0.25 (2H)	0.125	**I**	0.52 (1H)	0.52
D	0.41 (3H)	0.137	**J**	1.02 (2H)	0.51
			K	1.00 (2H)	0.50
Average integration per H atom		0.128	Average integration per H atom		0.51
Percentage *trans* $\frac{0.128}{0.128 + 0.51} \times \frac{100}{1}$ **20.1%**			**Percentage *trans*** $\frac{0.51}{0.51 + 0.128} \times \frac{100}{1}$ **79.9%**		

The same process was applied to establish the PSS_{420} and it was found to comprise of 21% *cis* isomer. Each compound in the series was then investigated in the same way and the photostationary state data is shown in the tables below.

The compounds **215**, **218**, **220** and **271** were investigated to explore the effect the biomolecule structure has on the PPS, table 3. In each compound within this family the azobenzene unit is linked directly to an isoxazole and a CH_2O spaces the isoxazole and sugar (**215**, **218** and **220**) or the nucleic acid (**271**).

As shown in figure 68, all of these molecules show approximately the same λmax for the $\pi \rightarrow \pi^*$ and $n \rightarrow \pi^*$ bands, meaning that each compound absorb equally as well at each of the isomerisation wavelengths and the photostationary states should be directly comparable.

*Table 3: Photostationary states of **215**, **218**, **220** and **271**.*

Compound number	Compound	% of *cis* isomer	
		PSS_{365}	PSS_{420}
215	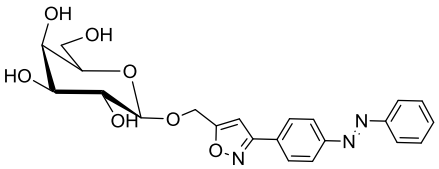	80.2	21.0
218	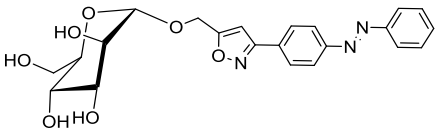	79.9	22.3
220	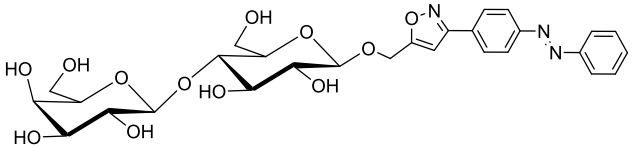	75.2	21.6
271	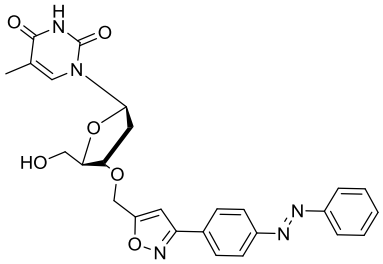	80.0	20.4

The data shows that the biomolecule has little bearing on either PPS_{365} or PSS_{420}. The lactose derivative **220** shows a slightly reduced *cis* content in the PSS_{365} sample, this may relate to the greater bulk of the disaccharide.

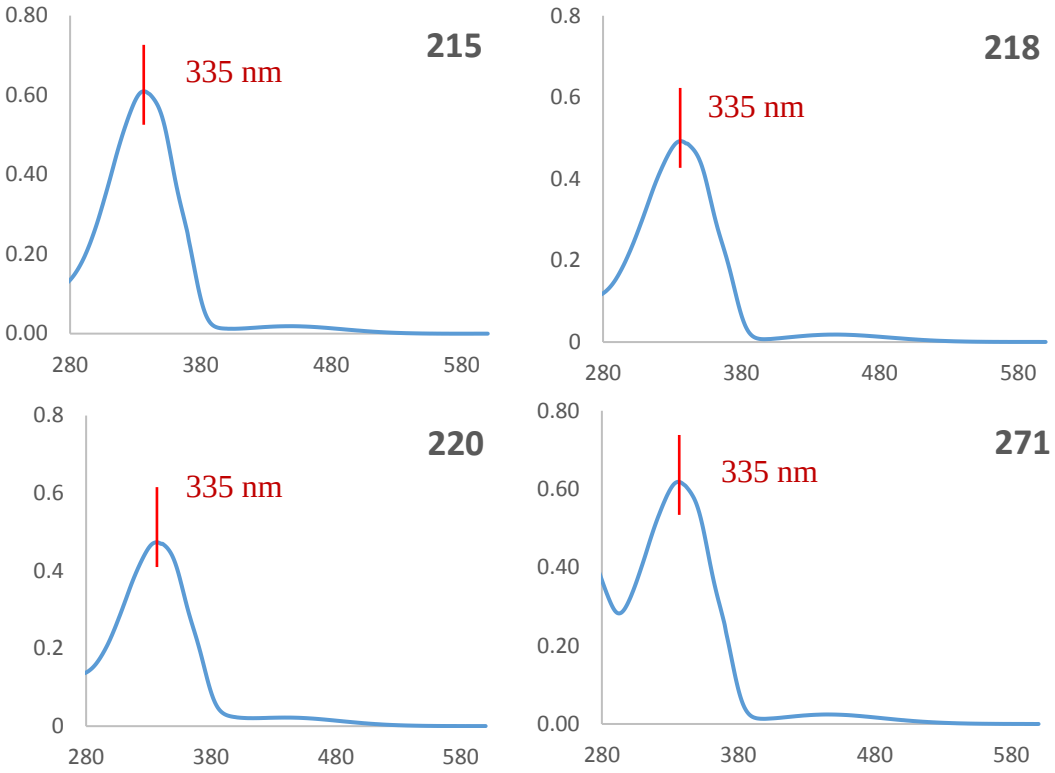

*Figure 68: UV/Vis spectra of the dark adapt samples of **215**, **218**, **220** and **271**; 25 µM DMSO*

(Y-axis: Absorbance (A.U.), X-axis: Wavelength (nm)

We next aimed to explore the effects of the relative orientation of the biomolecules with respect to the azo linkage. The *para* ligated azobenzene-mannose conjugate **218** and its *meta* derivative **229,** as well as the *para* and *meta* ligated azobenzene-thymidine conjugates **271** and **273** were studied. The data is summarised in table 4.

*Table 4: Photostationary states of **218**, **229**, **271** and **273**.*

Compound number	Compound	% of *cis* isomer	
		PSS_{365}	PSS_{420}
218	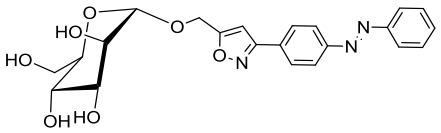	79.9	22.3
229	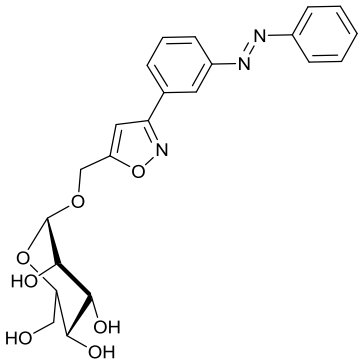	66.2	34.1
271	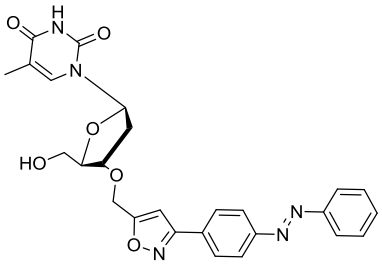	80.0	20.4
273	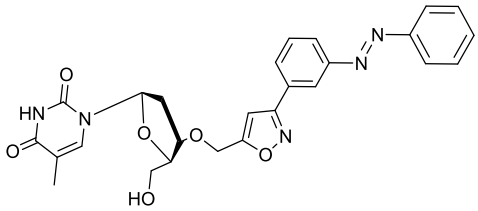	65.2	24.4

At the PSS_{365} the percentage of the *cis* isomer is significantly less than that of their *trans* counterparts. This may be explained by examining the UV/Vis spectra of the compounds. The spectra of the mannose conjugates **218** and **229**, and the thymidine conjugates **271** and **273** are shown in figure 69. It is noticeable that the $\pi \rightarrow \pi^*$ bands are less intense and shifted to a lower wavelength for the *meta* adducts **229** and **273**, with respect to their *para* substituted analogues **218** and **273**. This means that the *meta* compounds absorb less strongly at 365 nm than their *para* analogues. This would be expected to decrease the efficiency of *trans* to *cis* isomerisation, resulting in a lower percentage of the *cis* isomer being present.

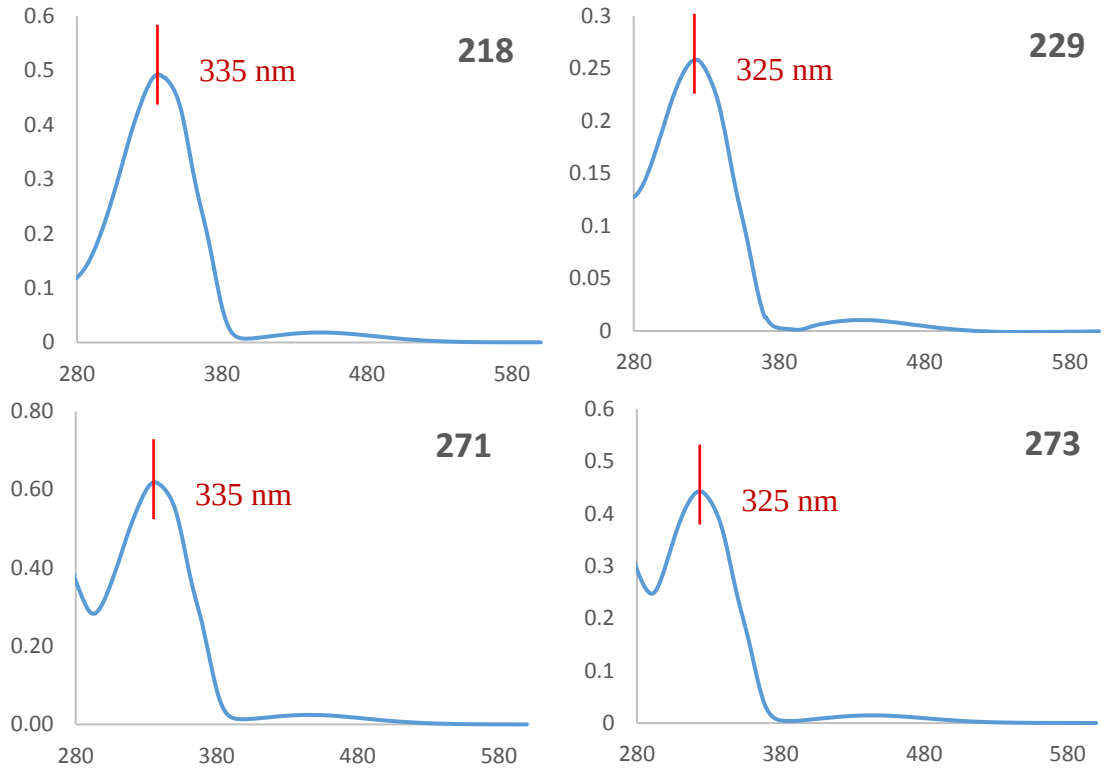

*Figure 69: UV/Vis spectra of the dark adapt samples of **218**, **229**, **271** and **273**; 25 μM DMSO;*

(Y-axis: Absorbance (A.U.), X-axis: Wavelength (nm)

We then set out to investigate the effects of valency on the PSS of the conjugates. The photostationary states of monovalent galactose conjugate **215**, its divalent analogue **222** and the divalent *m,m*-galactose conjugate **234** were determined, shown in table 5.

*Table 5: Photostationary states of **215**, **222** and **234**.*

Compound number	Compound	% of *cis* isomer	
		PSS_{365}	PSS_{420}
215	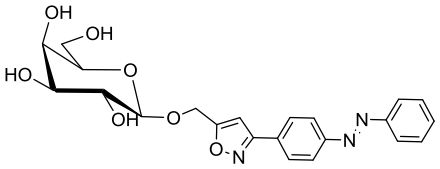	80.2	21.0
222	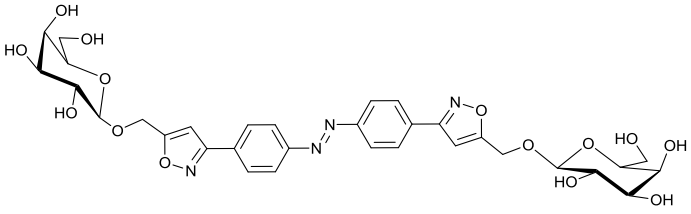	64.4	12.7
234	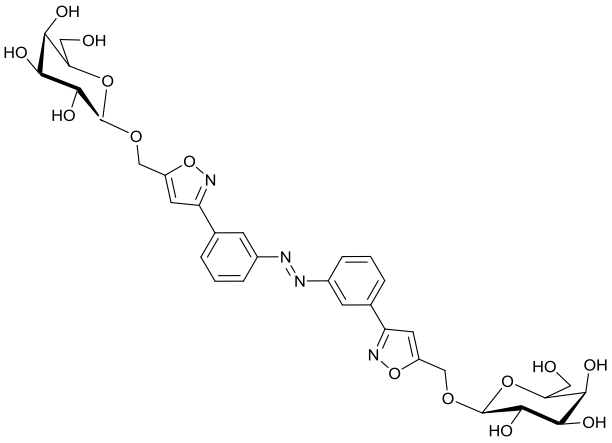	68.4	26.2

The isomeric divalent conjugates (*p,p*-) **222** and (*m,m*-) **234** both showed a moderate percentage of the *cis* isomer in the PSS_{365} sample. The UV/Vis spectra of the divalent compound **234**, shown in figure 70, shows a blue shifted $\pi \rightarrow \pi^*$ band with respect the monovalent analogue **215**. The *m,m*-disubstituted compound **234**, like the *m*-monosubstituted **229** and **273** has relatively low intensity absorbance bands with respect to their *p,p*-substituted analogues. The lower percentage of the *cis* isomer present in the PSS_{365} samples may reflect relative weak absorption at this wavelength.

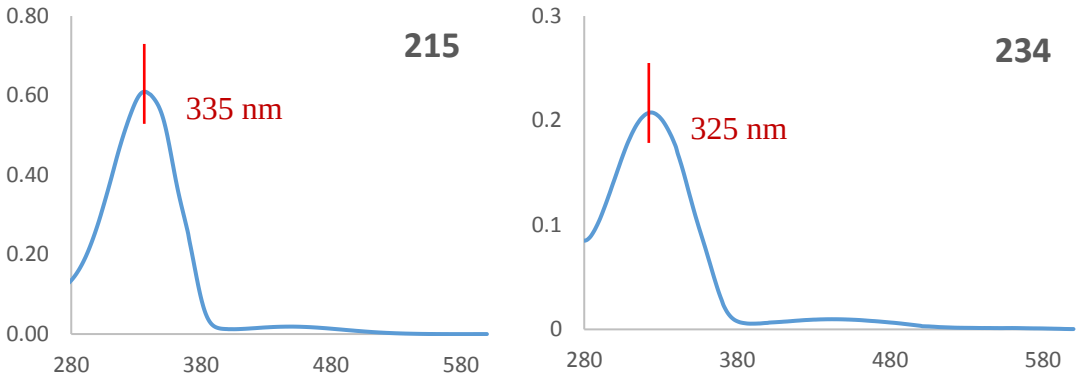

*Figure 70: UV/Vis spectra of the dark adapted samples of compounds **215** and **234**; 25 µM DMSO (Y-axis: Absorbance (A.U.), X-axis: Wavelength (nm)*

Next attention turned to a study of the effect on the photostationary state of the choice of ligation unit, and a series of compounds bearing a triazole or either linkage next to the azobenzene were studied.

The data, shown in table 6, indicates all of the compounds **238, 258** and **266** have highly efficient *trans* to *cis* isomerisation. In particular the ether linked **258** has a PSS_{365} with nearly 90% conversion to the *cis* isomer. This is perhaps an expected outcome considering that electron donating groups are known to cause shifts in the $\pi \rightarrow \pi^*$ band to higher wavelengths, meaning that the ether group of **258** should cause a shift bringing the irradiation wavelength (365 nm) close to the λmax of the $\pi \rightarrow \pi^*$ band for this compound. The closeness of the λmax and the irradiation wavelength should result in more efficient *trans* to *cis* isomerisation. The shift to longer wavelength for the $\pi \rightarrow \pi^*$ transition cause a greater overlap with the $n \rightarrow \pi^*$ absorbance, The same shift also moves the $\pi \rightarrow \pi^*$ closer to the 420 irradiation wavelength, explaining reduction in efficiently for the *cis* to *trans* isomerisation and PSS_{420} has 40 % *cis* isomer for conjugate **258**.

*Table 6: Photostationary states of **238, 258** and **266***

Compound number	Compound	% of *cis* isomer	
		PSS of 365 nm light irradiation	PSS of 420 nm light irradiation
238[§]	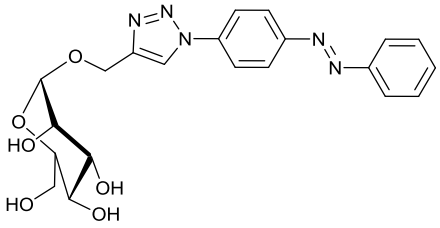	84.8	23.3
258	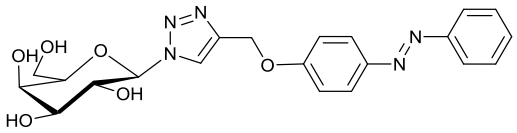	89.2	38.9
266	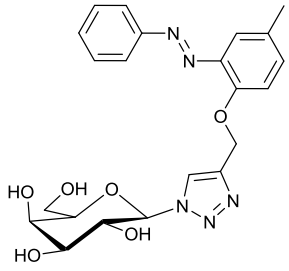	85.2	45.4

The absorption profile of **266**, with the biomolecule conjugation through *ortho* ligation, is distinctly different from the other compounds in this series. The difference is suggestive of partial destruction of planarity in the azobenzene unit, a known effect in *ortho* substituted azobenzene derivatives.[273] The effects of steric hindrance must also be considered for the isomerisation processes of compounds like **266**.[271] The electron donation for the *ortho* oxygen atom appears to influence the PSS_{365} of **266 (**85.2) in the same way as the similar *p*-ether linked **258** (89.2) and PSS_{420} (45.4) are likely attributed to the same structural features.

[§] This compound presented as having multiple conformations.

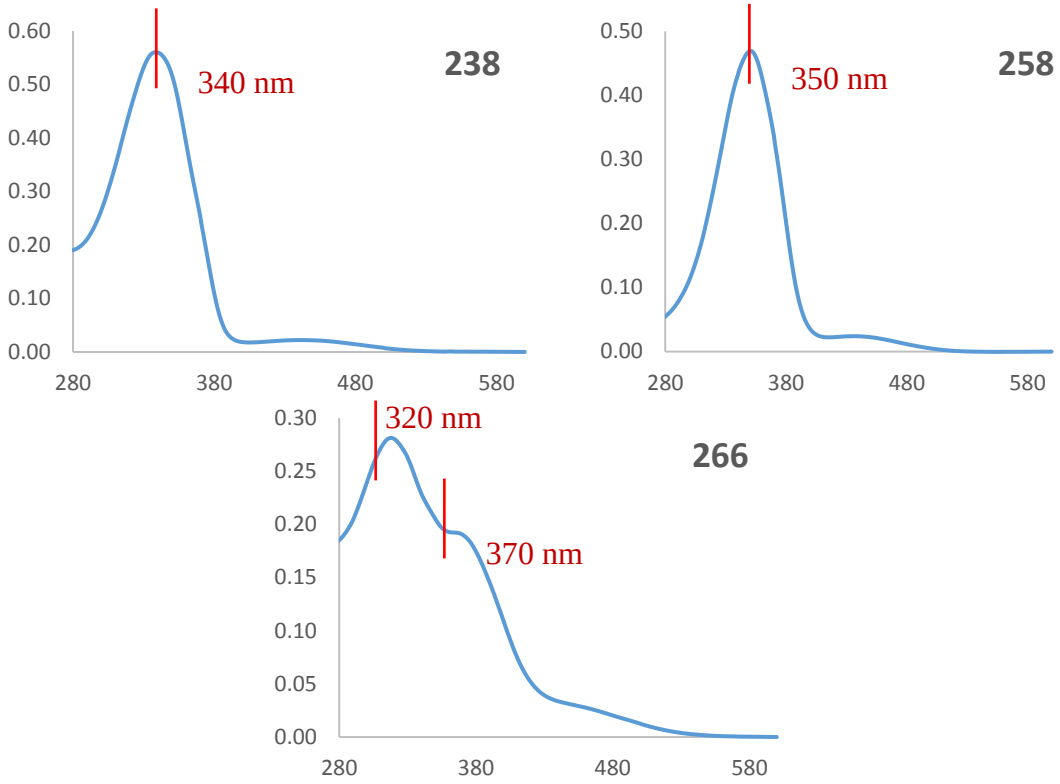

*Figure 71: UV/Vis spectra of the dark adapted samples of compounds **238, 258** and **266**; 25 µM DMSO; (Y-axis: Absorbance (A.U.), X-axis: Wavelength (nm)*

5.2 Determination of kinetic parameters for the thermal *cis* to *trans* isomerisation

The stability of the *cis* isomer of a given azobenzene is often viewed as one of the key parameters in determination of its usefulness as a photoswitch. For many applications it is desirable to have long term stability,[281] in effect giving precedence to photoisomerisation over thermal isomerisation. A search for more stable *cis* isomeric azobenzenes has led to several approaches to extending the *cis* life time including: ligation with peptides[179] binding to surfaces[282] and appropriate substitution.[283] In particular, it has been shown that there is a 100 fold decrease in the speed of thermal isomerisation for an azobenzene substituted with a range of tertiary amino functionalities in the *ortho*-substitution compared to their regioisomeric *para*-analogues.[284]

Whilst the thermal stability of azobenzene derivatives can be followed by ^{1}H-NMR studies UV/Vis spectroscopy is more commonly employed as it allows much more rapid data acquisition.[285-287] There are several possible methods of data acquisition when running UV/Vis spectra. In particular, a full spectrum can be run periodically giving data

like that shown for **215** in figure 72 at the extremes of the time course of the experiment. Alternatively, a fixed wavelength time course measurement can be adopted, often it offers the data in the most suitable form for analysis. The thermal relaxation profile plots measured at 335 nm, for **215** at a range of temperatures (60-90 ˚C) and over a time window of 0-3000 seconds are shown in figure 73.

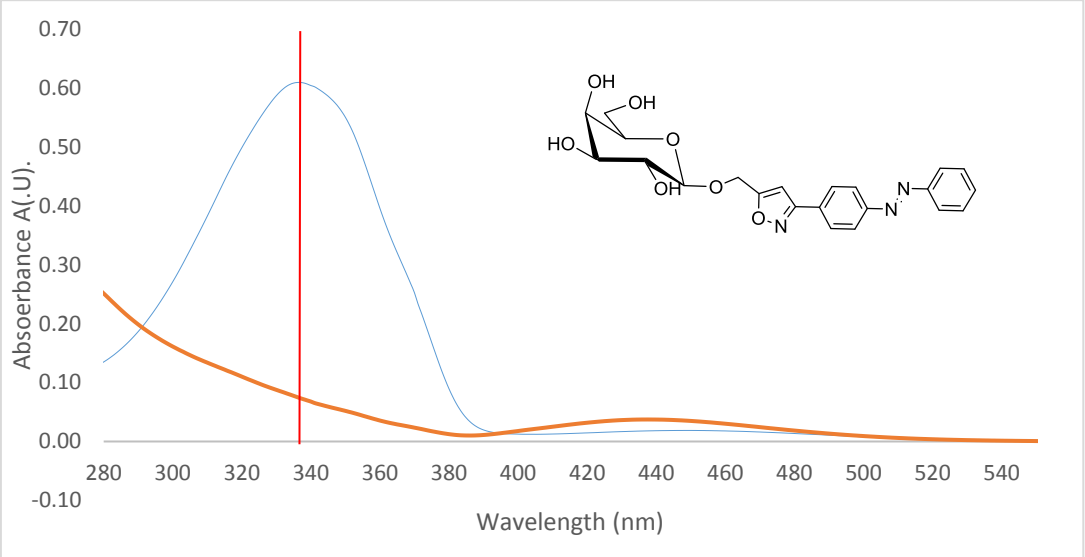

*Figure 72: UV/Vis spectra of **215** at the extremes of the time course of the experiment: dark-adapted sample in blue, PSS_{365} in orange. The red line indicates the absorption at 335 nm; 25 µM DMSO.*

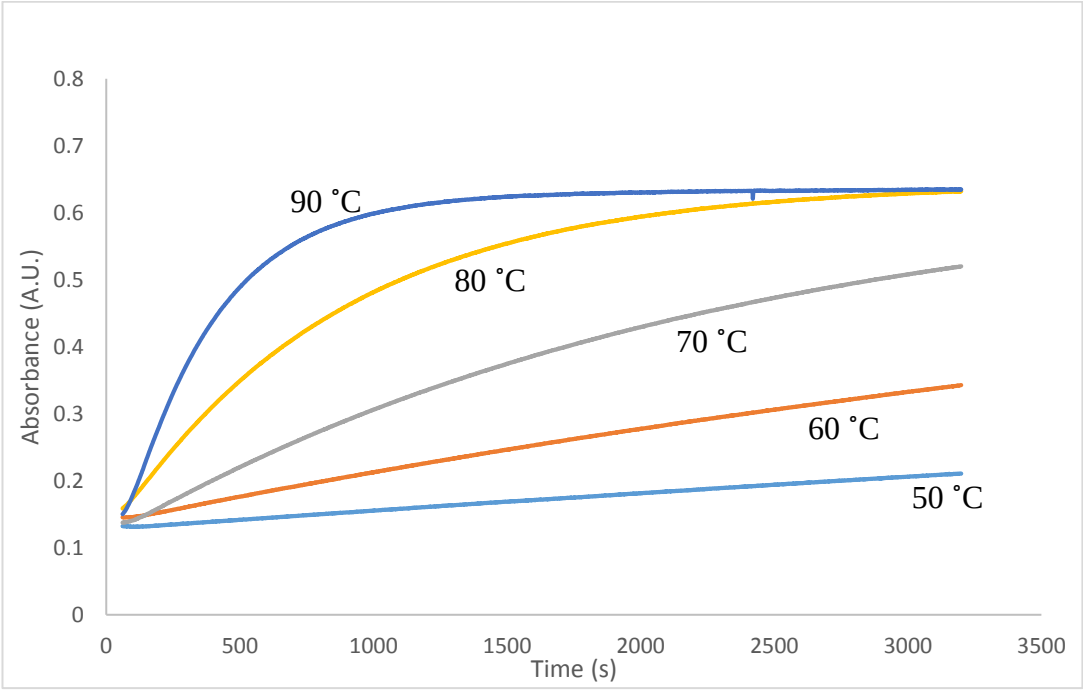

*Figure 73: Absorbance of **215** at 335 nm at various temperatures 25; µM DMSO.*

In this thesis, and taking compound **215** as an example, the thermal relaxation parameters for each compound were determined as follows:

- A UV/Vis of a sample kept in dark was recorded. This represents the spectrum for a sample of exclusively *trans* isomer – the "dark adapted sample"
- The sample was irradiated to its *cis* dominated photostationary state PSS_{365} , and a UV/Vis vis spectrum recorded.
- By comparing the two spectra, a suitable wavelength was selected to monitor the thermal relaxation rate. We selected the λmax of the $\pi \rightarrow \pi^*$, in this case 335 nm.
- The PSS_{356} (*cis* dominated) sample was placed in a spectrometer fitted with a Peltier unit to maintain a fixed temperature
- The absorption of the sample was continuously monitored at the selected wavelength
- The process was repeated over a range of temperatures (60 to 90/100 ^{o}C)

For each compound the data was manipulated in determination of a selected range of photophysical properties.

The data from the time course measurement was normalised using the equation $[(A_t-A_0)/(A_\infty-A_0)]$ where

A_t is the absorbance at 365 nm measured at a given time, t,
A_0 is the absorbance at t = 0 s (the PSS_{365})
$A\infty$ is the absorbance at the all trans form – the dark adapted sample.

The normalised plots of the absorbance of **215** over the temperature range is shown in figure 74.

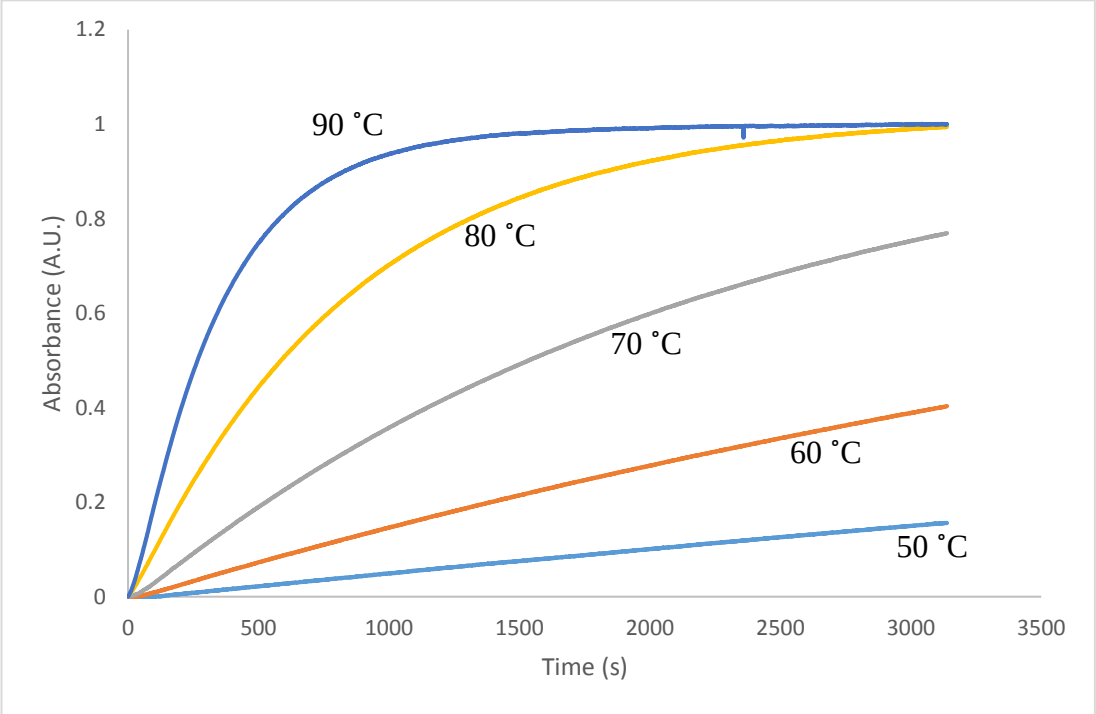

*Figure 74: Normalised plots of absorbance intensity, measured at 335 nm for **215** at various temperatures over a time period of 3200 s; 25 μM DMSO.*

The plot for **215** supports first order kinetics for the *cis* to *trans* thermal relaxation process.

Curve fitting was used to determine the isomerisation rate constant (k) at each temperature using GraphPad Prism 7.

The rate constants (k) determined for **215** at each temperature studied are listed in table 7.

*Table 7: Rate constant for the thermal relaxation of **215** at different temperatures.*

Temperature (K)	Rate constant (s^{-1})
333	$1.031X10^{-4}$
343	$2.248\ X10^{-4}$
353	$5.338\ X10^{-4}$
363	$13.35\ X10^{-4}$

The Arrhenius equation relates the rate constant with the activation energy required for the isomerisation process :

Arrhenius equation: $k = Ae^{Ea/RT}$

which can also be expressed in the linear form:

Arrhenius equation – **linear form**: $\ln(k) = \ln(A) - E_A/R(1/T)$

In the equation:

A is the Arrhenius pre-exponential factor, typically defined as the frequency of collisions in the correct orientation, it is a unique constant for each reaction.

E_A is the activation energy.

R is the gas constant (8.314 J K^{-1} mol^{-1}).

T is temperature (K).

An Arrhenius plot, -[ln(k) against 1/T], was constructed to determine A and E_a

The data for **215** is shown in Figure 75. From this linear plot

- The y-axis intercept is equal to in A.
- The slope is equal to ($-E_A/R$).

For **215** the y-axis intercept is at 21.75, giving a value for the Arrhenius pre-exponential factor, **A = 2.88 X 10^9 s^{-1}**. The slope of the graph is -10318 giving an **E_A = 85.9 kJ mol^{-1}** for the isoxazole linked galactose-azobenzene conjugate **215**.

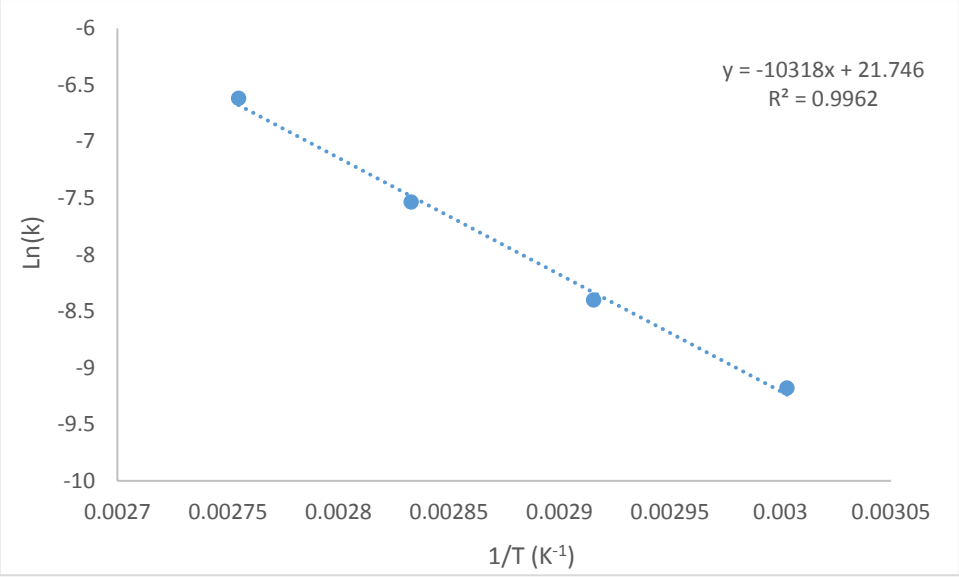

*Figure 75: Arrhenius plot following the thermal relaxation of **215**: plot of ln(k) against 1/T/*

The Eyring equation relates the rate constant for a given reaction with ΔG

Eyring equation $$k = \frac{k_B T}{h} e^{\frac{-\Delta G^{\ddagger}}{RT}}$$

It can be presented as a linear expression:

Eyring equation - linear form $\ln(k/T) = (-\Delta H^{\ddagger}/R)(1/T)+\ln(k_B/h)+\Delta S^{\ddagger}/R$

In the equation

$\Delta H^{\ddagger}$ is the enthalpy of activation.

R is the gas constant (8.314 J K^{-1} mol^{-1}).

k_B is the Boltzmann constant (1.380×10^{-23} $J\cdot K^{-1}$)

h is Plank's constant (6.626×10^{-34} J·s)

$\Delta S^{\ddagger}$ is the entropy of activation

R is the gas constant.

An Eyring plot, ln(k/T) against 1/T, was constructed to determine $\Delta H^{\ddagger}$ and $\Delta S^{\ddagger}$

The straight line plot for **215** is given in Figure 76. From this plot

- the slope represents $-\Delta H^{\ddagger}/R$
- the intercept of the y-axis gives $\ln(k_B/h)+\Delta S^{\ddagger}/R$.

For **215**, the y-axis intercept is at 14.90 and the slope -9970.Analysis of this data gives $\Delta H^{\ddagger}$ =83.0 kJ mol^{-1} and $\Delta S^{\ddagger}$ = -76.0 kJ $mol^{-1}K^{-1}$.

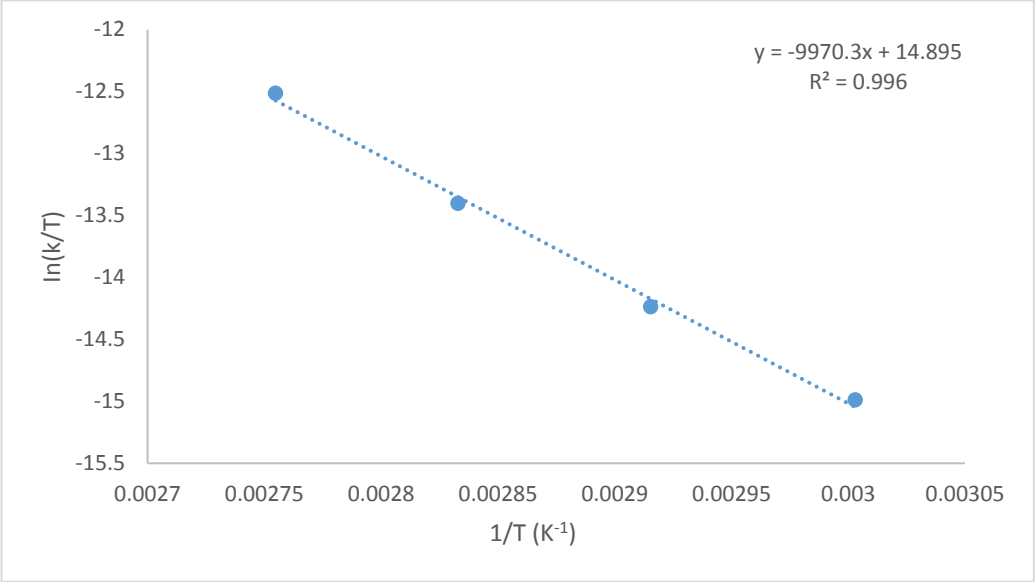

Figure 76: Eyring plot following the thermal relaxation of ***215****:plot of ln(k/T) against 1/T*

The analysis conducted for the isoxazole-linked galactose conjugate **215** was repeated and the data extracted for the range of conjugates shown in Tables 8-10.

The data in table 8 shows that the nature of the biomolecule has some effect on the characteristics of the molecule. The galactose **215** and its lactose analogue **220** show similar characteristics. The mannose **218** ($t_{1/2}$ ~ 40 hrs) and the thymidine conjugate **271** ($t_{1/2}$ ~30 hrs) are also similar with both showing larger activation energies and significantly longer half lives than **215** and **220** (~20 hrs).

*Table 8; Kinetic parameters for the thermal cis to trans isomerisation of compounds **215**, **218**, **220** and **271** determined via UV/Vis absorption spectroscopy in DMSO*

Compound Structure and Number	**EA** kJ mol^{-1}	**A** s^{-1} x 10^{10}	**$\Delta H^{\ddagger}$** kJ mol^{-1}	**$\Delta S^{\ddagger}$** kJ mol^{-1} K^{-1}	**$t_{1/2}$*** h*
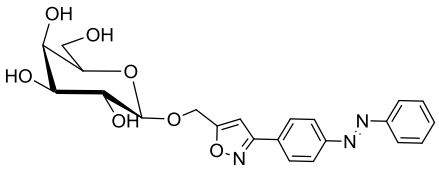 **215**	85.9	0.29	83.0	-76.0	20.6
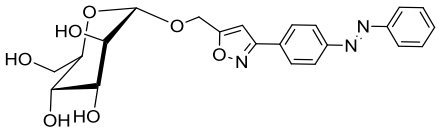 **218**	102.1	77.0	99.2	-29.5	42.5
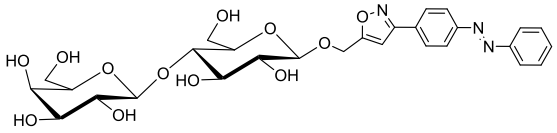 **220**	86.0	0.28	83.1	-76.2	21.6
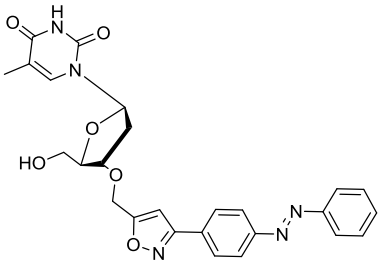 **271**	93.9	4.68	90.6	-54.0	28.3

*Measured at 37 ˚C

Conjugates **271** and **273** differ only the relative orientation of the thymidine unit with respect to the azolinkage. The *meta* adduct **273** has a much lower activation energy for the isomeriation process than its *para* counterpart **271**. Considering this difference it is somewhat surprising this pair have extremely similar half-lives (~30 hrs), table 9.

*Table 9: Kinetic parameters for the thermal cis to trans isomerisation of compounds **271** and **273** determined via UV/Vis absorption spectroscopy in DMSO.*

Compound Structure and Number	**EA** kJ mol^{-1}	**A** s^{-1} X 10^{10}	**$\Delta H^{\ddagger}$** kJ mol^{-1}	**$\Delta S^{\ddagger}$** kJ mol^{-1} K^{-1}	**$t_{1/2}$** * h
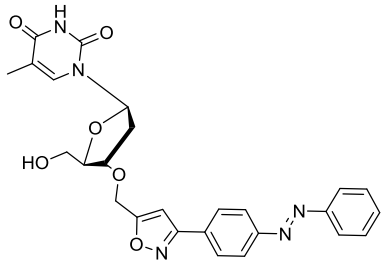 **271**	93.9	4.68	90.6	-54.0	29.3
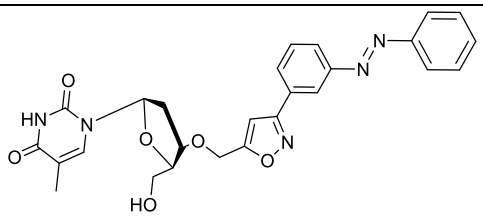 **273**	77.4	0.0059	74.4	-108.6	28.3

*Measured at 37 ˚C

The compounds in table 10 differ in their linkage between the carbohydrate and azobenzene units. Compound **238** can be directly compared with its isoxazole-ligated analogue **215**. It can be seen that the activation energy for isomerisation of the triazole ligated **238** is slightly higher and the half-life of the cis isomer slightly shorter than the isoxazole analogue **215**. Whilst the ether linked **258** does show a relatively long half-life, the activation energy for its isomerisation is similar, if not slightly lower, than many of the other compounds in this series.

The data shows the *ortho* substituted **266** has a higher activation barrier for the isomerisation that the two para-substituted sugar conjugates **238** and **258**. Significantly, the half-life of **266** is nearly double that of any of the other compounds investigated in this series. This observation fits with literature precedence suggesting steric bulk at the *ortho* position causes the resulting azobenzenes to experiencing slower thermal relaxation times.[288]

*Table 10: Kinetic parameters for the thermal cis to trans isomerisation of compounds **238**, **258** and **266** determined via UV/Vis absorption spectroscopy in DMSO*

Compound Structure and Number	**EA** kJ mol^{-1}	**A** s^{-1} X 10^{10}	**$\Delta H^{\ddagger}$** kJ mol^{-1}	**$\Delta S^{\ddagger}$** kJ mol^{-1} K^{-1}	**$t_{1/2}$** * h
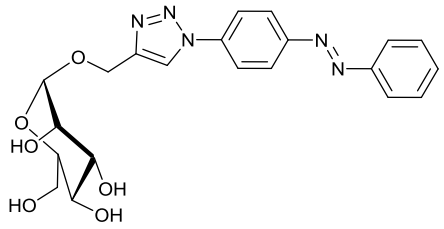 **238****	89.0	1.08	86.2	-65.1	18.4
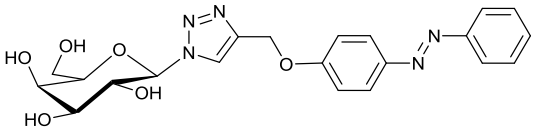 **258**	83.9	0.083	80.9	-86.47	33.5
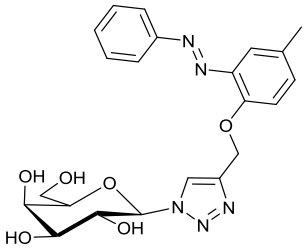 **266**	98.5	10.3	95.6	-46.5	78.1

** This compound presented as having multiple conformations.

*Measured at 37 ˚C

Whilst the results of these experiments are interesting and whilst we can reliably report the orthosubstituted, ether linked **266** is the stand out compound in this series, further work is need to fully understand the relationship between the structural features of the conjugated azobenzenes and the kinetic parameters of their thermal relaxation. In particular, it is acknowledged that before a more robust relationship is established the experiments would need to be repeated in triplicate.

5.3 Summary

- The photophysical properties of several of the carbohydrate-azobenzene conjugates were studied.
- The photostationary states of the compounds at 365 nm and 420 nm, PS_{365} and PS_{420} were determined by ^{1}H-NMR spectroscopy.
- The position of the conjugated group relative to the azo linkage and the opportunity, or not, for electron donation into the azobenzene unit were important influences on the PSS.The structure of the adduct had little bearing on the PSS.
- The thermal relaxation process of the adducts was studied by UV/Vis spectroscopy and the thermodynamic and kinetic properties of the process determined.
- The electron donating potential of the substituents and the substitution position relative to the azo linkage were found to impact on the thermal relaxation parameters.

6. Conclusions

This project has achieved the following:

A broad range of azobenzenes bearing oxime and chlorooxime functionalities were successfully synthesised. The reactive species were designed to offer, following cycloaddition, access to regioisomeric heterocycle linked azobenzene conjugates.

Azobenzenes with the cycloaddition partner in the *para* and *meta* positions were prepared. Substrates were designed to allow formation of both the *mono* and divalent compounds. Unfortunately *ortho* functionalised dipole precursors could not be accessed due to complications, not least the formation of indazoles.

Azidoazobenzenes and azobenzenes bearing nitrile oxide precursor functionalities were prepared. Reaction conditions were explored to find those best suited for nitrile oxide generation from an oxime – the Ch-T and NCS methods.

The synthesis of both mono- and disubstituted propargylated azobenzene derivatives were also successful and initial test reactions showed they were suitable for cycloaddition with azido-substrates as well as nitrile oxides generated through both NCS and Ch-T NOAC methodologies. *Meta* and *ortho* dipolarphilic azobenzenes were synthesised.

The integration of a dipolarphilic functionality into a carbohydrate substrates was readily achieved through glycosylation chemistry.

The cycloaddition alkyne-bearing sugars reaction with the nitrile oxide dipoles was found to be challenging especially for the divalent cycloaddition reactions. A range of conditions were explored and ultimately good yields were achieved utilising controlled formation of the dipole via the slow addition of base to the chlorooxime bearing azobenzenes.

Azidoazobenzene was found to readily undergo cycloaddition with propargylated carbohydrates. Ultimately a wide range of adducts were synthesised through these reactions, producing conjugates with varying regiochemistry and valency.

The introduction of an oxime functionally into carbohydrates was found to be difficult and the only conjugates that could be formed were *mono* and divalent allose-azobenzene compounds. In contrast azides were easily introduced into carbohydrate substrates and their cycloaddition with propargylated azobenzenes was found to be highly effective.

In terms of future work in this area, the development of asymmetric glycoconjugates is of interest, in particular for the functionalisation of surfaces, peptides or other biomolecules.

The chemistry developed during the conjugation of saccharides was found to be effective for creating nucleoside adducts and a range of isoxazole and triazole linked compounds were synthesised. There is much scope to further investigate these compounds. In particular, the integration of the conjugates into oligonucleotide may offer an insight into the effects of the photoiswitch upon DNA and RNA structures.

For the creation of peptide-azobenzene conjugates, the azide functionality was introduced into peptides at both internal and terminal positins. These peptides were found to be good substrates for cycloaddition with alkyne bearing azobenzenes. Higher yields were obtained when working with the resin supported peptides, however the chemistry was also shown to be viable in solution. A peptide with an internal propargyl functionality was shown to undergo cycloaddition with both azide and nitrile oxide dipolarohiles. The is still much scope for optimising the reaction conditions, in particular with nitrile oxides-peptide conjugation.

The CuAAC chemistry was also used during the ligation of a saccharide onto a peptide structure through an azobenzene linker. This reaction shows the potential to explore the use of asymmetric azobenzene units as linker for creating cyclic peptides or for chemical ligation in peptide synthesis.

Finally the effects of variation in biomolecules type, regiochemistry, valency and linker type upon the photophysical properties of a range of azobenzenes was explored. The photostationary states (PSS), determined by NMR study, showed the importance of electron donating and withdrawing effects upon the azobenzenes PSS.

Upon determining the kinetic parameters of the thermal relation process by UV/Vis studies, we found that bulky *ortho* –substituents had a dramatic effect on thermal isomerisation parameters.

7. Experimental

7.1 Materials and instrumentation

Standard reagents were supplied by: TCI Europe, Sigma Aldrich, Acros Organics or Alfa Aesar and were used as received without the need for further purification. Solvents were supplied in HPLC grade or higher. Solvents were used as supplied unless the reaction was moisture sensitive, in which case they were distilled and dried according to reported protocols.[289,290]

Analytical TLC was performed on pre-coated silica gel 60 F_{254} plates from Merck. Visualisation was achieved by UV irradiation or with the use of a carbohydrate stain (5% H_2SO_4 in EtOH) followed by charring.

Flash chromatography was performed on silica gel (40-62 μM, 60 Å).

NMR spectra were recorded on a Bruker Advance spectrometer at 300 K. NMR were recorded in $CDCl_3$ or DMSO-d_6, ^1H spectra were recorded at 300 or 500 MHz; ^{13}C spectra were recorded at 75 or 125 MHz, as indicated. Chemical shifts are reported in ppm downfield from TMS as a standard.

UV-Vis spectra were recorded on a Jasco V-630 Bio spectrometer at 25 ˚C unless otherwise stated. Temperature control was maintained by a Jasco ETC717 Peltier.

Infrared spectra were recorded as a sample prepared as a KBr disc or by ATR using a Perkin Elmer system 2000 FT-IR spectrophotometer.

Melting points were obtained with a Stewart scientific SMP 11 melting point apparatus

Electrospray (ESI) mass spectra were obtained on an Agilent Technologies 6410 time of flight LC/MS. They were interpreted with 'Agilent MassHunter workstation software'.

HPLC was undertaken on system built with a Gilson 322 pump, a 172 diode array detector and a GX-272 liquid handler; using either a Macherey-Nagel C18, 21.0 mm x 25 cm column for semi-preparative work or a Phenomenex C18, 4.6 mm x 15 cm column for analytical work.

Automated peptide synthesis was undertaken at Royal college of Surgeons Ireland on an Applied Biosystems 433A Peptide Synthesiser with the ‘Synthesis Assistant 3.1 Software’.

7.2 Structural numbering and nomenclature.

Azobenzene core:

To facilitate assignment of NMR data the following structural numbering systems were used:

For the purposes of discussion in this thesis, the numbering of the azobenzene core will supersede other standard numbering systems.

(1)The numbers of asymmetric azobenzene molecules begins at the unsustituted phenyl C atom *para* to the azo group.

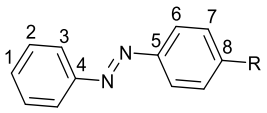

(2) With symmetrical azobenzenes, the numbering will originate from the aryl C atom adjacent to the azo linkage

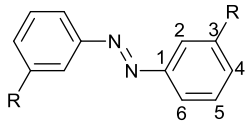

Carbohydrate nuclei:

Carbohydrate nuclei are numbered according to the standard numbering system; starting with the anomeric position as C-1. Disaccharide units carry the prime (‘) designation on the second sugar unit.

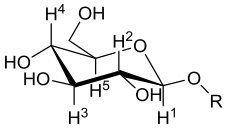

Nucleic acids:

The ribose unit is labelled 1’ to 5’ going from the anomeric position. The base is referred to by its functionality as necessary.

Peptides:

Peptides are ‘constructed’ using the standard one letter and three letter codes for their constituent amino acids, as is appropriate. Terminal positions are labelled post C=O or NH functionality, e.g

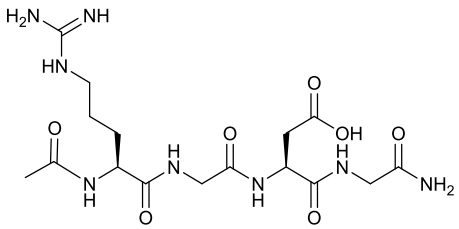

would be represented as Ac-RGDG-NH_2 or Ac-arg-gly-asp-gly-NH_2.

7.3 Protocols for SPPS

General method for manual preparation of a peptide on the solid phase:

Rink amide resin (0.50 g, 0.5-1.0 g/mmol) was swelled in DMF (5 mL) in a SPPS vessel with mild agitation for 30 minutes. The DMF was drained and fresh DMF (5 mL) was added, followed by 30 minutes of mild agitation. This process was repeated once more. Then a solution of 20% v/v piperidine in DMF (5 mL) was added and the vessel was agitated for 10 minutes, before being drained and a further portion of the piperdine solution (5 mL) added, followed by agitation for a further 10 minutes. The piperdine solution was drained and the resin was washed consecutively with DMF (3 x 5 mL), DCM (3 x 5 mL) and DMF (3x 5 mL). A solution of *N*-α Fmoc protected amino acid (4 eq.) PyBOP (4 eq., 1.04 g) and NMM (8 eq., 0.414 g, 0.44 mL) in DMF (5 mL) were added to the resin in the SPPS reaction vessel, followed by agitation for 40 minutes. The reaction solution was drained and the resin was washed with DMF (3 x 5 mL), DCM (3 x 5 mL) and DMF (3x 5 mL).

Resin loading was determined as follows:

Three samples of the resin then removed and accurately weighed (each 5-10 mg), and transferred to a flask followed by addition of 1.0 mL of 20% v/v piperidine in DMF to each portion of resin, followed by agitation for 20 minutes. 100 µl of each solution was added to DMF (10 mL), of this 2 mL was taken forward for UV/Vis spectroscopic analysis. The intensity of the absorbance at 301 nm ($\lambda\,(301)$ was recorded for each of the three samples and used in the following equation:

$$resin\ loading = \frac{101\ \times (\lambda\,(301)}{7.8\ \times\ Weight}$$

The average of the three readings were used to determine the resin loading.

The remaining sample was N-terminal deprotected through the addition of 20% v/v piperdine in DMF (5 mL) with 10 minutes of agitation, before draining and a further 10 minutes of agitation with fresh piperidine solution (5 mL). The piperidine solution was again drained and the resin washed with DMF (3 x 5 mL), DCM (3 x 5 mL) and DMF (3x 5 mL).

Each new residue was added as a solution of *N*-α Fmoc protected amino acid (3 eq. of determined resin loading) PyBOP (3 eq. of determined resin loading) and NMM (6 eq. of determined resin loading) in DMF (5 mL) to resin, where it was agitated for 40 minutes, followed by draining of the solution and consecutive washings with DMF (3 x 5 mL), DCM (3 x 5 mL) and DMF (3 x 5 mL). With each being followed by deprotection involving two 10 minute reactions with 20% v/v piperidine solution, followed by draining and finally washing with DMF (3 x 5 mL), DCM (3 x 5 mL) and DMF (3x 5 mL).

If the SPPS needed to be interrupted (e.g. the end of a working day) and storage of the peptide was required, the resin was shrunk by washing with DMF (3 x 5 mL), DCM (3 x 5 mL), DMF (3x 5 mL), DCM (3 x 5 mL) and dried under vacuum before being stored at 5 ˚C. To reswell the resin it was twice agitated in DMF (5 mL) for 20 miniutes.

General procedure for capping peptides: To the swelled, N-deprotected peptide bearing resin was added a fresh solution of acetic anhydride in pyridine (20% v/v, 5 mL). The reaction vessel was agitated for 5 minutes before being drained of the solution. Fresh acetic anhydride solution (5 mL) was added and the mixture was agitated for 5 minutes before being drained again. This process was repeated once more before the resin was washed with consecutively with DMF (3 x 5 mL), DCM (3 x 5 mL), DMF (3x 5 mL) and DCM (3 x 5 mL). When using the automated synthesiser acetylation was achieved by the standard coupling protocol with acetic acid (10 eq.) on to the final residue.

General procedure for cleavage of peptides from Rink amide resin: To the swelled peptide bearing resin in a SPPS vessel, a solution of TFA, triisopropylsilane and water (95:2.5:2.5; 5 mL) was added. The vessel was agitated for 1 hour, if two arginine residues were present this was increased by 30 minutes. Solution was then drained from the reaction vessel and three quarters of the TFA was removed by passing dry air over the solution. Diethyl ether was then added to the solution until no more precipitate formed. The resulting suspension was then pelleted by centrifuging (2800 rpm, 5 mins). The pellet was twice dispersed in fresh diethyl ether (10 mL), followed by pelleting by centrifugation (2800 rpm, 5 mins). Finally the pellet was dissolved in distilled water (1-2 mL) and minimum of acetonitrile before being lyophilised to give the crude material as a powdery solid.

For automated synthesis: an Applied Biosystems 433A Peptide Synthesiser was used at Royal collage of Surgeons Ireland. The syntheses were performed on 0.1 mmol scale, therefore a rink amide resin (128 mg of 0.78 mmol per gram of known loading was used). N-Methyl-2-pyrrolidone (NMP) was used as the general solvent, with DCM for washing, Fresh HATU solution (1 M) was used for coupling and piperidine for deprotections Each of these solutions was fitted to the synthesiser in the correct positions. Each coupling used 10 equivalents of Fmoc protected amino acid (1.0 mmol), which were weighed into individual cartridges. The cartridges were placed into the machine in order of sequence. Once ready, the sequence was loaded in the synthesiser through the Synthesis Assistant 3.1 software. The peptide was then automatically synthesised with monitoring of the process through observation of the UV/Vis signature of the dibenzofulvene generated in the Fmoc deprotections.

Purification: All peptides were purified by semi-preparative HPLC (Gilson 322 pump, 172 diode array detector and GX-272 liquid handler, Macherey-Nagel C18, 21.0 mm x 25 cm column) using 'Trilution LC' software. The mobile phase was a 0-100% gradient of H_2O/CH_3CN, with 1% TFA, run over the course of a 20 or 30 minute period. Absorption was monitored at 256 nm.

7.4 Protocols for determination of photostationary states (PSS) and thermal relaxation measurements

Photostationary state determination:

A 5 mM solution of the compound was made up in DMSO-d_6. The solution was kept in the dark for period of no less than 3 days. 400 μL of the solution was transferred to a quartz NMR tube (Norell inc.) and a ^{1}H-NMR spectrum was recorded. The resonance position and the relative integrations of the Ar-H and heterocycle-H were identified and recoreded as those representing the *trans* isomer.

The sample was irradiated directly in the quartz NMR tube.[††] The tube was aligned with the light source (Thorlabs, M365L2, 365 nm[‡‡]) at distance of 5 cm; the NMR tube was propped up in an open box in room with no lights on. The sample was irradiated for a period of 1 minute and immediately placed into the NMR magnet (automatic shim, 16 scans) and the ^{1}H-NMR spectrum recorded. This process was repeated until no change was observed and the photostationary state was reached.

For the final spectrum, the signals clearly identified as respresentive of the *trans* isomer were integrated and normalised by dividing each intergral by the number of protons the signal represented. The average of these numbers was calculated as the relative size of a 1H signal of the *trans* isomer. The same process was then applied to those signals representing the *cis* isomer[§§]. The two averages were used to calculate the percentage of *trans* and *cis* isomers present in each sample; the called PSS_{365} and PSS_{420}.

[††] Whenever the diode lamps were on, protective lab glasses were worn.
[‡‡] The LEDD1B LED driver console unit was set to continuous wave (CW) and the current limit to 0.7 A, the limit dial on the front was set to its maximum.
[§§] Thorlabs M420L3 diode lamp, 420 nm.

Thermal relaxation measurements:

A 25 μM solution of the compound was made up from the stock 5 mM solution prepared for the NMR PSS study. The solution was kept in the dark for period of no less than 3 days. The UV-VIS spectrum was recorded (250-600 nm, 25 ˚C) for this dark adapted sample. The sample 3000 μL was irradiated with light at 365 nm following the same methodology as Photostationary study. After an irradiation period of 1 minute the UV-VIS spectra was recorded. This process was repeated until no change was observed in the UV/Vis and the sample was deemed to be at the PSS_{365}.

The Peltier unit was set 60 ˚C and the system left to equilibrate for 30 minutes. The PSS_{365}, freshly irradiated, was placed in the heated sample holder and allowed to equilibrate for 1 minute. The absorbance of the sample was continuously recorded at 335 nm for a period of no less than 3000 seconds.

This process was repeated with a freshly irradiated sample at 10 ˚C intervals over the 60-100 ˚C range, until the absorbance reached a plateau (measuring data at no less than 4 different temperatures for each sample).

The data, manipulated as discussed in the research and discussion section (5.2 thermal stability studies), was used to determine a range of thermal relaxation parameters.

7.5 General experimental

3-Propargyloxy(azobenzene) ***108***

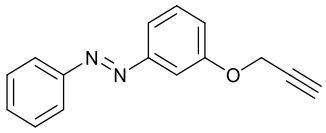

3-Hydroxyazobenzene, **141,** (70 mg, 0.35 mmol), propargyl bromide (131 mg, 0.88 mmol) and K_2CO_3 (235 mg, 1.7 mmol) were added to anhydrous CH_3CN (10 mL). The reaction mixture was allowed to stir at room temperature for 16 hrs. It was then concentrated under vacuum, the resulting slurry was dissolved in diethyl ether (20 mL). The solution was washed with water (30 mL), then brine (30 mL), dried over anhydrous magnesium sulphate and concentrated under vacuum to give the crude product as an orange oil (101 mg). Following flash chromatography (ether: pet ether 1:4) desired product was isolated as an orange sticky solid 72 mg, 87%.

^{1}H-NMR: δ_H (500 MHz) ($CDCl_3$): 2.55 (t, 1H, CH, J = 2.5 Hz), 4.78 (d, 2H, CH_2, J = 2.5 Hz), 7.11 (ddd, 1H, Ar-H, J = 8.0, 3.0, 1.0 Hz) 7.42-7.54 (m, 5H, Ar-H), 7.60 (ddd, 1H, Ar-H, 8.0, 2.0, 1.0 Hz) 7.91-7.93 (m, 2H, Ar-H)

The ^{1}H-NMR spectrum shows a series of low intensity peaks consistent with the presence of the *cis* isomer; 10:1 *trans* to *cis* ratio

^{13}C-NMR: δ_C (125 MHz) ($CDCl_3$): 56.1 (CH_2), 75.8 (CH), 78.3 (C≡CH), 107.3, 117.7, 118.4, 122.9, 129.1, 129.9, 131.1 (Ar-H), 152.6, 153.9 (Ar q-C) 158.3 (Ar qC-O)

The ^{13}C-NMR spectra shows a series of low intensity peaks consistent with the presence of the *cis* isomer

R_f: (diethyl ether: pet. ether 1:2) 0.76

IR (KBr disc): 3293.6 (C-H), 1598.0 (C=C), 1478.2 (N=N) 1238.6 (C-N) cm^{-1}.

HRMS (direct injection) $[M+H]^+$, $[C_{15}H_{13}N_2O]^+$ calculated: 237.1022, found: 237.1030; difference 3.23 ppm

2-Propargyloxy-3-methyl(azobenzene) ***144***

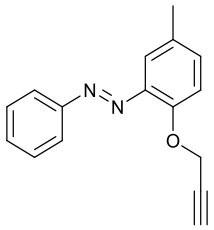

2-Hydroxy-3-methylazobenzene, **143**, (1.01 g, 4.6 mmol), propargyl bromide (1.80 g, 15.1 mmol) and K_2CO_3 (3.29 g, 23.8 mmol) were added to anhydrous CH_3CN (40 mL). The reaction mixture was allowed to stir at room temperature for 18 hrs. It was then concentrated under vacuum, the resulting mixture was partitioned in diethyl ether (50 mL) and water (100 mL). The organics were washed with brine (100 mL), dried over anhydrous magnesium sulphate and concentrated under vacuum to give the crude product (1.40 g). Following flash chromatography (pet. ether) the desired product was isolated as an orange oil 0.94 g, 82%.

^{1}H-NMR: δ_H (500 MHz) ($CDCl_3$): 2.34 (s, 3H, CH_3) 2.52 (t, 1H, CH, J = 2.5 Hz), 4.90 (d, 2H, CH_2, J = 2.5 Hz), 7.13 (d, 1H, Ar-H, J = 8.5 Hz), 7.24 (dd, 1H, Ar-H, 8.5, 2.5 Hz) 7.42-7.52 (m, 4H, Ar-H), 7.89-7.93 (m, 2H, Ar-H)

The ^{1}H-NMR spectrum shows a series of low intensity peaks consistent with the presence of the *cis* isomer

^{13}C-NMR: δ_C (125 MHz) ($CDCl_3$): 20.6 (CH_3), 58.3 (CH_2), 75.9 (CH), 78.8 (C≡CH), 116.5, 117.3, 123.0, 129.1, 130.9, 132.8 (Ar-H), 132.0 (q-C-CH_3) 142.9, 153.1 (Ar q-C) 153.3 (Ar qC-O)

The ^{13}C-NMR spectrum shows a series of low intensity peaks consistent with the presence of the *cis* isomer

R_f (diethyl ether: pet. ether 1:19) 0.64

IR (KBr disc): 3291.6 (C-H), 1500.8.0 (C=C), 1467.6 (N=N) 1219.3 (C-N) cm^{-1}.

HRMS (direct injection) $[M+H]^+$, $[C_{16}H_{15}N_2O]^+$ calculated: 252.1210, found: 252.1223; difference 4.95 ppm

1-[3-[[Phenylisoxazole-5-yl]methoxy]phenyl]-2-phenyldiazine ***153***

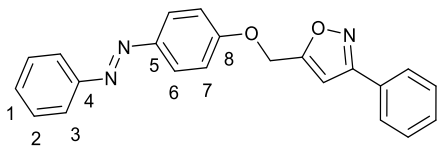

Route A:[183] Benzaldehyde oxime **103** (154 mg, 1.68 mmol) was dissolved in ethanol (5 mL), chloramine-T (574 mg, 2.56 mmol) was added, followed by distilled water (1 mL). the reaction mixture was left to stir for 10 minutes. The propargylated azobenzene **107** (100 mg, 0.42 mmol) was added and the reaction was left to stir over night at room temperature. Ethyl acetate (30 mL) was added followed by consecutive washing with water and brine (50 mL each). The organics were dried over anhydrous magnesium sulphate and concentrated under vacuum to give the crude product as an orange solid (834 mg). Purification by flash chromatography (diethyl ether: pet. ether, 1:1) and crystallisation from diethyl ether and pet. ether gave the product as a crystalline orange solid 132 mg, 88%.

Route B: Benzohydroximoyl chloride **97** (200 mg, 1.29 mmol) and the Propargylated azobenzene **107** (101 mg 0.43 mmol) were dissolved in EtOAc (10 mL), followed by addition of NEt_3 (130 mg, 0.18 mL 1.29 mmol). The reaction mixture was stirred for 16 hrs at room temperature. Ethyl acetate (20 mL) was added, followed by sequential washing with distilled water and brine (30 mL each). The organics were dried over anhydrous sodium sulphate and concentrated under vacuum to give the crude product as an orange solid (278 mg). Purification by flash chromatography (diethyl ether: pet. ether, 1:1) gave the desired product as a crystalline orange solid 116 mg, 76%.

^{1}H-NMR: δH (500 MHz) ($CDCl_3$): 5.30 (s, 2H, OCH_2), 6.69 (s, 1H, CH-isoxazole) 7.09-7.13 (m, 2H, H-7), 7.44-7.47 (m, 4H, Ar-H), 7.51 (t, 2H, Ar-H, J = 7.5 Hz), 7.80-7.83 (m, 2H, Ar-H), 7.87-7.90 (m, 2H, Ar-H), 7.93-7.97 (m, 2H, H-6).

The ^{1}H-NMR spectrum shows a series of low intensity peaks consistent with the presence of the *cis* isomer

^{13}C-NMR: δC (125 MHz) ($CDCl_3$): 62.6 (OCH_2), 101.6 (CH-isoxazole) 115.1 (C-6/7), 122.7 (Ar-H), 124.8 (C-6/7), 126.9 (Ar-H), 128. 7 (q-Ph), 129.0, 129.1, 130.2, 130.6

(Ar-H), 147.8 (C-5) 152.7 (C-4), 160.0 (C-8), 162.6 (CN-isoxazole), 167.9 (CO-isoxazole).

The ^{13}C-NMR spectrum shows a series of low intensity peaks consistent with the presence of the *cis* isomer

m.p.: 122-124 ℃

IR (KBr disc): 3260.9, 3136.4 3058.5 (C-H), 1601.4, 1585.9, 1581.4 (C=C), 1502.3 (C=N) 1441.1 (N=N), 1257.9 (C-O) cm^{-1}

HRMS (direct injection) $[M+H]^+$, $[C_{22}H_{18}N_3O_2]^+$ calculated: 356.1394, found: 356.1409; difference: 4.36 ppm

1,2-Bis[4-[[3phenylisoxazol0-5y]methoxy]phenyl]diazine ***154***

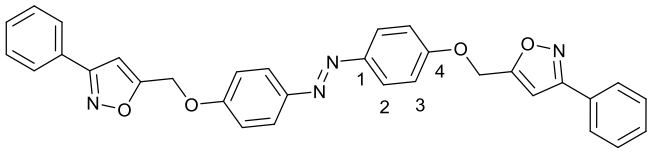

A solution of triethylamine (293 mg, 0.404 mL, 2.9 mmol) in ethyl acetate (0.6 mL) was added over 4 hours with a syringe pump to a solution of the *p,p*-bis propargyloxy-azobenzene **113** (140 mg, 0.48 mmol) and benzohydroximoyl chloride, **97** (450 mg, 2.9 mmol) in ethyl acetate (30 mL). The reaction mixture was heated to reflux for 16 hours. The reaction mixture was washed consecutively with water (60 mL) and brine (60 mL). The organics were dried over anhydrous magnesium sulphate and concentrated under vacuum to give the crude product as an orange solid (576 mg). Purification by flash chromatography (1:1 to 2:1 diethyl ether: pet. ether) to give the product as a yellow solid 189 mg, 74%.

The same experiment was conducted (scale x 1.45), with $CHCl_3$ in the place of EtOAc; **152** was furnished in 81% yield.

^{1}H-NMR: δH (500 MHz) ($CDCl_3$): 5.31 (s, 2H, OCH_2), 6.69 (s, 1H, CH-isoxazole) 7.05-7.11 (m, 2H, H-3), 7.45-7.49 (m, 3H, *m*- & *p*-Ph), 7.79-7.82 (m, 2H, *o*-Ph), 8. 22-8.27 (m, 2H, H-2).

The ^{1}H-NMR spectrum shows a series of low intensity peaks consistent with the presence of the *cis* isomer

^{13}C-NMR: δC (125 MHz) ($CDCl_3$): 61.6 (OCH_2), 101.0 (CH-isoxazole) 115.8 (C-3), 126.1 (C-2), 126.9 (Ph), 128.5 (q-Ph), 129.0, 130.4 (Ph), 142.5 (C-1) 162.5 (C-4), 162.7 (CN-isoxazole), 166.8 (CO-isoxazole).

The ^{13}C-NMR spectrum shows a series of low intensity peaks consistent with the presence of the *cis* isomer

m.p.: 136-139 ˚C

IR (KBr disc): 3116.3 (C-H), 1593.7(C=C), 1507.3 (C=N) 1442.5 (N=N), 1254.9 (C-O) cm^{-1}

HRMS (direct injection) $[M+H]^+$, $[C_{32}H_{25}N_4O_4]^+$ calculated: 529.1870, found: 529.1875; difference: 0.97 ppm

1-[-4-[1-Benzyl-1H-123-triazolo-4-yl]methoxy]phenyl]-2-phenyldiazine **156**

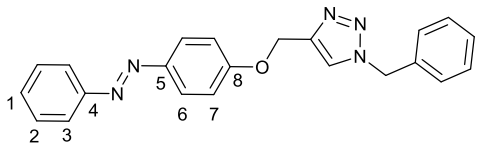

Benzyl azide **155** (226 mg, 0.206 mL, 1.69 mmol) and the 4-propargylated azobenzene **107** (200 mg, 0.85 mmol) were added to DMSO (30 mL). Distilled water (10 mL) was added followed by $CuSO_4.5H_2O$ (88 mg, 0.17 mmol) and sodium ascorbate (68 mg, 0.17 mmol). The reaction mixture was stirred overnight at room temperature. Distilled water (50 mL) was added, followed by extraction with ethyl acetate (2 X 30 mL). The organic layers were combined, washed sequentially with distilled water (50 mL) and saturated brine (50 mL), dried over anhydrous sodium sulphate and concentrated under vacuum to give an orange solid (346 mg). The material was loaded on to a silica plug. Diethyl ether (100 mL) was passed through to elute impurities, subsequent elution with acetone (100 mL) gave, after evaporation of the solvent, the pure compound as an orange solid 227 mg, 89%.

^{1}H-NMR: δ_H (500 MHz) (DMSO-d_6): 5.27 (s, 2H, OCH_2), 5.63 (s, 2H, NCH_2), 7.25 (d, 2H, H-7, J = 9.0 Hz), 7.31-7.41 (m, 5H, Ar-H), 7.52-7.61 (m, 3H, Ar-H), 7.85 (d, 2H, Ar-H, J = 7.5 Hz), 7.90 (d, 2H, H-6, J = 9.0 Hz), 8.34 (s, 1H, CH-triazole).

The ^{1}H-NMR spectrum shows a series of low intensity peaks consistent with the presence of the *cis* isomer

^{13}C-NMR: δ_C (125 MHz) (DMSO-d_6): 53.4 (NCH_2), 62.0 (OCH_2), 115.9, 122.7, 125.0, 125.4, 128.5, 128.7, 129.3, 129.9, 131.4 (Ar-H & CH-triazole), 136.4 (C-8), 143.0 (triazole-qC), 146.8 (C-1a), 152.5 (C4/5), 161.3 (qC-Ph)

The ^{13}C-NMR spectrum shows a series of low intensity peaks consistent with the presence of the *cis* isomer

m.p.: 187-189 ˚C

IR (KBr disc): 3133.6 (C-H), 3055.0 (C-H), 1601.4 (C=C), 1581.3 (C=C triazole), 1495.1 (N=N), 1238.9 (C-N), 1224.7 (C-O) cm^{-1}

HRMS (direct injection) $[M+H]^+$, $[C_{22}H_{20}N_5O]^+$ calculated: 370.1662, found: 370.1662; difference 0.23 ppm.

1E-1,2-Bis[4-[1-Benzyl-1H-1,2,3-triazolo-4-yl]methoxy]phenyl]diazine ***157***

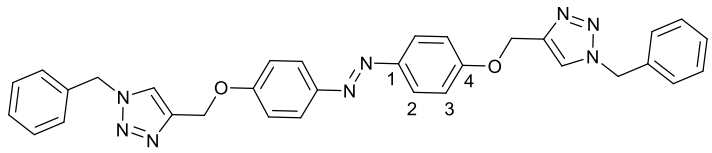

Benzyl azide **155** (183 mg, 0.17 mL, 1.38 mmol) and the 4,4'-bispropargylated azobenzene **113** (100 mg, 0.34 mmol) were added to DMSO (30 mL). Distilled water (10 mL) was added followed by $CuSO_4.5H_2O$ (69 mg, 0.28 mmol) and sodium ascorbate (55 mg, 0.28 mmol). The reaction mixture was stirred overnight at room temperature. Distilled water (50 mL) was added, extraction with ethyl acetate (2 x 30 mL) followed. The organic layers were combined, washed with distilled water (50 mL) and saturated brine (50 mL), dried over anhydrous sodium sulphate and concentrated under vacuum to give a yellow sticky solid (224 mg). The material was loaded on to a silica plug. Diethyl ether (150 mL) was passed through to elute impurities, a subsequent acetone (100 mL) elution gave, after evaporation of the solvent, the pure compound as a yellow solid 166 mg, 87%.

^{1}H-NMR: δ_H (500 MHz) (DMSO-d_6): 5.26 (s, 2H, OCH_2), 5.65 (s, 2H, NCH_2), 7.22 (d, 2H, H-3, J = 8.5 Hz), 7.31-7.42 (m, 5H, Ph), 7.85 (d, 2H, H-2, J = 8.5 Hz), 8.34 (s, 1H, CH-triazole).

The ^{1}H-NMR spectrum shows a series of low intensity peaks consistent with the presence of the *cis* isomer

^{13}C-NMR: δ_C (125 MHz)(DMSO-d_6): 53.4 (NCH_2), 62.0 (OCH_2), 115.8 (C-3), 124.6 (C-2), 125.3(C-H triazole), 128.4 , 128.7, 129.3 (Ph) 136.5 (q-Ph), 143.1 (q-triazole), 146.9 (C-1), 160.7 (C-4)

The ^{13}C -NMR shows a series of low intensity peaks consistent with the presence of the *cis* isomer

m.p.: 190-192 ˚C

IR (KBr disc): 3079.5, 2925.5 (C-H), 1603.2 (C=C), 1583.6 (C=C triazole), 1496.2 (N=N), 1455.7 (C-N), 1248.4 (C-O) cm^{-1}

HRMS (direct injection) $[M+H]^+$, $[C_{34}H_{29}N_8O_2]^+$ calculated: 557.2408, found:557.2404; difference 0.73 ppm

4-(Phenylazo)benzaldehyde ***160***

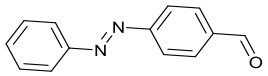

4-(Phenylazo)benzyl alcohol, **159**, (100 mg, 0.47 mmols) and NMM (83 mg, 0.71 mmol) were dissolved in DCM (3 mL). TPAP (8.3 mg, 0.023 mmols, 5 mol%) and 4Å molecular sieves were added. The reaction was stirred gently at room temperature for 2 hours. The reaction mixture was then washed through a silica plug (diethyl ether 30 mL). The filtrate was concentrated under vacuum to give the desired product as an orange solid 77 mg, 78%.

^{1}H-NMR spectral data agreed with that reported in the literature.[183]

*4-[Phenylazo]hydroxyimino]benzaldehyde **110***

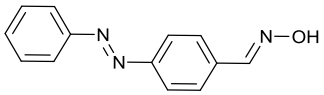

Route 1: 4-(Phenylazo)benzaldehyde, **160,** (0.263 g, 1.25 mmol), hydroxylamine hydrochloride (0.139 g, 2.00 mmol) and pyridine (0.146 g, 0.15 mL, 1.85 mmol) were added to ethanol (10 mL) in a 35 mL microwave vessel. The sealed vessel was then heated by microwave irradiation (T = 125 ˚C, Pmax = 300 W) for 60 mins. Distilled water (10 mL) was added, the reaction mixture was left to stand for 5 mins while a precipitate formed. The precipitate was filtered and dried to give the desired product as an orange solid (0.242 g, 86%) which required no further purification.

Route 2: 4-(Phenylazo)benzaldehyde, **160,** (1.97 g, 9.4 mmol), hydroxylamine hydrochloride (0.97 g, 14.0 mmol) and pyridine (0.83 g, 0.85 mL, 10.5 mmol) were added to ethanol (80 mL). The reaction mixture was heated to reflux for 4 hours. Distilled water (80 mL) was added, the reaction mixture was left to stand for 25 mins while a precipitate formed. The precipitate was filtered and dried to give the desired product as an orange solid (1.50 g, 71%) which required no further purification.

^{1}H-NMR spectral data agreed with that reported in the literature.[183]

4,4'-Azobis[hydroxyimino]benzaldeyde ***116***

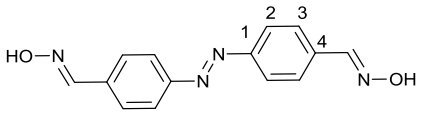

Route 1: Bis[4-(1,3-dioxolan-2-yl)phenyl]diazene, **166,** (0.451 g, 1.38 mmol), hydroxylamine hydrochloride (0.64 g, 9.21 mmol) and pyridine (0.36 g, 0.37 mL, 4.6 mmol) were added to ethanol (10 mL) in a microwave vessel. The sealed vessel was then heated by microwave irradiation (T = 125 ˚C, Pmax = 300 W) for 90 mins. Distilled water (15 mL) was added, the reaction mixture was left to stand for 10 mins while a precipitate formed. The precipitate was filtered and dried to give the desired product as an orange solid 0.198 g, 53%.

Route 2: Bis[4-(1,3-dioxolan-2-yl)phenyl]diazene **166,** (3.02 g, 9.3 mmol), hydroxylamine hydrochloride (5.79 g, 55.5 mmol) and pyridine (2.20 g, 2.25 mL, 27.8 mmol) were added to ethanol (75 mL). The reaction mixture was heated to reflux for 4 hours. Distilled water (150 mL) was added, the reaction mixture was left to stand for 30 mins while a precipitate formed. The precipitate was filtered and dried to give the desired product as an orange solid 1.1 g, 44%.

^{1}H-NMR: δ_H (300 MHz) (DMSO-d_6): 7.86 (d, 4H, Ar-H, J = 7.0 Hz), 8.25 (d, 4H, Ar-H, J = 7.0 Hz), 8.29 (s, 1H, C<u>H</u>=NOH), 11.85 (s, 1H, CH=NO<u>H</u>),

The ^{1}H-NMR spectrum shows a series of low intensity peaks consistent with the presence of the *cis* isomer

^{13}C-NMR: δ_C (75 MHz) (DMSO-d_6): 129.2, 132.9 (Ar-CH), 139.5 (CH=NOH), 143.4 (C-4), 153.7 (C-1)

The ^{13}C -NMR shows a series of low intensity peaks consistent with the presence of the *cis* isomer

r.f. 0.39 (pet. Ether: EtOAc 6:1)

IR (KBr disc): 2982.1 (br.) (O-H), 1588.6 (C=C), 1467.1 (N=C), 1414.9 (N=N), 1011.4 (N-O),

HRMS (direct injection) $[M+H]^+$, $[C_{14}H_{11}Cl_2N_4O_2]^+$ calculated:, found:; difference ppm.

3,3'-Azobis[hydroxyimino]benzaldehyde ***117***

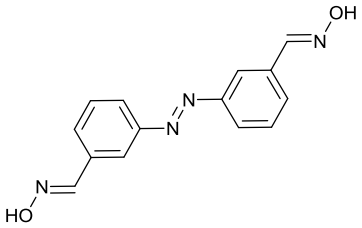

The acetal protected azobenzene **169** (3.16 g, 9.7 mmol), hydroxylamine hydrochloride (3.38 g, 48.6 mmol) and pyridine (2.37 g, 2.43 mL, 30.0 mmol) were added to ethanol (80 mL). The reaction mixture was heated to reflux for 4 hours. Distilled water (150 mL) was added, and the mixture was extracted with diethyl ether (3 x 50 mL). The organics were combined, dried over anhydrous magnesium sulphate and concentrated under vacuum to give the crude product. Purification by flash chromatography (diethyl ether: pet. ether 1:2 > 1:1) gave the desired product as an orange solid 1.24 g, 48%.

^{1}H-NMR spectral data agreed with that reported in the literature.[189]

*1[[4-[5-(Phenoxymethyl)isoxazol-3yl]phenyl]-2-phenyldiazine **172***

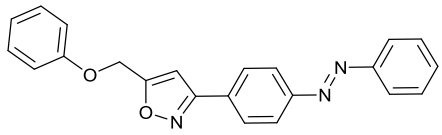

Route 1: To a solution of 4-(phenylazo)benzaldehyde oxime, **110,** (150 mg, 0.66 mmol) in EtOH (3 mL) and H_2O (1 mL) was added Ch-T (152 mg, 0.66 mmol). The reaction mixture was stirred at room temperature 10 min. a solution of propargyloxybenzene, **173**, (29 mg, 0.222 mmol) in EtOH/H_2O (3:1, 2 mL). The reaction mixture was heated to 40 ˚C for 60 mins. H_2O (30 mL) was added, followed by extraction with DCM (20 mL). The combined organics were dried over anhydrous magnesium sulphate and concentrated under reduced pressure to give the crude product (244 mg). Purification by flash column chromatography (pet. ether:EtOAc, 4:1) yielded the desired product as an orange solid 209 mg, 89%.[183]

Route 2: 4-(Phenylazo)benzaldehyde oxime **110** (30 mg, 0.133 mmol) was dissolved in DMF (1.0 mL) followed by cooling to 0 ˚C. NCS (34 mg, 0.26 mmol) was added portionwise to the reaction mixture over the course of an hour. The reaction mixture was stirred at room temperature for a further hour. Propargyloxybenzene, **173**, (5.8 mg, 0.044 mmol) and triethylamine (14 mg, 0.019 mL, 0.133 mmol) were added, followed by stirring overnight at room temperature. DCM (3 x 4 mL) was added and the organics were washed with water (10 mL) and brine (10 mL). The organics were then dried over magnesium sulphate and concentrated under vacuum to give the crude product as an orange solid (37.4 mg). Purification by flash chromatography (pet ether:EtOAc, 4:1) gave the yielded the desired product as an orange solid 11.4 mg, 73%.

Route 3: Propargyloxybenzene **173** (9.7 mg, 0.075 mmol) and NEt_3 (22 mg, 0.22 mmol) were dissolved in DMF (0.5 mL), to this a solution of the chlorooxime **174** (57 mg, 0.22 mmol) in DMF (0.5 mL) was added. The reaction mixture was left to stir for 2 hours at room temperature. Distilled water was added (10 mL) followed by extraction with DCM (3 x 4 mL). The combined organics were dried over anhydrous magnesium sulphate and concentrated under vacuum to give the crude product (31 mg). Purification by flash

chromatography (pet ether:EtOAc, 4:1) gave the yielded the desired product as an orange solid 19.6 mg, 76%.

^{1}H-NMR spectral data agreed with that reported the literature.[183]

4-[[Phenylazo]chloro(hydroxyimino)]benzaldehyde ***174***

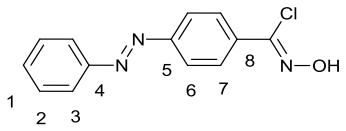

A solution of the oxime **110** (100 mg, 0.44 mmol) in DMF (0.45 mL) was cooled in an ice bath. To this *N*-chlorosuccinimide (72 mg, 0.54 mmol) was added in four portions over 1 hr. The resulting solution was stirred at room temperature for 4 hrs. The reaction was quenched with iced water (1.2 mL) followed by extraction with diethyl ether (4 x 0.6 mL). The organic layers were combined, dried over anhydrous Na_2SO_4 and concentrated under vacuum pressure to give the product as a flaky orange solid 93 mg, 81%.

^{1}H-NMR: δ_H (500 MHz) ($CDCl_3$): 7.50-7.56 (m, 3H, Ar-H), 7.93-7.97 (m, 4H, Ar-H), 8.00-8.03 (m, 2H, Ar-H) 8.13 (s, 1H, OH)

The ^{1}H-NMR spectrum shows a series of low intensity peaks consistent with the presence of the *cis* isomer; 5:1 *trans* to *cis*.

^{13}C-NMR: δ_C (125 MHz) ($CDCl_3$): 122.9, 123.1, 128.1, 129.2, 131.6 (Ar-CH), 134.4 (C-8), 139.4 (C-Cl), 152.6, 152.7 (C-4 & C-5)

The ^{13}C -NMR shows a series of low intensity peaks consistent with the presence of the *cis* isomer

m.p.: 157-161 ˚C

IR (KBr disc): 3453.2 (O-H), 1633.9 (C=C), 1439.9 (N=N), 998.3 (N-O), 681.3 (C-Cl)

HRMS (direct injection) $[M+H]^+$, $[C_{13}H_{11}ClN_3O]^+$ calculated: 260.0585, found: 260.0597; difference 4.72 ppm.

4,4'-Azobis[chloro(hydroxyimino)]benzaldehyde ***176***

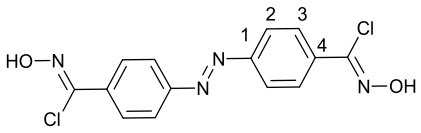

N-Chlorosuccinimide (72 mg, 0.54 mmol) was added in 4 portions over 1 hr to a ice cooled solution of the bis-oxime **116** (50 mg, 0.17 mmol) in DMF (0.5 mL). The reaction mixture was allowed to warm to room temperature and stirred for 4 hrs. Iced water (1.2 mL) was added, followed by extraction with diethyl ether (4 x 1.0 mL). The organic layers were washed with brine (2 x 1mL) and dried over magnesium sulphate. The solvent was removed under vacuum to give the product as an orange solid 41 mg, 72%.

^{1}H-NMR: δ_H (300 MHz) (DMSO-d_6): 8.09 (d, 2H, Ar-H, J = 3Hz), 8.09 (d, 2H, Ar-H, J = 3Hz), 12.80 (s, 1H, OH)

^{13}C-NMR: δ_C (75 MHz) (DMSO-d_6): 129.2, 132.9 (Ar-CH), 139.5 (C-Cl), 143.4 (C-4), 153.7 (C-1)

The ^{13}C -NMR shows a series of low intensity peaks consistent with the presence of the *cis* isomer

m.p.: 157-160 ˚C

IR (KBr disc): 2914.9 (br.) (O-H), 1595.0 (C=C), 1460.0 (N=C), 1404.1.9 (N=N), 1003.3 (N-O), 685.4 (C-Cl)

HRMS (direct injection) $[M+H]^+$, $[C_{14}H_{11}Cl_2N_4O_2]^+$ calculated: 337.0254, found: 337.0267; difference 4.07 ppm.

*(E)-1,2-Bis[4-[5-(phenoxymethyl)isoxazol-3-yl]phenyl]diazene **175***

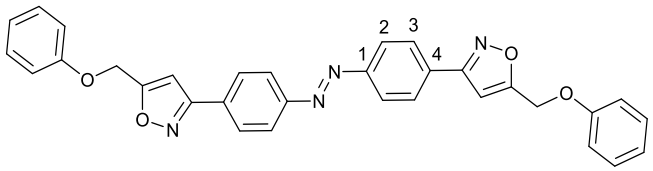

*Table E1: Experimental conditions explored for the synthesis of **175***

Experiment number	Starting material	Solvent	Con[c] 116/175 (mol/L)	Dipole precursor: alkyne ratio[ǂ]	Reaction duration (hrs)	Temp (˚C)	Out come (isolated product)
A.1	Oxime **116**	EtOH	0.11	1:3	4	40	No **175**
A.2	Oxime **116**	EtOH	0.11	1:6	4	40	No **175**
A.3	Oxime **116**	EtOH	0.11	1:3	4	78	No **175**
B.1	Chloro-oxime **176**	EtOH	0.046	1:6	20	r.t.	**175** - 2% yield
B.2	Chloro-oxime **176**	EtOH	0.046	1:6	20*	r.t.	**175** - 21% yield
C.1	Chloro-oxime **176**	Toluene	0.015	1:6	24	110	**175** - 32% yield
B.4	Chloro-oxime **176**	EtOH	0.046	1:6	20*	83	**175** - 46% yield

[ǂ] Dipole precursor: alkyne ratio is interpreted as the number of mole equivalents of alkyne to each dipole precursor. Therefore, a 1:3 molar ratio of ratio implies a ratio of 2:3 alkyne to dipole precursor in terms of functional groups, since the oxime **116** or chlorooxime **176** potentially furnish 2 equivalents of nitrile oxide.

*In these experiments a solution of NEt_3 (total volume 1 mL) was added slowly over a 40 minute period, using a syringe pump.

Route A: Reaction temperatures, molar ratio of the reactants and concentration of the oxime are as per table E1. The bis-oxime **176** and Ch-T were added to ethanol (10 mL) and stirred for 10 minutes, propargyloxybenzene **173** was added. The reaction mixture was left to stir for four hours. Distilled water (50 mL) was added, followed by extraction with DCM (3 x 30 mL). The combined organics were dried over anhydrous sodium sulphate and concentrated under vaccum to give the crude mixture which did not contain any **175.**

Route B: Reaction temperatures, molar ratio of the reactants and concentration of the chlorooxime are as per table E1. Bis-chlorooxime **176** and propargyloxybenzene **173** were dissolved in EtOH. NEt_3 was added and the mixture was left to stir. The reaction mixture was partitioned between distilled water (100 mL) and DCM (50 mL). The organics were washed with distilled water (50 mL) and brine (50 mL), followed by drying over anhydrous sodium sulphate and concentrating under vaccum. Purification by flash chromatography (diethyl ether: pet ether, 1:4 > 1:2) gave the title compound **175**, yields shown in the table.

Route C: Bis-chlorooxime **176** (160 mg, 0.47 mmol) and propargyloxybenzene **173** (393 mg, 2.97 mmol) were dissolved in toluene (30 ml). NEt^3 was added and the reaction was left to stir. The solvent was removed under vacuum and the residue was dispersed in DCM. The organics were washed with distilled water (2 x 50 mL) and brine (50 mL), followed by drying over anhydrous sodium sulphate and concentrating under vacuum. Purification by flash chromatography (diethyl ether: pet ether, 1:4 > 1:2) gave the title compound **175**, yields shown in the table.

^{1}H-NMR: δ_H (300 MHz) ($CDCl_3$): 5.25 (s, 2H, CH_2), 6. 73 (s, 1H, isoxazole-CH), 6.99-7.06 (m, 3H, Ar-H), 7.31- 7.37 (m, 2H, Ar-H) 7.93-8.05 (m, 4H, Ar-H)

The ^{1}H-NMR shows a series of low intensity peaks consistent with the presence of the *cis* isomer

^{13}C-NMR: δ_C (75 MHz) ($CDCl_3$): 61.4 (CH_2) 101.43 (isoxazole-CH) 114.8, 122.0, 123.6, 127.7 129.74 (Ar-CH) 131.4 (C-4), 153.4 (C-1), 157.8 (O-Ar-C), 161.8 (isoxazole-CN), 169.0 (isoxazole-CO)

The ^{13}C -NMR shows a series of low intensity peaks consistent with the presence of the *cis* isomer

R.f. (diethyl ether: pet. ether 1:2) 0.52

IR (KBr disc): 3108.7, 2917.0, 2865.8 (C-H), 1616.8 (C=N), 1600.8 (C=C), 1434.4 (N=N), 1247.0 (C-O).

HRMS (direct injection) $[M+H]^+$, $[C_{32}H_{25}N_4O_4]^+$ calculated: 529.1870, found: 529.1876; difference 0.99 ppm.

2-(2H-Indazol-2yl)benzaldehyde oxime ***198***

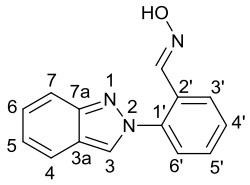

(i) Lithium aluminum hydride (0.49 g, 13 mmol) was added to diethyl ether (30 mL) which was cooled to -82 °C ($N_{2(Lq)}$/ EtOAc slush bath). The suspension was vigorously stirred and the protected nitrobenzene, **196**, (0.52 g, 2.7 mmol) in diethyl ether (50 ml) was added dropwise. The resulting reaction mixture was allowed to slowly warm to room temperature and was left to stir for 3 hours. The reaction cooled to -82 °C ($N_{2(Lq)}$/ EtOAc slush bath) and quenched by the slow, dropwise consecutive addition of EtOAc (3 mL), MeOH (3 mL) and distilled water (3 mL). 5% H_2SO_4 solution was added until all the salts dissolved. EtOAc (50 mL) was added and the organics were separated from the aqueous phase and washed with distilled water (50 mL) and brine (50 mL). The organics were dried over anhydrous magnesium sulphate and concentrated under vacuum to give the crude product was an orange solid (0.43 g). the crude material was dissolved in ethanol (20 ml) and hydroxylamine hydrochloride (0.38 g, 5.4 mmol) and pyridine (0.41 g, 5.3 mmol) were added. The mixture was heated to reflux for 14 hrs. The ethanol was removed under vacuum and the residue dissolved in diethyl ether (30 mL), followed by washing with water and brine (30 mL each). The organics were dried over anhydrous sodium sulphate and concentrated under vacuum to give the crude product as an orange/brown solid (0.34g). The residue was triturated with ether/pet ether (1:1), and the title compound obtained as an off white solid 0.24g, 37%.

(ii) Lithium aluminum hydride (1.51 g, 40 mmol) was added to diethyl ether (100 mL) which was cooled to -82 °C (N_2(Lq)/ EtOAc slush bath). With vigorous stirring the protected nitrobenzene, **196**, (1.47 g, 7.5 mmol) in diethyl ether (150 ml) was added dropwise. The resulting reaction mixture was allowed to slowly warm to room temperature and was left to stir for 3 hours. The reaction cooled to -82 °C (N_2(Lq)/ EtOAc slush bath) and quenched by the slow, dropwise addition of distilled water (10 ml), 10% NaOH solution (10 mL) and distilled water (20 mL). The organics were decanted from the precipitate, which were washed with further ether (50 mL). The

combined organics were dried over anhydrous sodium sulphate and concentrated under reduced vacuum to give the crude product was an off white solid (1.54 g). The crude material, hydroxylamine hydrochloride (2.30 g, 33 mmol) and pyridine (1.30 g, 1.30 mL, 16.5 mmol) were added to ethanol (30 mL). The mixture was heated to reflux for 14 hrs. The ethanol was removed under vacuum and the residue dissolved in diethyl ether (50 mL), followed by washing with water and brine (50 mL each). The organics were dried over anhydrous sodium sulphate and concentrated under vacuum to give the crude product as an orange/brown solid residue (1.39 g), which was triturated with diethyl ether (1:1) to give the title compound as an off white solid 0.82 g, 46%.

^{1}H-NMR: δ_H (500 MHz) (DMSO-d_6): 7.14-7.18 (m, 1H, H-5/6), 7.34-7.38 (m, 1H, H-5/6) 7.60-7.66 (m, 3H, Ar-CH) 7.74 (dd, 1H, H-4/7, J = 9.0, 1.0 Hz), 7.79 (s, 1H, C<u>H</u>=NOH), 7.82 (dt, 1H, H-4/7, J = 8.5, 1.0 Hz) 8.00-8.02 (m, 1H, Ar-CH) 8.73 (s, 1H, H-3) 11.52 (s, 1H, CH=NO<u>H</u>)

^{13}C-NMR: δ_C (125 MHz) (DMSO-d_6): 117.8 121.4 (Ar-CH) 122.4 (C-3a) 122.5, 126.5, 126.8, 127.2, 127.2 (Ar-CH), 128.7 (C-2') 129.8 (C-3), 130.5 (Ar-CH) 139.4 (C-1') 144.6 (<u>C</u>H=NOH) 149.4 (C-7a)

m.p.: 229-233 ˚C.

IR (KBr disc): 3169.2 (O-H), 3118.1, 3074.9 (C-H), 1629.0 (C=N), 1519.8, 1313.6 (N-O), 982.2 (N-O) cm^{-1}.

HRMS (direct injection) $[M+H]^+$, $[C_{14}H_{12}N_3O]^+$ calculated: 238.0975; found: 238.0986. Difference 4.66 ppm.

Experimental conditions explored for the synthesis of the o,o-bisoxime ***118*** *(2,2'-azobis(hydroxyimino)benzaldehyde*

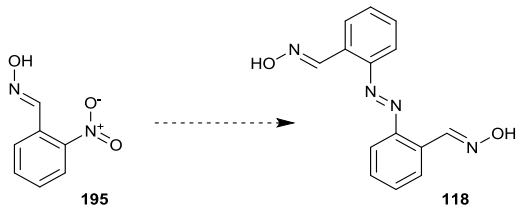

2-Nitrobenzaldehyde oxime **195** (0.20 g, 1.20 mmol) was added to a suspension of $NaBH_4$ (0.27 g, 7.2 mmol) in DMSO (10 mL) with vigorous stirring. Reaction times are indicated in table E2. All experiments were carried out at 80 °C apart from experiment **6** which was heated to 150 ˚C. After the indicated reaction duration the DMSO mixture was cooled and diluted with H_2O (50 mL) and extracted with DCM (2 x 20 mL). The combined organics were washed with water (3 x 30 mL), dried over anhydrous magnesium sulphate and concentrated under vacuum to give the crude product mixture as summarised in table E2.

Table E2: Experimental conditions explored for the synthesis of **118**

Experiment	Time	Outcome‡
1	5 mins	Starting material returned 73%
2	1.5 hrs	Starting material returned 76%
3	6 hrs	starting material returned, with benzaldehyde oxime and other minor impurities 71% (Crude)
4	14 hrs	Complex mixture, (84% crude)
5	16 hrs	Mixture of benzaldehyde oxime and 2-amino benzaldehyde oxime (0.25:1 ratio) 68% (crude)
6	16 hrs	Complex mixture, DMSO decomposition (reaction heated to 150 ˚C). 77% (crude)
7	24 hrs	Complex mixture, including 2-amino benzaldehyde oxime and benzaldehyde oxime 74% (crude)

‡ estimated by examining the relative integrations of key signals in ^{1}H-NMR spectra of the crude products

Bis[2-[(hydroxyimino)methyl)phenyl)diazene 1-oxide ***201***

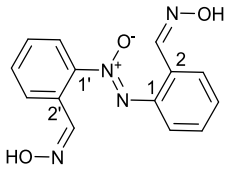

Protected nitrobenaldehyde **196** (0.50 g, 2.56 mmol) was added to EtOH (20 mL), followed by addition of Zn dust (1.71 g, 26.13 mmol) and NaOH (1.04 g, 26.11 mmol). The reaction mixture was heated to reflux for 3 hours. The residue was concentrated under vacuum and the residue partitioned between diethyl ether (50 mL) and distilled water (50 mL). The organics were dried over anhydrous sulphate and concentrated under vacuum. Purification by flash chromatography (diethyl ether: pet. ether, 1:2 > 1:1) gave the azoxybenzene product **200** as an off white solid (278 mg, 63%).[***] Hydroxylamine hydrochloride (0.088 g, 1.27 mmol) was added to a solution of **200** (0.217 g, 0.64 mmol) in acetonitrile (20 mL) and water (20 mL). The resulting solution was stirred at 60 ˚C for 2 hours. Upon cooling to room temperature distilled water was added (50mL) followed by extraction with diethyl ether (2 X 25 mL). The organics layers were combined, dried over anhydrous magnesium sulphate and concentrated under vacuum to afford the title compound as a light orange solid 0.132 g, 72%.

1H-NMR: δ_H (500 MHz) (DMSO-d_6): 7.46 (t, 1H, Ar-H, J = 7.5 Hz), 7.55 (t, 1H, Ar-H, J = 8.0 Hz), 7.62- 7.68 (m, 2H, Ar-H), 7.86 (d, 1H, Ar-H, J = 8.0 Hz), 7.91 (d, 1H, Ar-H, J = 7.0 Hz), 7.95 (d, 1H, Ar-H, J = 8.0 Hz), 8.03 (d, 1H, Ar-H, J = 8.0 Hz), 8.31 (s, 1H, C<u>H</u>=NOH), 8.33 (s, 1H, C<u>H</u>=NOH), 11.47 (s, 1H, CH=NO<u>H</u>), 11.63 (s, 1H, CH=NO<u>H</u>),

13C-NMR: δ_C (125 MHz) (DMSO-d_6): 122.4, 124.6 (Ar-CH), 126.6, (C-2/2') 127.2, 127.9 (Ar-CH), 128.3 (C-2/2'), 129.4, 129.9, 130.6, 131.4 (Ar-CH), 141.6 (C-1/1'), 144.6 (<u>C</u>H=NOH), 145.5 (<u>C</u>H=NOH), 147.8 (C-1/1').

m.p.: 186-188 ˚C.

IR (KBr disc): 3253.1 (O-H), 1631.9 (C=N), 1440.9 (N=N), 975.1 (N-O) cm^{-1}.

[***] Canadian Journal of Chemistry, 1973, 51(23): 3827-3841

HRMS (direct injection) $[M+H]^+$, $[C_{14}H_{13}N_4O_3]^+$ calculated: 285.0982; found: 285.0971. Difference 3.79 ppm.

*Isoxazole linked protected galactose azobenzene conjugate **214***

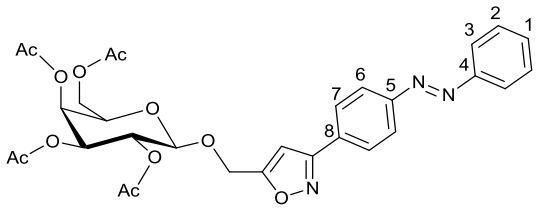

The chloro-oxime **174** (200 mg, 0.77 mmol) and the 1-*O*-propargyloxy galactose **209** (100 mg, 0.26 mmol) were added to EtOAc (20 mL). To this, a solution of triethylamine (79 mg, 0.78 mmol) and EtOAc (1.0 Ll) was added over 4 hours with a syringe pump. The reaction mixture was heated to reflux for 24 hours. Water (50 mL) was added, followed by extraction with DCM (2 X 50 mL). The combined organic layers were washed sequentially with water, brine (30 mL each), and dried over anhydrous $NaSO_4$. The organic phase was concentrated under reduced pressure to give the crude product as a sticky orange solid (172 mg). The crude material was subjected to flash chromatography (DCM/MeOH, 99:1) to give the desire product as an orange solid 125 mg, 79 %, the furoxan byproduct 216 was also recovered from the chromatography franctions, (49 mg, 0.11 mmol).

^{1}H-NMR: δ_H (300 MHz) ($CDCl_3$): 2.00, 2.07, 2.07, 2.18 [4 X (s, 3H, C(O)$\underline{C}H_3$)], 3.97 (app. t, 1H, H^5, J = 6.5 Hz), 4.13-4.25 (m, 2H, H^6), 4.66 (d, 1H, H^1, J = 8.0 Hz) 4.84 (d, 1H, OCH_2, J = 14.0 Hz), 4.97-5.07 (m, 2H, OCH_2 & H^3), 5.29 (dd, 1H, H^2, J = 8.0, 3.5 Hz), 5.43 (d, 1H, H^4, J = 3.5 Hz) 6.65 (s, 1H, CH-isoxazole), 7.50-7.57 (m, 3H, Ar-H) 7.50-7.57 (m, 6H, Ar-H).

^{13}C-NMR: δ_C (75 MHz) ($CDCl_3$): 20.6, 20.6, 20.7, 20.8 (C(O)$\underline{C}H_3$), 61.3 (C^6), 61.6 (OCH_2), 66.9 (C^4), 68.6 (C^2), 70.7 (C^3), 71.0 (C^5), 100.5 (C^1), 101.7 (CH-isoxazole) 123.0, 123.5, 127.6, 129.2 (Ar-CH), 129.7 (C-8), 131.4 (C-1), 152.6, 153.5 (C-4 & C-5) 161.8 (CN-isoxazole) 168.8 (CO-isoxazole), 169.5, 170.1, 170.2, 170.4 ($\underline{C}$(O)CH_3)

m.p.: 56-59 ˚C

IR (KBr disc): 3135.6, 2956.9 (C-H), 1757.8 (C=0) 1614.8 (C=C triazole), 1431.3 (N=N) 1369.8 (C-N), 1226.7 (C-O) cm^{-1}.

HRMS (direct injection) $[M+H]^+$, $[C_{30}H_{32}N_3O_{11}]^+$ calculated: 610.2031, found: 610.2051; difference 3.24 ppm

3,4-(diazobenzene)-1,2,5-oxadiazole 2-Oxide

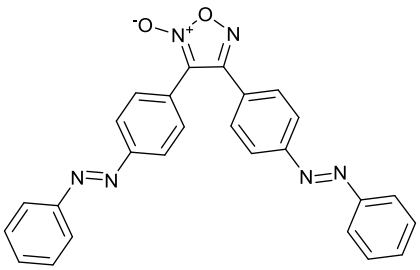

^{1}H-NMR: δ_H (500 MHz) ($CDCl_3$): 7.43-7.50 (m, 6H, Ar-H), 7.65-7.69 (m, 4H, Ar-H), 7.86-7.95 (m, 8H, Ar-H).

Isoxazole linked galactose azobenzene conjugate ***215***

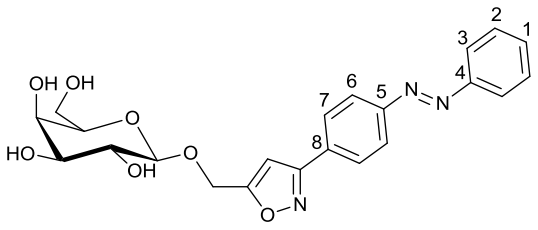

Isoxazole linked protected galactose azobenzene conjugate 214 (108 mg, 0.18 mmol) was added to THF (10ml) followed by methanol (50 mL) and water (10 mL). Sodium methoxide (catalytic amount) was added, the mixture was then allowed to stir overnight at room temperature. Acidic Dowex resin was added to adjust the pH to 6. The resulting mixture was then filtered under gravity. The solid collected, comprising of the precipitated product and the resin beads, was washed with DMF (50 mLs) the resulting solution was concentrated under reduced pressure to yield the product as an orange solid 63 mg, 79%.

^{1}H-NMR: δ_H (500 MHz) (DMSO-d_6): 3.30-3.45 (m, 3H, $H^{2,3,5}$), 3.53-3.58 (m, 2H, H^6) 3.67 (dd, 1H, H^4, J = 3.0, 1.0 Hz) 4.30 (d, 1H, H^1, J = 7.5 Hz), 4.82 (d, 1H, OCH_2, J = 14.0 Hz) 4.96 (d, 1H, CH_2, J = 14.0 Hz) 7.23 (s, 1H, CH-isoxazole) 7.59-7.66 (m, 3H, Ar-H) 7.93-7.97 (m, 2H, Ar-H) 8.02-8.06 (m, 2H, Ar-H) 8.10-8.13 (m, 2H, Ar-H)

^{13}C-NMR: δ_C (125 MHz) (DMSO-d_6): 60.9 (C^6) 61.0 (OCH_2) 68.5 (C^4), 71.0, 73.8, 76.0 (C^2, C^3 &C^5) 102.6 (C^1) 103.5 (CH-isoxazole) 123.2, 123.8, 128.3, 130.0, 132.4 (Ar-H), 131.6, 153.2, 152.4 (Ar-q) 161.6 (CN-isoxazole), 170.8 (CO-isoxazole)

m.p. 158- 163 ˚C

IR (KBr disc): 3402.7 (OH), 2924.7 (CH) 1610.2 (C=N), 1433.4 (N=N), 1056.5 (C-O) cm^{-1}.

HRMS (direct injection) $[M+Na]^+$, $[C_{22}H_{23}N_3O_7Na]^+$ calculated: 464.1428, found: 464.1671; difference: 5.23 ppm

*Isoxazole linked protected mannose azobenzene conjugate **217***

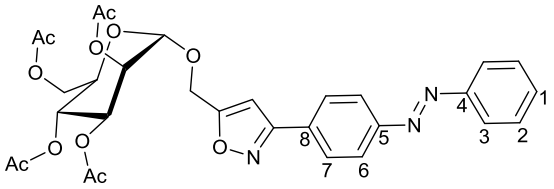

A solution of the propargyl mannose **211** (0.250 g, 0.65 mmol) and the chlorooxime **174** (0.049 g, 0.22 mmol) in ethyl acetate (10 mL) was heated to reflux. Triethlyamine (0.033 g, 0.22 mmol) in ethyl acetate (1.0 mL) was added dropwise over 4 hours. The reaction mixture was heated to reflux overnight. Further ethyl acetate (20 mL) was added followed by consecutive washing with water (20 mL) and brine (20 mL). The organics were then dried over anhydrous magnesium sulphate and concentrated under vacuum to give the crude product as a sticky orange solid (309 mg). The crude material was purified by flash chromatography (DCM/MeOH 100:0 > 95:5) to give the title compound as an orange sticky solid 98 mg, 73 %.

^{1}H-NMR: δ_H (300 MHz) ($CDCl_3$): 2.01, 2.05, 2.12, 2.16 [4 X (s, 3H, C(O)$\underline{C}H_3$)], 3.99-4.17 (m, 2H, H^5 & H^6), 4.23-4.33 (m, 1H, H^6), 4.78 (d, 1H, OCH_2, J = 14.0 Hz), 4.85 (s, 1H, OCH_2, J = 14.0 Hz), 5.00 (s, 1H, H^1), 5.24-5.40 (m, 3H, H^2 & H^3 & H^4), 6.71 (s, 1H, CH-isoxazole), 7.47-7.56 (m, 3H, Ar-H) 7.91-8.03 (m, 6H, Ar-H).

The ^{1}H-NMR spectrum shows a series of low intensity peaks consistent with the presence of the *cis* isomer.

^{13}C-NMR: δ_C (75 MHz) ($CDCl_3$): 20.6, 20.7, 20.7, 20.8 (C(O)$\underline{C}H_3$), 60.3 (OCH_2), 62.3 (C^6), 65.9, 68.9, 69.2, 69.3 (C^2-C^5), 97.4 (C^1), 102.0 (CH-isoxazole) 123.0, 123.5, 127.7, 129.2 (Ar-CH), 131.3 (C-1) 153.6, 153.5 (C-4 & C-5) 161.9 (CN-isoxazole) 168.2 (CO-isoxazole), 169.7, 1169.9, 170.0, 170.6 ($\underline{C}$(O)CH_3)

The ^{13}C -NMR shows a series of low intensity peaks consistent with the presence of the *cis* isomer.

m.p. 174-179 ˚C

IR (KBr disc): 3459.1 (C-H), 1721.0 (C=0) 1618.4 (C=C triazole), 1377.9 (C-N), 1209.9 (C-O) cm^{-1}.

HRMS (direct injection) $[M+H]^+$, $[C_{30}H_{32}N_3O_{11}]^+$ calculated: 610.2031, found:610.2041; difference: 1.57 ppm

*Isoxazole linked mannose azobenzene conjugate **218***

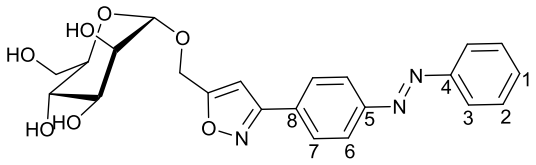

Isoxazole linked protected mannose azobenzene conjugate **217** (108 mg, 0.18 mmol) was added to THF (10ml) followed by methanol (40 mL) and water and (10 mL). Sodium methoxide (catalytic amount) was added, the mixture was then allowed to stir overnight. Acidic Dowex resin was added to adjust the pH to 6. The acidified solution was concentrated until an orange coloured precipitate formed. Following filtration the precipitate was separated from the resin beads by washing with DMF (50 mL). The resulting solution was concentrated under reduced pressure to yield the product as an orange solid 58 mg, 87 %.

^{1}H-NMR: δ_H (500 MHz) (DMSO-d_6): 3.07-3.83 (m, very broad, H^{2-6} & H'^{2-6}), 4.22-4.26 (m, 1H, H'^{1}), 4.41 (d, 1H, H^{1}, J = 8.0 Hz) 4.84 (d, 1H, OCH_2, J = 14.0 Hz) 4.97 (d, 1H, CH_2, J = 14.0 Hz) 7.18 (s, 1H, CH-isoxazole), 7.58-7.65 (m, 3H, Ar-H), 7.93 (d, 2H, Ar-H, J= 6.5 Hz), 8.02 (d, 2H, Ar-H, J = 8.5 Hz) 8.07 (d, 2H, Ar-H, J = 8.5 Hz).

The ^{1}H-NMR spectrum shows a series of low intensity peaks consistent with the presence of the *cis* isomer.

^{13}C-NMR: δ_C (125 MHz) (DMSO-d_6): 60.8, 60.9. 61.2 (OCH2, C^{6} & C'^{6}), 68.6, 71.0, 73.6, 73.7, 75.4, 75.5, 76.0, 81.1 ($^{C2-5}$), 102.5 (CH-isoxazole), 102.7, 104.3 (C^{1} & C'^{2}) 123.2, 123.8, 128.3, 130.0, 132.4 (Ar-H), 152.4, 153.2 (Ar-q), 161.6 (CN-isoxazole), 162.8 (Ar-q), 170.6 (CO-isoxazole).

The ^{13}C -NMR shows a series of low intensity peaks consistent with the presence of the *cis* isomer.

R_f: 0.2 (MeOH

IR (KBr disc): 3390.0 (O-H), 2932.1, 2780.7 (C-H), 1617.5 (C=N), 1430.2 (N=N), 1066.6 (C-O) cm^{-1}

HRMS (direct injection) $[M+H]^+$, $[C_{28}H_{34}N_3O_{12}]^+$ calculated:, found: difference: ppm

*Isoxazole linked lactose azobenzene conjugate **220***

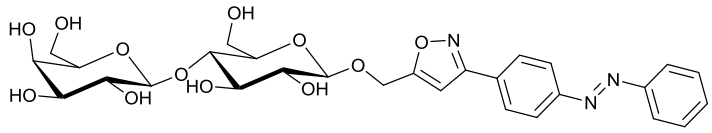

A solution of the propargylated lactose **213** (200 mg, 0.30 mmol) and the chlorooxime **174** (231 mg, 0.89 mmol) in ethyl acetate (15 mL) was heated to reflux. Triethlyamine (0.10 g, 0.1 mmol) in ethyl acetate (1.0 mL) was added dropwise over 4 hours. The reaction mixture was heated to reflux overnight. Further ethyl acetate (20 mL) was added followed by consecutive washing with water (30 mL) and brine (30 mL). The organics were then dried over anhydrous magnesium sulphate and concentrated under vacuum to give the crude product as a sticky orange solid. The crude material was purified by flash chromatography (DCM/MeOH 100:0 > 95:5) to give the adduct as an orange solid which was deprotected without further characterisation.

The protected adduct was added to THF (10 mL) followed by methanol and water (40 mL and 10 mL) in a 100 mL round bottom flask. Sodium methoxide (catalytic amount) was added, the mixture was then allowed to stir overnight. Acidic Dowex resin was added to adjust the pH to 6, whereupon an orange precipitate formed. The resulting mixture was filtered under gravity. The solids comprising of the precipitated product and the resin beads were washed with DMF (50 mL). The resulting solution was concentrated under reduced pressure to yield the product as an orange solid 99 mg, 55 %.

^{1}H-NMR: δ_H (500 MHz) (DMSO-d_6): 3.07-3.83 (m, very broad, $H^{2\text{-}6}$ & $H'^{2\text{-}6}$), 4.22-4.26 (m, 1H, H'^{1}), 4.41 (d, 1H, H^1, J = 8.0 Hz) 4.84 (d, 1H, OCH_2, J = 14.0 Hz) 4.97 (d, 1H, CH_2, J = 14.0 Hz) 7.18 (s, 1H, CH-isoxazole), 7.58-7.65 (m, 3H, Ar-H), 7.93 (d, 2H, Ar-H, J= 6.5 Hz), 8.02 (d, 2H, Ar-H, J = 8.5 Hz) 8.07 (d, 2H, Ar-H, J = 8.5 Hz).

The ^{1}H-NMR spectrum shows a series of low intensity peaks consistent with the presence of the *cis* isomer;

^{13}C-NMR: δ_C (125 MHz) (DMSO-d_6): 60.8, 60.9. 61.2 (OCH2, C^6 & C'^6), 68.6, 71.0, 73.6, 73.7, 75.4, 75.5, 76.0, 81.1 ($^{C2\text{-}5}$), 102.5 (CH-isoxazole), 102.7, 104.3 (C^1 & C'^2) 123.2, 123.8, 128.3, 130.0, 132.4 (Ar-H), 152.4, 153.2 (Ar-q), 161.6 (CN-isoxazole), 162.8 (Ar-q), 170.6 (CO-isoxazole).

The ^{13}C -NMR shows a series of low intensity peaks consistent with the presence of the *cis* isomer

R_f: material failed to move in 100% MeOH

IR (KBr disc): 3402.0 (O-H), 2921.9 (C-H), 1607.3 (C=N), 1431.8 (N=N), 1065.5 (C-O) cm^{-1}

HRMS (direct injection) $[M+Na]^+$, $[C_{28}H_{33}N_3O_{12}Na]^+$ calculated: 626.1956, found: 626.1938; difference: 2.92 ppm

*Divalent isoxazole linked protected galactose azobenzene conjugate **221***

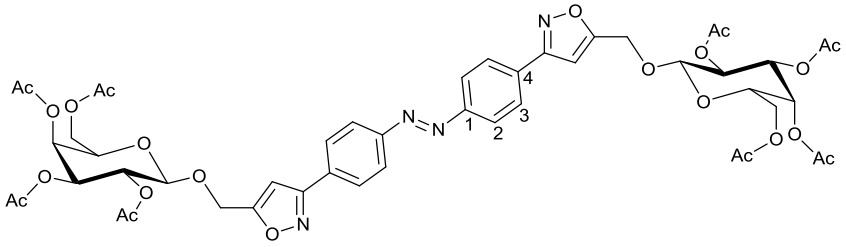

To a solution containing the bis-chlorooxime **176** (135 mg, 0.4 mmol) and the propargylated galactose **209** (308 mg, 0.80 mmol) in ethanol or EtOAc (25 mL) a solution of triethylamine (0.23 mL. 1.6 mmol) in ethanol or EtOAc (0.77 mL) was added over 4 hours. The resulting solution was heated to reflux for 16 hrs. Distilled water (25 mL) was added, followed by extraction with DCM (3 X 25 mL). The combined organic layers were washed with water and brine (25 mL each) and dried over anhydrous Na_2SO_4. Following concentration under vacuum the crude product was isolated as a sticky orange solid (452 mg EtOH; 463 mg EtOAc). The crude material was further purified by flash chromatography (DCM/MeOH, 99:1) to give the desired product as an orange solid; 141 mg 34% EtOH; 285 mg, 69% EtOAc

^{1}H-NMR: δ_H (300 MHz) ($CDCl_3$): 2.00, 2.07, 2.07, 2.18 [4 X (s, 3H, C(O)$\underline{C}H_3$)], 3.98 (t, 1H, H^5, J = 6.5 Hz), 4.13-4.26 (m, 2H, H^6), 4.67 (d, 1H, H^1, J = 8.0 Hz) 4.85 (d, 1H, OCH_2, J = 14.0 Hz), 4.97-50.8 (m, 2H, OCH_2 & H^3), 5.30 (dd, 1H, H^2, J = 8.0, 3.5 Hz), 5.43 (d, 1H, H^4, J = 3.5 Hz) 6.66 (s, 1H, CH-isoxazole), 7.98 (d, 2H, Ar-H J= 9.0 Hz), 8.06 (d, 2H, Ar-H J= 9.0 Hz).

^{13}C-NMR: δ_C (75 MHz) ($CDCl_3$): 20.6, 20.7, 20.7, 20.8 (C(O)$\underline{C}H_3$), 61.3 (C^6), 61.7 (OCH_2), 67.0.0 (C^4), 68.6 (C^2), 70.7 (C^5), 71.1 (C^3), 100.6 (C^1), 101.7 (CH-isoxazole) 123.7, 127.7 (C-2/3), 131.3 (C-4), 153.5 (C-1) 161.8 (CN-isoxazole) 168.9 (CO-isoxazole), 169.5, 170.1, 170.2, 170.4 ($\underline{C}$(O)CH_3).

m.p. 98- 101 ℃

IR (KBr disc): 3132.5, 2980.2 (C-H), 1750.2 (C=0) 1611.4 (C=C triazole), 1433.9 (N=N) 1370.6 (C-N), 1226.8, 1079.7 (C-O) cm^{-1}.

HRMS (direct injection) $[M+H]^+$, $[C_{30}H_{32}N_3O_{11}]^+$ calculated: 1037.3146, found: 1037.3138; difference 0.79 ppm

*Divalent isoxazole linked galactose azobenzene conjugate **222***

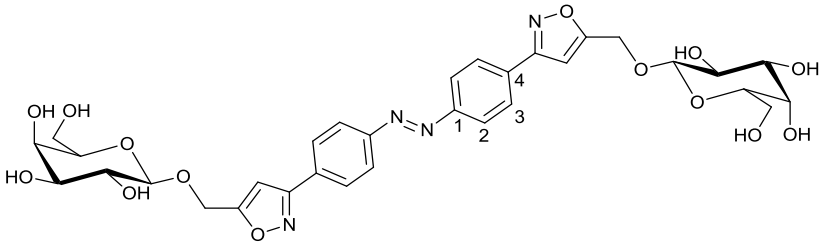

Divalent isoxazole linked protected galactose azobenzene conjugate **221** (104 mg, 0.10 mmol) was added to THF (10 mL) followed by methanol/water (50 mL/10 mL). Sodium methoxide (catalytic amount) was added, the reaction mixture was allowed to stir overnight. Acidic Dowex resin was added to adjust the pH to 6. The resulting mixture was then filtered under gravity. The residue comprising of the precipitated product and the resin beads was washed with DMF (50 mL) the resulting solution was concentrated under reduced pressure to yield the product 38 mg, 56% yield.

^{1}H-NMR: δ_H (500 MHz) (DMSO-d_6 (+ D_2O ex.)): 3.30-3.39 (m, 2H, H^2 & H^3), 3.40-3.46 (m, 1H, H^5) 3.54 (d, 1H, H^6, J = 6.0 Hz) 3.66 (d, 1 H, H^4, J = 2.0 Hz), 4.29 (d, 1H, H^1, J = 7.0 Hz) 4.81 (d, 1H, OCH_2, J = 14.0 Hz) 4.93 (d, 1H, CH_2, J = 14.0 Hz) 7.14 (s, 1H, CH-isoxazole) 8.03 (d, 2H, H-2/3, J = 8.5 Hz) 8.07 (d, 2H, H-2/3, J = 8.5 Hz).

The ^{1}H-NMR spectrum shows a series of low intensity peaks consistent with the presence of the *cis* isomer.

^{13}C-NMR: δ_C (125 MHz) (DMSO-d_6): 60.9 (C^6) 61.0 (OCH_2) 68.5 (C^4), 70.8, 73.5 (C^2 & C^3), 75.7 (C^5) 102.6 (C^1) 103.2 (CH-isoxazole) 128.3 (C-2 & C-3) 131.7 (C-4), 153.1 (C-1), 161.7 (CN-isoxazole), 170.7 (CO-isoxazole).

The ^{13}C -NMR shows a series of low intensity peaks consistent with the presence of the *cis* isomer.

m.p. 184- 206 ℃ (decomposition)

IR (KBr disc): 3391.2 (O-H) 2929.7, 2780.4 (C-H) 1617.0 (C=N), 1430.0 (N=N), 1066.5 (C-O) cm^{-1}

HRMS (direct injection) $[M+H]^+$, $[C_{32}H_{37}N_4O_{14}]^+$ calculated: 701.2301, found: 701.2326; difference: 3.57 ppm

*Divalent isoxazole linked protected mannose azobenzene conjugate **223***

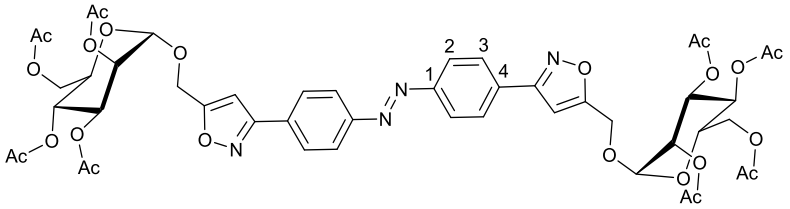

A solution of the propargylated galactose **209** (921 g, 2.4 mmol) and the bis-chlorooxime **176** (0.100 g, 0.3 mmol) in ethyl acetate (20 mL) was heated to reflux. A solution triethylamine (0.045 g, 0.062 mL, 0.45 mmol) in ethyl acetate (0.95 mL) was added dropwise over 4 hours. The reaction mixture was heated to reflux overnight. DCM (50 mL) was added followed by consecutive washing with water (75 mL) and brine (75 mL). The organics were dried over anhydrous magnesium sulphate and concentrated under vacuum to give the crude product as a sticky orange solid (879 mg). The crude material was purified by flash chromatography (DCM/MeOH 100:0 > 98:2) to give the title compound as an orange sticky solid 213 mg, 68 %.

^{1}H-NMR: δ_H (500 MHz) ($CDCl_3$): 2.01, 2.06, 2.12, 2.17 [4 X (s, 3H, C(O)$\underline{C}H_3$)], 4.05-4.10 (m, 1H, H^5), 4.13 (dd, 1H, H6, J =12.5, 2.5 Hz) 4.32 (dd, 1H, H^6, J = 12.5, 5.0 Hz) 4.79 (d, 1H, OCH_2, J = 13.5 Hz), 4.86 (d, 1H, OCH_2, J = 13.5 Hz), 5.01 (s, 1H, H^1), 5.30-5.40 (m, 3H, H^2 & H^3 & H^4) 6.72 (s, 1H, CH-isoxazole), 7.98-8.02 (m, 2H, H-2/3), 8.04-8.7 (m, 2H, H-2/3).

Minor peaks at 6.71 (s), 6.725 (s), 7.95-7.98 (m) 8.31-8.33 (m) 8.44-8.46 (m)

The ^{1}H-NMR spectrum shows a series of low intensity peaks consistent with the presence of the *cis* isomer.

^{13}C-NMR: δ_C (125 MHz) ($CDCl_3$): 20.7, 20.7, 20.8, 20.9 (C(O)$\underline{C}H_3$), 60.3 (OCH_2), 62.3 (C^6), 65.9, 68.8, 69.2, 69.3 (C^2, C^3, C^4, C^5), 97.5 (C^1), 102.0 (CH-isoxazole), 123.7, 127.8 (C-2/3), 131.2 (C-4), 153.9 (C-1) 161.9 (CN-isoxazole) 168.3 (CO-isoxazole), 169.7, 169.9, 170.0, 170.6 ($\underline{C}$(O)CH_3)

The ^{13}C -NMR shows a series of low intensity peaks consistent with the presence of the *cis* isomer.

R.f.: (DCM: MeOH 99:1) 0.35

HRMS (direct injection) $[M+H]^+$, $[C_{48}H_{53}N_4O_{22}]^+$ calculated: 1037.3146, found: 1037.3119; difference: 2.63 ppm

*Divalent isoxazole linked mannose azobenzene conjugate **224***

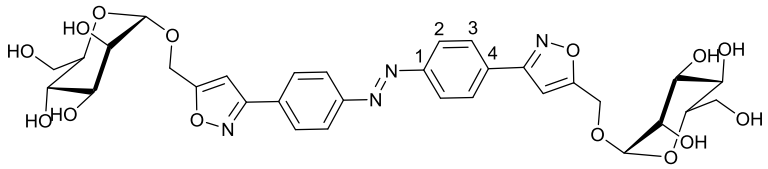

Divalent isoxazole linked protected mannose azobenzene conjugate **223** (103 mg, 0.99 mmol) was added to THF (10 mL) followed by methanol/water (50 mL/10 mL. Sodium methoxide (catalytic amounts) was added, the reaction mixture was allowed to stir overnight. Acidic Dowex resin was added to adjust the pH to 6. The resulting mixture was then filtered under gravity. The residue comprising of the precipitated product and the resin beads was washed with DMF (50 mL) the resulting solution was concentrated under reduced pressure to yield the product a sticky orange solid 57 mg 82%.

^{1}H-NMR: δ_H (500 MHz) (DMSO-d_6): 3.36-3.53 (m, 4H, H^3 H^4, H^5 & H^6), 3.66-3.73 (m, 2H, H^2 & H^6), 4.53 (t, 1H, OH, J = 6.0 Hz), 4.62 (d, 1H, OH, J = 6.5 Hz), 4.72-4.86 (m, 5H, OH x 2, H^1 & OCH_2) 7.23 (s, 1H, CH-isoxazole) 8.07-8.10 (m, 2H, H-2/3) 8.15-8.18 (m, 2H, H-2/3).

Minor peaks at 7.20 (s), 7.25 (s), 8.25-8.27 (m) 8.42-8.44 (m)

The ^{1}H-NMR spectrum shows a series of low intensity peaks consistent with the presence of the *cis* isomer.

^{13}C-NMR: δ_C (125 MHz) (DMSO-d_6): 58.9 (OCH_2), 61.7 (C^6), 67.3, 70.5, 71.3, 75.0 (C^{2-5}) 100.1 (C^1) 102.6 (CH-isoxazole) 124.0, 128.4 (C-2 & C-3) 131.8 (C-4), 153.2 (C-1), 161.7 (CN-isoxazole), 170.6 (CO-isoxazole).

The ^{13}C -NMR shows a series of low intensity peaks consistent with the presence of the *cis* isomer.

R_f: compound does not move in 100% MeOH

IR (KBr disc): 2923.1 (C-H), 1610.9 (C=C isoxazole), 1434.0 (N=N) 1295.6, 1055.0 (C-O) cm^{-1}.

HRMS (direct injection) $[M+Na]^+$, $[C_{32}.H_{36}N_4O_{14}Na]^+$ calculated: 723.212, found: 723.2129; difference 1.24 ppm

3-[[Phenylazo]chloro(hydroxyimino)]benzaldehyde ***225***

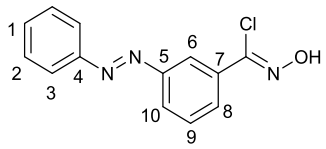

The oxime **111** (1.852 g, 8.22 mmol) was dissolved in DMF (10 mL) and the reaction solution cooled in an ice bath for 5 minutes. Whilst still in the ice bath *N*-chlorosuccinimide (1.65 g, 12.3 mmol) was added portion wise over 1 hr. The solution was stirred at room temperature for 3 hrs. Ice/water (50 mL) was added followed by extraction with diethyl ether (2 x 30 mL). The organics were combined, dried over anhydrous magnesium sulphate and concentrated under vacuum to give the desired product as an orange solid without the need for further purification 1.94 g, 91%.

^{1}H-NMR: δ_H (500 MHz) ($CDCl_3$): 7.49-7.59 (m, 4H, Ar-H), 7.93-8.02 (m, 4H, Ar-H), 8.06 (s, 1H, OH) 8.42 (br s, 1H, H-6)

The ^{1}H-NMR spectrum shows a series of low intensity peaks consistent with the presence of the *cis* isomer.

^{13}C-NMR: δ_C (125 MHz) ($CDCl_3$): 122.0 (C-6), 123.1, 124.7, 129.2, 129.2, 129.3, 131.5 (Ar-CH), 133.6 (C-7), 139.4 (C-Cl), 152.5, 152.6 (C-4 & C-5)

The ^{13}C -NMR shows a series of low intensity peaks consistent with the presence of the *cis* isomer.

m.p.: 172-176 ˚C

IR (KBr disc): 3233.1 (O-H) 3035.9, 2865.7 (C-H), 1613.6 (C=C), 1443.4 (N=N), 998.0 (N-O), 682.5 (C-Cl) cm^{-1}

HRMS (direct injection) $[M+H]^+$, $[C_{13}H_{11}ClN_3O]^+$ calculated: 260.0585, found: 260.0575; difference 4.08 ppm.

Isoxazole linked protected galactose-azobenzene conjugate **226**

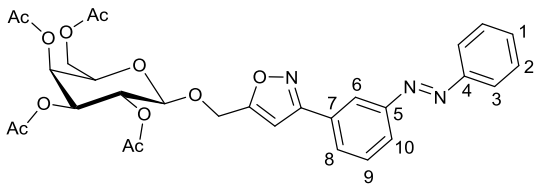

A solution of the propargylated galactose **209** (0.143 g, 0.37 mmol) and the chlorooxime **225** (0.250 g, 1.11 mmol) in ethyl acetate (20 mL) was heated to reflux. Triethylamine (0.131 g, 0.18 mL, 1.3 mmol) in EtOAc (1.0 mL) was added dropwise over 4 hours. The reaction mixture maintained at reflux overnight. Further ethyl acetate (30 mL) was added followed by consecutive washing with water (50 mL) and brine (50 mL). The organics were dried over anhydrous magnesium sulphate and concentrated under vacuum to give the crude product as a sticky orange solid (367 mg). The crude material was purified by flash chromatography (diethyl ether: Pet ether: DCM 1:3:3) to give the title compound as an orange sticky solid 169 mg, 76%.

^{1}H-NMR: δ_H (500 MHz) ($CDCl_3$): 2.00, 2.07, 2.08, 2.18 [4 X (s, 3H, C(O)$\underline{C}H_3$)], 3.98 (app. t, 1H, H^5, J = 6.5 Hz), 4.15-4.24 (m, 2H, H^6), 4.66 (d, 1H, H^1, J = 8.0 Hz) 4.86 (d, 1H, OCH_2, J = 13.5 Hz), 4.99 (d, 1H, OCH_2, J = 13.5 Hz), 5.05 (dd, 1H, H^3, J = 10.5, 3.5 Hz), 5.28 (dd, 1H, H^2, J = 10.5, 8.0 Hz), 5.43 (d, 1H, H^4, J = 3.5 Hz) 6.69 (s, 1H, CH-isoxazole), 7.50-7.57 (m, 3H, Ar-H), 7.64 (t, 1H, Ar-H, J= 7.5 Hz), 7.94-7.97 (m, 3H, Ar-H), 8.03 (d, 1H, Ar-H. J = 8.0 Hz), 8.32 (s, 1H, H-6).

The ^{1}H-NMR spectrum shows a series of low intensity peaks consistent with the presence of the *cis* isomer.

^{13}C-NMR: δ_C (125 MHz) ($CDCl_3$): 20.6, 20.7, 20.7, 20.8 (C(O)$\underline{C}H_3$), 61.3 (C^6), 61.6 (OCH_2), 67.0 (C^4), 68.5 (C^2), 70.7 (C^3), 71.1 (C^5), 100.4 (C^1), 101.8 (CH-isoxazole) 120.9 (C-6) 123.0, 124.9, 129.0, 129.2 (Ar-CH), 129.7 (C-7) 129.9, 131.4 (Ar-CH), 152.5, 153.0 (C-4 & C-5) 162.0 (CN-isoxazole) 168.7 (CO-isoxazole), 169.5, 170.1, 170.2, 170.4 ($\underline{C}(O)CH_3$)

The ^{13}C -NMR shows a series of low intensity peaks consistent with the presence of the *cis* isomer.

m.p. 56-58 ℃

IR (KBr disc): 2973.3 (C-H), 1752.2 (C=0) 1612.5 (C=C isoxazole), 1369.4 (C-N), 1225.1 (C-O) cm^{-1}.

HRMS (direct injection) $[M+H]^+$, $[C_{30}H_{32}N_3O_{11}]^+$ calculated: 610.2031, found:610.2022; difference 1.46 ppm

Isoxazole linked protected mannose-azobenzene conjugate ***228***

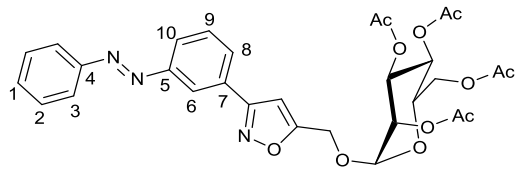

A solution of the propargylated mannose **211** (0.144 g, 0.37 mmol) and the chlorooxime **225** (0.251 g, 1.11 mmol) in ethyl acetate (20 mL) was heated to reflux. Triethylamine (0.132 g, 0.18 mL, 1.3 mmol) was added dropwise over 4 hours. The reaction mixture was maintained at reflux overnight Further ethyl acetate (30 mL) was added followed by consecutive washing with water (50 mL) and brine (50 mL). The organics were dried over anhydrous magnesium sulphate and concentrated under vacuum to give the crude product as a sticky orange solid (349 mg). The crude material was purified by flash chromatography (diethyl ether: Pet ether: DCM 1:3:3) to give the title compound as an orange sticky solid 153 mg, 68 %.

^{1}H-NMR: δ_H (500 MHz) ($CDCl_3$): 2.01, 2.06, 2.12, 2.17 [4 X (s, 3H, C(O)$\underline{C}H_3$)], 4.05-4.14 (m, 2H, H^5 & H^6), 4.33 (dd, 1H, H^6, J = 12.5, 5.0 Hz) 4.79 (d, 1H, OCH_2, J = 13.5 Hz), 4.85 (d, 1H, OCH_2, J = 13.5 Hz), 5.01 (d, 1H, H^1, J = 1.5 Hz), 5.30-5.40 (m, 3H, H^2 & H^3 & H^4) 6.75 (s, 1H, CH-isoxazole), 7.49-7.57 (m, 3H, Ar-H), 7.64 (t, 1H, Ar-H, J = 8.0 Hz), 7.94-7.99 (m, 3H, Ar-H), 8.02 (ddd, 1H, Ar-H. J = 8.0, 2.0, 1.0 Hz), 8.34 (t, 1H, H-6, J = 1.5 Hz).

The ^{1}H-NMR spectrum shows a series of low intensity peaks consistent with the presence of the *cis* isomer.

^{13}C-NMR: δ_C (125 MHz) ($CDCl_3$): 20.7, 20.7, 20.8, 20.9 (C(O)$\underline{C}H_3$), 60.3 (OCH_2), 62.3 (C^6), 65.9, 68.9, 69.2, 69.2 (C^2 & C^3 & C^4 & C^5), 97.4 (C^1), 102.1 (CH-isoxazole) 121.1 (C-6) 123.0, 124.8, 129.0, 129.2 (Ar-CH), 129.7 (C-7) 129.8, 131.4 (Ar-CH), 152.5, 153.0 (C-4 & C-5) 162.1 (CN-isoxazole) 168.2 (CO-isoxazole), 169.7, 169.9, 170.0, 170.6 ($\underline{C}(O)CH_3$)

The ^{13}C -NMR shows a series of low intensity peaks consistent with the presence of the *cis* isomer.

m.p. 57-59 ℃

IR (KBr disc): 2958.8 (C-H), 1751.7 (C=0) 1612.1 (C=C isoxazole), 1370.9 (C-N), 1226.3 (C-O) cm^{-1}.

HRMS (direct injection) $[M+H]^+$, $[C_{30}H_{32}N_3O_{11}]^+$ calculated: 610.2031, found:610.2029; difference 0.45 ppm

*Isoxazole linked mannose-azobenzene conjugate **229***

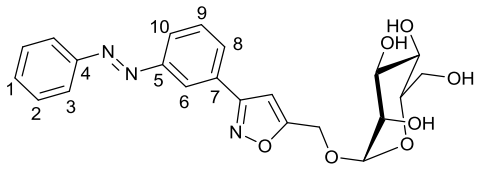

Isoxazole linked protected mannose-azobenzene conjugate **228** (98 mg, 1.61 mmol) in THF/MeOH/H_2O (5 mL : 20 mL : 5 mL) was added sodium methoxide (catalytic amount). The reaction solution was allowed to stir at room temperature overnight. Acidic Dowex resin was added until the solution was pH 8. The resin was filtered off and the solution was concentrated under vacuum until a precipitate formed. The precipitate was filtered and washed with distilled water (50 mL) and dried to give the desired product as an orange solid 54 mg, 76%.

^{1}H-NMR: δ_H (500 MHz) (DMSO-d_6): 3.40-3.62 (m, 4H, H^3, H^4, H^5 & H^6), 3.70- 3.79 (m, 2H, H^2 and H^6) 4.79 (d, 1H, OCH_2, J = 13.5 Hz), 4.85-4.90 (m, 2H, OCH_2 & H^1), 7.31 (s, 1H, CH-isoxazole), 7.62-7.75 (m, 3H, Ar-H), 7.81 (t, 1H, Ar-H, J = 8.0 Hz), 7.99 (d, 2H, Ar-H, J = 6.5 Hz), 8.06 (d, 1H, Ar-H. J = 8.0 Hz), 8.14 (t, 1H, Ar-H, J = 8.0 Hz), 8.41(s, 1H, Ar-H)

The ^{1}H-NMR spectrum shows a series of low intensity peaks consistent with the presence of the *cis* isomer.

^{13}C-NMR: δ_C (125 MHz) (DMSO-d_6): 58.5 (OCH_2), 61.6 (C^6), 67.3, 70.5, 71.3, 74.9 (C^2 & C^3 & C^4 & C^5), 97.4 (C^1), 100.1 (C^1) 102.6 (CH-isoxazole) 120.8, 123.2, 124.6, 129.9, 130.0, 130.9, 132.4 (Ar-CH), 152.3, 152.8 (Ar-q) 161.8 (CN-isoxazole) 170.5 (CO-isoxazole).

The ^{13}C -NMR shows a series of low intensity peaks consistent with the presence of the *cis* isomer.

R.f.: (DCM : MeOH 3:1) 0.42

IR (KBr disc): 3320.7 (O-H), 1611.4 (C=C isoxazole), 1419.9 (N=N), 1060.1 (C-O) cm^{-1}.

HRMS (direct injection) $[M+H]^+$, $[C_{22}H_{24}N_3O_7]^+$ calculated: 442.1609, found: 442.1618; difference 2.15 ppm

3,3'-Azobis[chloro(hydroxyimino)]benzaldehyde ***230***

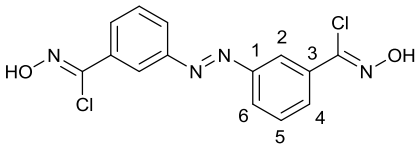

The bis-oxime **112** (2.55 g, 9.5 mmol) was dissolved in DMF (15 mL) and the reaction solution was cooled in an ice bath for 5 minutes. Whilst still in the ice bath *N*-chlorosuccinimide (3.80 g, 28.5 mmol) was added portion wise over 1 hour. The reaction mixture was stirred at room temperature for 3 hours. Ice/water (75 mL) was added followed by extraction with diethyl ether (2 x 50 mL). The organics were combined, dried over anhydrous magnesium sulphate and concentrated under vacuum to give the desired product as an orange solid without the need for further purification 2.98 g, 93%

^{1}H-NMR: δ_H (500 MHz) (DMSO-d_6): 7.74 (app. t, 1H, H-5, J = 8.0 Hz), 8.03 (d, 1H, H-4, J = 8.0 Hz), 8.08 (d, 1H, H-6, J = 8.0 Hz), 8.29 (s, 1H, H-2) 12.65 (s, 1H, OH)*

The ^{1}H-NMR spectrum shows a series of low intensity peaks consistent with the presence of the *cis* isomer.

^{13}C-NMR: δ_C (125 MHz) (DMSO-d_6): 120.4 (C-2), 125.6, 129.9 (C-4 & C-6), 130.7 (C-5), 134.4 (C-3), 135.2 (C-Cl), 152.2 (C-1)

The ^{13}C -NMR shows a series of low intensity peaks consistent with the presence of the *cis* isomer.

m.p.: 202-204 ˚C

IR (KBr disc): 3276.7 (O-H) 3088.8 (C-H), 1631.3(C=C), 1461.4 (N=N), 995.22 (C-O), 683.4 (C-Cl) cm^{-1}

HRMS (direct injection) $[M+H]^+$, $[C_{14}H_{11}Cl_2N_4O_2]^+$ calculated: 337.0254, found: 337.0267; difference 3.84 ppm.

*Divalent isoxazole linked protected galactose azobenzene conjugate **231***

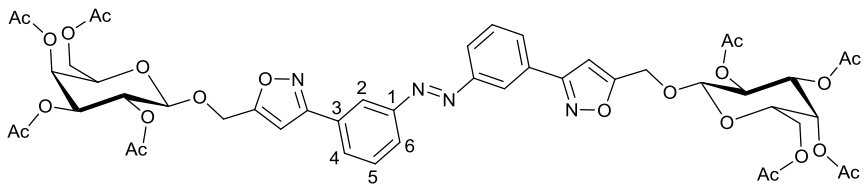

A solution of the propargylated galactose **209** (1.208 g, 3.13 mmol) and the bis-chlorooxime **230** (0.176 g, 0.521 mmol) in ethyl acetate (30 mL) was heated to reflux. Triethlyamine (0.116 g, 0.16 mL, 1.15 mmol) in EtOAc (1.0 mL) was added dropwise over 4 hours. The reaction mixture maintained at reflux overnight. Further ethyl acetate (50 mL) was added followed by consecutive washing with water (75 mL) and brine (75 mL). The organics were dried over anhydrous magnesium sulphate and concentrated under vacuum to give the crude product as a sticky orange solid (1.43 g). Purification by flash chromatography (diethyl ether: Pet ether: DCM 1:1:3) gave the title compound as an orange sticky solid 389 mg, 72 %.

^{1}H-NMR: δ_H (500 MHz) ($CDCl_3$): 1.99, 2.07, 2.08, 2.18 [4 X (s, 3H, C(O)$\underline{C}H_3$)], 3.98 (app. t, 1H, H^5, J = 6.5 Hz), 4.14-4.25 (m, 2H, H^6), 4.67 (d, 1H, H^1, J = 8.0 Hz) 4.87 (d, 1H, OCH_2, J = 14.0 Hz), 5.00 (d, 1H, OCH_2, J = 14.0 Hz), 5.04-5.07 (m, 1H, H^3), 5.30 (dd, 1H, H^2, J = 10.5, 5.0 Hz), 5.43 (d, 1H, H^4, J = 2.5 Hz) 6.70 (s, 1H, CH-isoxazole), 7.66 (t, 1H, H-5, J= 7.5 Hz), 7.98 (d, 1H, H-4/6, J = 7.5 Hz), 8.05 (d, 1H, H-4/6, J = 7.5 Hz), 8.36 (s, 1H, H-2).

The ^{1}H-NMR spectrum shows a series of low intensity peaks consistent with the presence of the *cis* isomer.

^{13}C-NMR: δ_C (125 MHz) ($CDCl_3$): 20.5, 20.6, 20.7, 20.8 (C(O)$\underline{C}H_3$), 61.3 (C^6), 61.6 (OCH_2), 67.0 (C^4), 68.6 (C^2), 70.7 (C^3), 71.1 (C^5), 100.5 (C^1), 101.7 (CH-isoxazole) 121.0 (C-2) 124.9, 129.3 (C-4 & C-6), 129.9 (C-3) 129.9, (C-5), 152.8 (C-1) 161.9 (CN-isoxazole) 168.8 (CO-isoxazole), 169.5, 170.0, 170.2, 170.4 ($\underline{C}$(O)CH_3)

The ^{13}C -NMR shows a series of low intensity peaks consistent with the presence of the *cis* isomer.

m.p. 71-74 ˚C

IR (KBr disc): 2980.5 (C-H), 1751.3 (C=0) 1612.3 (C=C isoxazole), 1423.6 (N=N) 1370.0 (C-N), 1224.6 (C-O) cm^{-1}.

HRMS (direct injection) $[M+H]^+$, $[C_{48}H_{53}N_4O_{22}]^+$ calculated: 1037.3146, found: 1037.3148; difference 0.20 ppm

*Divalent isoxazole linked galactose azobenzene conjugate **232***

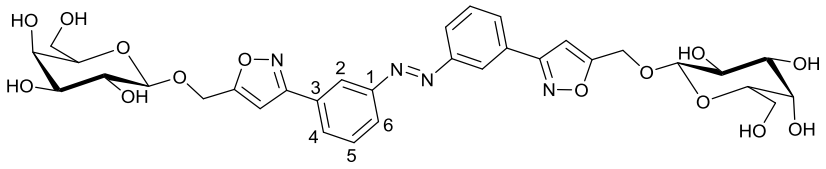

Divalent isoxazole linked protected galactose azobenzene conjugate **231** (264 mg, 0.25 mmol) was added to a THF/MeOH/H_2O mixture (5 mL: 20 mL: 5 mL) followed by sodium methoxide (catalytic amount). The reaction solution was allowed to stir at room temperature for 16 hrs. Acidic Dowex resin was added until the solution was pH 8. The resin was filtered off and the solution was concentrated under vacuum to give the desired product as an orange solid 149 mg, 83%.

^{1}H-NMR: δ_H (500 MHz) (DMSO-d_6): 3.29-3.44 (m, 3H, H^2, H^3 & H^5), 3.52-3.57 (m, 2H, H^6), 4.30 (d, 1H, H^1, J = 7.5 Hz) 4.82 (d, 1H, OCH_2, J = 14.0 Hz), 4.96 (d, 1H, OCH_2, J = 14.0 Hz), 7.25 (s, 1H, CH-isoxazole), 7.80 (t, 1H, H-5, J= 8.0 Hz), 8.07-8.10 (m, 2H, H-4 & H-6), 8.40 (t, 1H, H-2, J = 2.0 Hz).

The ^{1}H-NMR spectrum shows a series of low intensity peaks consistent with the presence of the *cis* isomer.

^{13}C-NMR: δ_C (125 MHz) (DMSO-d_6): 60.8 (C^6), 61.0 (OCH_2), 68.5 (C^4), 70.8, 73.6, 75.8 (C^2, C^3 & C^5), 102.6 (CH-isoxazole), 103.4 (C^1), 120.9 (C-2) 124.9, 130.3 (C-4 & C-6), 130.2 (C-3) 131.1, (C-5), 152.7 (C-1) 161.7 (CN-isoxazole) 170.9 (CO-isoxazole),

The ^{13}C -NMR shows a series of low intensity peaks consistent with the presence of the *cis* isomer.

m.p. 209-211 ˚C

IR (KBr disc): 3380.4 (O-H) 2925.7 (C-H), 1613.8 (C=C isoxazole), 1450.4 (N=N) 1369.5 (C-N), cm^{-1}.

HRMS (direct injection) $[M+Na]^+$, $[C_{32}H_{36}N_4O_{14}Na]^+$ calculated: 723.2120, found: 723.2115; difference: 0.66 ppm

Divalent isoxazole linked protected mannose azobenzene conjugate **233**

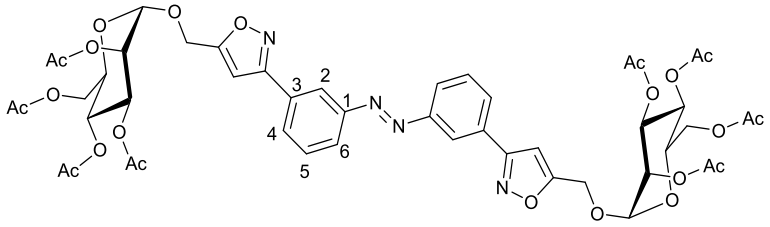

A solution of the propargylated mannose **211** (0.507 g, 1.31 mmol) and the bis-chlorooxime **230** (0.073 g, 0.22 mmol) in ethyl acetate (20 mL) was heated to reflux. Triethlyamine (0.085 g, 0.062 mL, 0.48 mmol) in EtOAc (1.0 mL) was added dropwise over 4 hours. The reaction mixture was maintained at reflux overnight. Further ethyl acetate (30 mL) was added followed by consecutive washing with water (50 mL) and brine (50 mL). The organics were dried over anhydrous magnesium sulphate and concentrated under vacuum to give the crude product as a sticky orange solid (1.43 g). Purification by flash chromatography (diethyl ether: Pet ether: DCM 1:1:3) gave the title compound as an orange sticky solid 169 mg, 74 %.

^{1}H-NMR: δ_H (500 MHz) ($CDCl_3$): 2.01, 2.06, 2.12, 2.17 [4 X (s, 3H, C(O)$\underline{C}H_3$)], 4.03-4.17(m, 2H, H^5 & H^6), 4.32 (dd, 1H, H^6, J = 12.0, 5.0 Hz) 4.80 (d, 1H, OCH_2, J = 13.5 Hz), 4.86 (d, 1H, OCH_2, J = 13.5 Hz), 5.02 (d, 1H, H^1, J = 1.0 Hz), 5.29-5.40 (m, 3H, H^2 & H^3 & H^4) 6.76 (s, 1H, CH-isoxazole), 7.66 (t, 1H, H-6, J = 8.0 Hz), 8.00 (d, 1H, H-4/6, J = 8.0 Hz), 8.06 (d, 1H, H-4/6, J = 8.0 Hz), 8.38 (s, 1H, H-2).

The ^{1}H-NMR spectrum shows a series of low intensity peaks consistent with the presence of the *cis* isomer.

^{13}C-NMR: δ_C (125 MHz) ($CDCl_3$): 20.6, 20.7, 20.7, 20.8 (C(O)$\underline{C}H_3$), 60.2 (OCH_2), 62.3 (C^6), 65.9, 68.9, 69.2, 69.3 (C^2, C^3, C^4, C^5), 97.4 (C^1), 102.1 (CH-isoxazole) 121.2 (C-2) 124.9, 129.4 (C-4/6), 129.8 (C-3) 129.9 (C-5), 152.8 (C-1) 162.0 (CN-isoxazole) 168.2 (CO-isoxazole), 169.7, 169.8, 169.9, 170.6 ($\underline{C}$(O)CH_3)

The ^{13}C -NMR shows a series of low intensity peaks consistent with the presence of the *cis* isomer.

m.p. 64-67 ˚C

IR (KBr disc): 2958.8 (C-H), 1751.8 (C=0) 1613.3 (C=C isoxaozle), 1423.3 (N=N) 1371.6 (C-N), 1226.8 (C-O) cm^{-1}.

HRMS (direct injection) $[M+H]^+$, $[C_{48}H_{53}N_4O_{22}]^+$ calculated: 1037.3146, found: 1037.3195; difference 4.70 ppm.

*Divalent isoxazole linked mannose azobenzene conjugate **234***

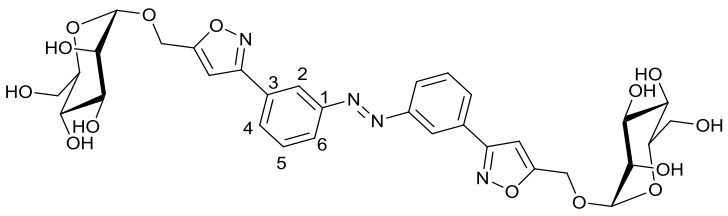

Divalent isoxazole linked protected mannose azobenzene conjugate **233** (188 mg, 0.18 mmol) was added to a THF/MeOH/H_2O mixture (5 mL: 20 mL: 5 mL) followed by sodium methoxide (catalytic amount). The reaction solution was allowed to stir at room temperature for 16 hrs. Acidic Dowex resin was added until the solution was pH 8. The resin was filtered off and the solution was concentrated under vacuum to give the desired product as an orange solid 103 mg, 81%.

^{1}H-NMR: δ_H (500 MHz) (DMSO-d_6): 3.38-3.452 (m, 4H, H^2, H^3, H^4 & H^6), 3.66-3.70 (m, 2H, H^5 & H^6), 4.82 (d, 1H, OCH_2, J = 13.5 Hz), 4.80 (d, 1H, H^1, J = 1.5 Hz), 4.83 (d, 1H, OCH_2, J = 13.5 Hz), 7.25 (s, 1H, CH-isoxazole), 7.80 (t, 1H, H-5, J= 7.5 Hz), 8.07-8.13 (m, 2H, H-4 & H-6), 8.42 (t, 1H, H-2, J = 1.5 Hz).

The ^{1}H-NMR spectrum shows a series of low intensity peaks consistent with the presence of the *cis* isomer.

^{13}C-NMR: δ_C (125 MHz) (DMSO-d_6): 58.9 (OCH_2), 61.5 (C^6), 67.2 70.4, 71.1, 74.9 (C^2, C^3 C^4 & C^5), 100.0 (C^1), 102.6 (CH-isoxazole), 121.0 (C-2) 124.8, 130.2 (C-4 & C-6), 130.2 (C-3) 131.0, (C-5), 152.7 (C-1) 161.8 (CN-isoxazole) 170.5 (CO-isoxazole),

The ^{13}C -NMR shows a series of low intensity peaks consistent with the presence of the *cis* isomer.

m.p. 159-163 ˚C

IR (KBr disc): 3380.4 (O-H) 2925.7 (C-H), 1617.1 (C=C isoxazole), 1422.4 (N=N) 1385.5 (C-N), cm^{-1}.

HRMS (direct injection) $[M+H]^+$, $[C_{32}H_{36}N_4O_{14}]^+$ calculated: 723.2120, found: 723.2116; difference 0.57 ppm

*Triazole linked protected galactose azobenzene conjugate **235***

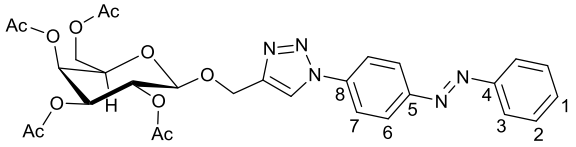

To a solution of the propargylated galactose **209** (347 mg, 0.90 mmol) and the 4-azido azobenzene **171** (200 mg, 0.90 mmol) in DMSO (30 mL), copper sulphate pentahydrate (90 mg, 0.36 mmol) and sodium ascorbate (72 mg, 0.36 mmol) were added, followed by water (10 mL). The reaction mixture was allowed to stir overnight at room temperature. Distilled water (100 mL) was added, followed by extraction with DCM (2 x 50 mL). The organics were combined, washed consecutively with water (2 x 100 mL) and brine (100 mL), followed by concentration under vacuum to give the crude product as an orange sticky solid (484 mg). Purification by flash chromatography (DCM: MeOH 100:0 to 98:2) gave the product as an orange foam 458 mg, 83%

^{1}H-NMR: δ_H (500 MHz) ($CDCl_3$): 1.99, 2.02, 2.06, 2.17 [4 X (s, 3H, C(O)CH_3)], 3.99 (t, 1H, H^5, J = 6.5 Hz), 4.15-4.24 (m, 2H, H^6), 4.73 (d, 1H, H^1, J = 8.0 Hz) 4.93 (d, 1H, OCH_2, J = 13.0 Hz), 5.04 2-5.10 (m, 2H, H^3 + OCH_2), 5.25-5.30 (m, 1H, H^2) 5.43 (d, 1H, H^4, J = 3.0 Hz) 7.51-7.57 (m, 3H, H-1 & H-2), 7.92 (d, 2H, H-6/7, J = 9.0 Hz) 7.96 (dd, 2H, H-3, J = 8.0, 1.5 Hz), 8.06 (s, 1H, CH-triazole), 8.10 (d, 2H, H-6/7, J = 9.0 Hz).

The ^{1}H-NMR spectrum shows a series of low intensity peaks consistent with the presence of the *cis* isomer.

^{13}C-NMR: δ_C (125 MHz) ($CDCl_3$): 20.6, 20.7, 20.7, 20.8 [4 x (C(O)$\underline{C}H_3$)], 61.4 (C^6), 63.0 (OCH_2), 67.1 (C^4), 68.8 (C^2), 70.8 (C^3), 71.0 (C^5), 100.7 (C^1), 120.8 (CH-triazole), 120.9 (C-6/7), 123.1 (C-3), 124.4 (C-6/7), 129.2 (C-2), 131.6 (C-1), 138.3 (C-5/8), 145.4 (q-triazole) 152.3, 152.5 (C-5/8 & C-4), 169.6, 170.1, 170.2, 170.4 [4 x ($\underline{C}$(O)CH_3)]

The ^{13}C -NMR shows a series of low intensity peaks consistent with the presence of the *cis* isomer.

m.p.: 65-69 ˚C.

IR (KBr disc): 2938.7 (C-H), 1750.3 (C=0) 1603.3 (C=C), 1509.5 (N=N), 1370.9 (C-N), 1228.1 (C-O) cm^{-1}.

HRMS (direct injection) $[M+H]^+$, $[C_{29}H_{32}N_5O_{10}]^+$ calculated: 610.2144; found: 610.2164; Difference: 3.35 ppm.

*Triazole linked galactose azobenzene conjugate **236***

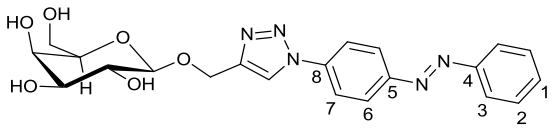

The triazole linked protected galactose azobenzene conjugate **235** (396 mg, 0.64 mmol) was dissolved in a THF/MeOH/H_2O mixture (10 mL:30 mL:10 mL), sodium methoxide (catalytic amount) was added and the resulting solution was left to stir over night at room temperature. Acidic Dowex resin was used to neutralise the solution to pH 7. The resin was removed by filtration and the solution was concentrated under vacuum until a precipitate formed. The precipitate was filtered and washed with distilled water (100 mL) to give the product as an orange solid, 247 mg 86%.

^{1}H-NMR: δ_H (500 MHz) ($CDCl_3$): 3.30-3.39 (m, 2H, H^2 & H^3), 3.44 (t, 1H, H^5, J = 6.0 Hz), 3.56-3.69 (Br H2O peak containing H^4 & H^6 (d, 1H, H^6, J = 6.0 Hz) 4.30 (d, 1H, H^1, J = 7.5 Hz), 4.77 (d, 1H, OCH_2, J = 12.5 Hz) 4.95 (d, 1H, OCH_2, J = 12. 5 Hz) 7.59-7.65 (m, 3H, H-1 & H-2), 7.94 (dd, 2H, H-3, J = 8.0, 2.0 Hz) 8.11 (d, 2H, H-6/7, J = 9.0 Hz), 8.15 (d, 2H, H-6/7, J = 9.0 Hz), 8.96 (s, 1H, CH-triazole).

^{13}C-NMR: δ_C (125 MHz) ($CDCl_3$): 61.0 (C^6), 61.8 (OCH_2), 68.6 (C^4), 70.9 73.7 (C^2 & C^3), 75.8 (C^5) 103.4 (C^1) 121.2 (C-6/7), 123.2, 123.2 (C-3 and CH-triazole), 124.6 (C-6/7), 130.0 (C-2), 132.4 (C-1), 138.8 (C-5/8), 146.0 (q-triazole) 151.7 (C-5/8), 152.3 (C-4).

m.p.: 211-214 ˚C.

IR (KBr disc): 3350.2(C-H), 2929.4 (C-H), 1597.0 (C=C), 1510.7 (N=N), 1383.7 (C-N), 1235.1, 1064.4 (C-O) cm^{-1}.

HRMS (direct injection) $[M+H]^+$, $[C_{21}H_{24}N_5O_6]^+$ calculated: 442.1721; found: 442.1735. Difference: 3.20 ppm.

*Triazole linked mannose azobenzene conjugate **238***

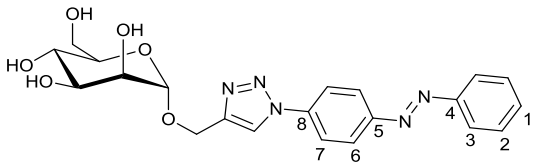

To a solution of the propargylated mannose **211** (0.250g, 0.65 mmol) and the 4-azidoazobenzene **171** (0.072 g, 0.32 mmol) in DMSO (30 mL), copper sulphate pentahydrate (95 mg, 0.38 mmol) and sodium ascorbate (76mg, 0.38 mmol) were added, followed by water (10 mL). The reaction mixture was allowed to stir overnight at room temperature. Distilled water (100 mL) was added, followed by extraction with DCM (2 x 50 mL). The organics were combined, washed consecutively with water (2 x 100 mL) and brine (100 mL), followed by concentration under vacuum to give the crude product as an orange sticky solid (319 mg). The crude material was incompletely purified by flash chromatography (DCM: MeOH 100:0 to 98:2). The resulting material was dissolved in a THF/MeOH/H_2O mixture (10 mL: 30 mL: 10 mL), sodium methoxide was added (catalytic amounts) and the resulting solution was left to stir over night at room temperature. Acidic Dowex resin was used to neutralise the solution to pH 7. The resin was removed by filtration and the solution was concentrated under vacuum until a precipitate formed. The precipitate was filtered and washed with distilled water (100 mL) to give the product as an orange solid, 117 mg, 80%.

^{1}H-NMR: δ_H (500 MHz) (DMSO-d_6): 3.43-3.56 (m, 2H, H^2 + H^5) 3.50-3.55 (m, 2H, H^4 + H^6), 3.66 (br s, 1H, H^3), 3.72 (d, 1H, H^6, J = 1.5 Hz) 4.66 (d, 2H, OCH_2, J = 11.0) 4.81 (d, 1H, OCH_2, J = 11.0 Hz), 4.82 (s, 1H, H^1) 7.55-7.62 (m, 3H, H-1 & H-2), 7.89 (d, 2H, H-3, J = 7.5 Hz) 8.06 (d, 2H, H-6/7, J = 9.0 Hz), 8.11 (d, 2H, H-6/7, J = 9.0 Hz), 8.88 (s, 1H, CH-triazole).

Minor peaks at 8.72 (s), 8.83 (s), 8.90 (s).

The ^{1}H-NMR spectrum shows a series of low intensity peaks consistent with the presence of the *cis* isomer.

^{13}C-NMR: δ_C (125 MHz) (DMSO-d_6): 59.5 (OCH_2), 61.6 (C^6), 67.3 (C^5), 70.5 (C^4), 71.2 (C^3) 74.5 (C^2), 99.7 (C^1) 121.3 (C-6/7), 123.1 (C-3), 124.6 (C-6/7), 130.0 (C-2), 132.4 (C-1), 138.6 (C-5/8), 145.5 (q-triazole) 151.7 (C-5/8), 152.3 (C-4).

The ^{13}C -NMR shows a series of low intensity peaks consistent with the presence of the *cis* isomer.

m.p. 58-61 ˚C

IR (KBr disc): 3380.6 (O-H), 2925.86 (C-H), 1448.6 (N=N), 1042.3 (C-O) cm^{-1}

HRMS (direct injection) $[M+H]^+$, $[C_{21}H_{24}N_5O_6]^+$ calculated: 442.1721, found: 442.1739; difference: 3.99 ppm

*Divalent isoxazole linked protected helicid-azobenzene conjugate **242***

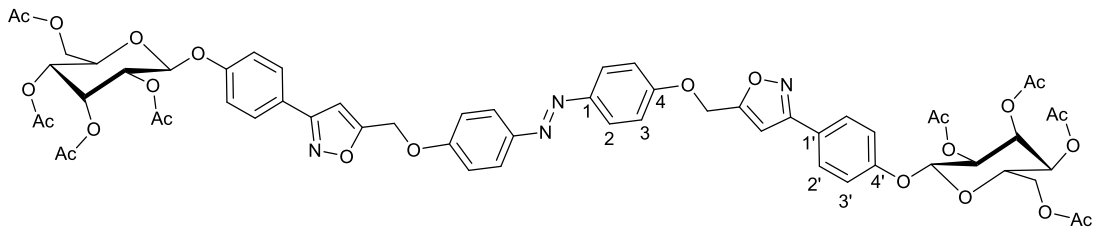

The propargylated azobenzene **113** (50 mg, 0.17 mmol) was dissolved in ethanol (5 mL) and the solution heated to reflux. Separately, the helicid oxime **241** (0.160, 0.34 mmol) and Ch-T (93 mg, 0.41 mmol) were added to ethanol (5 mL). After mixing for 10 minutes the solution was added dropwise to the refluxing azobenzene solution. After 90 minutes, a second freshly premixed solution of the oxime **241** (0.160, 0.34 mmol) and Ch-T (93 mg, 0.41 mmol) was added dropwise to the reaction mixture. The addition was repeated twice more on the same scale at 90 minutes intervals. The reaction mixture was heated to reflux overnight. It was then concentrated under vacuum before being dissolved in DCM (50 mL). The organics were washed with water (25 mL) aqueous NaOH (5% w/v, 25 mL) and brine (25 mL). the organics were dried over anhydrous magnesium sulphate, followed by concertation under vacuum to give the crude product (582 mg). Purification by flash chromatography (pet ether: EtOAc 3:1) gave the desired product as a yellow solid (124 mg, 59%)

^{1}H-NMR: δ_H (500 MHz) ($CDCl_3$): 2.03, 2.06, 2.09, 2.17 (s, 3H, C(O)C$\underline{H}_3$), 4.23-4.29 (m, 3H, H^5 & H^6) 5.06 (dd, 1H, H^4, J = 9.5, 3.0 Hz) 5.18 (dd, 1H, H^2, J = 8.0, 3.0 Hz) 5.29 (s, 2H, OCH_2) 5.42 (d, 1H, H^1, J = 8.0 Hz) 5.76 (app. t, 1H, H^3, J = 3.0 Hz) 6.64 (s, 1H, isoxazole-CH) 7.07-7.13(m, 4H, H-3' & H-2/3) 7.77 (d, 2H, H-2', J = 9.0 Hz) 7.91 (d, 2H, H-2/3, J = 9.0 Hz).

The ^{1}H-NMR spectrum shows a series of low intensity peaks consistent with the presence of the *cis* isomer.

^{13}C-NMR: δ_C (125 MHz) ($CDCl_3$): 20.5, 20.6 20.7 20.8 ($\underline{C}H_3C(O)$), 61.7 (OCH_2), 62.3 (C^6), 66.2 (C^4), 68.4 (C^3), 68.8 (C^2), 70.6 (C^5), 96.9 (C^1), 101.4 (isoxazole-CH), 115.1, 117.3 (Ar-CH), 123.6 (C-1') 124.6 128.3 (Ar-CH), 147.8 (C-1) 158.4 (C-4') 159.7 (C-4) 161.9 (isoxazole-CN) 168.0 (isoxazole-CO) 169.1, 169.1, 169.7, 170.7 ($\underline{C}(O)CH_3$)

The ^{13}C -NMR shows a series of low intensity peaks consistent with the presence of the *cis* isomer.

R.f.: (DCM) 0.38

IR (ATR): 1744.9 (C=O), 1616.6, 1582.6 (C=C), 1530.0 (N=N), 1370.8 (C-N), 1223.2, 1023.8, 1003.4 (C-O) cm^{-1}.

HRMS (direct injection) $[M+H]^+$, $[C_{60}H_{60}N_4O_{24}Na]^+$ calculated: 1243.3490; found: 1243.3496. Difference: 0.47 ppm.

*Divalent isoxazole linked helicid-azobenzene conjugate **243***

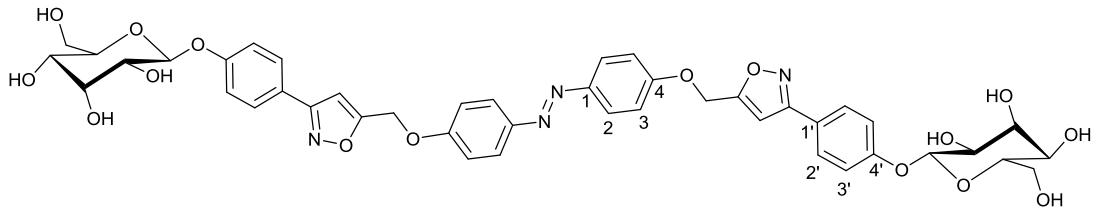

Divalent isoxazole linked protected helicid-azobenzene conjugate **242** (63 mg, 0.052 mmol) was dissolved in THF (10 mL) followed by addition of MeOH (40 mL) and distilled water (10 mL). Catalytic amounts of NaOMe were added and the mixture was left to stir at room temperature overnight. Acidic Dowex resin was added until the reaction mixture reached pH ~5. The solids were then separated by filtration and were washed with aqueous methanol (1:1, 25 mL). The product was then washed away from the resin with DMF (50 mL). The solvent was removed under vacuum to give the desired product as a yellow solid (44 mg, 95%)

^{1}H-NMR: δ_H (500 MHz) (DMSO-d_6): 3.40-3.53 (v. br. m, H_2O & OH, H^2 & H^3 & H^6), 3.65-3.70 (m, 1H, H^6), 3.71-3.76 (m, 1H, H^5), 3.95 (t, 1H, H4, J = 3.0 Hz), 5.20 (d, 1H, H^1, J = 8.0 Hz), 7.14 (d, 2H, H-3', J = 9.0 Hz), 7.17 (s, 1H, isoxazole-CH), 7.27 (d, 2H, H-2/3, J = 9.0 Hz) 7.83 (d, 2H, H-2', J = 9.0 Hz) 7.88 (d, 2H, H-2/3, J = 9.0 Hz)

^{13}C-NMR: δ_C (125 MHz) (DMSO-d_6): 61.1, 61.3 (OCH_2 & C^6), 67.4, 70.6 (C^2 & C^3), 71.8 (C^4), 75.1 (C^5), 98.7 (C-1), 102.9 (isoxazole-CH), 115.9 (C-2/3), 117.1 (C-3'), 122.1 (C-1'), 124.7 (C-2/3), 128.6 (C-2'), 147.2 (C-1) 159.6 (C-4') 160.2 (C-4) 162.0 (isoxazole-CN) 168.3 (isoxazole-CO)

R.f.: (DCM: MeOH 4:1) 0.31

IR (ATR): 1623.6, 1576.6 (C=C), 1499.7 (N=N), 1378.0 (C-N), 1224.4, 1014.8, (C-O) cm^{-1}.

HRMS (direct injection) $[M+H]^+$, $[C_{44}H_{45}N_4O_{16}]^+$ calculated: 885.2825; found: 885.2871. Difference: 5.15 ppm.

*Divalent isoxazole linked protected galactose-azobenzene conjugate **254***

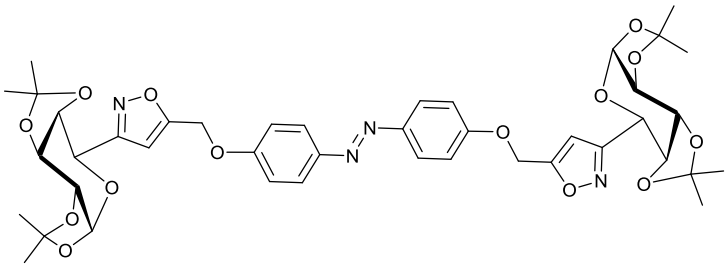

The chlorooxime **253** (1.019 g, 3.31 mmol) and the propargylated azobenzene **113** (0.246 g, 0.85 mmol) were dissolved in EtOAc (30 mL). Triethylamine (0.338 g, 3.34 mmol) in EtOAc (1 mL) was added over four hours with a syringe pump. The reaction mixture was heated to reflux for 16 hours. The organics were washed with water and brine (50 mL each), followed by drying over anhydrous magnesium sulphate and finally concentration under vacuum to give the crude product a sticky yellow solid (1.399 g). Despite several attempts at purification by flash chromatography (**1:** DCM: MeOH 99:1; **2:** EtOAc: pet. ether 1:3; **3**: EtOAc: cyclohexane: pet ether 1:1:2) the desired product could not be isolated.

*Triazole linked protected galactose-azobenzene conjugate **257***

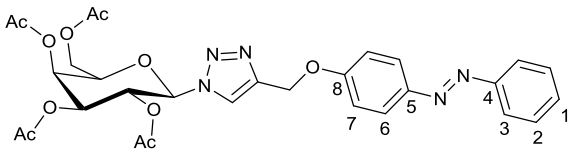

The galactose azide **255** (408 mg, 1.10 mmol) and the propargylated azobenzene **107** (1.5 eq., 387 mg, 1.65 mmol) were added to DMSO (30 mL) with vigorous stirring. Distilled water (10 mL) was added followed by copper sulphate pentahydrate (110 mg, 0.88 mmol) and sodium ascorbate (90 mg, 0.88 mmol). The reaction solution was stirred at room temperature overnight. DCM (80 mL) was added, followed by washing with distilled water (100 mL) and brine (100 mL). The organics were dried over anhydrous magnesium sulphate and concentrated under vacuum to give the crude product as a sticky orange solid (743 mg). Purification by flash chromatography (SiO_2, DCM: MeOH 99:1) gave the title compound as an orange foam, 519 mg, 0.85 mmol, 77%.

^{1}H-NMR: δ_H (500 MHz) ($CDCl_3$): 1.86, 2.01, 2.05, 2.22 [4 X (s, 3H, C(O)CH_3)], 4.13-4.25 (m, 3H, H^5 + H^6), 5.21 (dd, 1H, H^3, J = 3.5 Hz, 10.0 Hz) 5.31 (s, 2H, OCH_2), 5.52-5.59 (m, 2H, H^2 + H^4) 5.82 (d, 1H, H^1, J = 9.0 Hz) 7.12 (d, 2H, H-7, J = 9.0 Hz), 7.44 (t, 1H, H-1, J = 7.5 Hz) 7.50 (t, 2H, H-2, J = 7.5 Hz), 7.88 (d, 2H, H-3, J = 7.5 Hz), 7.91-7.96 (m, 3H, H-6 + C-H triazole.

^{13}C-NMR: δ_C (125 MHz) ($CDCl_3$): 20.2, 20.5, 20.6, 20.7 [4 x (C(O)$\underline{C}H_3$)], 61.2 (C^6), 62.0 (OCH_2), 66.9, 67.9 (C^2 + C^4), 70.8 (C^3), 74.19 (C^5) 86.4 (C^1) 115.1 (C-7), 121.3 (C-H triazole), 122.6 (C-3), 124.8 (C-6), 129.0 (C-2), 130.5 (C-1), 144.5 (q-triazole) 147.4 (C-5) 152.8 (C-4) 160.5 (C-8) 169.1, 169.8, 169.9, 170.3 [4 x ($\underline{C}$(O)CH_3)]

m.p.: 64-67 ˚C.

IR (KBr disc): 2973.3 (C-H), 1754.1 (C=0) 1600.4 (C=C), 1583.6 (C=C triazole), 1500.0 (N=N), 1370.9 (C-N), 1234.6 (C-O) cm^{-1}.

HRMS (direct injection) $[M+H]^+$, $[C_{29}H_{32}N_5O_{10}]^+$ calculated: 610.2144; found: 610.2160. Difference 2.63 ppm.

*Triazole linked galactose-azobenzene conjugate **258***

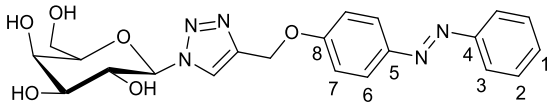

The triazole linked protected galactose-azobenzene conjugate 257 (478 mg, 0.78 mmol) was dissolved in THF (10 mL). MeOH (30 mL), distilled water (10 mL) and sodium methoxide (cat.) were added sequentially. The reaction mixture was stirred overnight at room temperature. Acidic Dowex resin was added until pH 8 was reached. The resin was filtered off and the solvent removed under vacuum to give the product as an orange solid, 318 mg, 0.72 mmol, 92%.

^{1}H-NMR: δ_H (500 MHz) (DMSO-d_6): 3.46-3.59 (m, 3H, H^5 + 2xH^6) 3.71-3.79 (m, 2H, H^3 + H^4), 4.04 (t, 1H, H^2, J = 9.5 Hz), 5.28 (s, 2H, OCH_2) 5.51 (d, 1H, H^1, J = 9.0 Hz,), 7.26 (d, 2H, H-7, J = 9.0 Hz), 7.52 (t, 1H, H-1, J = 7.0 Hz) 7.57 (t, 2H, H-2, J = 7.0 Hz), 7.84 (d, 2H, H-3, J = 7.5 Hz), 7.90 (d, 2H, H-6, J = 9.0 Hz), 8.42 (s, 1H, CH-triazole).

^{13}C-NMR: δ_C (125 MHz) (DMSO-d_6): 60.8 (C^6), 61.7 (OCH_2), 68.8 (C^4), 69.7 (C^2), 73.9 (C^3) 78.7 (C^5), 88.5 (C^1) 115.8 (C-7), 122.7 (C-3), 124.3 (C-H triazole), 125.1 (C-6), 129.9 (C-2), 131.4 (C-1), 142.8 (q-triazole) 146.8 (C-5) 152.4 (C-4) 161.2 (C-8).

The ^{13}C -NMR shows a series of low intensity peaks consistent with the presence of the *cis* isomer.

m.p.: 141-143 ˚C.

IR (KBr disc): 3393.2 (O-H), 2916.9 (C-H), 1600.5 (C=C triazole), 1500.2 (N=N), 1372.7 (C-N), 1249.6 (C-O) cm^{-1}.

HRMS (direct injection) $[M+H]^+$, $[C_{21}H_{24}N_5O_6]^+$ calculated: 442.1721; found: 442.1728. Difference 1.54 ppm.

*Triazole linked protected mannose-azobenzene conjugate **259***

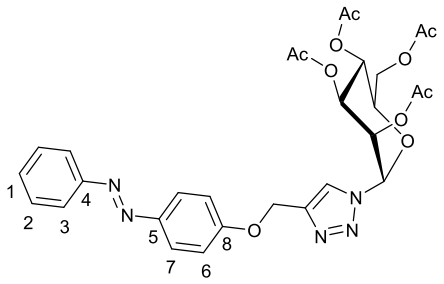

The mannose azide **256** (359 mg, 0.96 mmol) and the propargylated azobenzene **107** (1.5 eq., 342 mg, 1.44 mmol) were added to DMSO (30 mL) with vigorous stirring. Distilled water (10 mL) was added followed by copper sulphate pentahydrate (96 mg, 0.77 mmol) and sodium ascorbate (76 mg, 0.77 mmol). The reaction solution was stirred at room temperature overnight. DCM (80 mL) was added, followed by washing with distilled water (100 mL) and brine (100 mL). The organics were dried over anhydrous magnesium sulphate and concentrated under vacuum to give the crude product (761 mg). Purification by flash chromatography (SiO_2, DCM: MeOH 99:1) gave the title compound as an orange solid, 496 mg, 84%.

^{1}H-NMR: δ_H (500 MHz) ($CDCl_3$): 2.05-2.08 (s, 9H, 3 X C(O)$\underline{C}H_3$) 2.17 (s, 3H, C(O)$\underline{C}H_3$), 3.90-3.95 (m, 1H, H^5), 4.07 (dd, 1H, H^6, J = 2.5 Hz, 12.5 Hz), 4.07 (dd, 1H, H^6, J = 5.5 Hz, 12.5 Hz), 5.33-5.39 (m, 3H, H^4 + OCH_2), 5.91 (dd, 1H, H^3, J = 3.5 Hz, 8.5 Hz), 5.98 (t, 1H, H^2, J = 3.5 Hz), 6.03 (d, 1H, H^1, J = 3.5 Hz,), 7.12 (d, 2H, H-7, J = 9.0 Hz), 7.44 (t, 1H, H-1, J = 7.0 Hz) 7.50 (t, 2H, H-2, J = 7.0 Hz), 7.85 (s, 1H, CH-triazole), 7.88 (d, 2H, H-3, J = 7.5 Hz), 7.94 (d, 2H, H-6, J = 9.0 Hz).

The ^{1}H-NMR spectrum shows a series of low intensity peaks consistent with the presence of the *cis* isomer.

^{13}C-NMR: δ_C (125 MHz) ($CDCl_3$): 20.6, 20.7, 20.7, 20.7 [4 X (C(O)$\underline{\mathbf{C}}H_3$)] 61.5 ($C^6$), 62.1 ($OCH_2$), 66.1 ($C^4$), 68.3 ($C^2$), 68.7 ($C^3$) 72.4 ($C^5$), 83.6 ($C^1$) 115.0 (C-7), 122.6 (C-3), 123.1 (CH-triazole), 124.8 (C-6), 129.1 (C-2), 130.5 (C-1), 144.6 (q-triazole) 147.5 (C-5) 152.7 (C-4) 160.4 (C-8) 169.3, 169.6, 169.6, 170.5 [4 X ($\underline{\mathbf{C}}$(O)CH_3)]

The ^{13}C -NMR shows a series of low intensity peaks consistent with the presence of the *cis* isomer.

m.p.: 62-64 ˚C.

IR (KBr disc): 2990.2 (C-H), 1752.6 (C=0) 1600.4 (C=C triazole), 1500.4 (N=N), 1370.8 (C-N), 1240.3 (C-O) cm^{-1}.

HRMS (direct injection) $[M+H]^+$, $[C_{29}H_{32}N_5O_{10}]^+$ calculated: 610.2144; found: 610.2160. Difference 2.66 ppm.

*Triazole linked mannose-azobenzene conjugate **260***

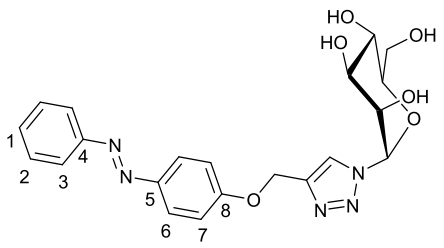

The triazole linked protected mannose-azobenzene conjugate **259** (487 mg, 0.80 mmol) was dissolved in THF (10mL). MeOH (30 mL), distilled water (10 mL) and sodium methoxide (catalytic amounts) were added sequentially. The reaction mixture was stirred overnight at room temperature. Acidic Dowex resin was added until the pH remained acidic. The resin was filtered off and the solvent removed under vacuum to give the product an orange solid which required no further purification, 314 mg, 89%.

^{1}H-NMR: δ_H (500 MHz) (DMSO-d_6): 3.30-3.35 (s, 1H, H^5) 3.56-3.63 (m, 3H, H^4 + H^6), 3.86 (dd, 1H, H^3, J = 3.5 Hz, 7.5 Hz) 5.28 (t, 1H, H^2, J = 3.5 Hz), 5.27 (s, 2H, OCH_2) 5.93 (d, 1H, H^1, J = 4.0 Hz,), 7.23 (d, 2H, H-7, J = 9.0 Hz), 7.51 (t, 1H, H-1, J = 7.0 Hz) 7.56 (t, 2H, H-2, J = 7.0 Hz), 7.82 (d, 2H, H-3, J = 7.5 Hz), 7.89 (d, 2H, H-6, J = 9.0 Hz), 8.36 (s, 1H, C-H triazole).

^{13}C-NMR: δ_C (125 MHz) (DMSO-d_6): 60.8 (C^6), 61.6 (OCH_2), 66.7 (C^4), 68.3 (C^2), 71.2 (C^3) 78.4 (C^5), 86.2 (C^1) 115.9 (C-7), 122.7 (C-3), 125.0 (C-6) 125.1 (C-H triazole), 129.9 (C-2), 131.5 (C-1), 142.9 (q-triazole) 146.8 (C-5) 152.4 (C-4) 161.1 (C-8)

(The ^{13}C -NMR shows low intensity peaks for the *cis* isomer)

m.p.: 135-138 ˚C.

IR (KBr disc): 3401.7.2 (O-H), 1606.3 (C=C triazole), 1502.8 (N=N), 1253.3 (C-O) cm^{-1}.

HRMS (direct injection) $[M+H]^+$, $[C_{21}H_{24}N_5O_6]^+$ calculated: 442.1721; found: 442.1725. Difference 0.88 ppm.

*Divalent triazole linked protected galactose-azobenzene conjugate **261***

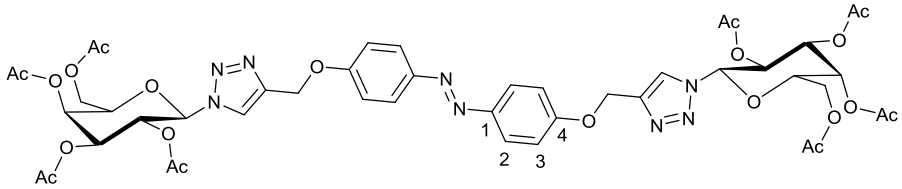

The galactose azide **255** (461 mg, 1.23 mmol) and the bis-propargylated azobenzene **113** (0.5 eq., 180 mg, 0.62 mmol) were added to DMSO (30 mL) with vigorous stirring. Distilled water (10 mL) was added followed by copper sulphate pentahydrate (124 mg, 0.50 mmol) and sodium ascorbate (98 mg, 0.50 mmol). The reaction solution was stirred at room temperature overnight. DCM (80 mL) was added, followed by washing with distilled water (100 mL) and brine (100 mL). The organics were dried over anhydrous magnesium sulphate and concentrated under vacuum to give the crude product as a sticky orange solid (690 mg). Purification by flash chromatography (SiO_2, DCM: MeOH 99:1) gave the title compound as a sticky orange solid, 471 mg, 74%.

^{1}H-NMR: δ_H (500 MHz) ($CDCl_3$): 1.83, 2.01, 2.05, 2.22 [4 x (s, 3H, C(O)CH_3)], 4.14-4.26 (m, 3H, H^5 + 2xH^6), 5.19-5.30 (m, 3H, H^3 & OCH_2), 5.55-5.59 (m, 2H, H^2 + H^4) 5.87 (d, 1H, H^1, J = 9.5 Hz) 7.10 (d, 2H, H-3, J = 9.0 Hz), 7.88 (d, 2H, H-2, J = 9.0 Hz), 7.95 (s, 1H, C-H triazole).

The ^{1}H-NMR spectrum shows a series of low intensity peaks consistent with the presence of the *cis* isomer.

^{13}C-NMR: δ_C (125 MHz) ($CDCl_3$): 20.2, 20.5, 20.6, 20.6 [4 x (C(O)$\underline{C}H_3$)], 61.2 (C^6), 62.1 (OCH_2), 66.9, 67.9 (C^2 + C^4), 70.8 (C^3), 74.2 (C^5) 86.4 (C^1) 115.1 (C-3) 121.3 (C-H triazole), 124.8 (C-2), 144.5 (q-triazole), 147.5 (C-1) 160.1 (C-4), 169.1, 169.8, 169.9, 170.3 [4 x ($\underline{C}$(O)CH_3)]

The ^{13}C -NMR shows a series of low intensity peaks consistent with the presence of the *cis* isomer.

m.p.: 207-210 ˚C.

IR (KBr disc): 3164.0, 2968.5 (C-H), 1752.6 (C=0) 1599.9 (C=C triazole), 1501.4 (N=N), 1372.1 (C-N), 1222.8 (C-O) cm^{-1}.

HRMS (direct injection) $[M+H]^+$, $[C_{46}H_{53}N_8O_{20}]^+$ calculated: 1037.3371; found: 1037.3411. Difference 3.86 ppm.

Divalent triazole linked galactose-azobenzene conjugate ***262***

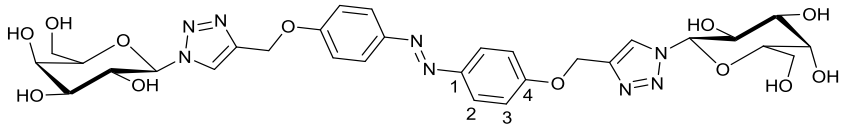

The divalent triazole linked protected galactose-azobenzene conjugate 261 (402 mg, 0.39 mmol) was dissolved in THF (10mL). MeOH (30 mL), distilled water (10 mL) and sodium methoxide (cat.) were added sequentially. The reaction mixture was stirred overnight at room temperature. Acidic Dowex resin was added until the pH remained acidic. The resin was filtered off and the solvent removed under vacuum to give the product an orange solid, which crystallised from a water/ethanol mixture, 239 mg, 88%.

^{1}H-NMR: δ_H (500 MHz) (DMSO-d_6): 3.48-3.57 (m, 3H, H^5 + 2xH^6) 3.72-3.77 (m, 2H, H^3 + H^4), 4.04 (t, 1H, H^2, J = 9.5 Hz), 5.27 (s, 2H, OCH_2) 5.51 (d, 1H, H^1, J = 9.0 Hz,), 7.23 (d, 2H, H-3, J = 9.0 Hz), 7.86 (d, 2H, H-2, J = 7.5 Hz), 8.42 (s, 1H, C-H triazole).

The ^{1}H-NMR spectrum shows a series of low intensity peaks consistent with the presence of the *cis* isomer.

^{13}C-NMR: δ_C (125 MHz) (DMSO-d_6): 60.9 (C^6), 61.8 (OCH_2), 68.9 (C^4), 69.8 (C^2), 74.2 (C^3) 78.9 (C^5), 88.6 (C^1) 115.7 (C-3), 124.2 (CH-triazole), 124.6 (C-2), 142.8 (q-triazole) 146.8 (C-1) 161.2 (C-4).

The ^{13}C -NMR shows a series of low intensity peaks consistent with the presence of the *cis* isomer.

m.p.: 198-202 ˚C.

IR (KBr disc): 3380.5 (O-H), 2925.6 (C-H), 1598.3 (C=C triazole), 1498.4 (N=N), 1240.5 (C-O) cm^{-1}.

HRMS (direct injection) $[M+H]^+$, $[C_{21}H_{24}N_5O_6]^+$ calculated: 723.2345; found: 723.2380. Difference 4.79 ppm.

Divalent triazole linked protected mannose-azobenzene conjugate ***263***

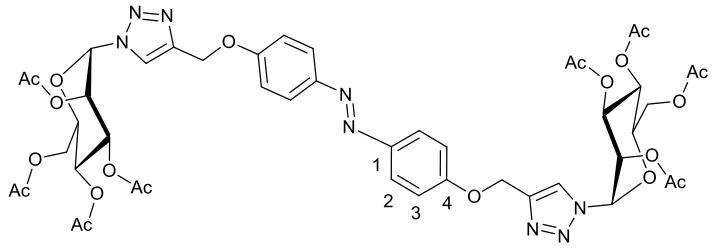

The mannose azide 256 (408 mg, 1.09 mmol) and the bis-propargylated azobenzene **113** (0.5 eq., 159 mg, 0.54 mmol) were added to DMSO (30 mL) with vigorous stirring. Distilled water (10 mL) was added followed by copper sulphate pentahydrate (108 mg, 0.43 mmol) and sodium ascorbate (86 mg, 0.43 mmol). The reaction solution was stirred at room temperature overnight. DCM (100 mL) was added, followed by washing with distilled water (100 mL) and brine (120 mL). The organics were dried over anhydrous magnesium sulphate and concentrated under vacuum to give the crude product as a sticky orange solid (721 mg). Purification by flash chromatography (SiO_2, DCM: MeOH 99:1) gave the title compound as a sticky orange solid, 401 mg, 71%.

^{1}H-NMR: δ_H (500 MHz) ($CDCl_3$): 2.06, 2.07, 2.07 (s, 3H, C(O)$\underline{C}H_3$) 2.17 (s, 3H, C(O)$\underline{\mathbf{C}}H_3$), 3.91-3.92 (m, 1H, H^5), 4.07 (dd, 1H, H^6, J = 2.5 Hz, 12.5 Hz), 4.37 (dd, 1H, H^6, J = 5.5 Hz, 12.5 Hz), 5.33-5.39 (m, 3H, H^4 + OCH_2), 5.91 (dd, 1H, H^3, J = 3.5 Hz, 8.5 Hz), 5.98 (t, 1H, H^2, J = 3.5 Hz), 6.04 (d, 1H, H^1, J = 3.5 Hz,), 7.10 (d, 2H, H-3, J = 9.0 Hz), 7.86-7.89 (m, 3H, H-2 & CH-triazole),

The ^{1}H-NMR spectrum shows a series of low intensity peaks consistent with the presence of the *cis* isomer.

^{13}C-NMR: δ_C (125 MHz) ($CDCl_3$): 20.6, 20.7, 20.7, 20.7 [4 x (C(O)$\underline{C}H_3$)] 61.5 (C^6), 62.1 (OCH_2), 66.1 (C^4), 68.2 (C^2), 68.7 (C^3) 72.4 (C^5), 83.6 (C^1) 115.0 (C-3), 123.1 (C-H triazole), 124.5 (C-2), 144.6 (q-triazole) 147.5 (C-1), 160.0 (C-4), 169.3, 169.6, 169.6, 170.5 [4 x ($\underline{C}$(O)CH_3)]

The ^{13}C -NMR shows a series of low intensity peaks consistent with the presence of the *cis* isomer.

m.p.: 77-81 ˚C.

IR (KBr disc): 2962.5 (C-H), 1752.5 (C=0) 1598.8 (C=C triazole), 1499.8 (N=N), 1371.6 (C-N), 1238.4 (C-O) cm^{-1}.

HRMS (direct injection) $[M+H]^+$, $[C_{46}H_{53}N_8O_{20}]^+$ calculated: 1037.3371; found: 1037.3409. Difference 3.66 ppm.

*Divalent triazole linked mannose-azobenzene conjugate **264***

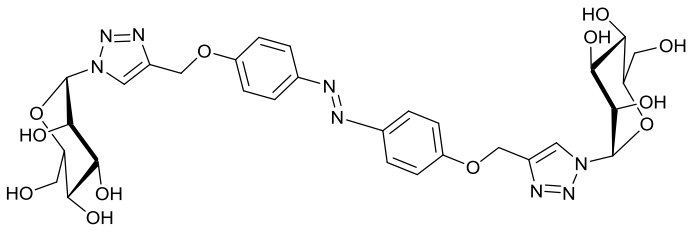

The divalent triazole linked protected mannose-azobenzene conjugate **263** (344 mg, 0.33 mmol) was dissolved in THF (10mL). MeOH (30 mL), distilled water (10 mL) and sodium methoxide (cat.) were added sequentially. The reaction mixture was stirred overnight at room temperature. Acidic Dowex resin was added until the pH remained acidic. The resin was filtered off and the solvent removed under vacuum to give the product an orange solid, which was crystallised from a water/ethanol mixture, 211 mg, 91%.

^{1}H-NMR: δ_H (500 MHz) (DMSO-d_6): 3.30-3.33 (m, 1H, H^5) 3.57-3.63 (m, 3H, H^4 + H^6), 3.86 (s, 1H, H^3) 4.43 (s, 1H, H^2), 5.30 (s, 2H, OCH_2) 5.95 (d, 1H, H^1, J = 4.0 Hz,), 7.26 (d, 2H, H-3, J = 9.0 Hz), 7.87 (d, 2H, H-2, J = 9.0 Hz), 8.42 (s, 1H, CH-triazole).

The ^{1}H-NMR spectrum shows a series of low intensity peaks consistent with the presence of the *cis* isomer.

^{13}C-NMR: δ_C (125 MHz) (DMSO-d_6): 61.2 (C^6), 61.8 (OCH_2), 66.1 (C^4), 68.6 (C^2), 71.7 (C^3) 78.9 (C^5), 86.2 (C^1) 115.8 (C-3), 124.6 (C-2), 125.1 (C-H triazole), 142.8 (q-triazole), 147.0(C-1) 161.0 (C-4)

The ^{13}C -NMR shows a series of low intensity peaks consistent with the presence of the *cis* isomer.

m.p.: thermal degradation at 208-215˚C.

IR (KBr disc): 3370.15 (O-H), 2924.0 (C-H), 1597.93.3 (C=C triazole), 1499.0 (N=N), 1246.6 (C-O) cm^{-1}.

HRMS (direct injection) $[M+Na]^+$, $[C_{30}H_{36}N_8O_{12}Na]^+$ calculated 700.2345, found: 700.2346; difference 0.14 ppm

Triazole linked protected galactose-azobenzene conjugate ***265***

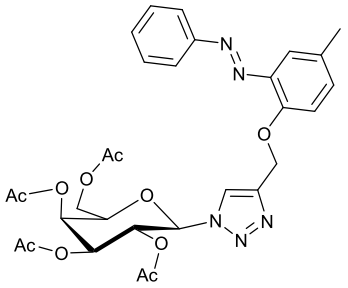

The galactose azide **255** (0.333 g, 0.89 mmol) and the propargylated azobenzene **144** (0.223g, 0.89 mmol) were added to DMSO (30 mL), to this mixture was added a solution of copper sulphate (89 mg, 0.46 mmol) and sodium ascorbate (71 mg, 0.46 mmol) in distilled water (10 mL). The reaction mixture was then left to stir at room temperature overnight. DCM (50 mL) was added and the reaction was washed with water (3 x 150 mL) and brine (150 mL). The organics were dried over magnesium sulphate and concentrated under vacuum to give the crude product as an orange oil. Flash chromatography (DCM/MeOH 99:1) gave the desired product as an orange foam, 0.487 g, 85%.

^{1}H-NMR: δ_H (500 MHz) ($CDCl_3$): 1.87, 2.01, 2.03, 2.137 (4 x s, 4 x 3H, C(O)C<u>H</u>3), 2.35 (s, 3H, CH_3), 4.08-4.24 (m, 3H, H^5 & H^6), 5.24 (dd, 1H, H^3, J = 9.5, 3.5 Hz), 5.45 (s, 1H, OCH_2) 5.53-5.59 (m, 2H, H^2 & H^4), 5.84 (d, 1H, H^1, J = 9.5 Hz), 7.10 (d, 1H, Ar-H, J = 8.5 Hz), 7.19-7.25 (m, 1H, Ar-H) 7.43-7.54 (m, 4H, Ar-H), 7.92-7.98 (m, 3H, Ar-H & triazole CH)

The ^{1}H-NMR spectrum shows a series of low intensity peaks consistent with the presence of the *cis* isomer.

^{13}C-NMR: δ_C (125 MHz) ($CDCl_3$): 20.2, 20.5, 20.6, 20.6, 20.6 (4 x C(O)<u>C</u>H3 & CH_3), 61.2 (C^6) 64.6 (CH_2), 66.9 (C^4), 67.9 (C^2), 70.9 (C^3), 74.0 (C^5), 86.3 (C^1), 116.2, 117.3 (Ar C-H), 121.4 (triazole C-H) 123.0, 129.1, 130.8, 133.0 (Ar C-H), 131.7 (C-CH_3) 142.7 (Ar q-C), 145.3 (CH2-<u>C</u>-N) 153.2 (Ar q-C) 153.3 (<u>C</u>-O-CH_2), 168.9, 169.8, 170.0, 170.3 (4 x <u>C</u>(O)CH_3)

The ^{13}C -NMR shows a series of low intensity peaks consistent with the presence of the *cis* isomer.

m.p.: 66-60 ˚C

IR (KBr disc): 2963.9 (C-H), 1754.6 (C=0) 1502.2 (C=C triazole), 1463.6 (N=N) 1370.8 (C-N), 1217.8 (C-O) cm^{-1}.

HRMS (direct injection) $[M+H]^+$, $[C_{30}H_{34}N_5O_{10}]^+$ calculated: 624.2300, found: 624.2268; difference 5.11 ppm

*Triazole linked galactose-azobenzene conjugate **266***

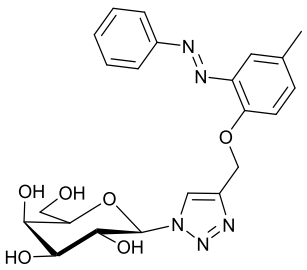

The Triazole linked protected galactose-azobenzene conjugate **265** (0.411 g, 0.643 mmol) was dissolved in a methanol/distilled water/THF mixture (40 mL: 10 mL: 10 mL). Sodium methoxide (catalytic amounts) was added and the reaction mixture was allowed to stir 16 hrs. The solution adjusted to pH 8 with acidic Dowex resin. The resin was filtered off and the solution was concentrated under vacuum to give the desired product as a red solid (0.261 g, 0.553 mmol, 86%).

^{1}H-NMR: δ_H (500 MHz) (DMSO-d_6): 2.32 (s, 3H, CH_3), 3.45-3.81 (m, 5H, H^3, H^4. H^5 & H^6), 4.05 (t, 1H, H^2, J = 9.5 Hz), 5.38 (s, 1H, OCH_2) 5.52 (d, 1H, H^1, J = 9.5 Hz), 7.34-7.42 (m, 3H, Ar-H) 7.52-7.62 (m, 3H, Ar-H), 7.81-7.84 (m, 2H, Ar-H), 8.40 (s, 1H, triazole CH)

The ^{1}H-NMR spectrum shows a series of low intensity peaks consistent with the presence of the *cis* isomer.

^{13}C-NMR: δ_C (125 MHz) (DMSO-d_6): 20.5, (CH_3), 60.9 (C^6) 63.1 (OCH_2), 68.9, 74.2, 79.0 (C^3, C^4, C^5), 69.8 (C^2), 88.6 (C^1), 116.0, 123.0 (Ar C-H), 124.1 (triazole C-H) 129.0, 129.9, 131.6, 133.9 (Ar C-H), 130.8 (C-CH_3) 142.0 (Ar q-C), 143.3 (CH2-<u>C</u>-N) 153.2 (Ar q-C) 154.7 (<u>C</u>-O-CH_2),

The ^{13}C -NMR shows a series of low intensity peaks consistent with the presence of the *cis* isomer.

R.F.: (DCM : MeOH 9:1) 0.45

IR (ATR): 3412.5 (O-H) 2919.4 (C-H), 1503.5 (C=C triazole), 1455.1 (N=N) 1279.6 (C-N), 1226.7, 1045.4 (C-O) cm^{-1}.

HRMS (direct injection) $[M+H]^+$, $[C_{22}H_{26}N_5O_6]^+$ calculated: 456.1878, found: 456.1888; difference 2.34 ppm

Isoxazole linked protected thymidine-azobenzene conjugate ***270***

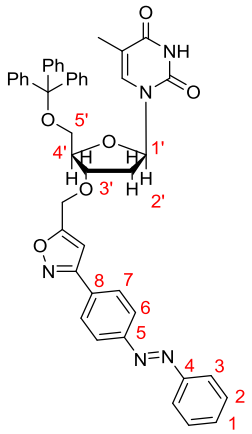

To solution of the propargylated thymidine **269** (0.514 g, 0.98 mmol) and the chlorooxime **174** (0.75 g, 2.94 mmol) in EtOAc (20 mL) triethylamine (0.38 g, 0.48 mL, 3.43 mmol) in EtOAC (1.0 mL) was added over 40 mins by syringe pump. The reaction mixture was heated to reflux and left to stir overnight. Distilled water (50 mL) was added, followed by extraction with further EtOAc (2 X 30 mL). The combined organics were dried over anhydrous magnesium sulphate and concentrated under vacuum to give the crude product (1.21 g). Purification by flash chromatography (SiO_2, Diethyl ether: DCM: Pet diethyl ether 4.5 : 4.5 : 1) gave the product as an orange foam, 0.42 g, 57%.

1H-NMR: δH (500 MHz) ($CDCl_3$): 1.53 (s, 3H, CH_3), 2.22-2.31 (m, 1H, H-2'), 2.51-2.59 (m, 1H, H-2'), 3.37 (d, 1H, H-5', J= 11.5 Hz), 3.52 (d, 1H, H-5', J= 11.5 Hz), 4.20 (br s, 1H, H-4'), 4.37 (br s, 1H, H-4'), 4.62 (d, 1H, O-CH_2, J= 13.5 Hz), 4.67 (d, 1H, O-CH_2, J= 13.5 Hz), 6.38 (br t, 1H, H-1', J= 6.0 Hz), 6.59 (s, 1H, CH-isoxazole), 7.22-7.34 (m, 7H, Ar-H), 7.36-7.42 (m, 6H, Ar-H), 7.49-7.58 (m, 5H, Ar-H), 7.91-8.04 (m, 7H, Ar-H), 8.30 (s, 1H, NH).

The ^{1}H-NMR spectrum shows a series of low intensity peaks consistent with the presence of the *cis* isomer.

13C-NMR: δC (125 MHz) ($CDCl_3$): 11.9 (CH_3) ,37.8 (C-2'), 62.2 (O-CH_2), 63.8 (C-5'), 80.2 (C-3'), 83.8 (C-4'), 84.8 (C-1')87.6 (O$\underline{C}$Ph$_3$) 101.4 (CH-isoxazole) 111.4 (C-5) 123.05, 123.2, 127.5, 127.6, 128.1, 128.6 128.9 (Ar-CH), 130.9 (C8) 129.2, 131.4 (Ar-CH), 135.3 (CH-pyrimidine) 145.2, 150.1, 152.6, 153.5 (Ar-C) 161.8 (CN-isoxazole) 163.4 (C-4) 169.3 (CO-isoxazole)

The ^{13}C -NMR shows a series of low intensity peaks consistent with the presence of the *cis* isomer.

m.p. 111-115 ℃

IR (KBr disc): 3057.4 (N-H), 2923.2 (C-H), 1689.1 (C=O), 1594.2 (N=N) 1448.0 (N-O), 1101.7 cm (C-O) $^{-1}$

HRMS (direct injection) $[M+Na]^+$, $[C_{45}H_{39}N_5O_6Na]^+$ calculated: 768.2793, found: 768.2791; difference 0.17 ppm

Isoxazole linked thymidine-azobenzene conjugate ***271***

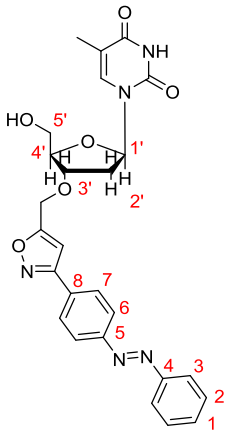

To a solution of the trityl protected isoxazole linked protected thymidine-azobenzene conjugate 270 (0.32 g, 0.43 mmol) in DCM (10 mL) was added DCA (4.0 mL, 6.25 g, 48 mmol). The solution was left to stir for 3 hours at room temperature. Further DCM (20 mL) was added followed by washing with distilled water (25 mL), saturated NaHCO3 (25 mL), further distilled water (25 mL) and finally brine (25 mL). The organics were dried over anhydrous magnesium sulphate and concentrated under vacuum to give the crude product (182 mg, 84 %), which was purified by passing the material through a silica plug (elution with acetone, followed by diethyl ether). Followed evaporation, the pure product was obtained by precipitation from a methanol/chloroform solution to give the pure product as an orange sticky solid, 145 mg, 67%.

1H-NMR: δH (500 MHz) (DMSO-d_6): 1.79 (s, 3H, CH_3), 2.17-2.25 (m, 1H, H-2'), 2.30-2.38 (m, 1H, H-2'), 3.63 (s, 2H, H-5'), 4.05 (s, 1H, H-4'), 4.30 (s, 1H, H-3'), 4.80 (s, 2H, O-CH_2), 5.19(s, 1H, OH) 6.18 (t, 1H, H-1', J= 7.0 Hz), 7.22 (s, 1H, CH isoxazole), 7.59-7.67 (m, 3H, H1 & H2), 7.72 (s, 1H, CH-pyrimidine), 7.95 (d, 2H, H3, J= 6.0 Hz), 8.04), 8.14 (2 X d, 2 X 2H, H6 & H7, J= 8.0 Hz), 11.33 (s, 1H, NH).

The ^{1}H-NMR spectrum shows a series of low intensity peaks consistent with the presence of the *cis* isomer.

13C-NMR: δC (125 MHz) (DMSO-d_6): 12.7 (CH_3) ,36.7 (C-2'), 61.7 (O-CH_2), 61.9 (C-5'), 80.4 (C-3'), 84.3 (C-4'), 85.0 (C-1') 102.4 (CH-isoxazole) 110.1 (C-5) 123.2, 123.7, 128.3, 130.0, (Ar-CH) 131.5 (C8) 132.4 (Ar-CH) 136.4 (C-6), 151.0 (NC(O)N), 152.4, 153.2 (C4 & C5), 161.7 (CN-isoxazole), 164.2 (CC(O)N), 170.7 (CO-isoxazole)

The ^{13}C -NMR shows a series of low intensity peaks consistent with the presence of the *cis* isomer.

m.p. 238-241 ˚C

IR (KBr disc): 3354.9 (O-H) 3061.9 (N-H), 2907.9(C-H) 1696.4(C=O), 1474.7 (N-O), 1282.1, 1110.1(C-O), 1092.04 (C-O-H) cm^{-1}

HRMS (direct injection) $[M+H]^+$, $[C_{26}H_{26}N_5O_6]^+$ calculated: 504.1878, found: 504.1892; difference 2.76 ppm

*Isoxazole linked protected thymidine-azobenzene conjugate **272***

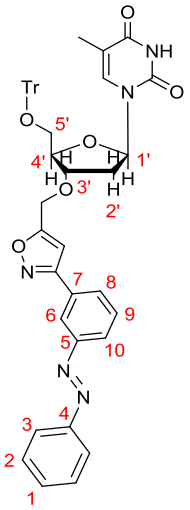

To solution of the propargylated thymidine **269** (0.517 g, 0.98 mmol) and the chlorooxime **225** (0.75 g, 2.94 mmol) in EtOAc (20 mL) a solution of triethylamine (0.38 g, 0.48 mL, 3.43 mmol) in EtOAc (1.0 mL) was added over 40 mins by syringe pump. The reaction mixture was stirred overnight at room temperature. Distilled water (50 mL) was added, followed by extraction with further EtOAc (2 X 30 mL). The combined organics were dried over anhydrous magnesium sulphate and concentrated under vacuum to give the crude product as an orange sticky solid (1.16 g). The product was purified by flash chromatography (SiO_2, Diethyl ether: DCM: Pet diethyl ether 4.5 : 4.5 : 1) to give the product as an orange foam, 0.54 g, 73 %

1H-NMR: δH (500 MHz) ($CDCl_3$): 1.52 (s, 3H, CH_3), 2.22-2.31 (m, 1H, H-2'), 2.51-2.58 (m, 1H, H-2'), 3.36 (d, 1H, H-5', J= 9.5 Hz), 3.52 (d, 1H, H-5',J= 9.5 Hz), 4.19 (br s, 1H, H-4'), 4.37 (br s, 1H, H-3'), 4.64 (d, 1H, O-CH_2, J= 13.5 Hz), 4.68 (d, 1H, O-CH_2, J= 13.5 Hz), 6.38 (t, 1H, H-1', J= 6.5 Hz), 6.62 (s, 1H, CH-isoxazole), 7.22-7.33 (m, 9H, Ar-H), 7.36-7.42 (m, 6H, Ar-H), 7.48-7.59 (m, 4H, Ar-H), 7.63 (t, 1H, Ar-H, J= 7.5 Hz), 7.92-7.98 (m, 2H, Ar-H), 8.03 (d, 1H, Ar-H, J= 7.5 Hz), 8.28 (s, 1H, NH), 8.30 (s, 1H, H6).

The ^{1}H-NMR spectrum shows a series of low intensity peaks consistent with the presence of the *cis* isomer.

13C-NMR: δC (125 MHz) ($CDCl_3$): 11.9 (CH_3), 37.9 (C-2'), 62.3 (O-CH_2), 63.8 (C-5'), 80.1 (C-3'), 83.8 (C-4'), 84.8 (C-1')87.6 (O<u>C</u>Ph_3) 101.5 (CH-isoxazole) 111.5 (<u>C</u>-

CH_3) 121.1, 123.0, 124.7, 127.5, 128.1, 128.6 129.0, 129.2 (Ar-CH), 129.8 (C-7), 131.4, 135.3 (Ar-CH) 143.2 (q-Ph_3), 150.1, 152.5, 153.0 (Ar-C) 162.0 (CN-isoxazole) 163.4 (CC(O)N) 169.3 (CO-isoxazole)

The ^{13}C -NMR shows a series of low intensity peaks consistent with the presence of the *cis* isomer.

m.p. 83-87 ℃

IR (KBr disc): 3059.0(N-H), 2925.7(C-H), 1692.9(C=O), 1449.0(N-O), 1274.4, 1096.2(C-O) cm^{-1}

HRMS (direct injection) $[M+Na]^+$, $[C_{45}H_{39}N_5O_6Na]^+$ calculated: 768.2793, found: 768.2794; difference 0.25 ppm

Isoxazole linked thymidine-azobenzene conjugate ***273***

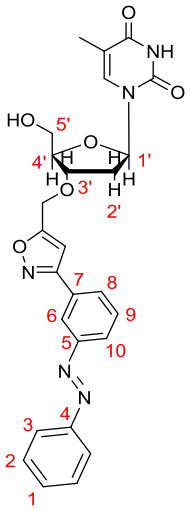

To a solution of the propargylated thymidine **169** (0.495 g, 0.66 mmol) in DCM (20 mL) was added DCA (3.0 mL, 4.69 g, 36 mmol), the solution was then left to stir overnight at room temperature. Further DCM (30 mL) was added followed by washing with distilled water (30 mL), saturated $NaHCO_3$ (30 mL), further distilled water (30 mL) and finally brine (30 mL). The organics were then dried over anhydrous magnesium sulphate and concentrated under vacuum to give the crude product (311 mg, 94 %). Purification by flash chromatography (diethyl ether: DCM: methanol 30:70:2) gave the product as a sticky orange solid, 231 mg, 70 %.

1H-NMR: δH (500 MHz) ($CDCl_3$): 1.84 (s, 3H, CH_3), 2.27-2.47 (m, 2H, H-2'), 3.59 (s, 1H, OH), 3.82 (d, 1H, H-5', J = 11 Hz), 3.82 (d, 1H, H-5', J = 11 Hz), 4.16 (br s, 1H, H-4'), 4.41 (br s, 1H, H-3'), 4.63-4.73 (m, 2H, O-CH_2), 6.18 (t, 1H, H-1', J= 6.5 Hz), 6.71 (s, 1H, CH isoxazole), 7.44-7.65, 7.89- 803 (2 X m, 5H & 4H, Ar-H and CH-pyrimidine), 8.31 (s, 1H, H6), 9.65 (s, 1H, NH or OH).

The ^{1}H-NMR spectrum shows a series of low intensity peaks consistent with the presence of the *cis* isomer.

Selected peaks for Z-isomer: 6.49 (s, 0.2H, CH isoxazole), 6.76 (d, 0.2H, Ar-H, J = 8.0 Hz), 6.87 (d, 0.4H, Ar-H, J = 7.0 Hz), 7.15 (t, 0.2H, Ar-H, J = 7.0 Hz), 7.21- 7.31 (m, 0.8H, Ar-H), 7.40 (s, 0.2H, Ar-H)

13C-NMR: δC (125 MHz) ($CDCl_3$): 12.5 (CH_3) ,37.2 (C-2'), 62.3 (O-CH_2), 62.5 (C-5'), 80.0 (C-3'), 85.1 (C-4'), 86.7 (C-1'), 101.6 (CH isoxazole) 111.1 (C-5) 121.0, 123.0, 124.6, 129.0, 129.2 (Ar-CH) 129.7 (C7) 129.8 (Ar-CH) 131.4 (Ar-CH) 137.0 (CH-pyrimidine), 150.6, 152.5, 152.9 (Ar-C) 162.0 (CN-isoxazole) 164.2 (C<u>C</u>(O)N), 169.5 (CO-isoxazole)

The ^{13}C -NMR shows a series of low intensity peaks consistent with the presence of the *cis* isomer.

m.p. 55-58℃

IR (KBr disc): 3418.3 (O-H) 3058.7 (N-H), 2925.7 (C-H), 1689.7 (C=O), 1472.7 (N-O), 1275.1, 1096.4, 1063.5.0 (C-O) cm^{-1}

HRMS (direct injection) $[M+H]^+$, $[C_{26}H_{26}N_5O_6]^+$ calculated: 504.1878, found: 504.1861; difference 3.22 ppm

Divalent i*soxazole linked* protected *thymidine-azobenzene conjugate* ***274***

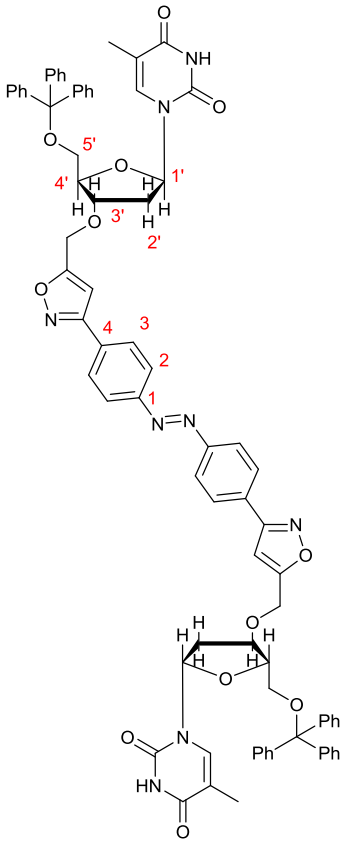

To solution of the propargylated thymidine **169** (714 mg, 1.4 mmol) and bis-chlorooxime **176** (81 mg, 0.24 mmol) in EtOAc (25 mL) a solution of triethylamine (49 mg, 0.067 mL, 0.15 mmol) in EtOAc (1.0 mL) was added over 4 hours by syringe pump. The reaction mixture was stirred overnight at room temprature. Distilled water (50 mL) was added, followed by extraction with further EtOAc (2 X 30 mL). The combined organics were dried over anhydrous magnesium sulphate and concentrated under vaccum to give the crude product as an orange sticky solid (588 mg). The product was further purified by flash chromatography (SiO_2, Diethyl ether: DCM: Pet diethyl ether 2 : 2 : 1) to give the product as an orange foam, 123 mg, 65 %.

1H-NMR: δH (500 MHz) ($CDCl_3$): 1.52 (s, 3H, CH_3), 2.22-2.32 (m, 1H, H-2'), 2.50-2.61 (m, 1H, H-2'), 3.37 (d, 1H, H-5', J= 10.0 Hz), 3.52 (d, 1H, H-5' J= 10.0 Hz), 4.20 (br s, 1H, H-4'), 4.37 (br s, 1H, H-3') 4.64 (d, 1H, O-CH_2, J= 13.5 Hz), 4.68 (d, 1H, O-CH_2, J= 13.5 Hz), 6.39 (t , 1H, H-1', J= 6.5 Hz), 6.61 (s, 1H, CH isoxazole), 7.22-7.43

(m, 15H, Ar-H), 7.57 (s, 1H, H-6), 7.96 (d, 2H, H2, J= 7.5 Hz), 8.05 (d, 2H, H3, J= 7.5 Hz), 8.48 (s, 1H, NH).

The ^{1}H-NMR spectrum shows a series of low intensity peaks consistent with the presence of the *cis* isomer.

13C-NMR: δC (125 MHz) ($CDCl_3$): 11.9 (CH_3) ,37.8 (C-2'), 62.3 (O-CH_2), 63.8 (C-5'), 80.2 (C-3'), 83.8 (C-4'), 84.8 (C-1') 87.6 (0$\underline{C}Ph_3$) 101.4 (CH isoxazole) 111.4 ($\underline{C}$-CH_3) 123.7, 127.5, 127.8, 128.1, 128.6 (Ar-CH) 131.3 (C4) 135.3 (CH-pyrimidine) 143.2 (q-Ph_3) 150.2 (NC(O)N) 153.4 (C1) 161.8 (CN-isoxazole) 163.5 (C$\underline{C}$(O)N) 169.4 (CO-isoxazole)

The ^{13}C -NMR shows a series of low intensity peaks consistent with the presence of the *cis* isomer.

m.p. 158-161 ℃

IR (KBr disc): 3057.8 (N-H), 2924.9 (C-H), 1689.0 (C=O), 1448.8 (N-O), 1274.1, 1096.1 (C-O) cm^{-1}

HRMS (direct injection) $[M+Na]^+$, $[C_{78}H_{68}N_8O12]^+$ calculated: 1331.4849, found: 1331.4818; difference 2.33 ppm

Divalent i*soxazole linked* protected *thymidine-azobenzene conjugate* ***27*****5**

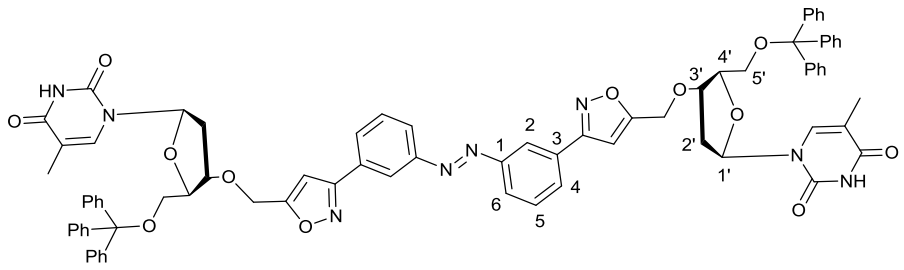

A solution of the propargylated thymidine **169** (0.988 g, 1.89 mmol) and bis-chlorooxime **230** (102 mg, 0.3 mmol) in ethyl acetate (15 mL) was heated to reflux. A solution of triethylamine (0.1 mL, 0.7 mmol), in a solution of ethyl acetate (0.9 mL), was slowly added over 4 hours with a syringe pump. The reaction mixture was left to heat at reflux overnight. Further ethyl acetate was added (30 mL) followed by consecutive washings with distilled water (50 mL) and brine (50 mL). The organics were dried over anhydrous sodium sulphate and concentrated under vacuum to give the crude product (1.03 g). Purification by flash chromatography (DCM:MeOH 100:0 to 98:2) gave the title compound as a sticky orange solid (180 mg, 0.14 mmol, 46%)

^{1}H-NMR: δH (500 MHz) ($CDCl_3$): 1.54 (s, 3H, CH_3), 2.20-2.27 (m, 1H, H-2'), 2.55-2.61 (m, 1H, H-2'), 3.35-3.40 (m, 1H, H-5'), 3.46-3.55 (m, 1H, H-5'), 4.21 (br s, 1H, H-4'), 4.32 (br s, 1H, H-3'), 4.60 (d, 1H, OCH_2, J= 13.0 Hz), 4.66 (d, 1H, OCH_2, J= 13.0 Hz), 6.38-6.42 (m, 1H, H-1'), 6.71 (s, 1H, CH-isoxazole), 7.24-7.42 (m, 15H, trityl), 7.58 (s, 1H, CH-pyrimidine) 7.64 (t, 1H, H-5, J= 7.5 Hz), 8.03-8.06 (m, 2H, H-4 & H-6), 8.31 (s, 1H, H-2), 9.56 (s, 1H, NH).

The ^{1}H-NMR spectrum shows a series of low intensity peaks consistent with the presence of the *cis* isomer.

^{13}C-NMR: δC (125 MHz) ($CDCl_3$): 12.0 (CH_3), 37.7 (C-2'), 62.4 (O-CH_2), 64.0 (C-5'), 80.9 (C-3'), 83.8 (C-4'), 84.9 (C-1'), 87.7 (O<u>C</u>Ph_3) 101.5 (CH-isoxazole) 111.5 (<u>C</u>-CH_3) 121.4 (C-2), 124.9(C-4/6), 127.6, 128.1, 128.6 (Ar-CH), 129.3 (C-4/6), 130.0 (C-5), 130.0 (Ar-C) 135.2 (CH-pyrimidine) 143.2 (q-Ph_3), 150.7 (N<u>C</u>(O)NH), 152.8 (Ar-C) 162.0 (CN-isoxazole) 163.9 (C<u>C</u>(O)N) 169.3 (CO-isoxazole)

The ^{13}C -NMR shows a series of low intensity peaks consistent with the presence of the *cis* isomer.

m.p. 148-152 ˚C

IR (KBr disc): 3057.1 (N-H), 2924.5 (C-H), 1689.8 (C=O), 1449.0(N-O), 1273.7, 1093.4 (C-O) cm^{-1}

HRMS (direct injection) $[M+H]^+$, $[C_{78}H_{68}N_8O_{12}Na]^+$ calculated: 1331.4849, found: 1331.4888; difference: 2.91 ppm

Triazole linked protected *thymidine-azobenzene conjugate* ***276***

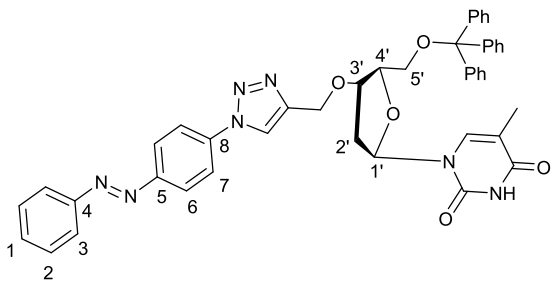

To a solution of the propargylated thymidine **169** (0.494g, 0.95 mmol) and the 4-azido azobenzene **171** (0.220 g, 0.95 mmol) in DMSO (30 mL), copper sulphate pentahydrate (95 mg, 0.38 mmol) and sodium ascorbate (78mg, 0.39 mmol) were added, followed by water (10 mL). The reaction mixture was allowed to stir overnight at room temperature. Distilled water (100 mL) was added, followed by extraction with DCM (2 x 50 mL). The organics were combined, washed consecutively with water (2 x 100 mL) and brine (100 mL), followed by concentration under vacuum to give the crude product (672 mg). Purification by flash chromatography (DCM: MeOH 100:0 to 98:2) followed by crystallisation from DCM/Pet ether (1:1) gave the product as an orange solid (0.595 g, 0.80 mmol, 84%)

^{1}H-NMR: δH (500 MHz) ($CDCl_3$): 1.50 (s, 3H, CH_3), 2.24-2.31 (m, 1H, H-2'), 2.53-2.59 (m, 1H, H-2'), 3.37 (dd, 1H, H-5', J= 10.5, 2.5 Hz), 3.49 (dd, 1H, H-5', J = 10.5, 2.5 Hz), 4.22 (br, 1H, H-4'), 4.44 (br, 1H, H-3'), 4.71 (d, 1H, O-CH_2, J= 12.5 Hz), 4.76 (d, 1H, O-CH_2, J= 12.5 Hz), 6.39 (dd, 1H, H-1', J = 8.0, 6.0 Hz), 7.24-7.43 (m, 15H, trityl), 7.50-7.60 (m, 4H, CH-pyrimidine & H-1 & H-2), 7.89 (d, 2H, H-6/7 , J = 9.0 Hz), 7.96 (dd, 2H, H-3, J = 8.0, 1.5 Hz), 8.02 (s, 1H, CH-triazole), 8.09 (d, 2H, H-6/7, J = 9.0 Hz)

The ^{1}H-NMR spectrum shows a series of low intensity peaks consistent with the presence of the *cis* isomer.

^{13}C-NMR: δC (125 MHz) ($CDCl_3$): 11.9 (CH_3), 37.9 (C-2'), 62.9 (O-CH_2), 63.9 (C-5'), 79.7 (C-3'), 83.9 (C-4'), 84.8 (C-1'), 87.6 (O<u>C</u>Ph_3) 101.5 (CH-isoxazole) 111.3 (<u>C</u>-CH_3) 120.1 (C-6/7) 123.1 (Ar-H), 124.4 (C-6/7), 127.5, 128.1, 129.8.6 (tritryl CH) 129.2,

131.6 (Ar-CH), 135.5 (CH-pyrimidine) 138.3 (C-5/8) 143.2 (qC-Ph_3), 145.6 (q-triazole), 150.1 (C-4), 152.3 (C-5/8), 152.5 (N<u>C</u>(O)NH), 163.3 (C<u>C</u>(O)N).

The ^{1}H-NMR spectrum shows a series of low intensity peaks consistent with the presence of the *cis* isomer.

m.p. 134-137 ℃

IR (KBr disc): 3057.6 (N-H), 2925.0 (C-H), 1689.1 (C=O), 1448.8 (N-N), 1274.0, 1099.3 (C-O) cm^{-1}

HRMS (direct injection) $[M+Na]^+$, $[C_{44}H_{39}N_7O_5Na]^+$ calculated: 768.2905, found: 768.2877; difference 3.61 ppm

*Triazole linked thymidine-azobenzene conjugate **277***

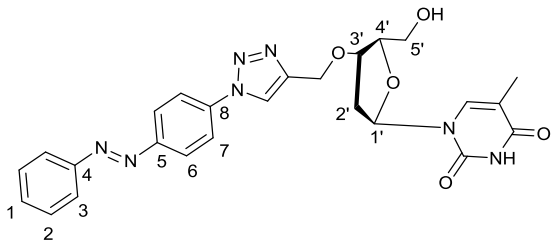

To a solution of the isoxazole linked protected thymidine-azobenzene conjugate **276** (0.381g, 0.51 mmol) in DCM (10 mL), DCA (4.0 mL, 0.39 mmol) was added (10 mL). The reaction mixture was allowed to stir overnight at room temperature. Distilled water (50 mL) was added, followed by extraction with DCM (2 x 25 mL). The organics were combined, washed consecutively with water (100 mL) and brine (100 mL), followed by concentration under vacuum to give the crude product (274 mg). purification by flash chromatography (DCM: MeOH 98:2) followed by crystallisation from DCM/Pet. ether (1:1) gave the product as an orange solid (0.195 g, 0.39 mmol, 76%)

^{1}H-NMR: δH (500 MHz) (DMSO-d_6): 1.80(s, 3H, CH_3), 2.16-2.24 (m, 1H, H-2'), 2.30-2.36 (m, 1H, H-2'), 3.63 (d, 1H, H-5', J= 3.0 Hz), 4.05-4.06 (m, 1H, H-4'), 4.29-4.33 (m, 1H, H-3'), 4.73 (s, 2H, O-CH2), 5.17 (br, 1H, OH), 6.18 (dd, 1H, H-1', J = 8.5, 6.0 Hz), 7.60-7.66 (m, 3H, & H-1 & H-2), 7.73 (d, 2H, CH-pyrimidine, J = 1.0 Hz), 7.95 (dd, 2H, H-3, J = 8.5, 2.0 Hz), 8.10-8.13 (m, 2H, H-6/7), 8.17-8.20 (m, 2H, H-6/7), 8.99 (s, 1H, triazole-CH)

The ^{1}H-NMR spectrum shows a series of low intensity peaks consistent with the presence of the *cis* isomer.

^{13}C-NMR: δC (125 MHz) (DMSO-d_6): 12.7 (CH_3), 36.8 (C-2'), 62.0 (O-CH_2), 62.2(C-5'), 79.7 (C-3'), 84.4 (C-1'), 85.1 (C-4'), 110.0 (<u>C</u>-CH_3) 122.9 (triazole-CH) 123.2 (C-2/3), 124.6 (C-6/7), 130.0 (C-2/3), 132.4 (C-1) 136.5 (CH-pyrimidine) 138.3 (C-5/8) 145.8 (q-triazole), 151.0 (N<u>C</u>(O)NH), 151.7 (C-5/8), 152.4 (C-4), 164.2 (C<u>C</u>(O)N).

The ^{13}C -NMR shows a series of low intensity peaks consistent with the presence of the *cis* isomer.

m.p. 224-227 ˚C

IR (KBr disc): 3033.35.0 (N-H), 1688.9 (C=O), 1465.9 (N-N), 1280.9, 1094.2 (C-O) cm^{-1}

HRMS (direct injection) $[M+Na]^+$, $[C_{25}H_{26}N_7O_5]^+$ calculated: 504.1990 found: 504.2007; difference 3.29 ppm

4-[4-[(1E)-2-phenyldiazenyl]phenoxy]methyl]-1H-1,2,3-triazolo acetic acid ***290***

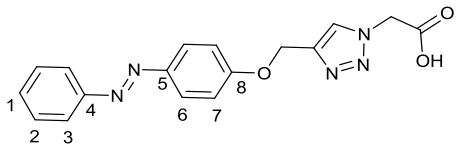

2-Azidoacetic acid, **289,** (0.202 g, 1.98 mmol) and the propargylated azobenzene **107** (0.701 g, 2.97 mmol) were dissolved in DMSO (30 mL), distilled water (10 mL) was added, followed by copper sulphate (0.396 g, 1.58 mmol) and sodium ascorbate (0.314 g, 1.58 mmol). The reaction mixture was stirred overnight. Distilled water (100 mL) was added, followed by extraction with diethyl ether (2 x 50 mL). The organics were combined, washed consecutively with water (2 x 100 mL) and brine (100 mL), and dried over anhydrous magnesium sulphate. After concentration under vacuum the crude product was obtained (706 mg). The crude material was passed through a silica plug (diethyl ether: pet. ether 1:1; followed by acetone) to give the title product **290** as an orange solid (408 mg, 1.20 mmol, 61%)

^{1}H-NMR: δ_H (500 MHz) (DMSO-d_6): 4.72 (s, 2H, C$\underline{H}_2$-COOH), 5.26 (s, 2H, O-C$\underline{H}_2$) 7.26 (d, 2H, H-7, J = 8.5) 7.48-7.64 (m, 3H, H-1 + H-2), 7.85 (d, 2H, H-3, J = 8.5), 7.91 (d, 2H, H-6, J = 8.5) 8.11 (s, 1H, triazole).

The ^{1}H-NMR spectrum shows a series of low intensity peaks consistent with the presence of the *cis* isomer.

^{13}C-NMR: δC (125 MHz) (DMSO-d_6): 54.2($\underline{C}H_2$-CO_2H), 62.1 (OCH_2), 115.8 (C-7), 122.7 (C-3), 125.0 (C-6), 126.2 (CH-triazole), 129.9 (C-2), 131.8 (H-1), 141.8 (q-triazole), 146.7 (C-5), 152.5 (C-4), 161.4 (C-8)

The ^{13}C -NMR shows a series of low intensity peaks consistent with the presence of the *cis* isomer.

m.p.: thermal degradation at 240 ˚C

IR (KBr disc): 1624.2 (C=0), 1581.3 (C=C triazole), 1500.5 (N=N), 1404.2 (N-N), 1253.8 (C-0) cm^{-1}

HRMS (direct injection) $[M+H]^+$, $[C_{17}H_{16}N_5O_3]^+$ calculated: 338.1248, found: 338.1247; difference 0.22 ppm

Azobenzenze-triazole-GRGDG-NH_2 ***295***

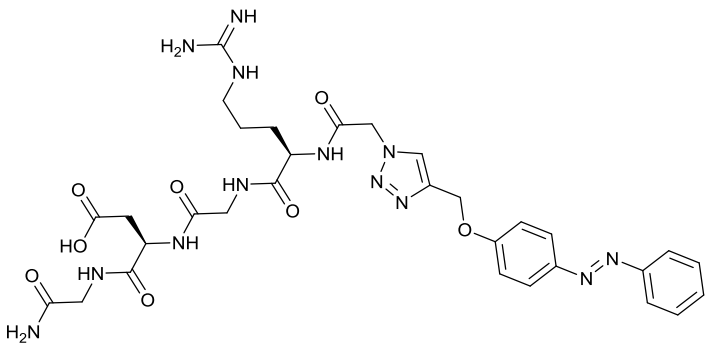

Method 1: The standard Fmoc SPPS protocol was used to manually synthesis H-Arg-Gyl-Asp-Gly-Resin (0.31 mmol) on a rink amide resin. A solution of **290** (0.315 g, 0.933 mmol, 3 eq.) PyBOP (486 mg, 0.933 mmol) and NMM (1.89 g, 0.205ml, 1.866 mmol, 6 eq.) in DMF (5mL) was added to the resin suppoerted peptide chain. The SPPS vessel was agitated for 40 minutes. The vessel was drained of the reaction solution and the resin was washed with DMF (3 x 5 mL), DCM (3 x 5 mL), DMF (3x 5 mL) and DCM (3 x 5 mL), the resin was dried under vacuum. The resin was then agitated in a solution of TFA, triisopropylsilane and water (95: 2.5: 2.5; 8 mL) for 1 hour. The solution containing the cleaved and deprotected peptide was then drained into a 15 mL falcon tube and air was blown over the solution until the volume was reduced to ~2 mL. Diethyl ether was added dropwise until no more precipitate formed. The precipitate was pelleted by centrifugation (5 mins, 2800 rpm) and the remaining liquid was decanted. Further ether was added to the pellet was dispersed through agitation and sonication. The pellet was regenerated from the suspension by centrifugation (5 mins, 2800 rpm) and removal of the liquid, this process was repeated once more. The pellet was then dissolved in distilled water (2 ml) and a minimum of acetonitrile, the resulting solution was lyophilised to give the crude product. which was subjected to semi-preparative HPLC. The seperated HPLC fractions were combined and lyophilised to give the product **295** as an orange solid (64%).

Method 2: The supported peptide H-GRGDG-resin **291** (0.1 mmol) was automatically synthesised using the standard Fmoc SPPS protocol on a rink amide resin. Imidazole-1-sunfunyl azide[260] **280** (63 mg, 0.3 mmol) and DIEA (58 mg. 0.078 mL, 0.45 mmol) were

dissolved in DMF (8 mL), the solution added to the supported peptide H-GRGDG-resin (0.1 mmol) in a SPPS vessel. The reaction mixture was agitated for 1 hour. The liquid was drained from the SPPS vessel and the resin was washed with DMF (3 x 5 mL), DCM (3 x 5 mL) and DMF (3 x 5 mL). A second solution of imidazole-1-sunfunyl azide (63 mg, 0.3 mmol) and DIEA (58 mg. 0.078 mL, 0.45 mmol) in DMF (8 mL) was added to the peptide and the reaction mixture was agitated over 1 hour. . The liquid was drained from the SPPS vessel and the resin was washed with DMF (3 x 5 mL), DCM (3 x 5 mL) and DMF (3 x 5 mL). The resin was agitated in a solution of TFA, triisopropylsilane and water (95: 2.5: 2.5; 6 mL) for 1 hour. The solution of containing the cleaved and deprotected peptide was then drained into a 15 mL falcon tube and air was blown over the solution until the volume was reduced to ~2 mL. Diethyl ether was added dropwise until no more precipitate formed. The precipitate was pelleted by centrifugation (5 mins, 2800 rpm) and the remaining liquid was decanted. Further ether was added to the pellet was dispersed through agitation and sonication. The pellet was regenerated from the suspension by centrifugation (5 mins, 2800 rpm) and removal of the liquid, this process was repeated once more. To a mixtuere of N_3-GRGDG-NH_2 **296** and propargylated azobenzene **107** (0.047 g, 0.2 mmol) in DMF (5mL) was added a solution of $CuSO_4$. $5H_2O$ (0.013 g, 0.05 mmol and sodium ascorbate (0.010 g, 0.05 mmol) in distilled water (1 mL). The resulting reaction mixture was left to stir overnight at room temperature. The solvent was removed under vacuum without heating. The residue was dissolved in distilled water and acetonitrile (1:1, 2 mLs) and the resulting yellow solution was purified by semi-preparative HPLC. The HPLC fractions were combined and lyophilised to give the product **295** as an orange solid (51%).

HRMS (direct injection) $[M+H]^+$, $[C_{31}H_{40}N_{13}O_8]^+$ calculated: 722.3117, found: 722.3130; difference: 1.79 ppm

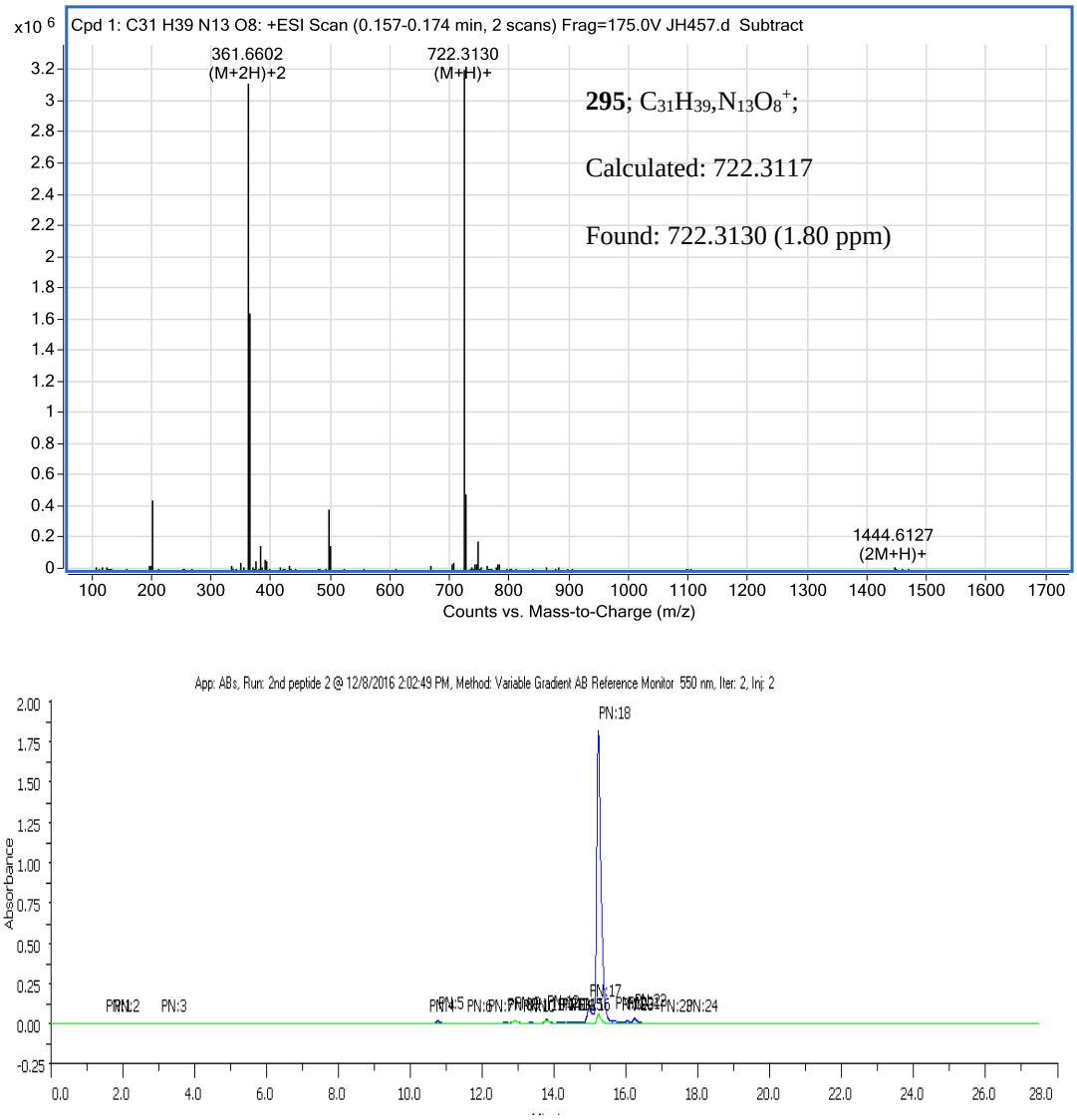

*Figure 77:HRMS and HPLC data of the conjugate **295**; 0-100% gradient of H2O/CH3CN, with 1% TFA, absorption monitored at 256 nm.*

Ac-RGDS(triazole-AB)TF-NH_2 ***300***

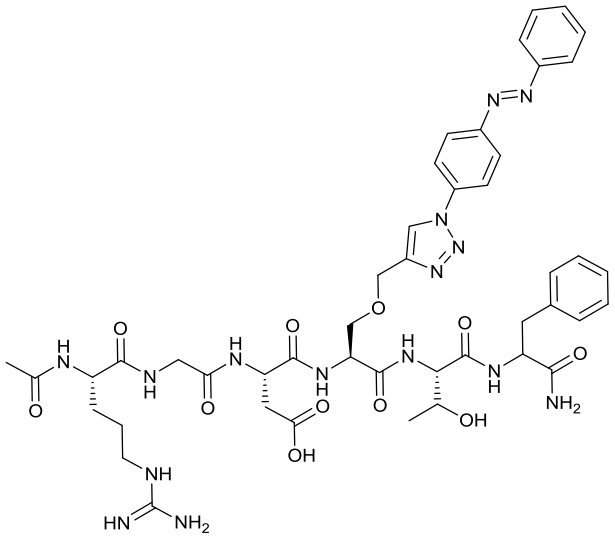

The supported peptide Ac-RGDS*TF-resin **297** (0.1 mmol) was automatically synthesised using the Fmoc SPPS protocol. A solution of 4-azidoazobenzene **171** (0.282 g, 1.26 mmol), copper sulphate (0.125 g, 0.5 mmol) and sodium ascorbate (0.099 g, 0.5mmol) in DMF/H_2O (5:1, 6 mL) was added to a SPPS vessel containing the on-resin propargylated peptide **297** (Ac-RGDS*TF-resin). The reaction mixture was agitated for 40 minutes, the solution was drained from the vessel and the resin was washed with DMF (3 x 5 mL), DCM (3 x 5 mL), DMF (3x 5 mL) and DCM (3 x 5 mL), the resin was dried under vacuum. The resin was agitated in a solution of TFA and water (95: 5; 8 mL) for 1 hour. The solution of containing the cleaved and deptroected peptide was then drained into a 15 mL falcon tube and air was blown over the solution until the volume was reduced to ~2 mL remained. Diethyl ether was added dropwise until no more precipitate formed. The precipitate was pelleted by centrifugation (5 mins, 2800 rpm) and the remaining liquid was decanted. Further ether was added to the pellet was dispersed through agitation and sonication. The pellet was regenerated from the suspension by centrifugation (5 mins, 2800 rpm) and removal of the liquid, this process was repeated once more. The pellet was dissolved in distilled water (1 mL) and a minimum of acetonitrile (~2 mL), the resulting solution was lyophilised to give the crude product. The residue was then dissolved in distilled water and acetonitrile (1:1, 2.5 mL) and the resulting yellow solution was purified by semi-preparative HPLC. The HPLC

fractions were combined and lyophilised to give the product **300** as an orange solid (73%).

HRMS (direct injection) $[M+H]^+$, $[C_{45}H_{58}N_{15}O_{11}]^+$ calculated: 984.4435, found: 984.4420; difference: 1.52 ppm

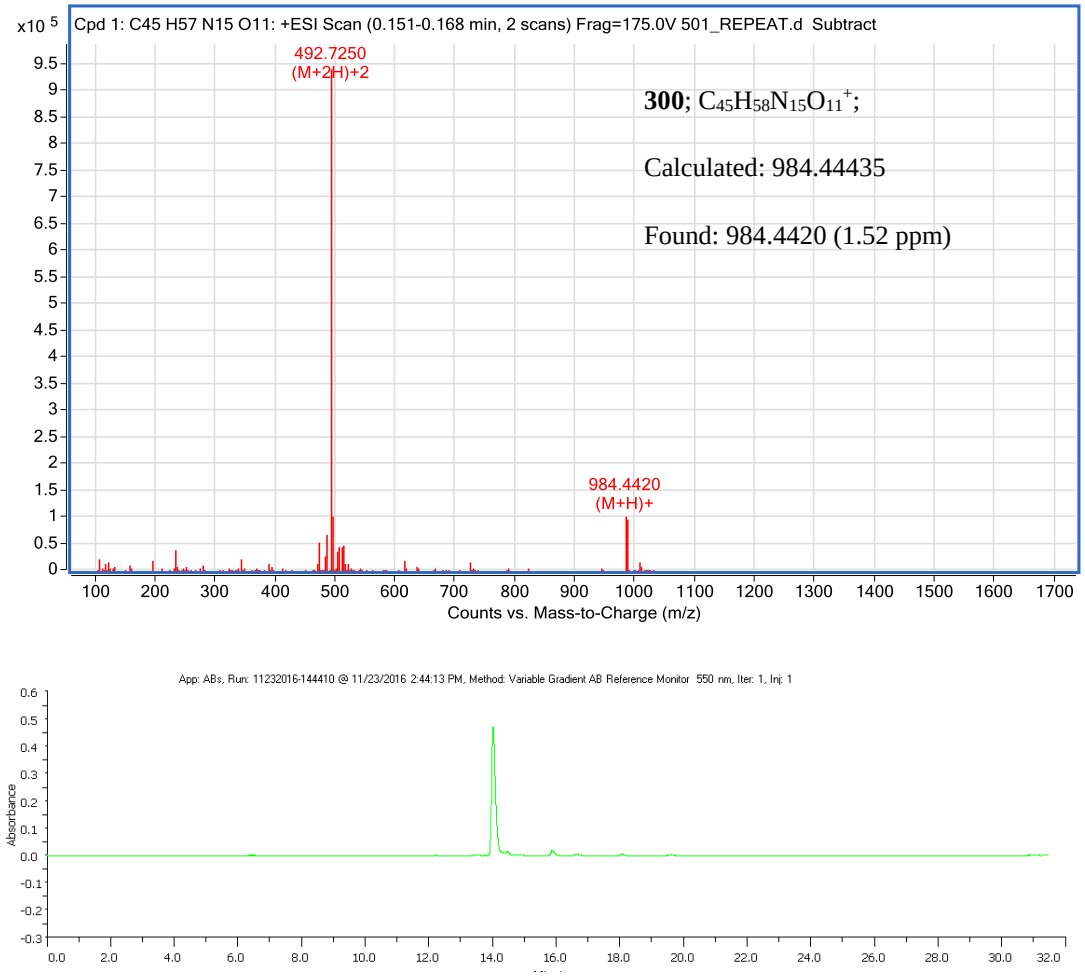

*Figure 78: HRMS and HPLC data of the conjugate **300**; 0-100% gradient of H2O/CH3CN, with 1% TFA, absorption monitored at 256 nm.*

Ac-SRK(triazole-AB)RGDS-NH_2 ***303***

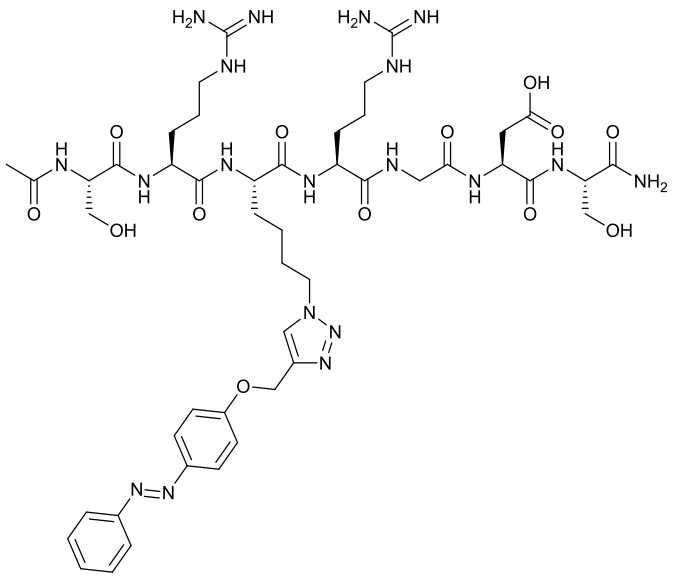

Method 1: The supported peptide Ac-SRK(N_3)RGDS-resin **302** (0.16 mmol) was manually synthesised using the Fmoc SPPS protocol on a rink amide resin. A solution of 4-propargylated azobenzene **107** (0.106 g, 0.45 mmol), copper sulphate (0.037 g, 0.15 mmol) and sodium ascorbate (0.030 g, 0.15mmol) in DMF/H_2O (5:1, 6 mL) was added to a SPPS vessel containing supported azido peptide **302** (Ac-SRK(N_3)RGDS-resin) (0.16 mmol). The reaction mixture was agitated for 1 hour, the solution was then drained from the vessel and the resin was washed with DMF (3 x 5 mL), DCM (3 x 5 mL), DMF (3x 5 mL) and DCM (3 x 5 mL). The resin was agitated in a solution of TFA and water (9.5:5; 7 mL) for 1.5 hour. The solution containing the cleaved and deprotected peptide was drained into a 15 mL falcon tube and air was blown over the solution until the volume was reduced to 2 mL. Diethyl ether was added dropwise until no more precipitate formed. The precipitate was pelleted by centrifugation (5 mins, 2800 rpm) and the remaining liquid was decanted. Further ether was added to the pellet was dispersed through agitation and sonication. The pellet was regenerated from the suspension by centrifugation (5 mins, 2800 rpm) and removal of the liquid, this process was repeated once more. The pellet was then dissolved in distilled water (1.5 mL) and a minimum of acetonitrile (~1 mL), the resulting solution was lyophilised to give the crude product as a light yellow solid. The residue was dissolved in distilled water and acetonitrile (1:1, 2 mL) and the resulting yellow solution was purified by semi-

preparative HPLC. The HPLC fractions were then combined and lyophilised to give the product **303** as an orange solid (56%).

Method 2: The supported peptide Ac-SRK(N_3)RGDS-resin **302** (0.16 mmol) was manually synthesised using the Fmoc SPPS protocol on a rink amide resin. The resin bound azidopeptide **302** (Ac-SRK(N_3)RGDS-resin) (0.16 mmol) was agitated in a solution of TFA, TIS and water (95: 2.5: 2.5; 6 mL) for 1.5 hour. The solution of containing the cleaved and deprotected peptide was drained into a 15 mL falcon tube and air was blown over the solution until the volume was reduced to ~2 mL. Diethyl ether was added dropwise until no more precipitate formed. The precipitate was pelleted by centrifugation (5 mins, 2800 rpm) and the remaining liquid was decanted. Further ether was added to the pellet was dispersed through agitation and sonication. The pellet was regenerated from the suspension by centrifugation (5 mins, 2800 rpm) and removal of the liquid, this process was repeated once more. The resulting white solid was then dissolved in DMF (5 mL) and propargylated azobenzene **107** (0.106 g, 0.45 mmol) was added. To this as solution of $CuSO_4$. $5H_2O$ (0.111 g, 0.45 mmol) and sodium ascorbate (0.091 g, 0.45 mmol) in distilled water (1 mL) was added. The resulting reaction mixture was left to stir over night. The solvent was removed under vacuum without heating. The residue was dissolved in TFA (5 mL) and diethyl ether was added until no more precipitated formed. The precipitate was pelleted by centrifugation (5 mins, 2800 rpm) and the remaining liquid was decanted. Further ether was added to the pellet was dispersed through agitation and sonication. The pellet was regenerated from the suspension by centrifugation (5 mins, 2800 rpm) and removal of the liquid, this process was repeated once more. The pellet was then dissolved in distilled water (1 mL) and a minimum of acetonitrile (~1 mL). The resulting solution was lyophilised to give the crude product as a light yellow solid. The material was dissolved in distilled water and acetonitrile (1:1, 2 mL) and the resulting yellow solution was purified by semi-preparative HPLC. The HPLC fractions were combined and lyophilised to give the product **303** as an orange solid (14%).

HRMS (direct injection) $[M+H]^+$, $[C_{47}H_{70}N_{19}O_{13}]^+$ calculated: 1108.5395, found: 1108.5432; difference: 3.34 ppm

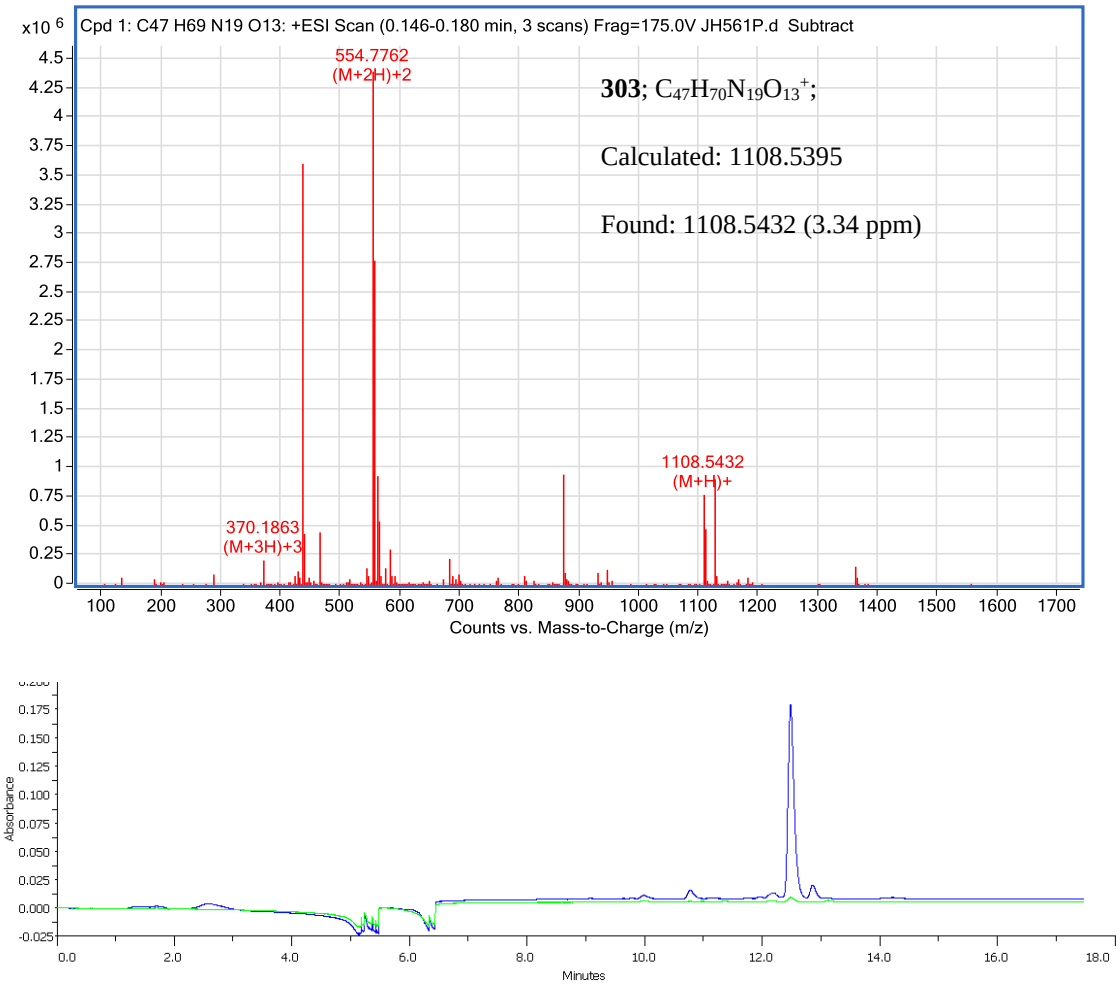

*Figure 79: HRMS and HPLC data for the conjugate **303**; 0-100% gradient of H2O/CH3CN, with 1% TFA, absorption monitored at 256 nm.*

Ac-RGDS(isoxazole-AB)TF-NH2 ***304***

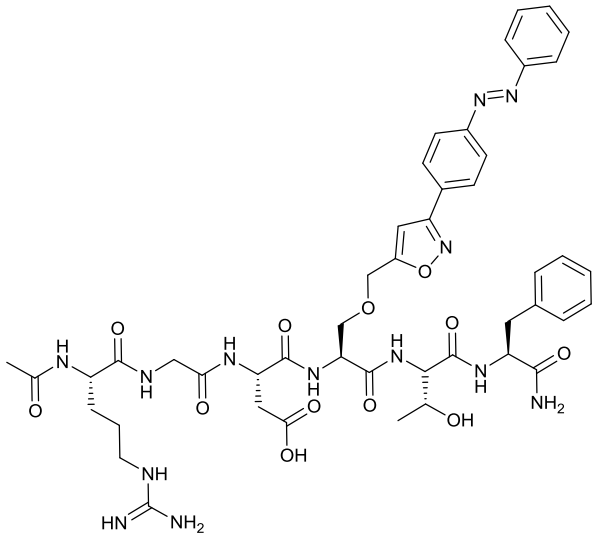

The supported peptide Ac-RGDS*TF-resin **297** (0.31 mmol) was manually synthesised using the Fmoc SPPS protocol on a rink amide resin. A solution of the chlorooxime **174** (241 mg, 0.93 mmol) and NEt_3 (0.17 ml, 1.2 mmol) in DMF/H_2O (7:1, 8 mL) was added to a SPPS vessel containing supported propargylated peptide **297** (RGDS*TF-resin). The reaction mixture was agitated for 30 minutes, the solution was drained from the vessel and the resin was washed with DMF (3 x 5 mL), DCM (3 x 5 mL) and DMF (3x 5 mL). A second solution of the chlorooxime **174** (241 mg, 0.93 mmol) and NEt_3 (0.17 ml, 1.2 mmol) in DMF/H_2O (7:1, 8 mL) was added to resin followed by a further 30 minutes of agitation. The solution was drained from the vessel and the resin was washed with DMF (3 x 5 mL), DCM (3 x 5 mL), DMF (3x 5 mL) and DCM (3 x 5 mL). The resin was agitated in a solution of TFA and water (95: 5; 8 mL) for 1 hour. The solution of containing the cleaved and deprotected peptide was decanted into a 15 mL falcon tube and air was blown over the solution until the volume was reduce to ~2 mL. Diethyl ether was added dropwise until no more precipitate formed. The precipitate was pelleted by centrifugation (5 mins, 2800 rpm) and the remaining liquid was decanted. Further ether was added to the pellet was dispersed through agitation and sonication. The pellet was regenerated from the suspension by centrifugation (5 mins, 2800 rpm) and removal of the liquid, this process was repeated once more. The pellet was dissolved in distilled water (2 mL) and a minimum of acetonitrile (~0.5 mL), the resulting solution was lyophilised to give the crude product as a faintly orange solid. The residue was then

dissolved in distilled water and acetonitrile (1:1, 2.5 mLs) and the resulting a pale yellow solution was purified by semi-preparative HPLC. The HPLC fractions were combined and lyophilised to give the product **304** as an orange solid (13%).

HRMS (direct injection) $[M+H]^+$, $[C_{46}H_{58}N_{13}O_{12}]^+$ calculated: 984.4322, found: 984.4353; difference: 3.15 ppm

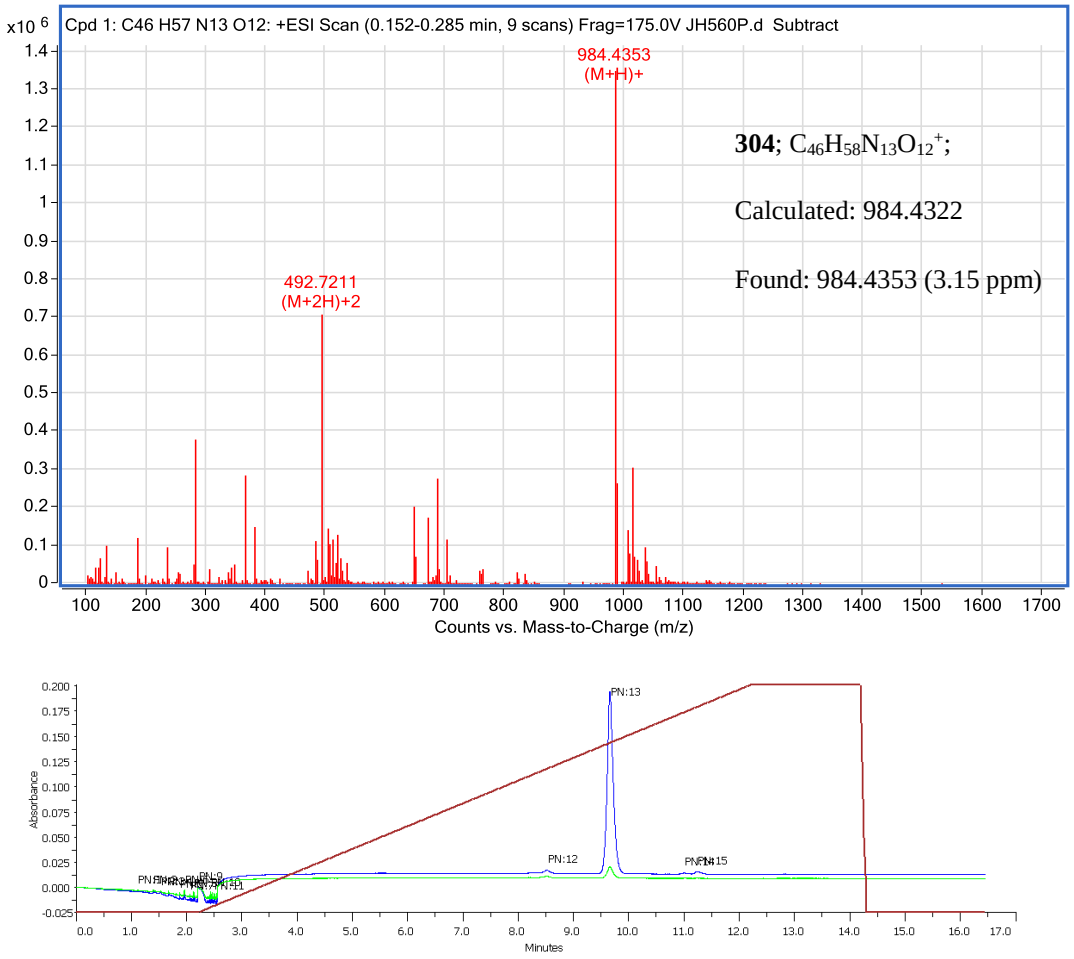

*Figure 80: HRMS and HPLC data for the conjugate **304**; 0-100% gradient of H2O/CH3CN, with 1% TFA, absorption monitored at 256 nm.*

Man-triazole-AB-GRGDG-NH2 ***306***

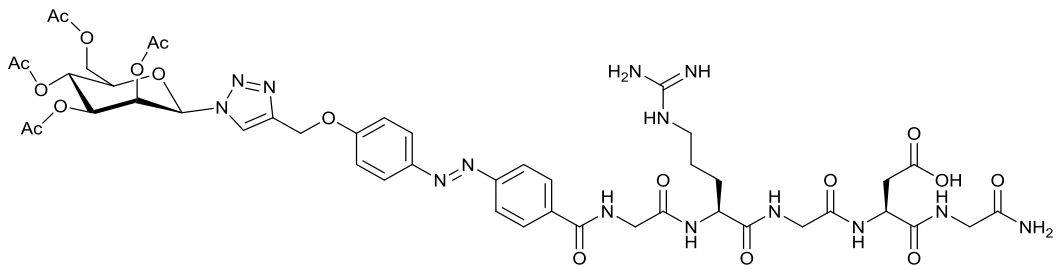

The supported peptide H-GRGDG-Resin **291** (0.31 mmol) was manually synthesised using the Fmoc SPPS protocol on a rink amide resin. A solution of the propargylated azobenzene **152** (0.315 g, 0.933 mmol, 3 eq.) PyBOP (486 mg, 0.933 mmol) and NMM (1.89 g, 0.205ml, 1.866 mmol, 6 eq.) in DMF (5mL) was added to a SPPS vessel containing the resin bound peptide **291**. The SPPS vessel was agitated for 40 minutes. The vessel was drained of the reaction solution and the resin was washed with DMF (3 x 5 mL), DCM (3 x 5 mL), DMF (3x 5 mL) and DCM (3 x 5 mL). A solution of azidogalactose **255** (347 mg, 0.93 mmol), copper sulphate (75 mg, 0.3 mmol) and sodium ascorbate (59 mg, 0.3 mmol) in DMF/H_2O (7:1, 8 mL) was added to a SPPS vessel containing the on resin propargylated azobenzene peptide **305**. The reaction mixture was agitated for 3 hours at room temprature. The solution was drained from the vessel and the resin was washed with DMF (3 x 5 mL), DCM (3 x 5 mL), DMF (3x 5 mL) and DCM (3 x 5 mL).

The resin was agitated in a solution of TFA, and water (9.5:5; 8 mL) for 1 hour. The solution of containing the cleaved peptide was then drained into a 15 mL falcon tube and air was blown over the solution until the volume was reduced to ~2 mL. Diethyl ether was added dropwise until no more precipitate formed. The precipitate was pelleted by centrifugation (5 mins, 2800 rpm) and the remaining liquid was decanted. Further ether was added to the pellet was dispersed through agitation and sonication. The pellet was regenerated from the suspension by centrifugation (5 mins, 2800 rpm) and removal of the liquid, this process was repeated once more. The pellet was then dissolved in distilled water (2 ml) and a minimum of acetonitrile (~2 mL), the resulting solution was lyophilised to give the crude product. The crude product was subjected to purifaction by semi-preparative HPLC. The HPLC fractions were combined and lyophilised to give the product as an orange solid (24%).

HRMS (direct injection) $[M+H]^+$, $[C_{47}H_{60}N_{12}O_{19}]^+$ calculated: 1095.4014, found: 1095.4191; difference: 1.62 ppm

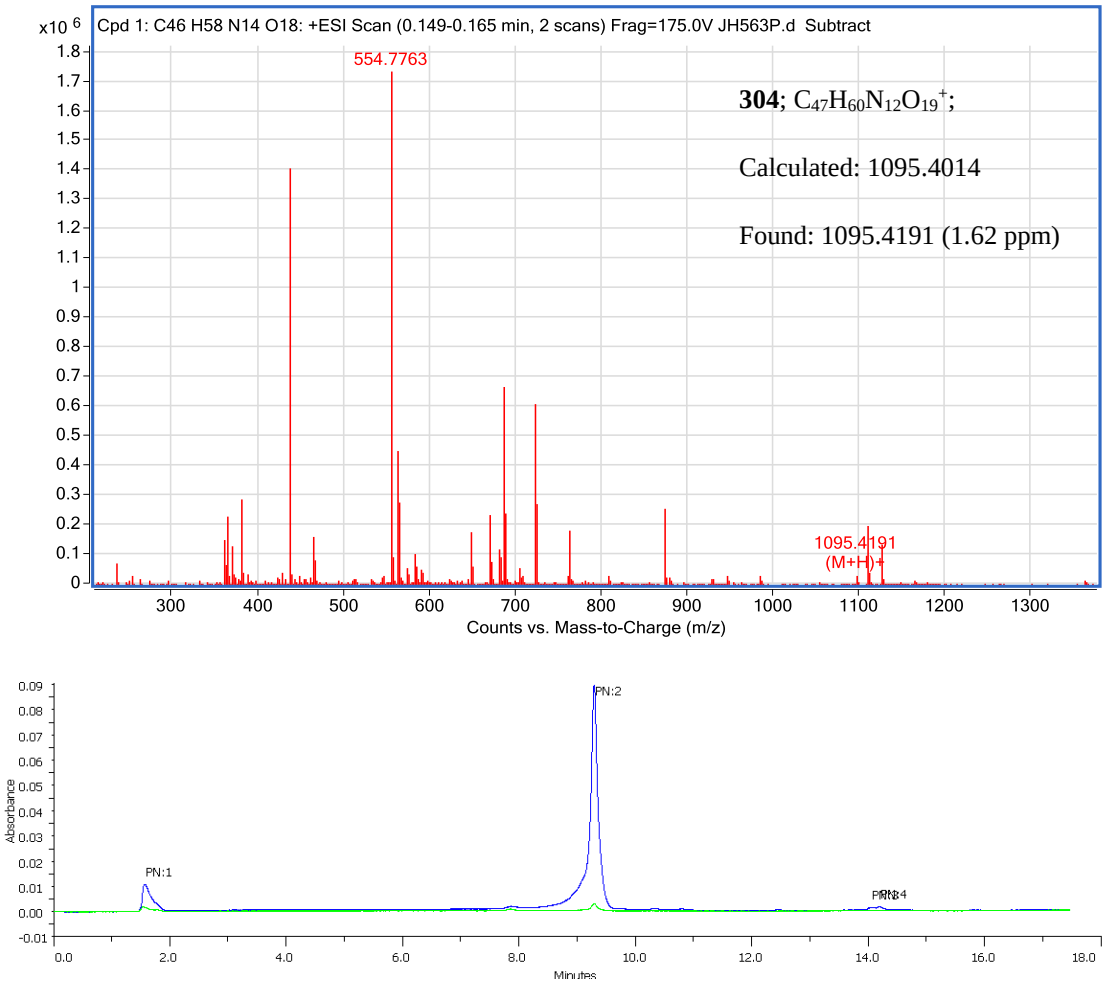

*Figure 81: HRMS and HPLC data for the conjugate **306**; 0-100% gradient of H2O/CH3CN, with 1% TFA, absorption monitored at 256 nm.*

(1) Pathem, B. K.; Claridge, S. A.; Zheng, Y. B.; Weiss, P. S. *Annu. Rev. Phys. Chem.* **2013**, *64*, 605.

(2) Grunder, S.; McGrier, P. L.; Whalley, A. C.; Boyle, M. M.; Stern, C.; Stoddart, J. F. *J. Am. Chem. Soc.* **2013**, *135*, 17691.

(3) Zhang, L.; Han, B.; Li, T.; Wang, E. *Chem. Commun.* **2011**, *47*, 3099.

(4) Goswami, S.; Aich, K.; Das, S.; Das, A. K.; Sarkar, D.; Panja, S.; Mondal, T. K.; Mukhopadhyay, S. *Chem. Commun.* **2013**, *49*, 10739.

(5) Chiang, W.-L.; Lin, T.-T.; Sureshbabu, R.; Chia, W.-T.; Hsiao, H.-C.; Liu, H.-Y.; Yang, C.-M.; Sung, H.-W. *J. Controlled Release* **2015**, *199*, 53.

(6) Nozaki, D.; Cuniberti, G. *Nano Research* **2009**, *2*, 648.

(7) Shiraishi, Y.; Tokitoh, Y.; Nishimura, G.; Hirai, T. *Org. Lett.* **2005**, *7*, 2611.

(8) Koshland, D. E. *Proc. Natl. Acad. Sci. U. S. A.* **1958**, *44*, 98.

(9) Smith, A. M.; Mancini, M. C.; Nie, S. *Nat Nano* **2009**, *4*, 710.

(10) Baylor, D. *Proc. Natl. Acad. Sci.* **1996**, *93*, 560.

(11) Baker, E. H. *J. Chem. Soc.* **1952**, 4518.

(12) Beyer, C.; Wagenknecht, H.-A. *J. Org. Chem.* **2010**, *75*, 2752.

(13) Klajn, R. *Chem. Soc. Rev.* **2014**, *43*, 148.

(14) Lee, C. K.; Davis, D. A.; White, S. R.; Moore, J. S.; Sottos, N. R.; Braun, P. V. *J. Am. Chem. Soc.* **2010**, *132*, 16107.

(15) Edahiro, J.-i.; Sumaru, K.; Takagi, T.; Shinbo, T.; Kanamori, T. *Langmuir* **2006**, *22*, 5224.

(16) Zhu, M.-Q.; Zhu, L.; Han, J. J.; Wu, W.; Hurst, J. K.; Li, A. D. Q. *J. Am. Chem. Soc.* **2006**, *128*, 4303.

(17) Lee, H.-i.; Wu, W.; Oh, J. K.; Mueller, L.; Sherwood, G.; Peteanu, L.; Kowalewski, T.; Matyjaszewski, K. *Angew. Chem. Int. Ed.* **2007**, *46*, 2453.

(18) Potisek, S. L.; Davis, D. A.; Sottos, N. R.; White, S. R.; Moore, J. S. *J. Am. Chem. Soc.* **2007**, *129*, 13808.

(19) Park, Y. S.; Ito, Y.; Imanishi, Y. *Macromolecules* **1998**, *31*, 2606.

(20) Zhu, M.-Q.; Zhang, G.-F.; Hu, Z.; Aldred, M. P.; Li, C.; Gong, W.-L.; Chen, T.; Huang, Z.-L.; Liu, S. *Macromolecules* **2014**, *47*, 1543.

(21) Zhu, J.-F.; Yuan, H.; Chan, W.-H.; Lee, A. W. M. *Tetrahedron Lett.* **2010**, *51*, 3550.

(22) Shao, N.; Jin, J. Y.; Wang, H.; Zhang, Y.; Yang, R. H.; Chan, W. H. *Anal. Chem.* **2008**, *80*, 3466.

(23) Sakata, T.; Jackson, D. K.; Mao, S.; Marriott, G. *J. Org. Chem.* **2008**, *73*, 227.

(24) Natali, M.; Giordani, S. *Org. Biomol. Chem.* **2012**, *10*, 1162.

(25) Zhu, M.-Q.; Zhang, G.-F.; Li, C.; Aldred, M. P.; Chang, E.; Drezek, R. A.; Li, A. D. Q. *J. Am. Chem. Soc.* **2011**, *133*, 365.

(26) Chan, Y.-H.; Gallina, M. E.; Zhang, X.; Wu, I. C.; Jin, Y.; Sun, W.; Chiu, D. T. *Anal. Chem.* **2012**, *84*, 9431.

(27) Chen, L.; Zhu, Y.; Yang, D.; Zou, R.; Wu, J.; Tian, H. *Scientific Reports* **2014**, *4*, 6860.

(28) Chen, L.; Wu, J.; Schmuck, C.; Tian, H. *Chem. Commun.* **2014**, *50*, 6443.

(29) Angelini, N.; Corrias, B.; Fissi, A.; Pieroni, O.; Lenci, F. *Biophys. J.* **1998**, *74*, 2601.

(30) Fujimoto, K.; Amano, M.; Horibe, Y.; Inouye, M. *Org. Lett.* **2006**, *8*, 285.

(31) Sakata, T.; Yan, Y.; Marriott, G. *Proc. Natl. Acad. Sci. U. S. A.* **2005**, *102*, 4759.

(32) Irie, M.; Mohri, M. *J. Org. Chem.* **1988**, *53*, 803.

(33) Kellogg, R. M.; Groen, M. B.; Wynberg, H. *J. Org. Chem.* **1967**, *32*, 3093.

(34) Tosic, O.; Altenhoner, K.; Mattay, J. *Photochemical & Photobiological Sciences* **2010**, *9*, 128.

(35) Irie, M.; Sakemura, K.; Okinaka, M.; Uchida, K. *J. Org. Chem.* **1995**, *60*, 8305.

(36) Irie, M. *Chem. Rev.* **2000**, *100*, 1685.

(37) Uchida, K.; Takata, A.; Saito, M.; Murakami, A.; Nakamura, S.; Irie, M. *Adv. Mater.* **2003**, *15*, 785.

(38) Uchida, K.; Saito, M.; Murakami, A.; Nakamura, S.; Irie, M. *Adv. Mater.* **2003**, *15*, 121.

(39) Matsuda, K.; Irie, M. *J. Am. Chem. Soc.* **2000**, *122*, 7195.

(40) Tsujioka, T.; Masuda, K. *Appl. Phys. Lett.* **2003**, *83*, 4978.

(41) Li, Y.; Urbas, A.; Li, Q. *J. Am. Chem. Soc.* **2012**, *134*, 9573.

(42) Vomasta, D.; Högner, C.; Branda, N. R.; König, B. *Angew. Chem. Int. Ed.* **2008**, *47*, 7644.

(43) Al-Atar, U.; Fernandes, R.; Johnsen, B.; Baillie, D.; Branda, N. R. *J. Am. Chem. Soc.* **2009**, *131*, 15966.

(44) Singer, M.; Jäschke, A. *J. Am. Chem. Soc.* **2010**, *132*, 8372.

(45) Rau, H. *Angew. Chem. Int. Ed.* **1973**, *12*, 224.

(46) Wei-Guang Diau, E. *J. Phys. Chem. A* **2004**, *108*, 950.

(47) Crecca, C. R.; Roitberg, A. E. *J. Phys. Chem. A* **2006**, *110*, 8188.

(48) Rau, H.; Lueddecke, E. *J. Am. Chem. Soc.* **1982**, *104*, 1616.

(49) Griffiths, J. *Chem. Soc. Rev.* **1972**, *1*, 481.

(50) Tamai, N.; Miyasaka, H. *Chem. Rev.* **2000**, *100*, 1875.

(51) Bandara, H. M. D.; Burdette, S. C. *Chem. Soc. Rev.* **2012**, *41*, 1809.

(52) Forber, C. L.; Kelusky, E. C.; Bunce, N. J.; Zerner, M. C. *J. Am. Chem. Soc.* **1985**, *107*, 5884.

(53) Lednev, I. K.; Ye, T. Q.; Matousek, P.; Towrie, M.; Foggi, P.; Neuwahl, F. V. R.; Umapathy, S.; Hester, R. E.; Moore, J. N. *Chem. Phys. Lett.* **1998**, *290*, 68.

(54) Bortolus, P.; Monti, S. *J. Phys. Chem.* **1979**, *83*, 648.

(55) Bandara, H. M. D.; Friss, T. R.; Enriquez, M. M.; Isley, W.; Incarvito, C.; Frank, H. A.; Gascon, J.; Burdette, S. C. *J. Org. Chem.* **2010**, *75*, 4817.

(56) Tan, E. M. M.; Amirjalayer, S.; Smolarek, S.; Vdovin, A.; Zerbetto, F.; Buma, W. J. *Nature Communications* **2015**, *6*, 5860.

(57) Shao, J.; Lei, Y.; Wen, Z.; Dou, Y.; Wang, Z. *J. Chem. Phys.* **2008**, *129*, 164111.

(58) Böckmann, M.; Doltsinis, N. L.; Marx, D. *J. Phys. Chem. A* **2010**, *114*, 745.

(59) Yuan, S.; Dou, Y.; Wu, W.; Hu, Y.; Zhao, J. *J. Phys. Chem. A* **2008**, *112*, 13326.

(60) Ciminelli, C.; Granucci, G.; Persico, M. *Chem. Eur. J.* **2004**, *10*, 2327.

(61) Fischer, E.; Frankel, M.; Wolovsky, R. *J. Chem. Phys.* **1955**, *23*, 1367.

(62) Yoshii, K.; Machida, S.; Horie, K. *J. Polym. Sci., Part B: Polym. Phys.* **2000**, *38*, 3098.

(63) Dokić, J.; Gothe, M.; Wirth, J.; Peters, M. V.; Schwarz, J.; Hecht, S.; Saalfrank, P. *J. Phys. Chem. A* **2009**, *113*, 6763.

(64) Blevins, A. A.; Blanchard, G. J. *J. Phys. Chem. B* **2004**, *108*, 4962.

(65) Toro, C.; Thibert, A.; De Boni, L.; Masunov, A. E.; Hernández, F. E. *J. Phys. Chem. B* **2008**, *112*, 929.

(66) Tsuji, T.; Takashima, H.; Takeuchi, H.; Egawa, T.; Konaka, S. *J. Phys. Chem. A* **2001**, *105*, 9347.

(67) Fliegl, H.; Köhn, A.; Hättig, C.; Ahlrichs, R. *J. Am. Chem. Soc.* **2003**, *125*, 9821.

(68) Kusebauch, U.; Cadamuro, S. A.; Musiol, H.-J.; Lenz, M. O.; Wachtveitl, J.; Moroder, L.; Renner, C. *Angew. Chem. Int. Ed.* **2006**, *45*, 7015.

(69) Beharry, A. A.; Woolley, G. A. *Chem. Soc. Rev.* **2011**, *40*, 4422.

(70) Sano, M.; Amaike, M.; Kamino, A.; Shinkai, S. *Langmuir* **2001**, *17*, 4367.

(71) Laurent, N.; Lafont, D.; Dumoulin, F.; Boullanger, P.; Mackenzie, G.; Kouwer, P. H.; Goodby, J. W. *J. Am. Chem. Soc.* **2003**, *125*, 15499.

(72) Ashby, J. *Br J Cancer* **1978**, *37*, 904.

(73) Lis Arias, M. J.; Girardi, E.; Navarro, J. A.; Savarino, P.; Valldeperas, J.; Viscardi, G. *Dyes and Pigments* **2000**, *46*, 37.

(74) Hu, Y.; Marlow, J. B.; Ramanathan, R.; Zou, W.; Tiew, H. G.; Pottage, M. J.; Bansal, V.; Tabor, R. F.; Wilkinson, B. L. *Aust. J. Chem.* **2015**, *68*, 1880.

(75) Srinivas, O.; Mitra, N.; Surolia, A.; Jayaraman, N. *Glycobiology* **2005**, *15*, 861.

(76) Weber, T.; Chandrasekaran, V.; Stamer, I.; Thygesen, M. B.; Terfort, A.; Lindhorst, T. K. *Angew. Chem. Int. Ed.* **2014**, *53*, 14583.

(77) Mockl, L.; Muller, A.; Brauchle, C.; Lindhorst, T. K. *Chem. Commun.* **2016**, *52*, 1254.

(78) Ma, X.; Wang, Q. C.; Tian, H. *Tetrahedron Lett.* **2007**, *48*, 7112.

(79) Ueno, A.; Kuwabara, T.; Nakamura, A.; Toda, F. *Nature* **1992**, *356*, 136.

(80) Fujimoto, T.; Nakamura, A.; Inoue, Y.; Sakata, Y.; Kaneda, T. *Tetrahedron Lett.* **2001**, *42*, 7987.

(81) Willner, I.; Rubin, S.; Riklin, A. *J. Am. Chem. Soc.* **1991**, *113*, 3321.

(82) Banghart, M. R.; Mourot, A.; Fortin, D. L.; Yao, J. Z.; Kramer, R. H.; Trauner, D. *Angew. Chem. Int. Ed.* **2009**, *48*, 9097.

(83) Fortin, D. L.; Banghart, M. R.; Dunn, T. W.; Borges, K.; Wagenaar, D. A.; Gaudry, Q.; Karakossian, M. H.; Otis, T. S.; Kristan, W. B.; Trauner, D.; Kramer, R. H. *Nat Methods* **2008**, *5*, 331.

(84) Jog, P. V.; Gin, M. S. *Org. Lett.* **2008**, *10*, 3693.

(85) Volgraf, M.; Gorostiza, P.; Numano, R.; Kramer, R. H.; Isacoff, E. Y.; Trauner, D. *Nat Chem Biol* **2006**, *2*, 47.

(86) Kramer, R. H.; Chambers, J. J.; Trauner, D. *Nat Chem Biol* **2005**, *1*, 360.

(87) Flint, D. G.; Kumita, J. R.; Smart, O. S.; Woolley, G. A. *Chemistry & Biology* **2002**, *9*, 391.

(88) Kumita, J. R.; Smart, O. S.; Woolley, G. A. *Proc Natl Acad Sci U S A* **2000**, *97*, 3803.

(89) Schierling, B.; Noël, A.-J.; Wende, W.; Hien, L. T.; Volkov, E.; Kubareva, E.; Oretskaya, T.; Kokkinidis, M.; Römpp, A.; Spengler, B.; Pingoud, A. *Proc. Natl. Acad. Sci.* **2010**, *107*, 1361.

(90) Renner, C.; Kusebauch, U.; Loweneck, M.; Milbradt, A. G.; Moroder, L. *J Pept Res* **2005**, *65*, 4.

(91) Behrendt, R.; Schenk, M.; Musiol, H. J.; Moroder, L. *J. Pept. Sci.* **1999**, *5*, 519.

(92) Dong, S. L.; Loweneck, M.; Schrader, T. E.; Schreier, W. J.; Zinth, W.; Moroder, L.; Renner, C. *Chemistry* **2006**, *12*, 1114.

(93) Tan, Z.-J.; Chen, S.-J. *Biophys. J.* **2008**, *95*, 738.

(94) Mathews, D. H.; Sabina, J.; Zuker, M.; Turner, D. H. *J. Mol. Biol.* **1999**, *288*, 911.

(95) Diguet, A.; Mani, N. K.; Geoffroy, M.; Sollogoub, M.; Baigl, D. *Chem. Eur. J.* **2010**, *16*, 11890.

(96) Dohno, C.; Uno, S.-n.; Nakatani, K. *J. Am. Chem. Soc.* **2007**, *129*, 11898.

(97) Yamana, K.; Yoshikawa, A.; Nakano, H. *Tetrahedron Lett.* **1996**, *37*, 637.

(98) Asanuma, H.; Ito, T.; Yoshida, T.; Liang, X.; Komiyama, M. *Angew. Chem. Int. Ed.* **1999**, *38*, 2393.

(99) Liang, X.; Asanuma, H.; Kashida, H.; Takasu, A.; Sakamoto, T.; Kawai, G.; Komiyama, M. *J. Am. Chem. Soc.* **2003**, *125*, 16408.

(100) Liu, Y.; Sen, D. *J. Mol. Biol.* **2004**, *341*, 887.

(101) Matsunaga, D.; Asanuma, H.; Komiyama, M. *J. Am. Chem. Soc.* **2004**, *126*, 11452.

(102) Goldau, T.; Murayama, K.; Brieke, C.; Steinwand, S.; Mondal, P.; Biswas, M.; Burghardt, I.; Wachtveitl, J.; Asanuma, H.; Heckel, A. *Chem. Eur. J.* **2015**, *21*, 2845.

(103) Chandrasekaran, V.; Jacob, H.; Petersen, F.; Kathirvel, K.; Tuczek, F.; Lindhorst, T. K. *Chem. Eur. J.* **2014**, *20*, 8744.

(104) Fraser-Reid, B.; Wu, Z.; Udodong, U. E.; Ottosson, H. *J. Org. Chem.* **1990**, *55*, 6068.

(105) Kleine, H. P.; Weinberg, D. V.; Kaufman, R. J.; Sidhu, R. S. *Carbohydr. Res.* **1985**, *142*, 333.

(106) Boutureira, O.; Bernardes, G. J. L. *Chem. Rev.* **2015**, *115*, 2174.

(107) Northrop, B. H.; Frayne, S. H.; Choudhary, U. *Polymer Chemistry* **2015**, *6*, 3415.

(108) Wu, D.; Dong, M.; Collins, C. V.; Babalhavaeji, A.; Woolley, G. A. *Advanced Optical Materials* **2016**, *4*, 1402.

(109) Shishido, H.; Yamada, M. D.; Kondo, K.; Maruta, S. *The Journal of Biochemistry* **2009**, *146*, 581.

(110) Patel, M. H.; Oswal, S. B. *International Journal of Polymeric Materials and Polymeric Biomaterials* **2011**, *60*, 542.

(111) Schlick, T. L.; Ding, Z.; Kovacs, E. W.; Francis, M. B. *J. Am. Chem. Soc.* **2005**, *127*, 3718.

(112) Hooker, J. M.; Kovacs, E. W.; Francis, M. B. *J. Am. Chem. Soc.* **2004**, *126*, 3718.

(113) Asanuma, H.; Ito, T.; Komiyama, M. *Tetrahedron Lett.* **1998**, *39*, 9015.

(114) Asanuma, H.; Liang, X.; Nishioka, H.; Matsunaga, D.; Liu, M.; Komiyama, M. *Nat. Protocols* **2007**, *2*, 203.

(115) Lan, T.; McLaughlin, L. W. *J. Am. Chem. Soc.* **2000**, *122*, 6512.

(116) Kolb, H. C.; Finn, M. G.; Sharpless, K. B. *Angew. Chem. Int. Ed.* **2001**, *40*, 2004.

(117) Kozikowski, A. P.; Chen, Y. Y. *J. Org. Chem.* **1981**, *46*, 5248.

(118) Tornøe, C. W.; Christensen, C.; Meldal, M. *J. Org. Chem.* **2002**, *67*, 3057.

(119) Boren, B. C.; Narayan, S.; Rasmussen, L. K.; Zhang, L.; Zhao, H.; Lin, Z.; Jia, G.; Fokin, V. V. *J. Am. Chem. Soc.* **2008**, *130*, 8923.

(120) Banerji, B.; Chandrasekhar, K.; Killi, S. K.; Pramanik, S. K.; Uttam, P.; Sen, S.; Maiti, N. C. *R. Soc. Open Sci.* **2016**, *3*.

(121) Himo, F.; Lovell, T.; Hilgraf, R.; Rostovtsev, V. V.; Noodleman, L.; Sharpless, K. B.; Fokin, V. V. *J. Am. Chem. Soc.* **2005**, *127*, 210.

(122) Makarem, A.; Berg, R.; Rominger, F.; Straub, B. F. *Angew. Chem. Int. Ed.* **2015**, *54*, 7431.

(123) Worrell, B. T.; Malik, J. A.; Fokin, V. V. *Science* **2013**, *340*, 457.

(124) Tiwari, V. K.; Mishra, B. B.; Mishra, K. B.; Mishra, N.; Singh, A. S.; Chen, X. *Chem. Rev.* **2016**, *116*, 3086.

(125) Ahmad Fuaad, A.; Azmi, F.; Skwarczynski, M.; Toth, I. *Molecules* **2013**, *18*, 13148.

(126) Horne, W. S.; Yadav, M. K.; Stout, C. D.; Ghadiri, M. R. *J. Am. Chem. Soc.* **2004**, *126*, 15366.

(127) El-Sagheer, A. H.; Brown, T. *Acc. Chem. Res.* **2012**, *45*, 1258.

(128) El-Sagheer, A. H.; Brown, T. *Chem. Soc. Rev.* **2010**, *39*, 1388.

(129) Chandrasekaran, V.; Lindhorst, T. K. *Chem. Commun.* **2012**, *48*, 7519.

(130) Liu, Y.; Yang, Z.-X.; Chen, Y. *J. Org. Chem.* **2008**, *73*, 5298.

(131) Casas-Solvas, J. M.; Martos-Maldonado, M. C.; Vargas-Berenguel, A. *Tetrahedron* **2008**, *64*, 10919.

(132) Müller, A.; Lindhorst, T. K. *Eur. J. Org. Chem.* **2016**, *2016*, 1669.

(133) Huisgen, R. *J. Org. Chem.* **1976**, *41*, 403.

(134) Pasinszki, T.; Hajgato, B.; Havasi, B.; Westwood, N. P. C. *PCCP* **2009**, *11*, 5263.

(135) Nguyen Minh, T.; Malone, S.; Hegarty, A. F.; Williams, I. I. *J. Org. Chem.* **1991**, *56*, 3683.

(136) Mukaiyama, T.; Hoshino, T. *J. Am. Chem. Soc.* **1960**, *82*, 5339.

(137) Erik Larsen, K.; Torssell, K. B. G. *Tetrahedron* **1984**, *40*, 2985.

(138) Gołebiewski, W.; Gucma, M. *Synthesis* **2007**, *2007*, 3599.

(139) Kesornpun, C.; Aree, T.; Mahidol, C.; Ruchirawat, S.; Kittakoop, P. *Angew. Chem. Int. Ed.* **2016**, *55*, 3997.

(140) Chiang, Y.-H. *J. Org. Chem.* **1971**, *36*, 2146.

(141) Kang, K. H.; Pae, A. N.; Choi, K. I.; Cho, Y. S.; Chung, B. Y.; Lee, J. E.; Jung, S. H.; Koh, H. Y.; Lee, H.-Y. *Tetrahedron Lett.* **2001**, *42*, 1057.

(142) Stevens, R. V.; Beaulieu, N.; Chan, W. H.; Daniewski, A. R.; Takeda, T.; Waldner, A.; Williard, P. G.; Zutter, U. *J. Am. Chem. Soc.* **1986**, *108*, 1039.

(143) Grundmann, C.; Richter, R. *J. Org. Chem.* **1968**, *33*, 476.

(144) Ahrens, H.; Lange, G.; Müller, T.; Rosinger, C.; Willms, L.; van Almsick, A. *Angew. Chem. Int. Ed.* **2013**, *52*, 9388.

(145) Galenko, A. V.; Khlebnikov, A. F.; Novikov, M. S.; Pakalnis, V. V.; Rostovskii, N. V. *Russian Chemical Reviews* **2015**, *84*, 335.

(146) Vinick, F. J.; Pan, Y.; Gschwend, H. W. *Tetrahedron Lett.* **1978**, *19*, 4221.

(147) Stork, G.; Mcmurry, J. E. *J. Am. Chem. Soc.* **1967**, *89*, 5464.

(148) Barco, A.; Benetti, S.; Pollini, G. P.; Baraldi, P. G.; Simoni, D.; Guarneri, M.; Gandolfi, C. *J. Org. Chem.* **1980**, *45*, 3141.

(149) Benltifa, M.; Hayes, J. M.; Vidal, S.; Gueyrard, D.; Goekjian, P. G.; Praly, J.-P.; Kizilis, G.; Tiraidis, C.; Alexacou, K.-M.; Chrysina, E. D.; Zographos, S. E.; Leonidas, D. D.; Archontis, G.; Oikonomakos, N. G. *Biorg. Med. Chem.* **2009**, *17*, 7368.

(150) Jawalekar, A. M.; Reubsaet, E.; Rutjes, F. P. J. T.; van Delft, F. L. *Chem. Commun.* **2011**, *47*, 3198.

(151) Heaney, F. *Eur. J. Org. Chem.* **2012**, *2012*, 3043.

(152) Mukherjee, S.; Mandal, S. B.; Bhattacharjya, A. *RSC Advances* **2012**, *2*, 8969.

(153) Sengupta, J.; Mukhopadhyay, R.; Bhattacharjya, A.; Bhadbhade, M. M.; Bhosekar, G. V. *J. Org. Chem.* **2005**, *70*, 8579.

(154) Shing, T. K. M.; Wong, W. F.; Cheng, H. M.; Kwok, W. S.; So, K. H. *Org. Lett.* **2007**, *9*, 753.

(155) Zlatopolskiy, B. D.; Kandler, R.; Kobus, D.; Mottaghy, F. M.; Neumaier, B. *Chem. Commun.* **2012**, *48*, 7134.

(156) Ning, X.; Temming, R. P.; Dommerholt, J.; Guo, J.; Ania, D. B.; Debets, M. F.; Wolfert, M. A.; Boons, G.-J.; van Delft, F. L. *Angew. Chem.* **2010**, *122*, 3129.

(157) Gutsmiedl, K.; Wirges, C. T.; Ehmke, V.; Carell, T. *Org. Lett.* **2009**, *11*, 2405.

(158) Singh, I.; Heaney, F. *Chem. Commun.* **2011**, *47*, 2706.

(159) Freeman, C.; Ni Cheallaigh, A.; Heaney, F. *Tetrahedron* **2011**, *67*, 7860.

(160) Merino, E. *Chemical Society Reviews* **2011**, *40*, 3835.

(161) Nystrom, R. F.; Brown, W. G. *Journal of the American Chemical Society* **1948**, *70*, 3738.

(162) Di Gioia, M. L.; Leggio, A.; Guarino, I. F.; Leotta, V.; Romio, E.; Liguori, A. *Tetrahedron Letters* **2015**, *56*, 5341.

(163) Srinivasa, G. R.; Abiraj, K.; Gowda, D. C. *Australian Journal of Chemistry* **2004**, *57*, 609.

(164) Surampudi, S. K.; Patel, H. R.; Nagarjuna, G.; Venkataraman, D. *Chemical Communications* **2013**, *49*, 7519.

(165) Khan, A.; Hecht, S. *Chemistry – A European Journal* **2006**, *12*, 4764.

(166) Flatt, A. K.; Dirk, S. M.; Henderson, J. C.; Shen, D. E.; Su, J.; Reed, M. A.; Tour, J. M. *Tetrahedron* **2003**, *59*, 8555.

(167) Baer, E.; Tosoni, A. L. *J. Am. Chem. Soc.* **1956**, *78*, 2857.

(168) Takeda, Y.; Okumura, S.; Minakata, S. *Angew. Chem. Int. Ed.* **2012**, *51*, 7804.

(169) Wawzonek, S.; McIntyre, T. W. *J. Electrochem. Soc.* **1972**, *119*, 1350.

(170) Saeid Farhadi, P. Z., Reza Zarei Sahamiehb *Acta Chim. Slov.* **2007**, *54*, 647.

(171) Fu, G.-D.; Xu, L.-Q.; Yao, F.; Li, G.-L.; Kang, E.-T. *ACS Applied Materials & Interfaces* **2009**, *1*, 2424.

(172) Willstätter, R.; Benz, M. *Berichte der deutschen chemischen Gesellschaft* **1906**, *39*, 3492.

(173) Wei, W.-h.; Tomohiro, T.; Kodaka, M.; Okuno, H. *J. Org. Chem.* **2000**, *65*, 8979.

(174) Shimogaki, T.; Oshita, S.; Matsumoto, A. *Macromol. Chem. Phys.* **2011**, *212*, 1767.

(175) Harvey, J. H.; Butler, B. K.; Trauner, D. *Tetrahedron Lett.* **2007**, *48*, 1661.

(176) Mei, X.; Yang, S.; Chen, D.; Li, N.; Li, H.; Xu, Q.; Ge, J.; Lu, J. *Chem. Commun.* **2012**, *48*, 10010.

(177) Steinwand, S.; Halbritter, T.; Rastädter, D.; Ortiz-Sánchez, J. M.; Burghardt, I.; Heckel, A.; Wachtveitl, J. *Chem. Eur. J.* **2015**, *21*, 15720.

(178) Baker, J.; Wolinski, K. *J. Mol. Model.* **2011**, *17*, 1335.

(179) Chambers, E. J.; Haworth, I. S. *J. Chem. Soc., Chem. Commun.* **1994**, 1631.

(180) Black, M.; Cadogan, J. I. G.; McNab, H. *Org. Biomol. Chem.* **2010**, *8*, 2961.

(181) Gund, S. H.; Shelkar, R. S.; Nagarkar, J. M. *RSC Advances* **2014**, *4*, 42947.

(182) Poloni, C.; Szymanski, W.; Feringa, B. L. *Chem. Commun.* **2014**, *50*, 12645.

(183) Freeman, C.; Vyle, J. S.; Heaney, F. *RSC Advances* **2013**, *3*, 1652.

(184) Freeman, C. *Thesis* **2012**.

(185) Ramón, R. S.; Bosson, J.; Díez-González, S.; Marion, N.; Nolan, S. P. *J. Org. Chem.* **2010**, *75*, 1197.

(186) Queiroz, L. H. K.; Giraudeau, P.; dos Santos, F. A. B.; de Oliveira, K. T.; Ferreira, A. G. *Magnetic Resonance in Chemistry* **2012**, *50*, 496.

(187) Masciello, L.; Potvin, P. G. *Canadian Journal of Chemistry* **2003**, *81*, 209.

(188) Nanasawa, M.; Nishiyama, T.; Kamogawa, H. *Polym. J.* **1991**, *23*, 127.

(189) Su, R.; Lü, L.; Zheng, S.; Jin, Y.; An, S. *Chemical Research in Chinese Universities* **2015**, *31*, 60.

(190) Kutonova, K. V.; Trusova, M. E.; Postnikov, P. S.; Filimonov, V. D.; Parello, J. *Synthesis* **2013**, *45*, 2706.

(191) Goyard, D.; Telligmann, S. M.; Goux-Henry, C.; Boysen, M. M. K.; Framery, E.; Gueyrard, D.; Vidal, S. *Tetrahedron Letters* **2010**, *51*, 374.

(192) Bigdeli, M. A.; Halimehjani, A. Z.; Mohammadipour, M.; Sagharichi, P. *Journal of Heterocyclic Chemistry* **2012**, *49*, 926.

(193) Pérez-Balderas, F.; Hernández-Mateo, F.; Santoyo-González, F. *Tetrahedron* **2005**, *61*, 9338.

(194) Freeman, C., unpublished work.

(195) Cai, S.; Lin, S.; Yi, X.; Xi, C. *J. Org. Chem.* **2017**, *82*, 512.

(196) Yi, X.; Jiao, L.; Xi, C. *Org. Biomol. Chem.* **2016**, *14*, 9912.

(197) Li, H.; Li, P.; Wang, L. *Organic Letters* **2013**, *15*, 620.

(198) Shirtcliff, L. D.; Rivers, J.; Haley, M. M. *J. Org. Chem.* **2006**, *71*, 6619.

(199) Peters, M. V.; Stoll, R. S.; Goddard, R.; Buth, G.; Hecht, S. *J. Org. Chem.* **2006**, *71*, 7840.

(200) Counceller, C. M.; Eichman, C. C.; Wray, B. C.; Stambuli, J. P. *Org Lett* **2008**, *10*, 1021.

(201) Davey, M. H.; Lee, V. Y.; Miller, R. D.; Marks, T. J. *J. Org. Chem.* **1999**, *64*, 4976.

(202) Shiravanate Atmaram, A. R. F., Melvyn Gill, Russell J. Napier, Ronald H. Thomson *Acta Chemica Scandinavica* **1982**, *36*, 641

(203) Hwu, J. R.; Das, A. R.; Yang, C. W.; Huang, J.-J.; Hsu, M.-H. *Organic Letters* **2005**, *7*, 3211.

(204) Kumar, H. M. S.; Mohanty, P. K.; Kumar, M. S.; Yadav, J. S. *Synthetic Communications* **1997**, *27*, 1327.

(205) Horning, E. C.; Stromberg, V. L. *Journal of the American Chemical Society* **1952**, *74*, 5151.

(206) Li, D.; Shi, F.; Guo, S.; Deng, Y. *Tetrahedron Letters* **2005**, *46*, 671.

(207) Chilin, A.; Battistutta, R.; Bortolato, A.; Cozza, G.; Zanatta, S.; Poletto, G.; Mazzorana, M.; Zagotto, G.; Uriarte, E.; Guiotto, A.; Pinna, L. A.; Meggio, F.; Moro, S. *Journal of Medicinal Chemistry* **2008**, *51*, 752.

(208) Singh, M. K.; Lakshman, M. K. *J. Org. Chem.* **2009**, *74*, 3079.

(209) Menendez-Rodriguez, L.; Tomas-Mendivil, E.; Francos, J.; Najera, C.; Crochet, P.; Cadierno, V. *Catalysis Science & Technology* **2015**, *5*, 3754.

(210) Enthaler, S.; Weidauer, M.; Schröder, F. *Tetrahedron Letters* **2012**, *53*, 882.

(211) Gawley, R. E. In *Organic Reactions*; John Wiley & Sons, Inc.: 2004.

(212) Bordwell, F. G.; Algrim, D. J. *Journal of the American Chemical Society* **1988**, *110*, 2964.

(213) Bordwell, F. G.; Ji, G. Z. *J. Org. Chem.* **1992**, *57*, 3019.

(214) Blackburn, O. A.; Coe, B. J.; Helliwell, M. *Organometallics* **2011**, *30*, 4910.

(215) Ohsawa, A.; Kawaguchi, T.; Igeta, H. *CHEMICAL & PHARMACEUTICAL BULLETIN* **1982**, *30*, 4352.

(216) Zuman, P.; Shah, B. *Chemical Reviews* **1994**, *94*, 1621.

(217) Pizzolatti, M. G.; Yunes, R. A. *Journal of the Chemical Society, Perkin Transactions 2* **1990**, 759.

(218) Armstrong, B. M.; Shevlin, P. B. *J. Chem. Soc.* **1994**, *116*, 4071.

(219) Magano, J.; Dunetz, J. R. *Organic Process Research & Development* **2012**, *16*, 1156.

(220) Yildiz, I.; Ray, S.; Benelli, T.; Raymo, F. M. *Journal of Materials Chemistry* **2008**, *18*, 3940.

(221) Hutchins, R. O.; Lamson, D. W.; Rua, L.; Milewski, C.; Maryanoff, B. *J. Org. Chem.* **1971**, *36*, 803.

(222) Li, G.; Xu, W.; Zhang, C.; Wang, J.; Liu, C. *Journal of Theoretical & Computational Chemistry* **2006**, *5*, 111.

(223) Maguire, E. *Thesis* **2015**.

(224) Vogel, A. I.; Watling, A.; Watling, J. *Journal of Chemical Education* **1958**, *35*, 40.

(225) Srivastava, A.; Ghorai, S.; Bhattacharjya, A.; Bhattacharya, S. *J. Org. Chem.* **2005**, *70*, 6574.

(226) Goon, D. J. W.; Murray, N. G.; Schoch, J.-P.; Bunce, N. J. *Can. J. Chem.* **1973**, *51*, 3827.

(227) Bamberger, E. *Berichte der deutschen chemischen Gesellschaft* **1911**, *44*, 1966.

(228) Pigman, W. W. *(Book)* **212**.

(229) Jiang, K.; Fan, D.; Belabassi, Y.; Akkaraju, G.; Montchamp, J.-L.; Coffer, J. L. *ACS Applied Materials & Interfaces* **2009**, *1*, 266.

(230) Yu, Z.-X.; Caramella, P.; Houk, K. N. *J. Am. Chem. Soc.* **2003**, *125*, 15420.

(231) Ren, B.; Wang, M.; Liu, J.; Ge, J.; Zhang, X.; Dong, H. *Green Chemistry* **2015**, *17*, 1390.

(232) Sharma, M. K.; Bharadwaj, P. K. *Inorg. Chem.* **2011**, *50*, 1889.

(233) Chiacchio, M. A.; Borrello, L.; Di Pasquale, G.; Pollicino, A.; Bottino, F. A.; Rescifina, A. *Tetrahedron* **2005**, *61*, 7986.

(234) Castellano, S.; Tamborini, L.; Viviano, M.; Pinto, A.; Sbardella, G.; Conti, P. *J. Org. Chem.* **2010**, *75*, 7439.

(235) Mabrour, M.; Bougrin, K.; Benhida, R.; Loupy, A.; Soufiaoui, M. *Tetrahedron Letters* **2007**, *48*, 443.

(236) Wen, H.; Lin, C.; Que, L.; Ge, H.; Ma, L.; Cao, R.; Wan, Y.; Peng, W.; Wang, Z.; Song, H. *European Journal of Medicinal Chemistry* **2008**, *43*, 166.

(237) Yi, W.; Cao, R.; Wen, H.; Yan, Q.; Zhou, B.; Ma, L.; Song, H. *Bioorg. Med. Chem. Lett.* **2009**, *19*, 6157.

(238) Sartori, G.; Ballini, R.; Bigi, F.; Bosica, G.; Maggi, R.; Righi, P. *Chem. Rev.* **2004**, *104*, 199.

(239) Zaliz, C. L. R.; Varela, O. *J. Carbohydr. Chem.* **2001**, *20*, 689.

(240) Sach, N. W.; Richter, D. T.; Cripps, S.; Tran-Dubé, M.; Zhu, H.; Huang, B.; Cui, J.; Sutton, S. C. *Org. Lett.* **2012**, *14*, 3886.

(241) Gouéth, P.; Ramiz, A.; Ronco, G.; Mackenzie, G.; Villa, P. *Carbohydr. Res.* **1995**, *266*, 171.

(242) Dijkstra, G.; Kruizinga, W. H.; Kellogg, R. M. *J. Org. Chem.* **1987**, *52*, 4230.

(243) Paton, R. M.; Young, A. A. *J. Chem. Soc., Chem. Commun.* **1994**, 993.

(244) Streicher, B.; Wünsch, B. *Carbohydr. Res.* **2003**, *338*, 2375.

(245) Percec, V.; Leowanawat, P.; Sun, H.-J.; Kulikov, O.; Nusbaum, C. D.; Tran, T. M.; Bertin, A.; Wilson, D. A.; Peterca, M.; Zhang, S.; Kamat, N. P.; Vargo, K.; Moock, D.; Johnston, E. D.; Hammer, D. A.; Pochan, D. J.; Chen, Y.; Chabre, Y. M.; Shiao, T. C.; Bergeron-Brlek, M.; André, S.; Roy, R.; Gabius, H.-J.; Heiney, P. A. *J. Am. Chem. Soc.* **2013**, *135*, 9055.

(246) Badía, C.; Souard, F.; Vicent, C. *J. Org. Chem.* **2012**, *77*, 10870.

(247) Dong, S. L.; Löweneck, M.; Schrader, T. E.; Schreier, W. J.; Zinth, W.; Moroder, L.; Renner, C. *Chemistry - A European Journal* **2006**, *12*, 1114.

(248) Behrendt, R.; White, P.; Offer, J. *J. Pept. Sci.* **2016**, *22*, 4.

(249) Harris, P. W. R.; Brimble, M. A. *Peptide Science* **2013**, *100*, 356.

(250) Moss, J. A. In *Current Protocols in Protein Science*; John Wiley & Sons, Inc.: 2001.

(251) Brinckerhoff, L. H.; Kalashnikov, V. V.; Thompson, L. W.; Yamshchikov, G. V.; Pierce, R. A.; Galavotti, H. S.; Engelhard, V. H.; Slingluff, C. L. *International Journal of Cancer* **1999**, *83*, 326.

(252) Yun Yang, B.; Montgomery, R. *Carbohydr. Res.* **1999**, *323*, 156.

(253) Ruoslahti, E.; Pierschbacher, M. *Science* **1987**, *238*, 491.

(254) Pankov, R.; Yamada, K. M. *J. Cell Sci.* **2002**, *115*, 3861.

(255) Jeschke, B.; Meyer, J.; Jonczyk, A.; Kessler, H.; Adamietz, P.; Meenen, N. M.; Kantlehner, M.; Goepfert, C.; Nies, B. *Biomaterials* **2002**, *23*, 3455.

(256) Buckley, C. D.; Pilling, D.; Henriquez, N. V.; Parsonage, G.; Threlfall, K.; Scheel-Toellner, D.; Simmons, D. L.; Akbar, A. N.; Lord, J. M.; Salmon, M. *Nature* **1999**, *397*, 534.

(257) Reitz, S.; Cebi, M.; Reiß, P.; Studnik, G.; Linne, U.; Koert, U.; Essen, L.-O. *Angew. Chem. Int. Ed.* **2009**, *48*, 4853.

(258) Sminia, T. J.; Pedersen, D. S. *Synlett* **2012**, *23*, 2643.

(259) Johansson, H.; Pedersen, D. S. *Eur. J. Org. Chem.* **2012**, *2012*, 4267.

(260) Potter, G. T.; Jayson, G. C.; Miller, G. J.; Gardiner, J. M. *J. Org. Chem.* **2016**, *81*, 3443.

(261) Pícha, J.; Buděšínský, M.; Macháčková, K.; Collinsová, M.; Jiráček, J. *J. Pept. Sci.* **2017**, *23*, 202.

(262) Wells, S. M.; Widen, J. C.; Harki, D. A.; Brummond, K. M. *Org. Lett.* **2016**, *18*, 4566.

(263) van Berkel, S. S.; van der Lee, B.; van Delft, F. L.; Wagenvoord, R.; Hemker, H. C.; Rutjes, F. P. J. T. *ChemMedChem* **2012**, *7*, 606.

(264) Srinivasan, R.; Tan, L. P.; Wu, H.; Yang, P.-Y.; Kalesh, K. A.; Yao, S. Q. *Org. Biomol. Chem.* **2009**, *7*, 1821.

(265) Sakamoto, K.; Ito, Y.; Mori, T.; Sugimura, K. *J. Biol. Chem.* **2006**.

(266) Aemissegger, A.; Hilvert, D. *Nat. Protocols* **2007**, *2*, 161.

(267) Morishima, Y.; Tsuji, M.; Seki, M.; Kamachi, M. *Macromolecules* **1993**, *26*, 3299.

(268) Morishima, Y.; Tsuji, M.; Kamachi, M.; Hatada, K. *Macromolecules* **1992**, *25*, 4406.

(269) Herkstroeter, W. G. *J. Am. Chem. Soc.* **1973**, *95*, 8686.

(270) Angelini, G.; Canilho, N.; Emo, M.; Kingsley, M.; Gasbarri, C. *J. Org. Chem.* **2015**, *80*, 7430.

(271) Merino, E.; Ribagorda, M. *Beilstein Journal of Organic Chemistry* **2012**, *8*, 1071.

(272) Carreño, M. C.; García, I.; Ribagorda, M.; Merino, E.; Pieraccini, S.; Spada, G. P. *Org. Lett.* **2005**, *7*, 2869.

(273) Han, M.; Honda, T. *Science China Chemistry* **2011**, *54*, 1955.

(274) Yin, T.-T.; Zhao, Z.-X.; Zhang, H.-X. *Org. Electron.* **2018**, *52*, 61.

(275) Wang, Q.; Gao, S.; Zhou, K.; Chen, W.; Niu, C.; Xi, Z. *Chin. J. Chem* . **2009**, *27*, 1582.

(276) Wazzan, N. A.; Richardson, P. R.; Jones, A. C. *Photochemical & Photobiological Sciences* **2010**, *9*, 968.

(277) Nagashima, T.; Ueda, K.; Nishimura, C.; Yamazaki, T. *Anal. Chem.* **2015**, *87*, 11544.

(278) Banghart, M. R.; Trauner, D. In *Chemical Neurobiology: Methods and Protocols*; Banghart, M. R., Ed.; Humana Press: Totowa, NJ, 2013, p 107.

(279) Tait, K. M.; Parkinson, J. A.; Jones, A. C.; Ebenezer, W. J.; Bates, S. P. *Chem. Phys. Lett.* **2003**, *374*, 372.

(280) Tait, K. M.; Parkinson, J. A.; Gibson, D. I.; Richardson, P. R.; Ebenezer, W. J.; Hutchings, M. G.; Jones, A. C. *Photochemical & Photobiological Sciences* **2007**, *6*, 1010.

(281) Han, M. R.; Hashizume, D.; Hara, M. *New J. Chem.* **2007**, *31*, 1746.

(282) Timm, J.; Schürmann, U.; Kienle, L.; Bensch, W. *Microporous Mesoporous Mater.* **2016**, *228*, 30.

(283) Dong, M.; Babalhavaeji, A.; Samanta, S.; Beharry, A. A.; Woolley, G. A. *Acc. Chem. Res.* **2015**, *48*, 2662.

(284) Sadovski, O.; Beharry, A. A.; Zhang, F.; Woolley, G. A. *Angew. Chem. Int. Ed.* **2009**, *48*, 1484.

(285) Briquet, L.; Vercauteren, D. P.; André, J.-M.; Perpète, E. A.; Jacquemin, D. *Chem. Phys. Lett.* **2007**, *435*, 257.

(286) Krekiehn, N. R.; Müller, M.; Jung, U.; Ulrich, S.; Herges, R.; Magnussen, O. M. *Langmuir* **2015**, *31*, 8362.

(287) Yeung, C. L.; Charlesworth, S.; Iqbal, P.; Bowen, J.; Preece, J. A.; Mendes, P. M. *PCCP* **2013**, *15*, 11014.

(288) Nishioka, H.; Liang, X.; Kato, T.; Asanuma, H. *Angew. Chem. Int. Ed.* **2012**, *51*, 1165.

(289) Williams, D. B. G.; Lawton, M. *J. Org. Chem.* **2010**, *75*, 8351.

(290) Casey, M.; Leonard, J.; Lygo, B.; Procter, G. In *Advanced Practical Organic Chemistry*; Casey, M., Leonard, J., Lygo, B., Procter, G., Eds.; Springer US: Boston, MA, 1990, p 28.

8. Appendix

Full NMR characterisation and assignment of 242

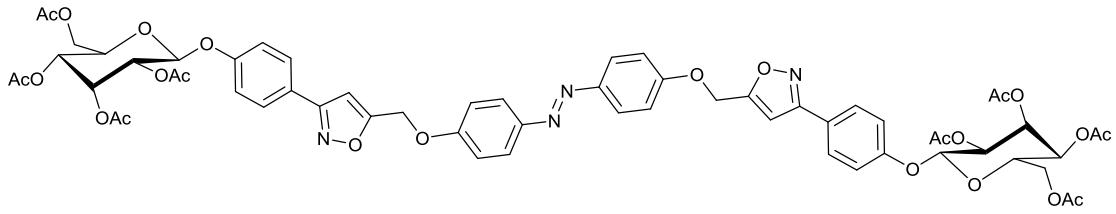

^{1}H-NMR: δ_H (500 MHz) ($CDCl_3$): 2.03, 2.06, 2.09, 2.17 (s, 3H, C(O)C<u>H</u>$_3$), 4.23-4.29 (m, 3H, H^5, H^6 & $H^{6'}$) 5.06 (dd, 1H, H^4, J = 9.5, 3.0 Hz) 5.18 (dd, 1H H^2, J = 8.0, 3.0 Hz) 5.29 (s, 2H, OCH_2) 5.42 (d, 1H, H^1, J = 8.0 Hz) 5.76 (t, 1H, H^3, J = 3.0 Hz) 6.64 (s, 1H, isoxazole-CH) 7.07-7.13(m, 4H, Ar-<u>H</u>) 7.77 (d, 2H, H-2') 7.91 (d, 2H, Ar-<u>H</u>)

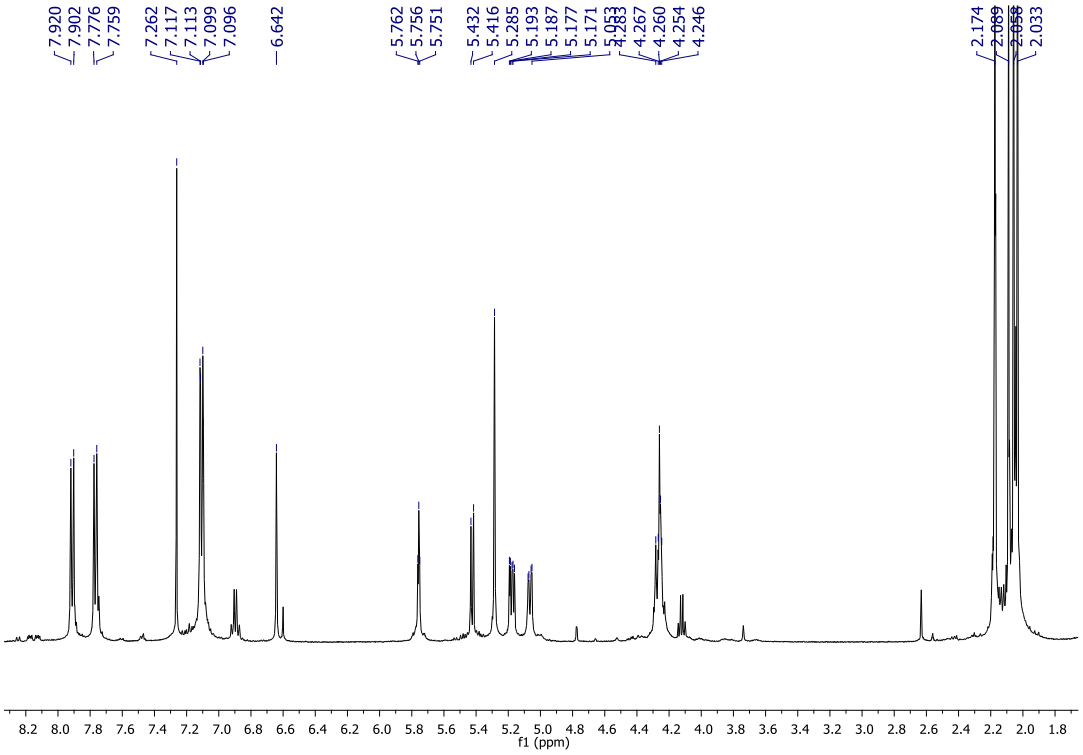

*Figure 82:^{1}H-NMR spectrum of **242.***

To assign these first the following assumptions where made: that the peak that 6.64 was the isoxazole CH due to it being a singlet in the region expected for such a shielded aromatic hydrogen. Also that the doublet at 5.42 is the H^1 of the allose sugar unit, as H^1

is the only carbohydrate proton expected to be a doublet. The acetyl hydrogen are also easily identified by their integration and shielded position from ~1.8-2.2 ppm.

The remaining carbohydrate hydrogens where assigned with a COSY: showing a correlation between H^1 and H^2, H^2 and H^3, etc. The multiplicity for H^2, H^3 and H^4 are all expected to be doublets of doublets, this is true of H2 and H4, H3 is an apparent triplet but this in fact just where the J values are equal for the doublet of doublets. H^3 also has low J-values because it is the epimeric hydrogen. H^5 and H^6 are overlapping and therefore cannot be differentiated from each other.

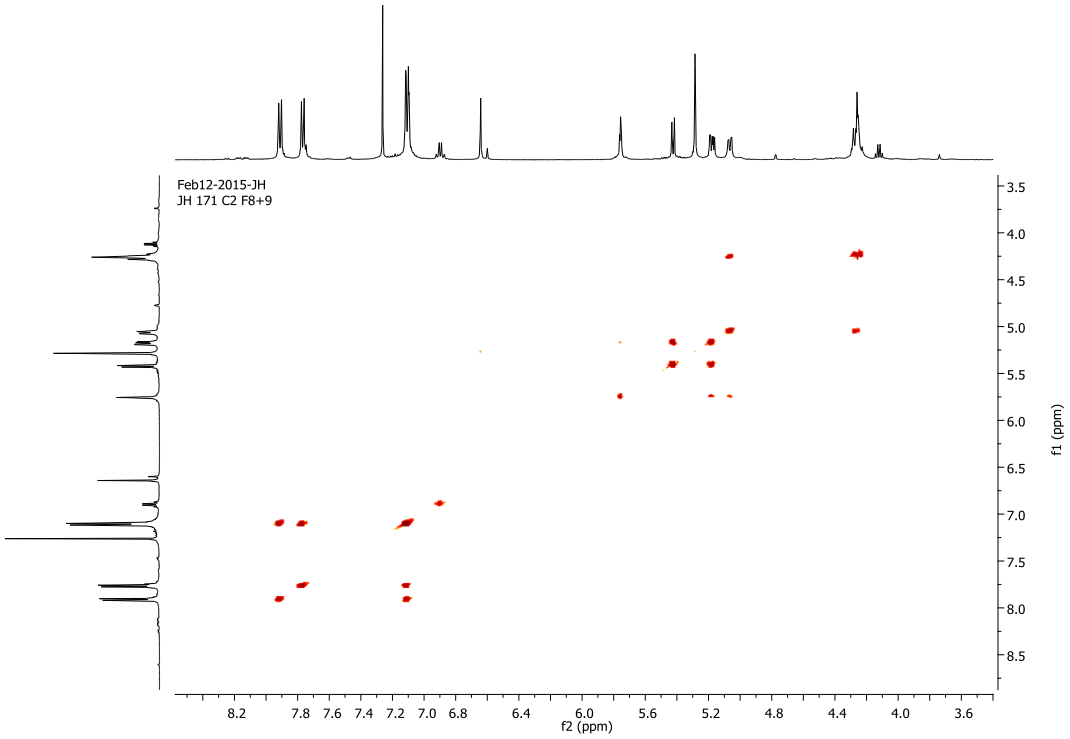

*Figure 83: COSY spectrum of **242.***

A weak correlation between the peak at 5.29 and 6.64 confirms at these are the CH_2 next to the isoxazole and the CH in the ring. They are too far apart for coupling and therefore appear as singlets with the former integrating for twice of the later. The remaining peaks all feature in the aromatic region. The first doublet (7.11) integrates for 8 which indicates that it is in fact two sets of doublets in the same position. The COSY shows both the latter two doublet (7.76 & 7.91) coupling in the first peak (7.11) indicating that the superimposed doublets belong to belong to different rings. These will later be shown in the HMBC carbon correlation that the peak at 7.76 is from the helicid and 7.91 is from the azobenzene aryl and they are both adjacent to oxygen.

^{13}C-NMR: δ_C (125 MHz) ($CDCl_3$): 20.5, 20.6 20.7 20.8 ($\underline{C}H_3C(O)$), 61.7 (OCH_2), 62.3 (C^6), 66.2 (C^4), 68.4 (C^3), 68.8 (C^2), 70.6 (C^5), 96.9 (C^1), 101.4 (isoxazole-CH), 115.1, 117.3 (Ar-CH), 123.6 (C-1') 124.6 128.3 (Ar-CH), 147.8 (C-1) 158.4 (C-4') 159.7 (C-4) 161.9 (isoxazole-CN) 168.0 (isoxazole-CO) 169.1, 169.1, 169.7, 170.7 ($\underline{C}(O)CH_3$)

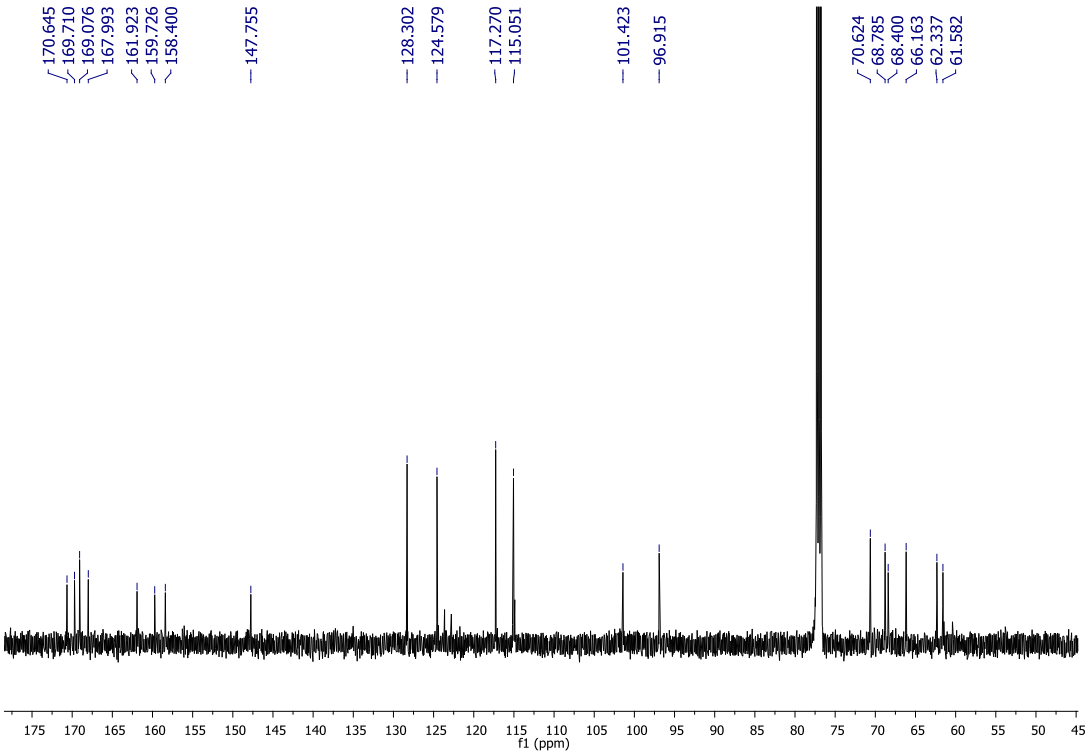

*Figure 84: ^{13}C spectrum of **242.***

From the dept carbon experiments the following information can be gained: the peaks at 61.7 and 62.3 are both CH_2 from the depth 135.

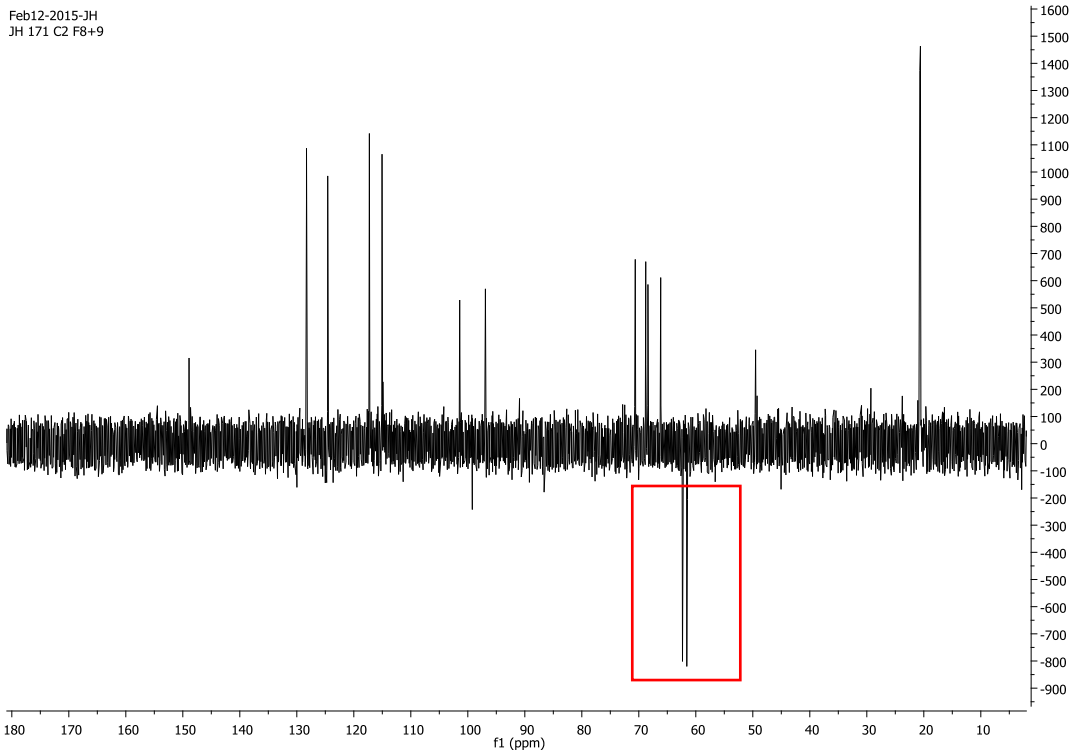

*Figure 85: Dept 135 spectrum of **242.***

The peaks at 123.6 and the 9 peaks between 147.8 and 170.7 are all quaternary. The remaining peaks are all CH.

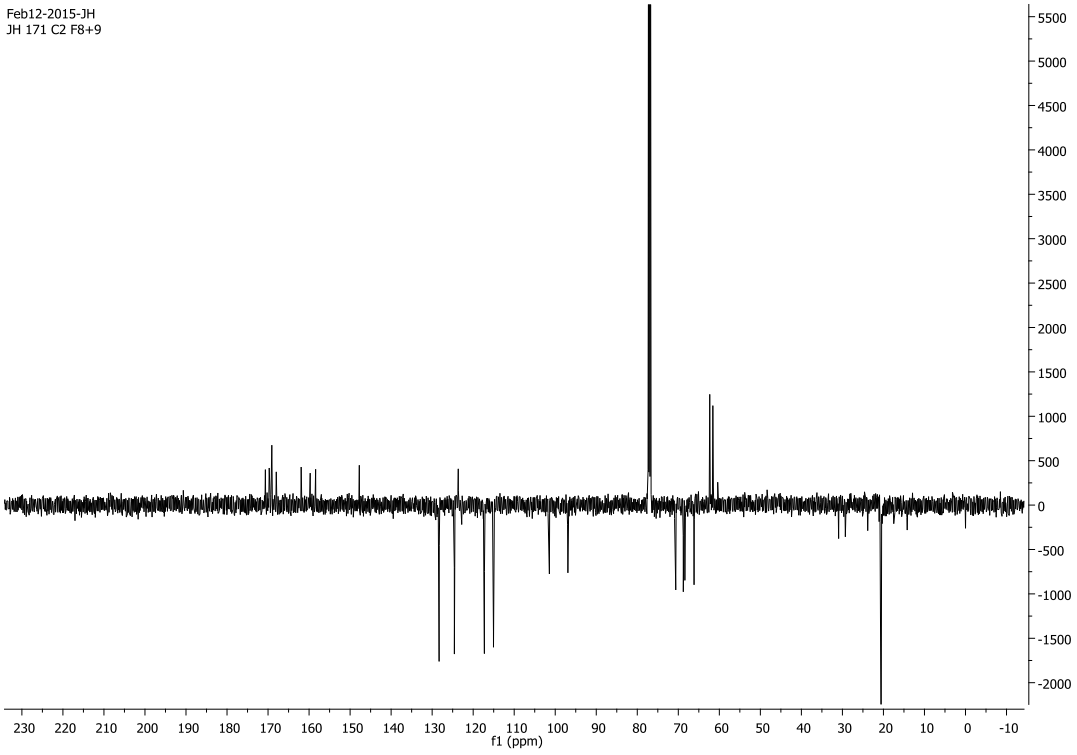

Figure 86: DeptQ-135 spectrum of 242.

The CH_2 and CH peaks can all be assigned by direct correlation on the HSQC. The quaternary carbons can be assigned with the HMBC experiment.The last four peaks (169.1, 169.7 169.7, 170.7) all show a correlation with the CH_3 of the acetyl groups indicating that that they represent the adjacent carbonyl carbons. The peak nearest these (168.0) correlates with CH of the isoxazole and the CH_2 next to the isoxazole, this is therefore the carbon between these two also next to the oxygen in the isoxazole. The peak at 161.9 shows a correlation to the CH of the isoxazole and CH doublet of the aryl ring at 7.76 making this the other quaternary isoxazole carbon which is double bonded to the nitrogen. The peak at 159.7 correlates to the aryl hydrogen (7.91 and 7.11) and the CH_2 next to the isoxazole showing it to be the quaternary peak of the azobenzene aryl which is adjacent to the oxygen. This also shows that the doublet at 7.91 of the ^{1}H NMR is from the azobenzene aryl, making the doublet at 7.76 from the helicid. The peak at 158.4 correlates to the two aryl peaks from the helicid aryl (7.76 and 7.11) and C^1 of the sugar, it is therefore the quaternary carbon of the helicid aryl nearest the allose sugar unit. 147.8 correlates to 7.11 and 7.91 making it the azobenzene quaternary adjacent to the azo functionality. The peak at 123.6 is therefore the remaining quaternary carbon of the helicid aryl, connecting to the isoxazole unit

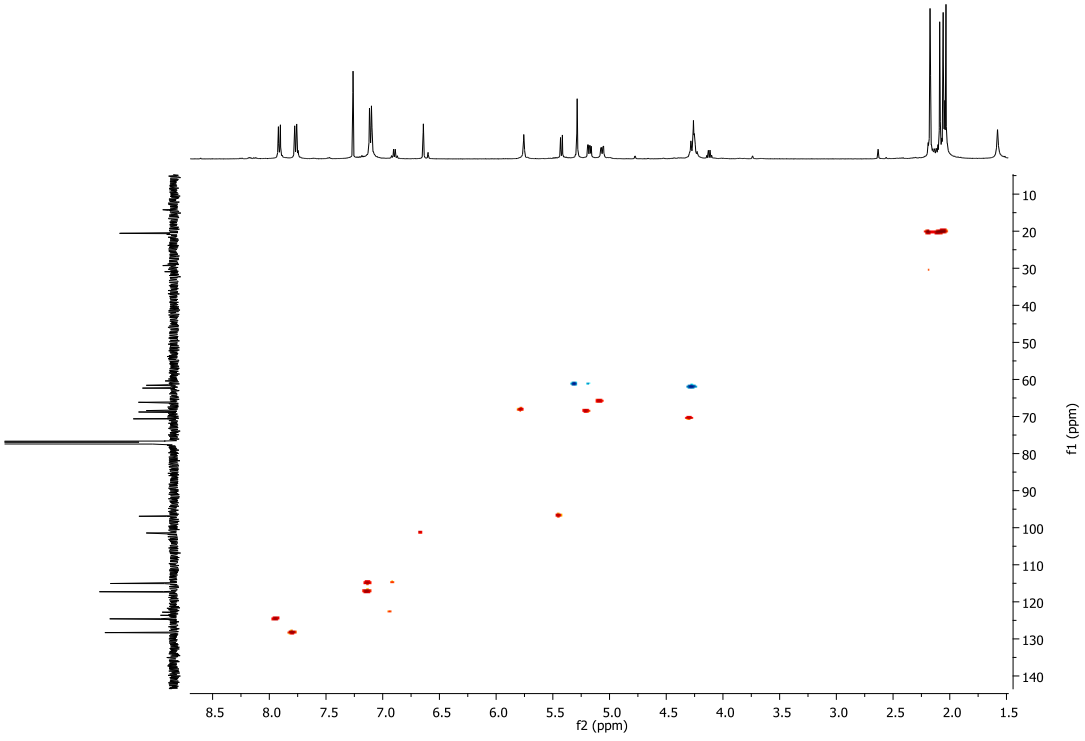

*Figure 87:HSQC spectrum of **242.***

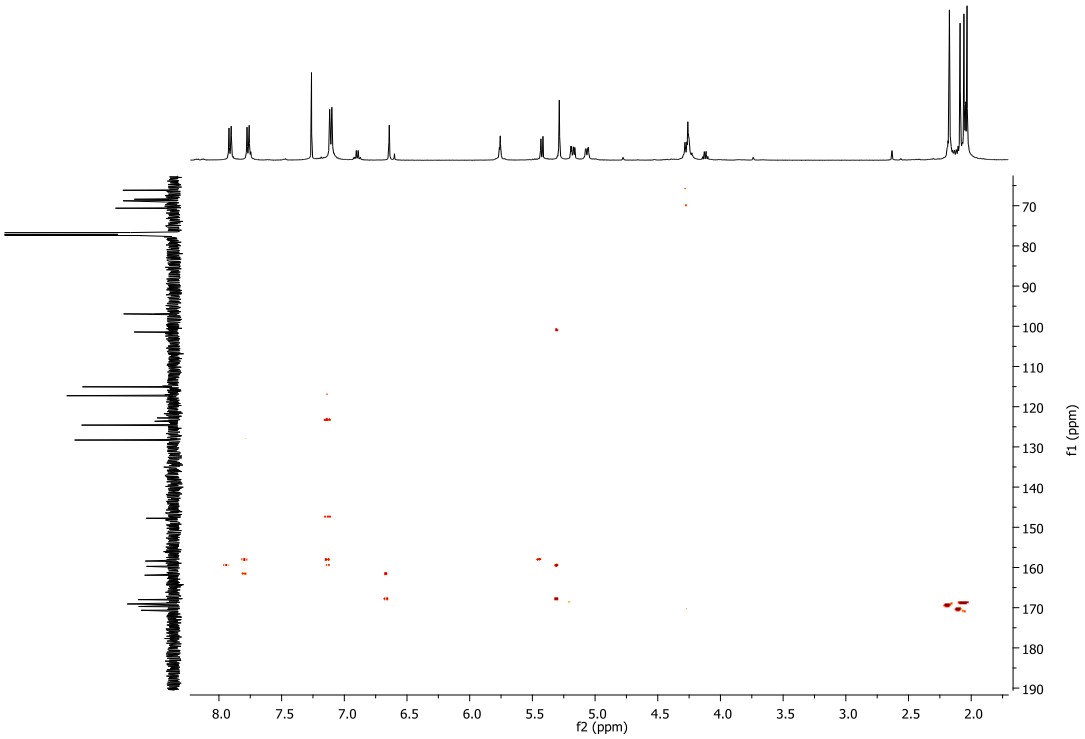

*Figure 88: HMBC spectrum of **242.***